EVALUATION OF LLTR SERIES II TEST A-6 RESULTS

by

DOE/SF/70030--T50

DE82 005340

J. C. Amos
D. E. Knittle
K. Chen
T. K. Odegaard
T. M. Yang

ADVANCED REACTOR SYSTEMS DEPARTMENT
General Electric Company
Sunnyvale, California

June 1981

Prepared for

U. S. Department of Energy
Under Contract No. DE-AT03-76SF70030
Work Package AF 15 40 10.1, WPT No.SG037

DOE/SF/70030--T50

TABLE OF CONTENTS

TABLE OF CONTENTS (cont'd)

LIST OF FIGURES

LIST OF FIGURES (cont'd)

LIST OF FIGURES (cont'd)

LIST OF FIGURES (cont'd)

LIST OF TABLES

I. INTRODUCTION

This report presents an evaluation of the data from Large Leak Test Program Series II Test A-6 performed November 26, 1980 in the Large Leak Test Rig at the Energy Technology Engineering Center (ETEC). This test program is being conducted to determine the effects of intermediate size to large size tube leaks in sodium heated steam generators. The principal objectives of the Series II program (Reference 1) are to define the potential for secondary tube failures in order to establish a basis for selection of design basis leaks (DBL's), to determine experimentally the peak pressures produced from large leak events and, to provide data for confirming or modifying design analysis methods. Data from the large leak tests in this series are also used to confirm or modify the Large Leak Standary Methodology developed from the Series I tests and presented in Reference 2. These tests also provide performance data on CRBR prototype rupture disc assemblies and materials data needed to requalify a system following a large leak event.

Series II Test A1-a and A1-b, evaluated in Reference 3, were double ended guillotine (DEG) size inert gas injection tests performed to separate the non-reactive and reactive effects of the large sodium steam generator leak. Test A-2, evaluated in Reference 4, was a DEG size sodium water reaction leak. Test A-3, evaluated in Reference 5, addressed the effects of a centrally located intermediate size ($\sim$0.1 lb/sec) leak representative of a leak which might be produced by impingement wastage from a smaller leak or by enlargement of a smaller leak by self wastage. Test A-6 covered by this report addresses a peripherally located DEG size leak.

This report summarizes the intertest examination work and evaluates the extent of damage experienced in the test article due to sodium-water reaction (SWR) effects, assesses the capability of the analytical methodology (established as a result of Series I program) to predict the thermal/hydraulic phenomena associated with large SWR events in LMFBR and provides an evaluation of test data not covered by the aforementioned methodology.

II. SUMMARY AND CONCLUSIONS

A. TEST SUMMARY

Series II test A-6 employed a DEG tube rupture located 222.9 inches above the bottom of the LLTI shroud at the periphery of the tube bundle. The test yielded a peak pressure at the leak site of 340 psia and peak measured temperatures of 2150°F. The initial acoustic pressure spike measured upstream of the RD-1 rupture disc assembly of 295 psia was insufficient to burst the upstream rupture membrane. [The LLTV was supposed to be completely filled with sodium. However, review of test data has indicated that $\sim$8 ft^3 of gas was present in the upper region of the LLTV at the time of test. The presence of this gas in the test article contributed to the reduction in the magnitude of the acoustic pressure spike.] The acoustic pressure spikes diminished and a gradual system pressure rise controlled by the compression of the cover gas in the surge tank occurred. When the system pressure increased to 340 psia about 6.5 seconds after leak initiation, the upstream rupture disc burst followed by burst of the downstream disc about 54 milliseconds later. Calculations indicated that about 195 lbs of water was injected into the sodium at an average flow rate of about 5.3 lb/sec. No secondary tube leaks occurred and only minimal tube wastage (0.004 inches maximum) resulted from this test. Tube bowing out to the 4th row from the leak site to a maximum of 1.5 inches was measured by Isotope Scanning Tests (IST).

New knife blades were used in the prototype rupture disc assembly. Rupture disc membrane openings for Test A-6 were 75% and 90%, for the upstream and downstream discs, respectively. These percent openings were significantly greater than for previous Series II tests. Examination of selected areas of the relief system and U-bend corrosion specimens installed in the Reactor Projects Tank (RPT) and a relief system penetration disclosed no evidence of stress corrosion cracking.

B. CONCLUSIONS

1. The analytical results confirm that a gas void was present at the top of the LLTV at the start of the A-6 test.

2. The analytical models and an evaluation of the test data indicate that the average SWR rate was reduced by approximately 35% in the A-6 test compared with the A-2 test. This reduction was probably caused by the proximity of the shroud to the rupture tube (e.g., peripheral rupture tube).

3. The Standard Methodology (Reference 2) has consistently overpredicted (by factors greater than 2) the initial acoustical pressurization rates throughout the LLTR Series II test program including Test A-6. This overprediction is probably caused by:

   a. The exclusion of the stagnant sodium in the cavity between the shroud and vessel wall, in the analytical pressurization model.
   b. The exclusion of the LLTI internals in the analytical model except when determining axial flow cross sections.
   c. The simplifying assumptions used in the analytical model for structure, flow paths, dampening effects, and fluid/structure interaction.

4. Adjustment of the analytical model to have an early transition from spherical to pancake reaction zone bubble improved the accuracy of the analytical predictions at the start of the transient.

5. The analytical models, including those which simulated the gas void at the top of the LLTV and matched the peak leak site acoustical pressure, predicted failure of the rupture discs early (during the acoustical phase of the transient), whereas, rupture disc failure did not actually occur until much later when sufficient energy had been generated by the continuing sodium-water reaction to pressurize the entire LLTR to the rated disc burst pressure (i.e., after about 6 seconds). This emphasizes the need for the piping designer to consider the SWR loads resulting from both an acoustical or quasi-static overpressurization type failure mode of the rupture disc.

6. Inability of the analytical model to accurately predict the rupture disc performance was probably caused by the following factors:

   a. Actual local non-axisymmetric disc buckling at sub-burst pressures which cannot be accounted for by the current analytical rupture disc model;
   b. Underprediction of acoustic pressure attenuation from leak site to rupture disc by the analytical model;
   c. Overprediction of acoustical pressurization rate by the analytical model.

7. The rupture discs would probably have burst during the acoustical phase of the A-6 transient had not the gas void been present at the top of the LLTV. Without the gas void, the acoustic pressure pulse would have built up sufficiently (due to reflections off the lower tube sheet) to burst the rupture disc.

8. LLTI internal thermocouples indicate that the active reaction zone was confined to a narrow (less than 10 inches radius) elongated shape. Similar reaction zone geometry was seen in previous Series II Test A-2.

9. A DEG leak occurring at the periphery of the tube bundle will not result in tube failure and will produce only minor wastage (maximum 0.004 inches).

10. Tube bowing in the vicinity of the leak site can be expected from a peripheral DEG leak under static or low flow conditions. The peripheral leak test A-6 produced tube bowing of about 1.5 inch maximum out to four rows from the leak tube or contrasted with approximately 0.5 inch maximum tube bowing realized from the centrally located test A-2. The increased tube bowing from the peripheral leak test was probably due to longer exposure at elevated temperatures due to the delayed rupture disc action ($\sim$6.5 seconds for A-6 as contrasted with $\sim$73 milliseconds for A-2) and slower complete drainage of the peripheral region.

11. Reverse Buckling rupture disc membranes do not open 100% of these cross-sections. Rupture disc assembly knife blades are dulled by disc rupture and should be replaced after each disc rupture in LMFBR Plant application. (In Test A-6, with new sharp knife blades, the rupture disc upstream and downstream membranes opened ∿75% and 90% as contrasted with the previous Test A-3 where old, resharpened knife blades caused only partial tearing resulting in about 40% opening of both membranes.)

12. The response frequencies of measured accelerometers in the upper relief line were generally within the expected range. The "breathing" mode (i.e., uniform radial expansion and contraction) of the pipe seems to show up stronger than expected.

III. TEST AND FACILITY DESCRIPTION

A. FACILITY DESCRIPTION

The LLTR consists of a test article having representative CRBR steam generator geometry and those systems required to prepare for, conduct, and recover from large sodium-water reaction tests. These systems are the sodium system, the water/steam injection system, the reaction products relief system, and the instrumentation and control system. Each is briefly described in the following sections. A simplified schematic is shown as Figure III-1.

Test Article

The Series II test article shown in Figure III-2 consists of two major assemblies; the permanently installed Large Leak Test Vessel (LLTV) and the removable Large Leak Test Internals (LLTI). These assemblies, when combined, are representative of a full-scale LMFBR steam generator from the standpoint of the sodium/water reaction event. The vessel is comparable to the inside diameter of the CRBRP steam generators. The LLTI tube size, number and pitch is the same as the CRBRP, however, the LLTI tube bundle length is slightly less than half the length of the CRBRP tube bundle. Full scale test article diameter is considered necessary to obtain representative sodium ejection velocities and hydrogen bubble geometries under sodium-water reaction conditions which could be quite different in a scaled down diameter. Representative test article length is less important since the analytical methods can be readily adjusted for length. The test article assemblies are constructed of 2-1/4 Cr-1Mo.

The LLTV consists of a top hemispherical head, a cylindrical shell and a bottom hemispherical head. The top head secures the LLTI tubesheet in place and acts as a steam head for the LLTI secondary tubes. A gasket between the top head and the LLTI tubesheet provides the steam seal. The top head has three nozzles. One nozzle is for instrumentation, and the other two are positioned over the central and peripheral rupture tube

locations for attachment to the Large Leak Injection Device and the secondary tube steam supply line.

A seal ring provides the primary seal between the shell upper flange and the LLTI tubesheet. Provision is also made for a backup seal should sodium leakage be experienced at this location. The bottom head flange seal includes a metal O-ring and welded seal. Since removal of the bottom head would be required only if an adequate LLTV sodium drain is not obtained, the lower seal is welded in place.

The LLTI consists of a thick upper tubesheet with tubes attached by full penetration internal bore welds similar to the welds being used for the CRBRP steam generator units. Additional tubes consisting of removable instrumentation tubes, removable dummy tubes and rupture tubes complete the tube array which simulates the full scale CRBRP tube bundle. The instrument tubes include pressure transducers, strain gage tubes, and thermocrouple tubes.

LLTI secondary tubes are capped at the bottom. However, a simulated tubesheet is located at the bottom of the LLTV to react to sodium pressure waves similarly to a steam generator lower tubesheet. The LLTI tubes are enclosed in a shroud prototypical of the CRBRP steam generator shroud except for length. Axial bolting flanges are provided to allow removal of the shroud in two clamshell halves for inspection and maintenance of the tube bundle. The LLTI contains tube spacer plates attached to the shrould similar to the CRBRP units. The LLTI shrould includes prototypic windows located with the same relation to the sodium inlet and outlet nozzles as the CRBRP units.

LLTI/LLTV Test Article includes the following pressure, temperature, and strain instrumentation located as shown in Table III-1 and III-2.

7 - Pressure Sensors (installed in instrumentation tubes)

3 - Pressure Sensors (installed on upper and lower tubesheets)

6 - Pressure Sensors (installed in penetrations on LLTV shell)

TABLE III-1

LLTI/LLTV PRESSURE TRANSDUCER LOCATIONS

SENSOR DESIGNATION	TUBE NO.	AXIAL DISTANCE FROM LEAK SITE (IN.)	RADIAL DISTANCE FROM LEAK SITE (IN.)
P-01-2	2107	- 121	24.4
P-02-2	4146	92	5.4
P-01-7A	2176	- 27	32.4
P-01-5	1119	- 171	15
P-01-8	1136	21	8.9
P-A-10	Lower Tube Sheet	- 236	6.4
P-01-7B	4182	- 27	4.2
P-615	LLTV Shell	21	14
P-616	LLTV Shell	- 51	14
P-617	LLTV Shell	- 103	14
P-618	LLTV Shell	- 151	14
P-619	LLTV Shell	- 183	14

TABLE III-2 LLTI THERMOCOUPLE LOCATION
(Sheet 1 of 3)

SENSOR NO.	TUBE NO.	LLTI HEIGHT (INCHES)	RADIAL DISTANCE FROM RUPTURE TUBE (INCHES)	DAS SEQUENCE NO.
TE-01-1	1026	41	17.69	1
TE-01-4	1026	101	17.69	49
TE-01-6	1026	149	17.69	81
TE-12-1	3002	65	16.9	97
TE-12-2	3002	89	16.9	113
TE-12-3	3002	105	16.9	129
TE-12-4	3002	109	16.9	2
TE-12-5	3002	113	16.9	18
TE-12-6	3002	121	16.9	34
TE-12-7	3002	149	16.9	50
TE-12-8	3002	197	16.9	94
TE-12-9	3002	267	16.9	66
TE-02-3	1052	81	28.52	67
TE-02-6	1052	137	28.52	115
TE-03-2	1077	81	24.30	4
TE-03-6	1077	149	24.30	68
TE-04-1	1100	41	27.47	82
TE-04-3	1100	81	27.47	114
TE-04-6	1100	137	27.47	19
TE-12-10	4182	65	2.11	36
TE-12-20	4182	89	2.11	52
TE-12-30	4182	105	2.11	90
TE-12-40	4182	109	2.11	130
TE-12-50	4182	113	2.11	3

TABLE III-2 LLTI THERMOCOUPLE LOCATION
(Sheet 2 of 3)

SENSOR NO.	TUBE NO.	LLTI HEIGHT (INCHES)	RADIAL DISTANCE FROM RUPTURE TUBE (INCHES)	DAS SEQUENCE NO.
TE-12-60	4182	121	2.11	5
TE-12-70	4182	149	2.11	21
TE-12-80	4182	197	2.11	37
TE-12-90	4182	267	2.11	53
TE-11-10	4166	41	2.11	69
TE-11-20	4166	81	2.11	85
TE-11-30	4166	89	2.11	101
TE-11-40	4166	93	2.11	117
TE-01-10	4116	41	6.11	58
TE-01-20	4116	81	6.11	92
TE-01-30	4116	89	6.11	74
TE-01-40	4116	101	6.11	110
TE-01-50	4116	113	6.11	111
TE-01-60	4116	149	6.11	112
TE-03-10	4075	41	9.76	126
TE-03-20	4075	81	9.76	127
TE-03-30	4075	89	9.76	128
TE-03-40	4075	111	9.76	142
TE-03-50	4075	113	9.76	108
TE-03-60	4075	149	9.76	132
TE-11-9	1013	233	16.47	133
TE-11-50	4166	97	2.11	17
TE-11-60	4166	101	2.11	33
TE-11-70	4166	113	2.11	65

TABLE III-2 LLTI THERMOCOUPLE LOCATION
(Sheet 3 of 3)

SENSOR NO.	TUBE NO.	LLTI HEIGHT (INCHES)	RADIAL DISTANCE FROM RUPTURE TUBE (INCHES)	DAS SEQUENCE NO.
TE-11-80	4166	120	2.11	35
TE-11-90	4166	233	2.11	51
TE-13-2	4010	113	13.73	99
TE-13-3	4010	207	13.73	131
TE-13-4	4010	255	13.73	20
TE-13-5	4010	283	13.73	70
TE-21-2	2084	23	21.35	86
TE-21-3	2084	25	21.35	102
TE- -	2084	105	21.35	7
TE-13-6	4010	291	13.73	39
TE-13-7	4010	307	13.73	118
TE-13-8	4010	311	13.73	134
TE-13-9	4010	315	13.73	23
TE-22-3	2183	25	33.55	55
TE-22-6	2183	105	33.55	103
TE-23-20	4095	23	7.93	71
TE-23-30	4095	25	7.93	87
TE-23-40	4095	101	7.93	105
TE-23-50	4095	103	7.93	79
TE-23-60	4095	105	7.93	83

77 - Sodium immersed thermocouples (installed in 12 tubes)

12 - Tube wall thermocouples (installed in 2 tubes)

5 - Strain gages (installed on the LLTI shroud)

Sodium System

Figure III-3 shows a pictorial representation of the sodium and relief system major components and piping. The main sodium piping is fabricated of 304 stainless steel and is designed for normal operation between 600°F and 900°F. The upper sodium line is 10 in. Schedule 80 pipe and has a total length of approximately 40 ft. The upper header is 18 in. Schedule 100 pipe and is approximately 25 ft. in length. Nozzles to the rupture disc attachment flanges are 18 in. diameter. A blank flange is installed at the upper disc location (RD-2) for the Series II tests. The system includes provisions for sodium filling from a 12,000 gallon drain tank, and for rapid sodium drain to the Reaction Products Tank (RPT).

Also shown on Figure III-3 are the locations of sodium system pressure and flow instrumentation. The instrumentation consists of thermocouples for measurement of fluid temperature, fast-response pressure transducers, a low-level pressure transducer to provide an accurate measure of initial sodium pressure, strain gages, and three drag-disc flowmeters (located in the relief lines and designated as sensors F506, F511 and F510 on Figure III-3) to provide information on sodium ejection velocities and bubble growth at the rupture site. Spark plug type flow meters (sensors F508A to F508H) provide information on the location of the fluid slug in the relief line.

Water Injection System

The primary tube water/injection system was filled with 1700 psig water for Test A-6. This system (Figure III-1) consists of water supply tanks (T1 and T2) and piping to and from the test article, the Large Leak

Injection Device (LLID) which is used to induce tube rupture, and a downstream flow control valve and condenser tank which can be used to initiate and control pretest water flowrate. The main water supply tanks, the interconnecting piping, and the LLID are electrically heated to condition water temperatures and pressures to the required test levels. Piping and components are fabricated of 2-1/4 Cr-1Mo material and are designed for operating temperatures between 500°F and 925°F.

The primary tube water injection system contains two 25 ft^3 supply tanks: Tank T-1 is connected to the normal water inlet at the bottom of the LLTV and Tank T-2 is connected to the LLID at the upper section of the primary rupture tube. The water injection system contains pressure, temperature and flow instrumentation. Tank T-3 was connected to the secondary tubes at the LLTV upper head.

The LLID is a piston-cyclinder device which is used to apply an axial load that causes separation of the notched rupture tube to which it is attached. The cylindrical body of the mechanism is rigidly attached to the shell of the LLTV via a series of mounting flanges; the piston rod extension is welded directly to the rupture tube. A bellows seal between the fixed mechanism and the piston rod maintains the integrity of the sodium boundary during the piston stroke. The piston rod is tubular and serves as an extension of the rupture tube. The LLID is pressurized with nitrogen gas to initiate tube rupture. Gas pressures between 1600 and 1800 psig (which yield forces of 7000 to 8000 lb) are utilized. A crushable structure is included at the top of the cylinder to absorb the kinetic energy of the piston rod and attached tube segment after rupture occurs. Pressure and displacement information from the LLID are monitored.

Reaction Relief System

The reaction relief system (Figure III-3) starts at the prototype 18 in. reverse buckling rupture discs assembly (RD-1), which protects the sodium system, and consists of the downstream piping, a large reaction

products tank (RPT) to which the sodium and reaction products are relieved after a sodium-water reaction (SWR) event, and a stack, with igniter, for burning the hydrogen evolved during the SWR. For test A-6, RD-1 contained two rupture discs in series. A blind flange replaced the upper rupture disc (RD-2) during Series II Tests. Thus, the only relief path during this test was through the lower rupture disc RD-1. The relief system line is approximately 53 ft. in length and is 16 inches in diameter. The relief system in the LLTR is instrumented with spark plug detectors in the piping downstream of the rupture discs to monitor sodium velocities. Relief system temperatures and pressures are monitored. Contact-type sensors are also provided downstream of each rupture disc to indicate the time of disc actuation.

B. TEST DESCRIPTION

Test A-6 was conducted on November 26, 1980 in accordance with the GE Test Request (Reference 1) under the following test conditions:

- DEG rupture of a single tube (Number 4175) located on the periphery of the LLTI 222.9 inches above the lower end of the LLTI shroud and 2 inches below Spacer No. 8.
- The test was initiated with dynamic water flow in the rupture tube prior to rupture. The LLTI/LLTV was in "evaporator startup power mode" with the test article full and, the sodium level specified to be in the lower part of the surge tank. (Post-test data review indicated that a gas volume of $\sim$8 ft^3 was present in the LLTV)
- Injection medium: subcooled water
- Rupture tube supply pressure: 1700 $\pm$ 50 psig
- Water/steam secondary system: 1700 $\pm$ 50 psig
- Water/steam tubes and lines: 580 $\pm$ 10F
- Initial sodium pressure (P-531): $\sim$125 psig
- LLTV with a linear temperature gradient from 570 $\pm$ 10F at the lower tubesheet to 590 $\pm$ 10F at the upper tubesheet.

- The RD-1 double rupture disc assembly was preheated isothermally to a temperature of 573 ± 20°F.

Table III-3 shows the time and sequence of significant events occurring during the A-6 test as deduced from the test data presented in Reference 6 and reproduced in Figures III-5 through III-14.

TABLE III-3

TEST A-6 SEQUENCE OF EVENTS

	Reference Sensor	Time (sec)	Figure
Leak Initiated by LLID	Z503 F502 F503	0	III-5 III-6 III-7
First accoustic pressure spike at leak site.	P-01-7B	0.005	III-8
First accoustic pressure spike up stream of Rupture Disc.	P525	0.010	III-9
Pressure up-stream of Rupture Disc indicating RD buckling.	P525	6.560	III-9
Cavity spark plug shorts indicating rupture up-stream.	Z504	6.590	III-10
Downstream disc buckling	PRP-1C	6.610	III-11
RD-1 downstream spark plug shorts indicating disc rupture.	Z505	6.620	III-12
Secondary tubes isolated and Blowdown started.	P506	18.00	III-13
Rupture tube Blowdown initiated.	P502 F502	38.00	III-14 III-6
Sodium Drain Valve opened.	Sequencer	72.00	

IV. ANALYTICAL METHODS & MODELS

The A-6 post test analytical evaluation was conducted using the RELAP 4 Mod5 computer code to calculate the water side parameters and the TRANSWRAP II computer code to calculate the reaction zone and sodium side parameters using the water side parameters as input.

After the A-2 post test report (Reference 4) was written the standard methodology SWR analytical model was changed as follows:

(1) An elastic-plastic rupture disc model was substituted for the elastic rupture disc model.

(2) The number of disc elements used was changed from 20 to 10.

(3) The transition between spherical and pancake reaction zone bubble models was changed from the time the reaction zone bubble growth achieved a given size to the first calculation time step.

The first change was made to improve the rupture disc simulation as explained in Section IV-B. The number of rupture disc elements was changed to correspond with the number being used for the CRBRP analysis. The spherical/pancake bubble model transition time was changed to eliminate model interface calculational instabilities.

Changes 1 and 3 were incorporated in the analytical model used for the A-6 pre test evaluation described in Reference 7. Change 2 was incorporated for the A-6 post test evaluation.

A. ANALYTICAL MODELS

The seven analytical models used for this analysis are described in Table IV-1. The reasons for using these models were as follows: Model A was used for the pretest predictions for test A-6 (Reference 7) and represents the changes made in the SWR standard methodology used for the A-2 post test evaluation represented by Model B. Model C was created to simulate the gas void which was present at the top of the LLTV at the start of the A-6 test, but in all other respects it was the same as Model A. Since Model C over predicted the leak site maximum acoustical pressure, Model D, which used a reduced SWR rate, was run. Model D, even though it accurately predicted the peak leak site acoustical pressure, over predicted the peak acoustical pressure upstream of the rupture disc. Models E-G were created to determine the reason(s) for over predicting the rupture disc pressure environment, Model E by changing one of the modeling assumptions used* and Model F by using the measured leak site pressure history as the source.** Model G was created to determine the combined effects of the changes made in Models E and F on the pressure history upstream of the rupture disc.

---

*Not including the large inventory of non-flowing sodium in the vessel cross section.

**To determine if the higher predicted leak site pressurization rate was the cause.

TABLE IV-1

ANALYTICAL MODELS USED

ANALYTICAL MODEL ID.	SODIUM-WATER REACTION RATE	CONDITION OF SYSTEM @ START OF TEST	OTHER MODEL CHANGES
A	Std. Methodology Rate*	hard (gas free) LLTV	
B	Std. Methodology Rate*	hard (gas free) LLTV	Late transition from spherical to pancake reaction zone bubble model
C	Std. Methodology Rate*	8 cu. ft. gas void at the top of the LLTV	
D	65% of Std. Methodology Rate*	8 cu. ft. gas void at the top of the LLTV	
E	Std. Methodology Rate*	8 cu. ft. gas void at the top of the LLTV	Non-flowing sodium between Shroud and Pressure Vessel included in LLTV pipe flow cross sections
F	N.A.	8 cu. ft. gas void at the top of the LLTV	Test measured leak site pressure history input as source
G	N.A.	8 cu. ft. gas void at the top of the LLTV	Combination of changes made for Models E and F

All of the analytical models except F & G used as input A-6 or A-2 water flow rate histories given in Figure IV-6. All of the models except B used transition from the spherical to the pancake reaction zone bubble model in the first time step and used the elastic-plastic rupture disc model. All of the models except A & B used 10 rupture disc elements. Models A & B employed 20 rupture disc elements.

*Std. Methodology Sodium-Water Reaction Rate - 65% of the available water reacting with the sodium.

B. WATER SIDE MODELING

The RELAP 4 computer code (Reference 8) was used to calculate the water flow rate history from the tube break into the sodium side of the system independently of the reaction zone conditions. The accuracy of this method of determining the water flow parameters depends upon the validity of the assumption of choked flow, which should be correct for the time period of interest, since the water side pressure remains considerably higher than that on the sodium side of the system.

The ruptured water tube was divided into 2 parts, an upper and a lower section, and the water flow rates from each were calculated independently. The resulting water flow histories predicted by the RELAP runs for the upper and lower sections (divided at the break) were added to obtain the total water flow into the reaction zone. The resulting water flow history was modified as follows to obtain the water flow history input into TRANSWRAP.

$$\dot{W}_{net} = \left[\dot{W}_{T1} + \dot{W}_{T2}\right] \cdot \overbrace{\frac{1700 + 460}{2600 + 460} \cdot 0.65}^{0.459} \cdot M.F.$$

$\dot{W}_{net}$: into Reaction Zone; $\dot{W}_{T1}$: RELAP (Lower); $\dot{W}_{T2}$: RELAP (Upper); 0.459 · 0.65 · M.F.: Modifying Factor

The first term in the modifying factor was to correct for reaction zone bubble temperature and the second term assumes that only 65% of the water reacts with the sodium. These corrections are based upon prior knowledge of the sodium water reaction and are part of the standard methodology. The third term M.F. is a multiplying factor which was used in Model D to obtain best fit pressure histories for the A-6 test data.

The RELAP models only differed from those used in the A-2 post test analytical predictions in the following respect. The tube break was moved to 222.87 inches above the bottom of the shroud (instead of the 122.25" used for the A-2 test).

The RELAP models used for the analysis are shown in Figures IV-1 (T1-Lower Tube Section fed by Tank T-1) and IV-2 (T2-Upper Tube Section fed by Tank T-2). Figure IV-3 shows the discharge coefficient vs tube opening used in this and previous analyses. The water flow histories for the lower and upper sections are given in Figures IV-4 & 5, respectively. TRANSWRAP used the mean values of the calculated water flow rates shown in the figures (ignoring the oscillations caused by calculational instabilities) multiplied by the constant factor defined above. The calculated water flow rate history for test A-6 is compared with that for LLTR-Series 2 test A-2 in Figure IV-6.

C. REACTION ZONE & SODIUM SIDE MODELING

The TRANSWRAP computer code, described in References 9 and 10, was used for the analytical predictions of the reaction zone and sodium system parameters during the acoustical phase of the transient. The TRANSWRAP computer code written in Fortran IV was developed to analytically predict the major consequences (e.g., acoustical pressure pulses) of large scale sodium water reactions in LMFBR secondary systems. The code provides the options, flexibility, and features necessary to consider any system configuration, the geometry of the system being input by the user in interconnected smaller segments. The code in its present form considers only the reaction zone and the sodium side of the system since experience at GE has shown that other general purpose fluid flow computer codes (e.g., RELAP) can better represent the water side of the system for most practical problems.

1. Method of Solution

TRANSWRAP divides the system into three parts; the reaction zone where the sodium water reaction takes place, the sodium side piping, and the relief lines. The reaction zone variables are calculated by simultaneously solving for the first derivative of the conservation of energy equation including reaction heat and the conservation of mass equation (perfect gas law) along with equations which relate the transient behavior of the sodium side and input from the water side with the reaction zone parameters. It solves the fluid dynamics equations for the sodium side by numerical finite difference techniques using the "Method of Characteristics" method. Rupture discs (singly and/or in pairs) can be considered using instantaneous, elastic, or elastic-plastic stress analysis models; the latter being used in this study, except for model B which used the elastic rupture disc model. Provisions have been made to incorporate empirical variables via user input into the rupture disc model to better represent real rupture disc behavior based on prototypical test data as discussed in Section IV-D.

2. TRANSWRAP Models

The basic TRANSWRAP analytical model used in this analysis is shown in Figure IV-7 and the data input given in Appendix A. This model differed from that used for the A-2 post test predictions in the following respects:

(a) The leak site was moved from 122.25" (Test A-2) to 222.87" above the bottom of the shroud (Test A-6). The modeling changes used to accomplish this are shown in Figure IV-7.

(b) The input water flow history used was obtained from new RELAP runs as discussed in Section IV-B.

(c) The rupture disc model was changed as described in Section IV-D.

(d) In models C through F, a 8 cu. ft. gas void* was added to end joint 12 (at the top of the LLTV). See Figure IV-7.

(e) In model D the SWR rate was changed from the standard methodology value to one that best fit the A-6 test data.

(f) The transition from spherical to pancake bubble took place in the first time step rather than after the bubble had grown to a given predetermined size (except in Model B).

(g) In model E & G the non-flowing sodium between the shroud and pressure vessel wall was included in the vessel sodium flow cross section. See Figure IV-9.

(h) In models F & G the measured leak site pressure history was used as the source pressure.

---

*The gas void was added to the model to simulate the A-6 test conditions as explained in Section V.

D. RUPTURE DISC MODELING

The present analytical modeling of the phenomena associated with the rupture discs has been evolved over time by incorporating an elastic-plastic rupture disc model from the SWAAM-I Code (Reference 5) and empirical parameters which were developed from the results of prior sodium water reaction tests. The rupture disc model is shown schematically in Figure IV-8.

1. Elastic-Plastic Rupture Disc Model

TRANSWRAP analyses conducted prior to the A-6 pre test analysis used either the instantaneous rupture disc model or the elastic rupture disc models. Neither model provided adequate simulation of rupture disc behavior. An adequate simulation of rupture disc behavior is, however, needed to reasonably predict the maximum loads one might expect from a SWR transient. The instantaneous rupture disc model, while it does burst the rupture discs at a user specified pressure, does not simulate the true behavior of the rupture disc or the effect of the disc rupture on the remainder of the system. The elastic rupture disc model does attempt to simulate the performance of the rupture discs when subjected to the over-pressures but the model proved to be inadequate since portions of the rupture disc undergo plastic strain prior to rupture. The elastic-plastic rupture disc model, which was developed at Argonne National Laboratories for the SWAAM-I computer Code (Reference 11), while it does not simulate rupture disc performance with complete accuracy, does a better job than the other models. However, it still does not adequately simulate rupture disc performance after the knife edges are contacted. In order to improve the rupture disc behavior simulation, G.E. has introduced empirical parameters which control the rupture disc model after the disc strikes the knife edges. These empirical parameters described in the next section were incorporated in the standard methodology starting with the A-2 post test evaluation.

2. Empirical Parameters

The values of the empirical parameters, along with the other rupture disc parameters used in this analysis, are presented in Table IV-2 and the empirical parameters are graphically shown in Figure IV-8.

TABLE IV- 2

RUPTURE DISC MODEL PARAMETERS

PARAMETER	VALUE OF PARAMETER USED FOR	
	First Disc	Second Disc
Type of Disc Model	Elastic-Plastic	Elastic-Plastic
Diameter (in)	18	18
Radius of Curvature (in)	12.675	12.675
Knife to Disc Clearance (in)	1.5	1.5
Disc Thickness (in)	.060	.060
Open Area Fraction	.50	0.6
Recovery Pressure (psi)	150	135
Hold Time (sec)	.025	.002
Rise Time (sec)	.010	.003
Tearing Time (sec)	.014	0.012
Young's Modulus (psi)	29.2×10^6	29.2×10^6
Poisson's Ratio	0.320	0.323
Density (lbm/ft^3)	512	512
Plastic Modulus (psi)	2.9×10^5	2.9×10^5
Yield Stress (psi)	5.25×10^4	4.75×10^4
Ultimate Stress (psi)	9.3×10^4	9.3×10^4
Number of Finite Elements	10	10

The empirical parameters include:

(a) RISETM

The time duration for the cavity pressure to rise at a given fixed rate once the 1st disc strikes the knife edges;

(b) HHOLD

The maximum pressure achieved upstream of the disc during the pressure rise.

(c) TOPEN

The length of time that pressure is held after contact of the 1st disc with the knife edge and before the disc starts to tear open;

(d) TMOPEN

The length of time it takes for the 1st disc to tear to a user specified maximum opening area from the time it starts to tear (using a linear increase in equivalent opening diameter with time);

(e) TIMOPEN

The length of time it takes for the 2nd disc to tear to a user specified maximum opening area from the time it strikes the knife edges (using a linear increase in equivalent opening diameter with time.

3. Problems Remaining in Rupture Disc Simulation

The elastic-plastic rupture disc model using the GE developed empirical parameters does do a much better job than prior rupture disc models in predicting rupture disc performance, but there are still important areas remaining where the simulation could be greatly improved. The most important problem areas remaining are sub-burst pressure local buckling and the loading and unloading rates for the disc. The sub-burst pressure local buckling phenomenon is discussed in Section VB. The piping loads created by the rupture disc behavior are dependent upon rate as well as amplitude. The real disc loads and unloads at slower rates than predicted by the analytical model, indicating that the actual disc behavior is more complex than that being simulated.

However, resulting dynamic loads on IHTS piping are conservatively predicted by the more rapid loading and unloading rates predicted by the model.

V. EVALUATION OF TEST RESULTS

A. LLTV AND SYSTEM PRESSURE EVALUATION

This section contains an evaluation of the A-6 test results and compares them with analytical predictions from the TRANSWRAP computer code. Analytical predictions are given for only the first 25 milliseconds of the transient because the TRANSWRAP computer code's forte is the acoustical wave phase which in the A-6 test was essentially completed by that time due to the presence of a gas void in the system.

Table V-1 presents the figure numbers where the prediction of pressure histories for the various locations and analytical models are given. Also included in the figures are the measured pressures at those locations. All pressures given are in absolute units.

Table V-2 presents the figure numbers where the predicted histories of parameters other than pressure are given.

The A-6 pre-test evaluation report (Reference 7) provided analytical pressure history predictions of the A-6 test configuration and anticipated conditions using the Reference 4 standard methodology analytical model with changes 1 and 3 described in Section IV. The predicted pressure history near the leak site is presented in Figure V-1. A comparison of that predicted pressure history with test data from pressure transducer (P-01-7B) near the leak site (Figure V-2) shows that the peak amplitude of the initial acoustical pressure wave was less than that predicted by the model (i.e., 307 psia measured vs 361 psia predicted). Also, the model predicted subsequent higher amplitude peaks as the result of reflected acoustical waves, whereas the test data indicates that these waves were dampened out. The standard methodology model predicted that the first rupture disc would buckle as a result of the acoustical pressure pulse within 4.35 msec of the DEG, whereas the test data shows that the disc did not burst until approximately 6 seconds into the transient as a result of system pressurization and not from acoustical pressure waves.

TABLE V-1

PRESSURE HISTORY PREDICTIONS TRANSWRAP MODEL VS. TEST PRESSURE TRANSDUCER LOCATIONS AND MEASUREMENTS

		Pressure Transducer Location			Nearest TRANSWRAP Output Location				Predicted Pressure History for TRANSWRAP Model							
Pressure Transducer Number	Tube Number or Location	Elevation Above Bottom of Shroud ~ Inches	Radial Location ~ Inches	Fig. No. (Showing Transducer Location)	Pipe Number	Node Number	Type of Piping	Elevation of TRANSWRAP Node ~ Inches	Model A A-6	Model A* A-2	Model B** A-2	Model C A-6	Model D A-6	Model E A-6	Model F A-6	Model G A-6
PT-02-1	4059	315.25	4.88	IV-7,9,10	12	6	LLTV	314.84				C.1	D.1	E.1		
PT-02-2	4146	315.25	17.09		12	6		314.84				C.2	D.2	E.2		
PT-02-8	4006	243.25	6.1		10	3		243.91				C.3	D.3	E.3		
PT-02-7A	4188	195.25	17.09		9	4		194.76				C.4	D.4	E.4		
PT-02-7B	2176	195.25	16.79		9	4		194.76	V-2	B-1		C.5	D.5	E.5		
PT-02-2	2107	101.00	8.55		2	4		99.11			V-3	C.6	D.6	E.6		
PT-01-5	1119	51.00	11.65		3	4		55.96				C.7	D.7	E.7		
PT-A-10	Lower Tube Sheet Edge				4	6		4.18				C.8	D.8	E.8		
P-614	Vessel Wall	288.00	LLTV Wall		12	4	LLTV			B-2		C.9	D.9	E.9		
P-615		244.00			10	3						C.10	D.10	E.10		
P-616		172.00			8	1						C.11	D.11	E.11		
P-617		120.00			2	2						C.12	D.12	E.12		
P-618		72.00			3	2						C.13	D.13	E.13		
P-619		3 0.00			4	2						C.14	D.14	E.14		
P-507	Sodium Sys. Piping		Piping Wall	III-3&IV-7	15	4	Upper Sodium Piping			B-3		C.15	D.15	E.15		
P-508					14	6				B-4		C.16	D.16	E.16		
P-509					16	7						C.17	D.17	E.17		
P-510					20	7						C.18	D.18	E.18		
P-516					18	7						C.19	D.19	E.19		
P-517					23	2						C.20	D.20	E.20		
P-519					28	3	Lower			B-5		C.21	D.21	E.21		
P-520					29	9						C.22	D.22	E.22		
P-521					30	11						C.23	D.23	E.23		
P-524					21	2	Upper					C.24	D.24	E.24		
P-525					31	6	Lower			B-6		C.25	D.25	E.25	V-11a	V-11b
Rupture Disc										B.7		C.26	D.26	E.26		
Rupture Disc Cavity												C.27	D.27	E.27		

* Table III Reference 7 for all figures.
** Reference 4 for all figures.

Note B, C, D and E refer to Appendices of this report

TABLE V-2

Figure Numbers Where Predicted Values for Parameters Other than Pressure are Given

Parameter	Figure No.*			
Model →	B	C	D	E
Rupture Disc Velocity	B.8	C.27	D.27	E.27
Pipe Velocity at Accelerometer F-506	-	C.28	D.28	E.28
Pipe Velocity at Accelerometer F-510	-	C.29	D.29	E.29
Pipe Velocity at Accelerometer F-511	-	C.30	D.30	E.30
Rupture Disc Displacement	B.9	C.31	D.31	E.31
Water Injection Rate	B.10	C.32	D.32	E.32
Bubble Temperature	B.11	C.33	D.33	E.33
Bubble Inventory of				
A) Solid Reaction Products by Weight	B.12	C.34	D.34	E.34
B) Hydrogen (by Weight)	B.13	C.35	D.35	E.35
C) Bubble Volume	B.14	C.36	D.36	E.36
Concentration of Reaction Products	B.15	C.37	D.37	E.37

* Figure Nos. refer to Appendices of this report.

The following is an explanation of the lack of correlation between the standard methodology analytical model pre test analysis and the A-6 test results.

1. Gas Void - During the post-test evaluation, it was found that a level change had occurred in the surge tank during the pre-test period after the rupture tube was being filled with water but prior to the start of the A-6 test. This change in surge tank sodium level indicates that approximately 8 cubic feet of gas was present in the upper region of the LLTV at the start of the A-6 test. The source of the leak was probably a very small defect in one of the welds of the rupture tube assembly. These welds were destroyed during the removal of the rupture tube for post-test inspection and, therefore, physical confirmation of the small leak scenario was not possible.

   A TRANSWRAP model (C) of the LLTR was prepared which included an 8 cu. ft. gas (nitrogen)* void at the top of the LLTV. The predicted (near leak site) pressure history curve using this model is strikingly similar in form to the measured pressure history (Figure V-2), analytically confirming that a gas void did exist at the top of the LLTV at the start of the A-6 test.

   It can be seen by comparing Figures V-1 and V-2 that the gas void does not affect the initial pressurization rate or the amplitude of the initial acoustical wave peak but does dampen out the subsequent higher amplitude acoustical wave peaks which would have occurred in a hard (i.e., gas free) system as the result of reinforcement waves reflecting from the

---

* Nitrogen was used because the Dieterici Gas law constants were readily available for that gas but not for hydrogen which was probably the gas present in the LLTV. The use of nitrogen versus hydrogen is expected to have a small effect on the results.

upper tube sheet.

2. Sodium Water Reaction (SWR) Rate

The TRANSWRAP model, incorporating the gas void and using the standard methodology SWR rate (Model C), predicted a peak acoustical pressure at a location near the leak site of 361 psia, but the test data indicated that this pressure did not exceed 307 psia. (See Figure V-2). Since the analytical model, using the standard methodology SWR rate, closely predicted the measured leak site maximum acoustical pressure for test A-2 (Figure V-3), the rate of reaction of the sodium with the incoming water must have been less for the A-6 test than for the A-2 test.

a. Effects of Early Transition from Spherical to Pancake Bubble

The A-2 post-test analysis report (Reference 4) using Model B, showed the standard methodology rate overpredicted the initial acoustical pulse but that the overall leak site source pressure history conformed reasonably closely with the test results (See Figure V-3). After issuance of Reference 4, the analytical model was changed so that the transition from the spherical bubble calculation method (which does not consider interactions with the sodium system) to the pancake bubble calculational method (which does interreact with the sodium system) takes place after the first calculational step.* This change was made to ensure that the calculational instabilities which occur at the transition occur at the start of the transient rather than at a time when peak acoustical wave pressures are expected. Also, the pancake bubble model appears to produce more accurate predictions. In the current version of Transwrap the spherical bubble model must be used in the first time step to initialize the values of a number of parameters. All of the models mentioned in this report except Model B used the early transition from spherical to pancake bubble. (See Figure V-2 for an example of the subject transition instability.)

* After 0.01 msec.

This alteration in the analytical model caused a considerable change in the calculated leak site pressure history in the initial phase of the transient only (i.e., that part which was characterized by the use of the spherical bubble method of calculation). The initial leak site pressure history calculated (using the standard methodology SWR rate and a first step transition from spherical to pancake bubble calculational method) more closely predicts the measured initial peak acoustical pressure (Model A) although it still achieves that value with a considerably steeper ramp than is shown by the test data (400 psi/msec predicted compared with approximately 182 psi/msec measured) as shown in Figure V-3.

The built-in conservatism of the standard methodology SWR rate in predicting the initial peak amplitude of the acoustical wave was eliminated when the spherical/pancake bubble transition criteria was changed after the A-2 post test evaluation report was written. Since the analytical model used for the A-6 pre- and post-test predictions incorporated this change, the reasons for the overprediction of the initial acoustical wave peak for the A-6 test must be found elsewhere.

b. Reduced SWR Rate for Test A-6

Measurement of the initial pressurization rate at the pressure transducers nearest the leak site for tests A-2 (pressure transducer P-01-1) and A-6 (pressure transducer PT-01-7B) shows that the rate for the A-2 test was approximately 35% higher as shown in Table V-3 below. (A-2 test analysis repeated using Model A for direct comparison with A-6.)

TABLE V-3

TEST NO.	INITIAL PREVALENT PRESSURIZATION RATE		FIGURE NO.
	MEASURED	PREDICTED	
A-2	182 psi/msec	400 psi/msec (Model A)	V-4a
A-6	118 psi/msec	400 psi/msec (Model A)	V-4b
A-6	118 psi/msec	261 psi/msec (Model D)	V-5b

In addition, the initial peak pressure of the acoustical wave was predicted reasonably accurately for test A-2 (307 psia predicted vs. 313 psia measured) but was over-predicted for test A-6 (361 psia predicted vs. 307 psia measured).

A TRANSWRAP model (D) of the A-6 test configuration with a SWR rate reduced by 35% from the Standard Methodology rate was run. The pressurization rate at a location near the leak site was reduced by 35% (261 psi/msec as compared with 400 psi/msec) and the amplitude of the initial peak acoustical pulse was reduced to 307 psia (the value measured at that location [in the A-6 test] from 361 psia, as shown in Figures V-5a for Model C and V-5b for Model D). Therefore, both the analytical and test data* indicate that the average initial sodium water reaction rate was reduced by approximately 35% in the A-6 test compared with the A-2 test. An explanation for the reduced sodium water reaction rate in test A-6 must, therefore, be found to explain the difference.

c. Causes for the Reduced SWR Rate in Test A-6

Of the major differences between the A-2 and A-6 tests, the most likely candidate to explain the reduced SWR rate in Test A-6 was its use of a peripheral rupture tube. The change in axial location and the presence of a gas void at the top of the LLTV for test A-6 should not have greatly affected the SWR rate. The water jets from the two sides of the break will probably impinge upon each other causing a lateral movement of the water as shown in Figure V-6b.

---

* The graphical measurement of the pressurization rates is subject to interpretation but the bases used for the measurements of similarly derived data was consistent.

The proximity of the rupture tube to the shroud reduces the volume of the reaction zone within a given radius of the leak site and could, therefore, reduce the rate at which the incoming water reacts with the sodium in the LLTV. As shown in Figure VI-6a, the proximity of the shroud reduces the LLTV volume within a given distance of the LLTV by up to 50%. For the time period of interest (<2 msec), the blockage is in the range of 30 to 40%, which is about the amount by which the SWR rate was apparently reduced in the A-6 test.

d. Variable SWR Rate

A comparison of the A-2 and A-6 test results and model predictions, Figures V-3 and V-2 respectively, indicates that the standard methodology with modifications as described in Section IV significantly overpredicts the acoustic pressures during the earliest time periods, i.e., <2 msec. for test A-2 and <3 msec. for test A-6. These overpredictions could be a result of either: (1) the standard methodology using a constant SWR rate throughout the transient, or (2) the standard methodology does not accurately predict the water flow rate during this period. The latter concern is complicated by the tube opening dynamics. While it is not possible to separate these combined effects, the standard methodology use of a constant SWR rate and the water flow rate as calculated by the RELAP code conservatively predicts the test data and the dynamic loads on the IHTS piping.

3. Acoustical Pressurization Rate - As indicated in Table V-3 the predicted LLTV initial pressurization rates, using the TRANSWRAP model, have been consistently greater by factors of 2 or more, than those measured in the LLTR/Series II Tests. A number of possible reasons for this conservatism have been explored. They include:

- The current TRANSWRAP model assumes that the sodium-water reaction rate is constant.
- The current TRANSWRAP model considers only the sodium inside the shroud* (except when calculating the equivalent sonic velocity).
- The current TRANSWRAP model does not consider the LLTV internals (e.g., tubes, spacers, supports, etc.) except when calculating the flow cross section.
- The current TRANSWRAP model assumes that the system is completely rigid.
- The current TRANSWRAP model is one dimensional.
- Analytical model start-up instabilities.

a. Constant SWR Rate

See Section V.2.d.

b. Sodium in the LLTV Outside the Shroud

A TRANSWRAP model (E) was run which included the sodium between the shroud and the pressure vessel wall in the LLTV flow cross section. The predicted initial pressurization rate was approximately 268 psi/msec near the leak site using this model compared with approximately 400 psi/msec for the standard methodology model (A)** (see Figure V-8 and V-2 respectively). An additional consequence of this change

* This was done to obtain the correct flow cross sections.

**Also Model C.

in the model was that the amplitude of the initial acoustical wave peak dropped from 361 psia to 305 psia.

The model had previously taken into account the flexibility of non-flowing sodium in the LLTV since the sonic velocity values input to the program were calculated based upon the non-flowing, as well as, the flowing sodium in the LLTV. However, the non-flowing sodium is not included when the conservation of energy equation is solved to established the relationship between potential energy (pressure) and kinetic energy (sodium velocity). The non-flowing sodium in the LLTV will absorb part of the energy created by the sodium-water reaction and will, therefore, tend to dampen the rate of pressurization as well as the maximum amplitude achieved. It will not however, change these values as much as predicted by model E, because the flow velocities were calculated incorrectly in this model. This indicates that making a change in one input parameter used in the analysis will necessitate changes in other parameters.

Including the inventory of sodium trapped between the shroud and the vessel wall in the analytical model cross section can account for more than half of the difference in pressurization rates between predicted and those measured in the LLTR Series II Test Program. Since the shroud is nearly transparent to pressure pulses, making this change would improve the validity of the analytical model. Some adjustment in the TRANSWRAP programming will allow it to calculate the correct sodium flow velocities in the LLTV and still account for the non-flowing sodium in the LLTV sodium inventory. However, in the interim, the resulting dynamic loads on IHTS piping are conservatively predicted using the standard methodology which neglects the non-flowing sodium between the shroud and the vessel wall in the energy equation.

c. LLTV Internals

The fact that the analytical model ignores the LLTV internals (except in calculating axial flow cross section) should increase the predicted initial pressurization rate by some as yet undetermined factor. The inclusion of the internals in the vessel flexibility would, however, probably not have as great an effect on the pressurization rate as inclusion of the non-flowing sodium.

d. Vessel Rigidity

The fact that the analytical model treats the LLTV as a rigid body, when in fact some movement is possible, would tend to increase the predicted pressurization rate over the actual rate by some as yet undetermined factor. The effect of this assumption should, however, be small compared with other causes. The transverse flexibility of the vessel is implicitly included in the equivalent sonic velocities used as input for the various sections of the LLTV, and this should account for the major effect of this parameter.

e. One Dimensional Model

Pressurization rates and peak acoustical pressures measured at two radial locations near the leaksite elevation (one near and one far from the leak site) are nearly identical. The 2-dimensional effect should, therefore, be negligible.

f. Analytical Startup Instability

The TRANSWRAP computer code (like most mathematical models using numerical solution techniques) experiences calculational instabilities at the start of the A-6 DEG transient as shown in Figure V-2. The instability occurs because TRANSWRAP initially overpredicts the reaction zone bubble size. TRANSWRAP quickly corrects the overshoot, however, when it factors the sodium side of the system into the calculation. The width of the acoustical pressure wave generated by the instability is narrow, < 0.2 msec and, therefore, it should have little effect on the subsequent pressure predictions for the system.

B. RUPTURE DISC PERFORMANCE

In the A-6 test, the measured pressure just upstream of the rupture disc did not achieve the maximum measured acoustical pressure at the leak site (307 psia maximum measured acoustical pressure at the leak site compared with 302 psia maximum acoustical pressure measured upstream of the rupture disc.) as shown in Figure V-9. Since the peak leak site acoustical pressure was less than the rated disc burst pressure, the rupture discs did not fail in the A-6 test during the acoustical wave pressurization phase.

In the analytical studies, however, the maximum acoustical pressure just upstream of the rupture discs exceeded the peak leak site acoustical pressure by an amount sufficient to fail the rupture discs (by 49 psi or 355 psi maximum pressure upstream of the R.D. versus 307 psia maximum near the leak site using model D) in 4.3 msec. This is shown in Figure V-9b.

The measured pressure at the pressure transducer just upstream of the rupture disc was 282 psia when the peak of the acoustical pressure wave arrived at that location. It then rose to 302 psia due to reinforcement from the wave reflection at the rupture disc face for a rise of 20 psi. The predicted pressure when the peak of the acoustical wave arrived just upstream of the R.D. was 306 psi which then rose to a peak of 355 psia with the arrival of the reinforcement wave for a rise of 49 psi, see Figure V-9.

The analytical model appears to predict a stronger reinforcement wave from the rupture disc face than was indicated by the test pressure transducer measurements, and the predicted pressure drop between the leak site and the rupture disc location appears to be too low.

The large differences between the predicted and measured maximum acoustical pressures just upstream of the rupture disc (in spite of the fact that the measured and predicted [for model D] leak site maximum acoustical pressures were identical) indicates that the upgraded rupture disc analytical model fails to simulate real rupture disc performance at sub-disc burst pressure conditions correctly.

It is also possible that the analytical model fails to predict the rupture disc environment correctly, due to inaccuracies elsewhere in the system (e.g., source pressurization rates, flow resistances), and for that reason failed to correctly predict rupture disc performance in the A-6 test.

Pressure Drop

A possible partial explanation for the difference between actual and analytical predicted conditions upstream of the rupture disc are the actual and predicted pressure drops from the source to the rupture disc.

The measured pressure difference in the peak acoustical pressure between the pressure transducer near the leaksite PT-07-B and the one upstream of the rupture disc was 25 psi. The predicted value was about 1 psi. Only part of this difference can, however, be accounted for by the difference between input and actual flow path resistance, the remainder being due to the strength of the pressure wave reflected from the disc face as explained later. This indicates that the flow coefficients used in the analytical model may be somewhat in error due to geometry and flow path simplifications. These differences can contribute to the rupture disc simulation problems by over-predicting the pressure history upstream of the rupture disc.

Source Loading Rates

A possible partial explanation for the difference between actual and analytically predicted conditions upstream of the rupture disc is the difference between the actual and predicted acoustical pressurization rates described in Section V-A.

In order to check out the effect of acoustical wave pressurization rates on rupture disc pressurization and performance, TRANSWRAP analytical models F and G were created. In Model F, the actual measured leak site pressure history was used as the source term and analytical predictions of the sodium side parameters only were made. In Model G, the non-flowing sodium between the shroud and the vessel wall was included in the LLTV flow cross section, in addition to the change denoted for Model F.

The results from the analytical runs for Models F and G are compared with those for Model D in Table V-4 below.

TABLE V-4

MODEL	MAXIMUM SOURCE PRESSURE PSIA	MAXIMUM PRESSURE UPSTREAM OF RUPTURE DISC	FIGURE NO.
D	307	355	V-9
F	307	342	V-10a
G	307	342	V-10b

Changing the source pressurization rate to that measured in the test did reduce the peak acoustical pressure predicted just upstream of the rupture disc by 13 psi (see Figure V-10) but the reduction was insufficient to prevent prediction of disc rupture during the acoustical phase of the transient. Inclusion of the stagnant LLTV sodium (model G) did not affect the predicted maximum acoustical pressure upstream of the rupture disc.

It can be concluded from the above that the overpredictions of the system pressurization rate by the analytical model does have an adverse effect on the accuracy of the prediction of conditions just upstream of the rupture disc but that other real/model discrepancies also contribute significantly to the problem.

Fluid Structure Interaction

Another possible partial explanation for the discrepancy between analytical and measured rupture disc performance may be that fluid/structure interaction, which is not accounted for in the analytical model, absorbs sufficient energy from the acoustical pulse to significantly reduce the amplitude of the reinforced acoustical pressure wave upstream of the rupture disc.

Sub-Burst Pressure Performance

From the test data it appears that the rupture disc locally buckles nonaxisymmetrically at sub-burst pressures thus reducing the pressure buildup on the disc face. The disc distortion, while sufficient to relieve the upstream pressure, was not great enough to propagate disc movement toward the knife edges and consequently disc rupture. The standard methodology - axisymmetric analytical model, on the other hand, retains its structural integrity at these pressures thus allowing buildup of the upstream pressure to the point where complete buckling of the disc occurs.

This phenomenon is the most likely major contributor to the rupture disc analytical simulation problems for the A-6 test. It would be very difficult to modify the rupture disc analytical model to be able to consider local disc buckling since a quantum increase in model complexity would be required. The alternative is for the piping designer to realize the limitations in the rupture disc treatment of the standard methodology and to design the piping system to accommodate both acoustical and quasi-static overpressurization type failure modes of the rupture discs. The acoustical failure mode is expected to produce the largest dynamic loads on the IHTS piping, but the overpressurization failure mode should also be considered for the SWR pressure relief system piping loads.

C. EVALUATION OF LLTI TEMPERATURES

The LLTI temperature data recorded during Test A-6 indicate both similarity and differences in thermal behavior with Test A-2 (previous DEG test conducted in the central region 101 inches below the Test A-6 peripheral leak site). The two tests were similar in that elevated temperatures of about 2200°F were recorded in the region of the leak sites and that the reaction zones were confined to narrow elongated shapes ($\leq$10 inches radius from the leak site). A-6 differed from A-2 in that a second, delayed high temperature period occurred in A-6 long after rupture disc operation ($\sim$14 seconds) whereas in A-2 LLTI high temperatures gradually diminished after rupture disc operation. This would indicate that a peripheral region does not drain as rapidly or completely as the central region, and thus is susceptible to delayed sodium-water reaction. The principal Test A-6 LLTI thermal behavior is described below.

The measured LLTI peak temperatures, the time of their occurrence along with the time of the initial temperature change are tabulated in Table V-5. Plots of axial temperature profiles vs. time data are shown on Figures V-11, V-12 and V-13 for the three temperature instrument tubes (numbers 4182, 4166 and 4116) closest to the rupture tube. The location of these tubes in the Test A-6 peripheral region is shown in Figure III-4.

During Test A-6 the reactions apparently occurred principally at or below the leak site as demonstrated in Figures V-14 and V-15 for thermocouples located in T/C tubes No. 4182 (26 inches below the leak site) and 4166 (10 inches above the leak site). [It should be noted that higher temperatures immediately above the leak site (<10 inches) could have been present but were not measured due to lack of instrumentation.] The temperatures above the leak site (Figure V-14) increased to a first maximum of about 1480°F in about 7 seconds (which corresponded approximately to the rupture disc activation time of $\sim$6.5 seconds). The temperatures below the leak site (Figure V-15) increased more rapidly to a higher maximum value about 2200°F in less time ($\sim$4.6 seconds). The higher temperatures were also more sustained in the lower region. Following rupture disc activation, both regions cooled to about 400°F (the lower region showing a rapid temperature drop to 900°F in less than a second followed by slower reduction to 400°F in about 8 seconds). At the lower

TABLE V-5 LLTI PEAK TEMPERATURE MEASUREMENTS
(Sheet 1 of 2)

Thermocouple Tube No.	T/C No.	Vertical* distance from the bottom of shroud, inches.	Center to center radial distance from the injection tube, inches.	First Peak Temp. °F	Time to reach first peak temp., sec.	Time for the first change of temp, sec.
4166	TC-11-10	41	2.11	815	10.4	7.2
	TC-11-30	89		1060	12.8	6.9
	TC-11-40	93		1080	8.4	6.9
	TC-11-50	97		1090	12.8	6.9
	TC-11-70	113		1210	11.7	6.7
	TC-11-80	120		1170	8.0	0.5
	TC-11-90	233		1480	7.0	0.0
4116	TC-01-20	81	6.11	895	8.8	8
	TC-01-40	101		945	9.2	7.8
	TC-01-50	113		1080	9.8	6.8
	TC-01-60	149		1140	8.9	6.8
4182	TC-12-10	65	2.11	880	12.2	6.8
	TC-12-20	89		1000	8.4	6.9
	TC-12-30	105		1005	8.0	7.0
	TC-12-40	109		1050	8.0	6.7
	TC-12-50	113		1050	8.0	6.3
	TC-12-60	121		1130	7.9	0.2
	TC-12-70	149		1560	7.2	1.0
	TC-12-80	197		2200	4.8	0.0
	TC-12-90	267		1330	7.8	0.3
4095	TC-23-20	23	7.93	-	-	-
	TC-23-30	25		597	10.0	8.0
	TC-23-40	101		800	12.0	7.4
	TC-23-50	103		810	12.0	7.5
	TC-23-60	105		-	-	-

* A-6 Leak Site @ 222.9 inches above bottom of shroud

TABLE V-5 LLTI PEAK TEMPERATURE MEASUREMENTS
(Sheet 2 of 2)

Thermocouple Tube No.	T/C No.	Vertical distance from the bottom of shroud, inches.	Center to center radial distance from the injection tube, inches.	First Peak Temp. °F	Time to reach first peak temp, sec.	Time for the first change of temp, sec.
4075	TC-03-10	41	9.76	910	13.7	8.5
↓	TC-03-20	81	↓	-	-	-
	TC-03-30	89		-	-	-
	TC-03-40	111		770	14.0	7.2
	TC-03-60	149		-	-	-
4010	TC-13-2	113	13.73	-	-	-
↓	TC-13-3	207	↓	700	11.6	6.6
	TC-13-4	255		-	-	-
	TC-13-5	283		-	-	-
	TC-13-6	291		-	-	-
	TC-13-7	307		-	-	-
	TC-13-8	311		-	-	-
	TC-13-9	315		-	-	-
3002	TC-12-1	65	16.9	735	13.7	8.0
↓	TC-12-2	89	↓			
	TC-12-3	105				
	TC-12-4	109				
	TC-12-5	113		725	13.2	7.5
	TC-12-6	121				
	TC-12-8	197				
	TC-12-9	267		607	7.5	6.9

* A-6 Leak site @ 222.9 inches above bottom of shroud

temperatures both regions were blanketed momentarily with water/steam. This condition was short lived as the temperatures rapidly rose again to about 1600°F as additional residual sodium reacted with water introduced at the leak site. As noted earlier, this delayed reaction is believed to be caused by incomplete draining of the peripheral region.

During the SWR prior to rupture disc activation at about 6.5 seconds, thermocouples in adjacent tubes 4182 and 4166 greater than 100 inches below the leak site remained at the initial ambient temperature of 580°F as shown in Figures V-16 and V-17. Following rupture disc activation the temperatures in the lower region increased as the sodium/reaction products moved rapidly downward toward the LLTV outlet nozzle. Higher maximum temperatures were noted in Tube 4166 indicating more hot sodium/reaction products were drained toward that tube than toward Tube 4182. This would be expected since Tube 4166 is located closer to the outlet nozzle than Tube 4182, and drainage would be expected to proceed preferentially toward Tube 4166.

T/C Tube 4116, located 6.1 inches away, showed similar behavior as the closer T/C tubes 4166 and 4182 in the lower regions below the leak site. Figure V-18 shows the temperature-time history for the Tube 4116 thermocouple located 74 inches below the leak site. As noted, the temperatures remained at the inital temperature of 580°F until rupture disc activation at which time they rapidly rose to peak values.

The LLTI temperature data indicate that the high temperature reaction zones did not extend radially beyond 6" from the leak site. Maximum temperatures about 1100°F were measured in Tube 4116; lesser maximum temperatures of about 800-900°F were measured in Tubes 4095 and 4075 located radially about 8 inches and 10 inches from the rupture tube. T/C tubes (Numbers 1026, 1077, 3002, 2183, 1100 etc.) located further away showed even lower maximum temperatures of about 700°F.

D. SYSTEM STRUCTURAL MEASUREMENTS

1. Loads on Upper Sodium Line from Accelerometer Measurements

Accelerometers were installed on the 10 inch and 18 inch diameter sodium piping connected to the LLTV upper nozzle to measure the dynamic response of this sodium filled pipe to dynamic acoustic pressure loading during an SWR event. The location of these accelerometers is shown in Figure V-19. Some of these accelerometers (A502, 503, 504, 506 and 508) exhibit clearly identifiable frequencies and amplitudes of response during the SWR event. Evaluation of these data was done in groups as follows:

a) Axial accelerometers A502 and A504 (Figures V-20 and V-21)
These accelerometers showed an approximate 400 Hz response which is the estimated frequency of the piping in the axial direction. A502 amplitude was approximately one-third of A504 due to its location at the large nozzle region. Because of use of a filter with a cut-off frequency at 100 Hz and a roll-off of 3dB per octave, the plotted amplitude is approximately 25% of the true amplitude. So the true maximum amplitude of A502 is appoximately $\pm$22g and $\pm$80 g for A504.

b) Vertical accelerometers A503 and A506 (Figures V-22 and V-23)
These accelerometers exhibit high amplitude response at approximately 500 to 600 Hz range. This is surprising because the prediction for this upper relief line and the prediction on similar CRBRP lines always indicate fundamental frequency in the range of 20 to 200 Hz range (with higher frequency for the upper relief line in the LLTR due to its configuration and supports). It is believed that the 500 to 600 Hz response is a "breathing" mode (i.e., uniform radial expansion and contraction) of the pipe, which was estimated to be in the 500 to 1000 Hz range.
A rather weak overall variation of the base line of the response plot at 40 Hz may indicate the vertical direction beam type response. Again, due to the use of the low pass filter, the true maximum amplitude of response is 5 times the plotted amplitude; $\pm$ 10g for A503, and $\pm$ 100g for A506.

c) Horizontal accelerometer A508 (Figure V-24).

This major response here is also at 600 Hz. "Breathing" mode response is again suspected. A more distinct response of 20 Hz is recognizable here, showing the beam-type horizontal response of the pipe. The maximum amplitude is ±20g after correction for the filter effect.

d) Support accelerometers.

Two accelerometers, A511 and A512 (Figures V-25 & V-26), were mounted on a snubber and a hanger, respectively. They show response frequencies of 400 Hz and 240 Hz, respectively. The response on the snubber shows rapid reduction of amplitude after a few cycles, reflecting the high damping of the snubber. The response of the pipe hanger shows slow amplitude reduction, reflecting the more elastic nature of the hanger. The amplitudes of these responses may be used to estimate the support forces during the SWR.

Summary

The response frequencies are generally within expected range. The "breathing" mode of the pipe seems to show up stronger than expected. The implication of this mode to the piping design should be studied. While LMFBR IHTS piping design does consider internal pressure due to SWR, the "breathing" mode response and the associated effects (such as fatigue) have not been considered in detail.

2. Structural Measurements for Lower Relief Line.

The high velocity flow of sodium and reaction products through the relief system and accompanying system pressure gradients caused appreciable forces on the piping system in Test A-6. Instrumentation provided to evaluate forces on the first piping elbow downstream of the rupture disc (RD-1) are listed below.

- Two load cells, W511 and W512, for measuring the loads transmitted through snubbers.
- A linear displacement gauge (Z506) to measure pipe motion.
- A drag disc flow meter (F506) to measure sodium velocity in the relief system.
- Sodium pressure upstream of RD-1 Rupture Disc (P-525).

Data obtained from this lower relief line instrumentation for Test No. A-6 is compared with data from Test A-2 and A-3 in Table V-6.

TABLE V-6 LOWER RELIEF LINE LOAD MEASUREMENTS

INSTRUMENT	UNITS	TEST A-2 @ 150 m sec* after RD-1 rupture	TEST A-3 @ ~50 m sec* after RD-1 rupture	TEST A-6 ~35 m sec*
W511	lbs	2300	2250	1200
W512	lbs	1500	3750	5500
Z506	in	0.02	0.075	0.16
Displacement converted to force	lbs	1180	4425	9440
TOTAL THRUST		4980	10,425	16,140
P-525	PSI	40	215	80
F506	FT/SEC	20	60	90

* Times at which maximum total load occurred after rupture disc activation.

The higher sodium velocity experienced in Test A-6 compared with A-3 is probably due to the greater opening of the rupture membranes. In Test A-6 the rupture disc membranes opened ~75% for the upstream membrane and 90% for the downstream membrane. The rupture disc opening for Test A-3 was about 40% of the cross-sectional area.

Similar data will be obtained on the lower relief line in future tests and additional evaluation of all the data including comparison with TRANS-WRAP code analysis results will be performed and presented in the summary Series II report for Test Group A.

E. EVALUATION OF LLTR STACK EFFLUENT DATA

Table V-7 shows the results of ground level deposition measurements taken at twelve locations at varying distances from the LLTR stack (Reference 12). Exposure time for the trays was 90 minutes. A high level of deposition (5.6×10^{-3} mg/cm^2/day) was collected at location No. 2 130 meters down wind of the stack. All other stations from 49 m to 370 m from the stack had less than 8×10^{-5} mg/cm^a/day. These results are very similar to those obtained for test A-3 as shown in Table V-8 which compares stack effluent data from Series I and Series II tests. Characterizations of the stack aerosol size and concentration was impractical since the quantity of material collected on the impactors was insufficient for quantative measurement.

TABLE V-7
SODIUM DEPOSITION FROM STACK

Tray Number	NaOH Deposition (mg/cm^2/day)	Distance from LLTR Stack (m)	Elevation
1	1.2×10^{-6}	49	1820
2	5600×10^{-6}	130	1810
3	3.1×10^{-6}	246	1785
4	9.3×10^{-6}	355	1780
5	$<1 \times 10^{-6}$	627	1775
6	76×10^{-6}	573	1765
7	1.6×10^{-6}	464	1765
8	20×10^{-6}	764	1760
9	22×10^{-6}	770	1760
10	1.9×10^{-6}	1215	1750
11	6.2×10^{-6}	1324	1725
12	7.8×10^{-6}	1370	1700

Blank subtracted from results

TABLE V-8

COMPARISON OF STACK EFFLUENT DATA
FROM SERIES I & II SWR TESTS

	SERIES III TEST A-6	SERIES II TEST A-3	SERIES II TEST A-2	SERIES I TEST 1*
WIND DIRECTION	FROM N	FROM NW	FROM NW	FROM NW
WIND SPEED	9 MPH	0 - 10 MPH	0 - 2 MPH	10 - 15 MPH
DURATION OF H_2O INJECTION, SEC	38	144	40	10
WATER ADDED, LBS	200	300	200	25
DOWN WIND DEPOSITION RATE				
Mg NAOH/cm^2-DAY				
RANGE	<1-5600 x 10^{-6}	3.5 to 4100x10^{-6}	1.6 to 340x10^{-6}	2.7 - 760x10^{-6}
AVERAGE	48 x 10^{-5}	36x10^{-5}	3.1 x 10^{-5}	7.2 x 10^{-5}
AVERAGE BACKGROUND	SUBTRACTED	6x10^{-5}	NOT REPORTED	7.1 x 10^{-5}
DOWN WIND AIRBORNE LEVEL				
MG/ m^3				
RANGE	NOT MEASURABLE	0.009 to 0.054	0.01 - 0.03	0.04 - 0.56
AVERAGE		0.026	0.02	0.24

*DATA TYPICAL OF SERIES I TESTS.

VI. INTERTEST EXAMINATION SUMMARY

A. General

Following Series II Test A-6, non-destructive examinations were performed in accordance with the Series II Test Request (Reference 1) to identify and evaluate any structural damage or other test consequences resulting from this test. These examinations included visual and borescopic examination of the LLTI interior; mass spectometer helium leak tests of the LLTI secondary tubes; radioisotope scanning tests of LLTI secondary tubes for tube bowing and reaction product deposition; ultrasonic examination of selected LLTI secondary tubes for tube wastage; dye penetrant examination and ultrasonic examination of selective relief line welds for stress corrosion cracking; dye penetrant examination of U-bend specimens removed from the Reaction Products Tank; radiographic examination of the LLTV drain line at the 8" tee and examination of the prototypical CRBR rupture disc assembly, RD-1. The findings from these examinations as reported in Reference 12 are summarized in the following sections.

B. Prototype Rupture Disc Examination

Both rupture disc membranes ruptured at approximately 325 psig pressure upstream as indicated by pressure P-525 trace shown in Figure III-7. The upstream disc opened about 75% and the downstream disc opened about 90% of cross-sectional area. New knife blades were installed for Test A-6 with a measured Rockwell hardness ranging from 40 to 48C. Measurements taken after the test indicated that the hardness had not changed. However, the blade edges were dulled and cracked in several places (Figure VI-1). Further confirming the earlier conclusion that blades in a plant application should be replaced after every operation, the new blades caused a cleaner cut of the disc membranes than Test A-3 where resharpened blades were used. The upstream and downstream discs after removal and cleaning, are shown in Figures VI-2 and VI-3, respectively.

The prototype rupture disc assembly was instrumented in the cavity between the discs and downstream of the second disc with electrical contact probes and Kaman-type pressure transducers immersed in sodium to minimize initial signal errors caused by abrupt temperature changes at the time of

arrival of sodium. These instruments (Z504, Z505 and PRD-1C traces shown in Figures III-8 thru III-10), are used to signal the time of disc rupture and are being evaluated for plant use in the automatic shutdown system. While both devices performed satisfactorily, the contact probe is considerably simpler and provides a sharper signal change when sodium passes through the disc.

C. LLTI Tube Leak Tests

After performance of Test A-6 and prior to removal of the LLTV upper head, an integrated helium leak test was performed on the LLTI secondary tubes by flooding the LLTV/LLTI shell side with helium at 1 to 2 psig and sniffing for helium in the LLTV steam head. No indication of leakage was obtained, eliminating the need for vacuum probe leak checking of individual tubes.

D. LLTI Tube Deformation Measurements

Tube deformation was measured by the Isotope Scanning Test (IST) as described in detail in Reference 12. Briefly, this test consists of simultaneously traversing two adjacent tubes with a Cobalt gamma source in one tube and a detector in the other tube. The gamma intensity varies inversely with the square of the distance between the source and the detector. A Cobalt-60 source was used to measure tube bowing and a Cobalt-57 source was used for SWR product deposition measurements.

Before IST measurements were made, the inside diameters of the tubes were scraped to remove loose scale and a go-no-go gauge was passed through the tube to determine if the tube bowing was sufficient to prevent freedom of travel of the IST and UT measurement devices. A total of 86 tube pairs were inspected by IST in the vicinity of the Test A-6 leak site. Tube bowing was identified between spacers 7 and 8, ranging from 0.25 inches to 1 inch in nine tubes including two tubes with sharp kinks. These tubes along with the tubes damaged in previous tests, A-3 and A-2 are shown in Figure VI-4. It is noted that the number of bowed tubes found in A-6 was about the same as experienced in the previous DEG test A-2 (e.g., 9 bowed tubes in A-6 versus 11 bowed tubes in A-2). Two of the tubes were kinked in A-6 whereas no tubes were kinked in A-2.

E. LLTI Tube Wastage Measurements

Eighteen (18) secondary tubes in the vicinity of the rupture tube were scanned by an internal bore UT technique described in Reference 12 to measure tube wastage. A maximum of 0.004 inches of wastage was measured in the plane of the leak site and within three tube rows. Wastage of about 0.004 inches was also observed at the reaction pool interface below the Lower LLTV sodium nozzle level (3.6 ft above the bottom of the LLTI shroud).

F. SWRP Deposition Measurements

IST measurements taken to detect SWRP deposition in the region between spacer 1 and 3 disclosed only minimal deposits which would not interfere with sodium flow in future testing.

G. Relief System Materials Evaluation:

1. Ultrasonic Examination of Relief Line Welds

Ultrasonic examination (UT) of certain welds (Figure VI-5) was performed to detect and monitor any stress corrosion cracking (SCC). The results of this investigation (reported in Reference 13) were compared with those for previous tests, and with baseline examination performed prior to the first of the Series II reactive tests (Test A2).

a) 2-1/4Cr-1Mo/stainless steel, Weld No. 8, upstream from the RD-1 rupture disc assembly.

1) No reportable indications were observed on the 2-1/4Cr-1Mo side of Weld No. 8. A reportable indication is one which registers at a magnitude of 40% or greater of the oscilloscope screen height; such indications represent sources which comprise at least 2% of the pipe wall thickness. This result agrees with the results of previous examinations (i.e., those following Test A-2, Test A-3 and the pre-Test A2 baseline examination).

2) No reportable indications were observed on the stainless steel side of Weld No. 8. This result is not in accord with the results obtained following Test A-3, for which two indications having amplitudes ranging from 40-50% of the screen height were reported. This anomaly is explained by the UT contractor in the following manner:

Prior to performing the UT evaluation, the system is calibrated such that a 2% reference notch results in an indication with an amplitude of 40% of the oscilloscope screen height. Scanning of the welds is subsequently performed at twice this sensitivity; however, the actual evaluation (i.e., determination of whether an indication is or is not reportable) is then performed using the original reference sensitivity. The contractor concluded that his evaluation of the Test A-3 results for this weld must have been performed at the scanning sensitivity, i.e., at a sensitivity twice that which should have been used. Had the proper sensitivity been employed for the evaluation, the low (40-55%) amplitude indications observed would not have been considered reportable.

Although this explanation appears reasonable, there are additional factors which complicate a ready resolution of this issue. Following Test A3, the dye penetrant inspection revealed numerous indications consisting of:

1) Three defects due to incomplete penetration, 3/16" L x 1/8" deep. The depth was measured by a scratch indicator. The location of these defects, circumferentially, is at 5 o'clock, and according to ETEC personnel, in the center of the weldment.

2) Cold laps due to a misalignment of the 2-1/4Cr-1Mo and SS pipe sections. These defects were located at several areas, primarily from 3-4 o'clock and from 7-9 o'clock. Some of the cold lap indications were as large as 1-1/2" in length (oriented circumferentially), and the total length of all overlap indications was 5-6".

These defects had been present since the fabrication of the system, yet three and possibly all four of the UT examinations (i.e., baseline and post-Test A2) revealed no indications. Although the cause of this discrepancy has not been conclusively determined, such factors as the geometry and the position of the defects could well result in their being "invisible" to UT. It should be noted that the UT procedure

being employed is optimized for SCC detection in the Heat Affected Zone (HAZ), not flaw detection in the weldment or weldment/base metal interface. This would require a transducer with a different frequency than the one currently employed; the task would still be difficult, at best.

An additional complicating factor is the inability of the UT contractor to precisely locate the source of the defects. Even with the knowledge that defects were present on the ID surface, the source of the UT indications could not be confidently correlated to these defects. The results of the UT evaluations for this weld underscore the uncertainties associated with the technique.

b) Carbon steel/stainless steel, Weld No. 46A, upstream from the RPT nozzle.

1) Carbon steel side - No additional indications were observed. There are slight variations in amplitude between the indications observed during this and the previous examinations; however, the locations of the indications exhibited a good correspondence. Currently, there are numerous (~7) indications ranging in source size from 2-5% of the wall thickness.

2) Stainless steel side - There are three new indications ranging in amplitude from 40% to 100% of the screen height (corresponding to sources comprising 2% to ~7% of the pipe wall thickness). Other observed indications (~8) correspond well (as regards amplitude and location) to previously observed indications. They range in source size from 2% to ~9% of the pipe wall thickness.

c) Carbon steel/carbon steel elbow, Weld No. 24, upstream from the RPT nozzle.

1) Carbon steel; elbow side - Indications are essentially unchanged from those previously observed. Currently there are several indications varying in amplitude from 15-45% of the screen height (representing sources comprising 1-2% of the wall thickness).

2) Carbon steel; straight pipe side - The two previously observed indications have increased very slightly in amplitude, from 25% to 35% and from 30% to 40%. Such an increase is probably not significant, especially at the low levels of amplitude (i.e., defect size) which were recorded.

d) Carbon steel/carbon steel, Weld No. 10, downstream from the RD-1 rupture disc assembly.

There were no reportable indications on either side of the weld. This weld had not been previously examined, but was included in the A-6 intertest examinations in an effort to provide an additional means to obtain a corelation between the UT and dye penetrant examination techniques (since the weld is accessible once RD-1 is removed).

In summary, the UT evaluations performed subsequent to Test A-6 revealed three new indications (stainless steel side of Weld No. 46A) having source sizes ranging from 2 to 7% of the wall thickness. Additionally, previously observed indications in Weld No. 24 (carbon steel - straight pipe side) increased slightly in amplitude. Finally, the previously reported anomalies associated with the UT and dye penetrant examination of Weld No. 8 were discussed with reasonable explanations proffered.

Indications (observed in the non-accessible welds) may be caused by weld defects, SWRP deposition or SCC. However, none of the observed indications (sources) has progressed to an extent which warrants destructive evaluation .

2. Examination of U-bend Specimens.

The evaluation for material susceptibility to caustic stress corrosion cracking consists primarily of introducing highly stressed U-bend coupons into the LLTR relief system environment, and following each test, inspecting these coupons using dye penetrant techniques in conjunction with a stereo microscope. Materials which were tested during Test A-6 (and also A-2 and A-3) included SA516, SA533 and stainless steel 304H. These specimens were in the unwelded, welded and post weld heat treated (PWHT), and welded and non-PWHT conditions (with the exception of the SA533 which was obtained from the CRBRP reaction products separator tank (RPST) fabricator in the unwelded, and welded and PWHT conditions only).

For Test A-6, specimens fabricated from prototypic transition joint spools were also included. These had been added to the separator tank and relief line racks for Test A-3. This addition was considered necessary because the transition joints are directly in the path of the SWRP during a large leak event in both the superheater and the evaporator. The materials comprising the transition joints include SS316H, SS304H, Incoloy 800, 2-1/4Cr-1Mo, and Inco 82 and 16-8-2 filler metals. The materials and material conditions included in the test represent the entire spectrum of anticipated metallurgical conditions for the CRBRP relief system, as well as relevant portions of the IHTS.

Two new types of specimen configurations were included in Test A6, namely, creviced U-bend coupons (double U-bend coupons) and stressed creviced tensile bars. These are shown in Figures VI-6 and VI-7, respectively. A number of studies have shown cracking to occur in creviced specimens, when, for the same bulk environment, uncreviced specimens did not exhibit cracking. The establishment of localized environmental conditions in the crevice was generally identified as the cause of the differential cracking behavior (References 14 and 15). The inclusion of these specimens into the system should provide a more severe test for the materials under consideration.

The results of the U-bend specimen examination indicated that stress corrosion cracking did not occur during Test A-6. A number of the U-bend specimens contained weld flaws, which had been photographically documented prior to the test; none of these flaws increased in size.

During the examination of the U-bend coupons for Test A-6, quite a number of the lock washers were found to be cracked. Four types of lock washers had been included in this test (in both the relief line port and the RPST); of the four types, two were extremely resistant and two were extremely prone to cracking. Similar lock washer cracking results were obtained following Tests A-2 and A-3.

These cracking events were felt to be highly significant, in that they could be an indication of the presence of stress corrosion cracking agents in the SWRP. However, the type of material used to fabricate the lock washers is also potentially susceptible to H_2 embrittlement.

Metallographic and failure analysis alone were inadequate to distinguish between the two failure mechanisms. Thus, a series of autoclave tests was initiated in an attempt to elucidate the cracking mechanism. Tests were run in both a 20% NaOH solution (@ 450°F) alone, and in a 20% NaOH solution with nascent hydrogen introduced to the lock washer surface via the reaction between Al foil (wrapped around the lock washer) and NaOH. This latter test was considered to be reasonably simulative of conditions at ETEC, with the exception that the autoclave solution is water based and the ETEC "solution" is sodium based.

Examination of the lock washers following the test runs has revealed no cracking. Lock washers identical to those used at ETEC for tests A-3 and A-6, which have been observed to fail at better than a 50% rate, were included in the autoclave tests.

Autoclave testing has been suspended (primarily) due to funding restrictions. A number of possible reasons for the lack of cracking in the autoclave tests have been identified. However, without further testing, these theories will remain conjecture.

H. Other Intertest Examinations

Visual inspection of the RD-1 rupture disc assembly and relief lines L-121 and 124 indicated that good sodium drainage was obtained. Radiographic examination of the drain line 8" tee indicated no flow restrictions in this area.

VII. REFERENCES

1. "LLTR Series II Test Request." GE Specification 23A2062, Revision 4, May 8, 1980.

2. J. O. Sane, et al., "Evaluation of Sodium Water Reaction Tests No. 1 through 6 Data and Comparison with TRANSWRAP Analyses Series I Large Leak Test Program," Vols. I and II, GEFR 00420, June, 1980.

3. B. F. Shoopak, et al., "Evaluation of the LLTR Series II, A-1a and A-1b Test Results," March, 1980, transmitted by GE letter XL-611-00026, March 31, 1980.

4. J. C. Whipple, et al., "Evaluation of LLTR Series II Test A-2 Results," July, 1980, transmitted by GE letter XL-796-00096, July 31, 1980.

5. J. C. Amos, et al., "Evaluation of LLTR Series II, Test A-3 Results" November 1980, transmitted by GE letter XL-796-00142, November 26, 1980.

6. W. J. Freede and H. H. Neely, "Progress Report on LLTR Series II Test A-6 (Part I)," ETEC-TDR-81-2, February 17, 1981.

7. D. E. Knittle, "Pre-test Evaluation of LLTR Series II Test A-6" November 1980, transmitted by G. E. Letter XL-611-00134. November 26, 1980.

8. "RELAP4/MOD5 A Computer Program for Transient Thermal-Hydraulic Analysis of Nuclear Reactors and Related Systems," ANCR-NERG-1335, September 1976.

9. D. E. Knittle, "TRANSWRAP II User's Manual," February 1981, transmitted by G. E. Letter XL-611-10011.

VII. REFERENCES (cont'd)

10. D. E. Knittle, "TRANSWRAP II Problem Definition Manual," February 1981, transmitted by G. E. Letter XL-611-10011.

11. Y. W. Shin, et al., "SWAMM-I" A Computer Code System for Analysis of Large Scale Sodium-Water Reactions in LMFBR Secondary Systems," ANL-80-4 February 1980.

12. W. J. Freede and H. H. Neely, "LLTR Series II Sodium Water Reaction Test SWR A-6 (Part II)," ETEC-TDR-81-4, March 16, 1981.

13. Ronald Nesbit Associates, Inc., "Ultrasonic Examination of Weld that Affected Zones," January 16, 1981.

14. H.R. Copson and S.W. Dean, "Effect of Contaminants on Resistance to Stress Corrosion Cracking of Ni-Cr Alloy 600 in Pressurized Water," Corrosion 21, 3-10 (1965).

15. H.R. Copson and G. Economy, "Effects of Some Environmental Conditions on Stress Corrosion Behavior of Ni-Cr-Fe Alloys in PRessurized Water," Corrosion 24, 55-65 (1968).

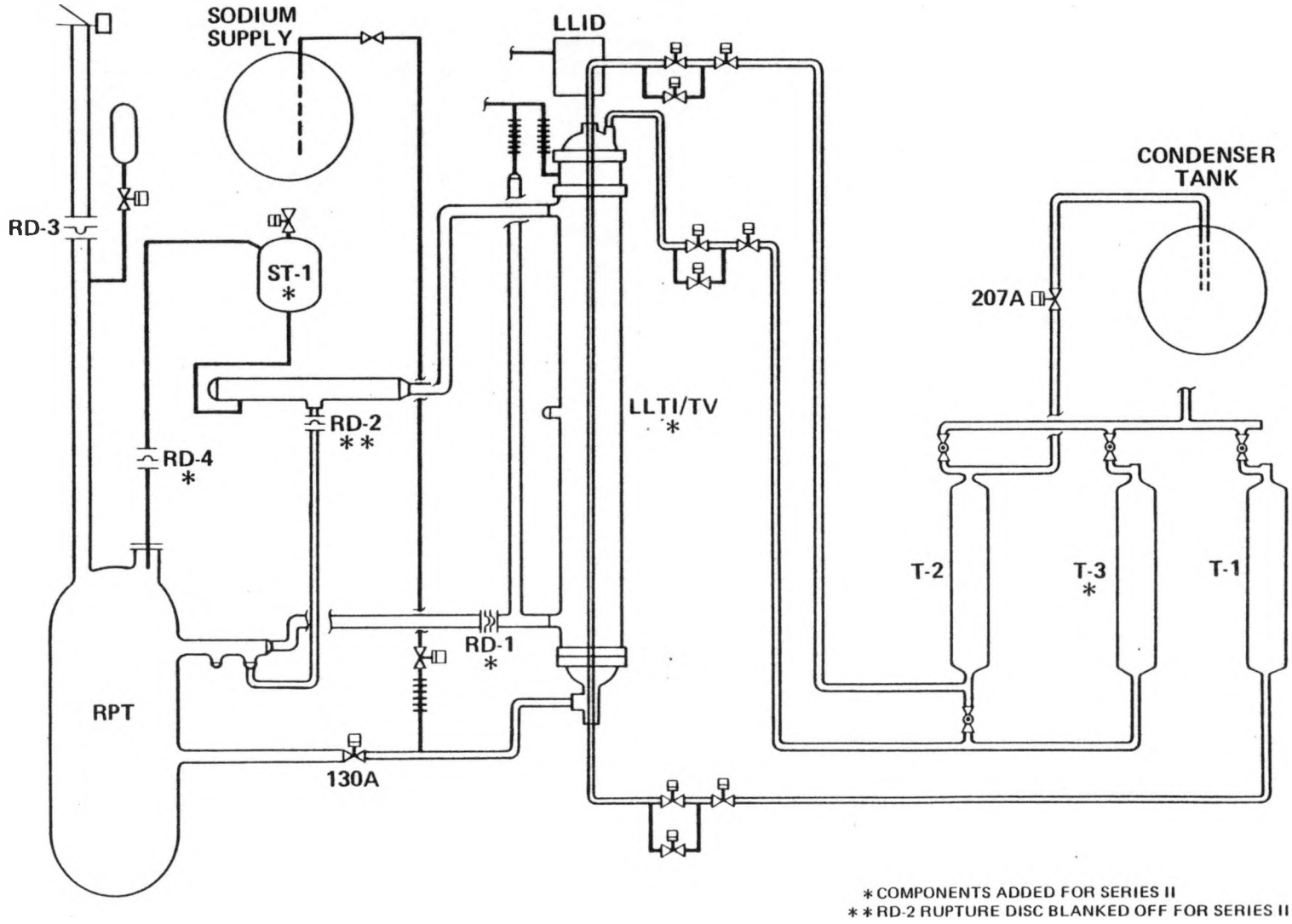

Figure III-1. LLTR SERIES II SCHEMATIC

81-204-14

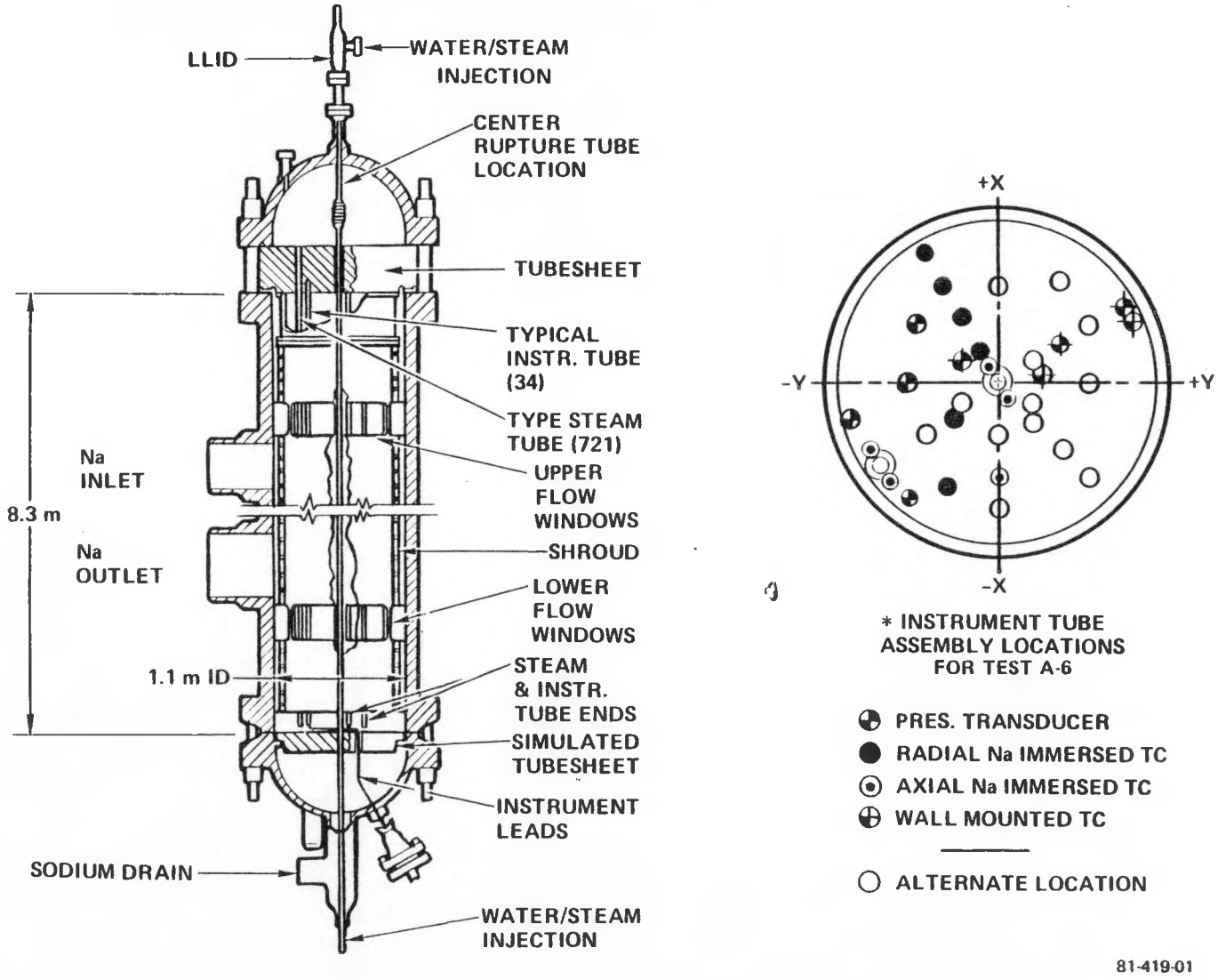

Figure III-2. LARGE LEAK TEST INTERNALS/LARGE LEAK TEST VESSEL

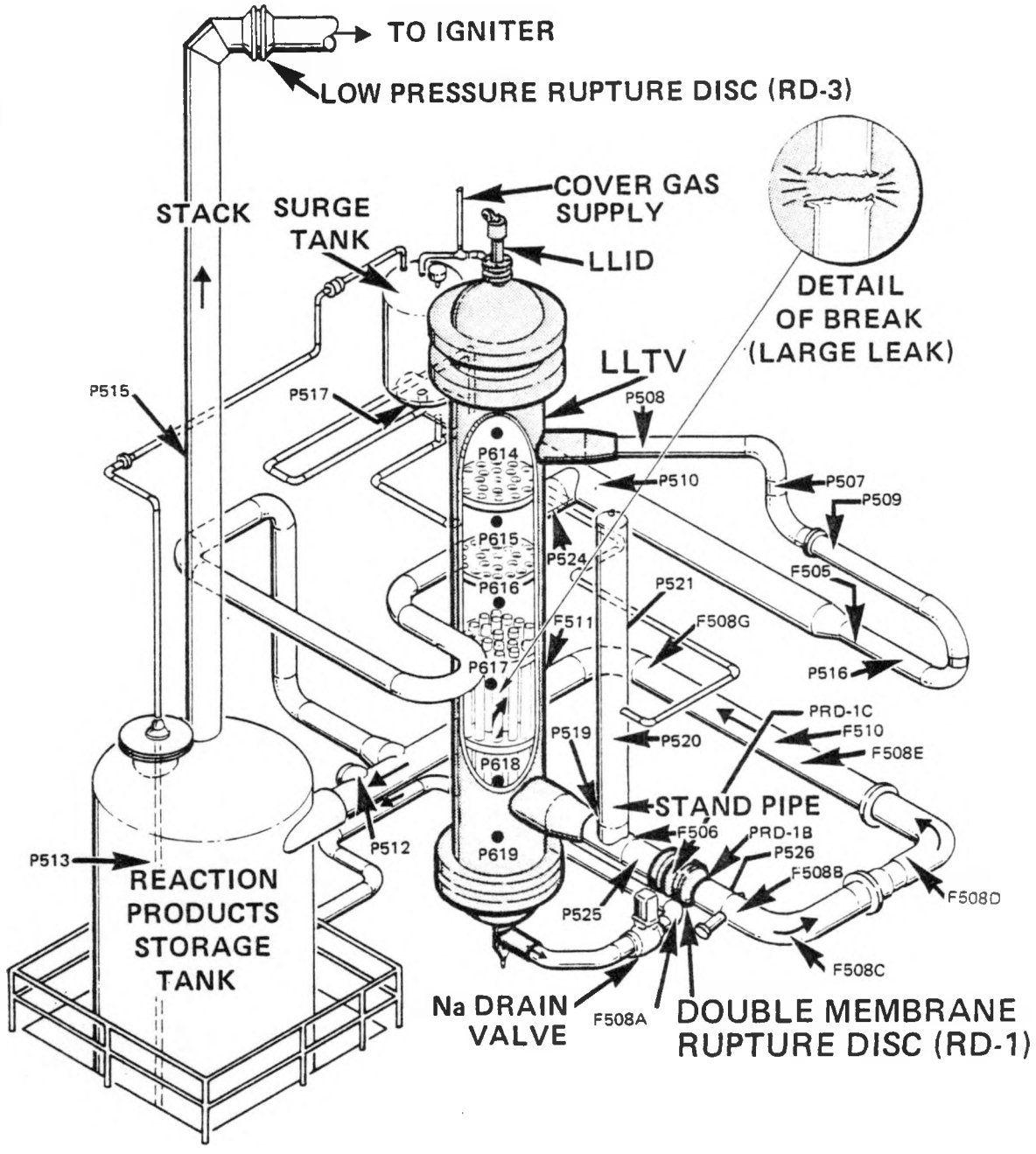

Figure III-3. LLTR SODIUM AND RELIEF SYSTEMS SHOWING SELECTED SENSOR LOCATIONS

81-435-01

PERIPHERAL TEST TUBE ARRAY

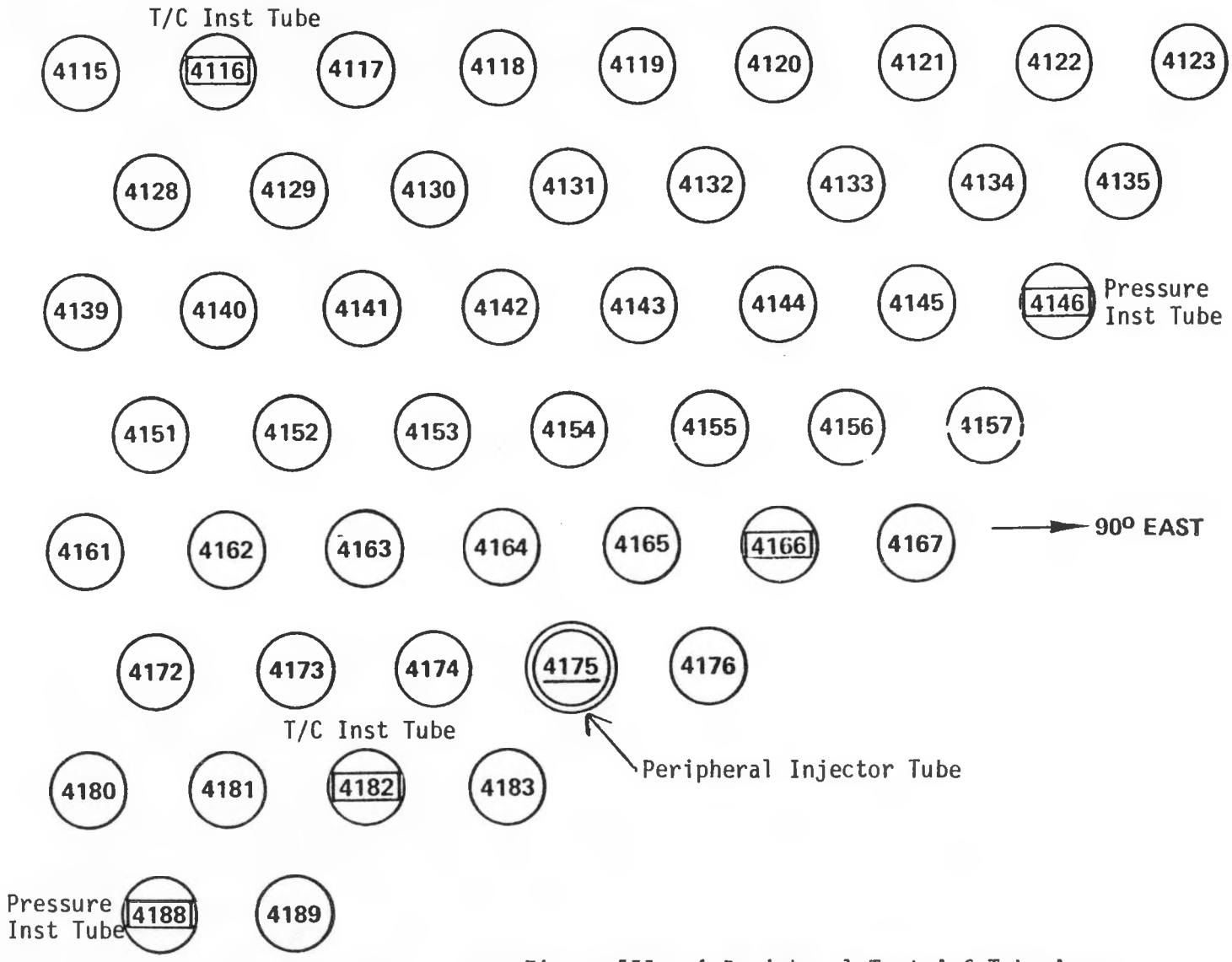

Figure III - 4 Peripheral Test A-6 Tube Array

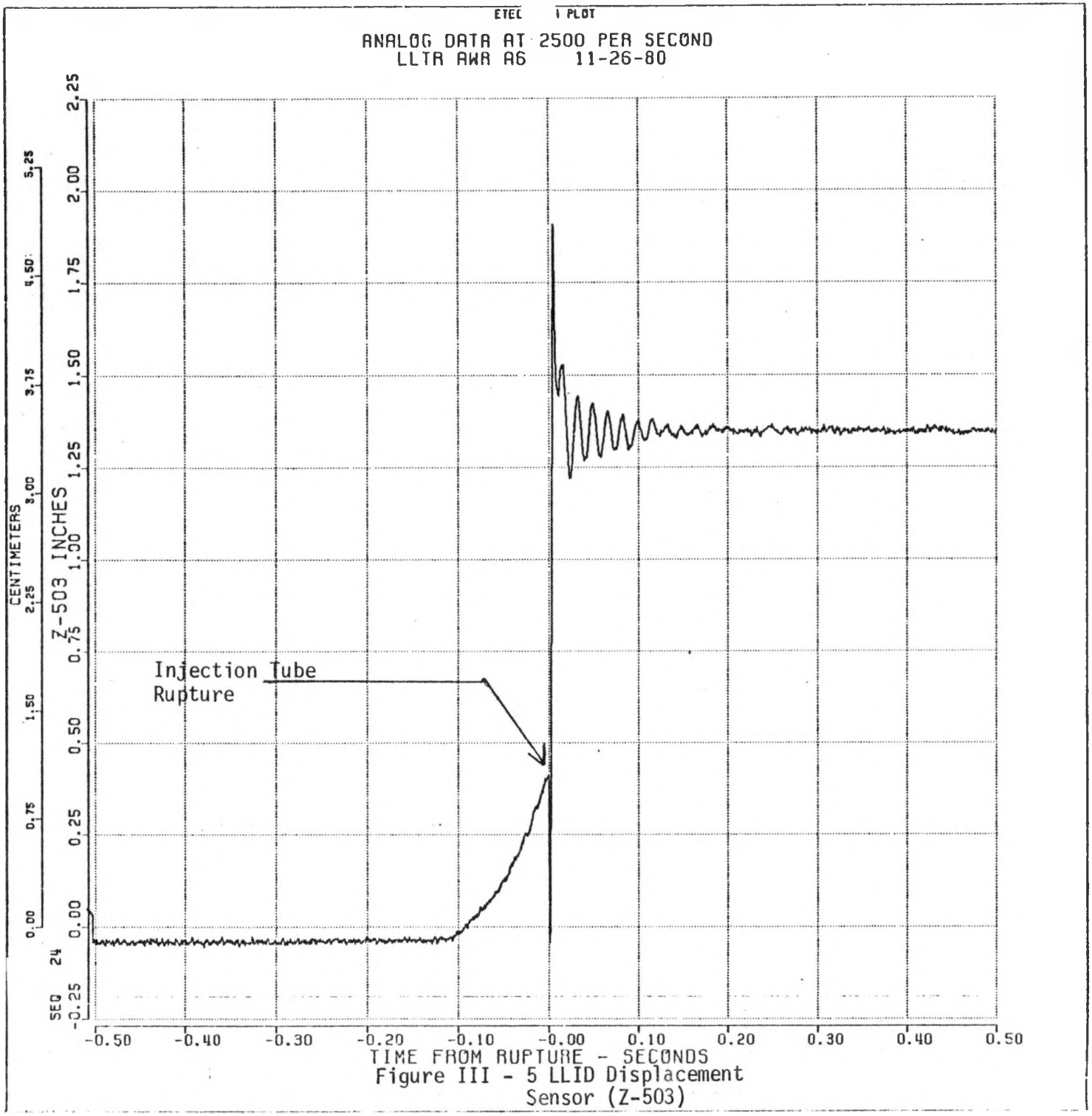

Figure III - 5 LLID Displacement Sensor (Z-503)

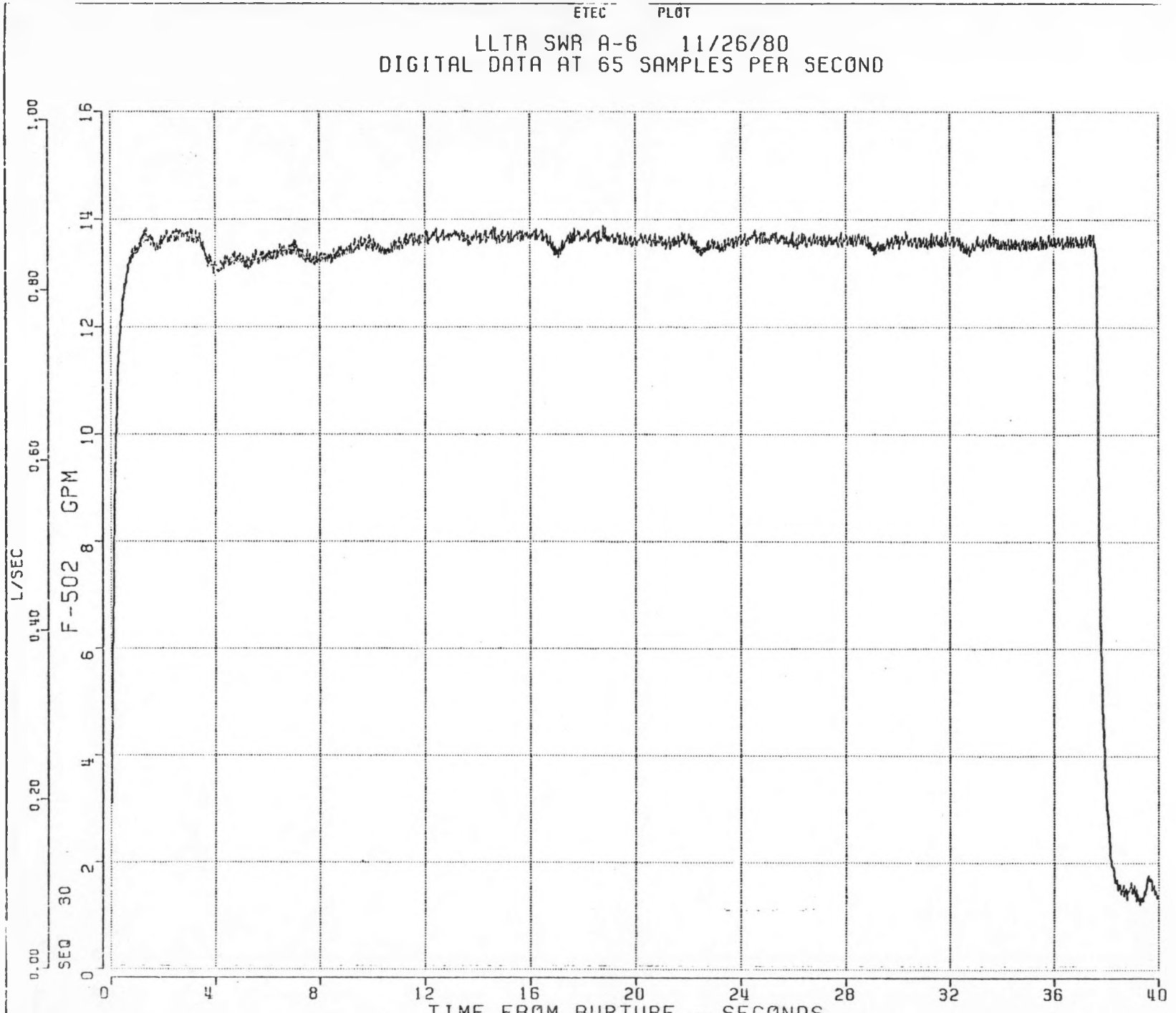

Figure III - 6 Rupture Tube
Bottom End Flow (F502)

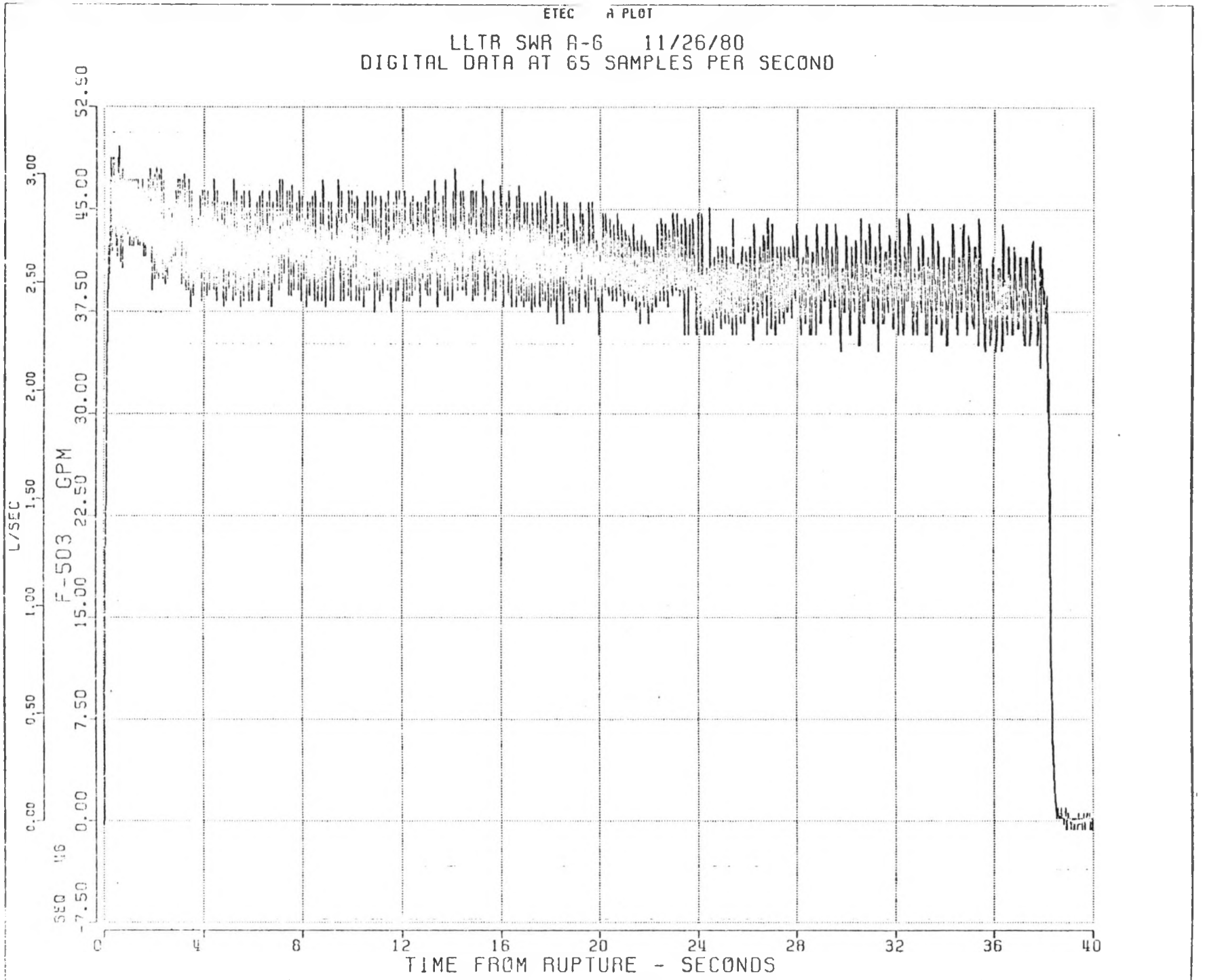

Figure III - 7 Rupture Tube Top End Flow (F-503)

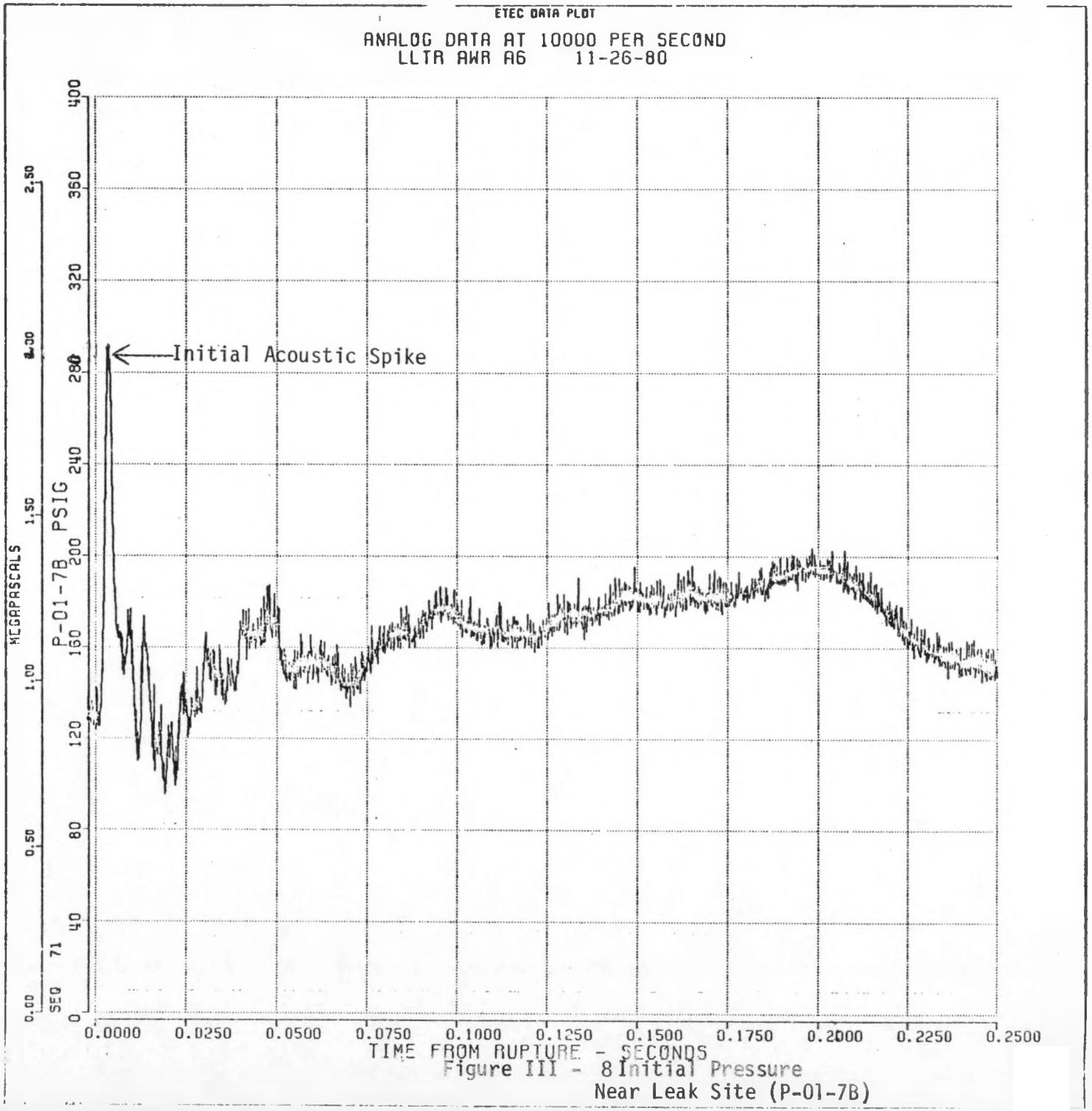

Figure III - 8 Initial Pressure
Near Leak Site (P-01-7B)

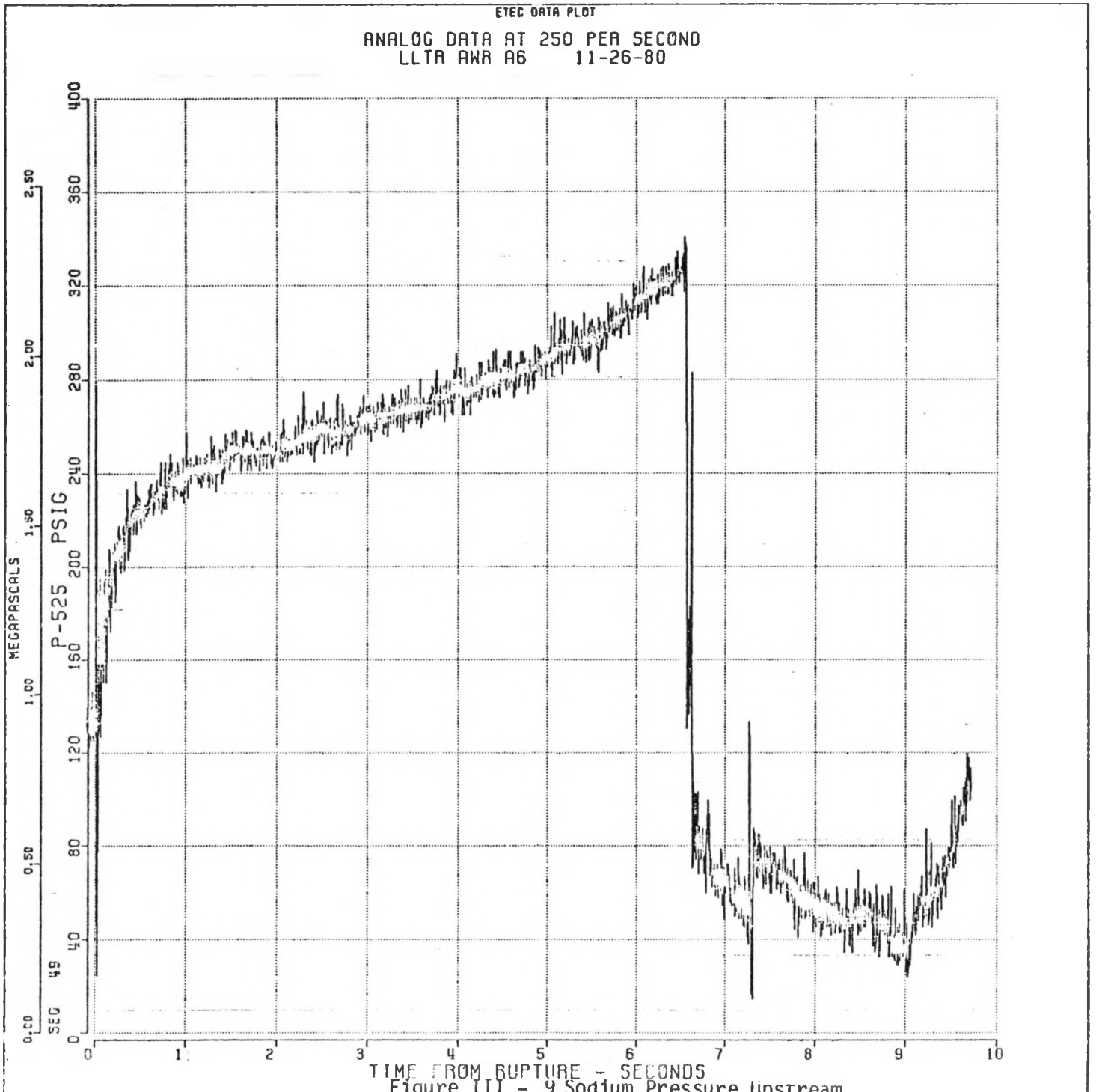

Figure III - 9 Sodium Pressure Upstream of Rupture Disc Assembly (P-525)

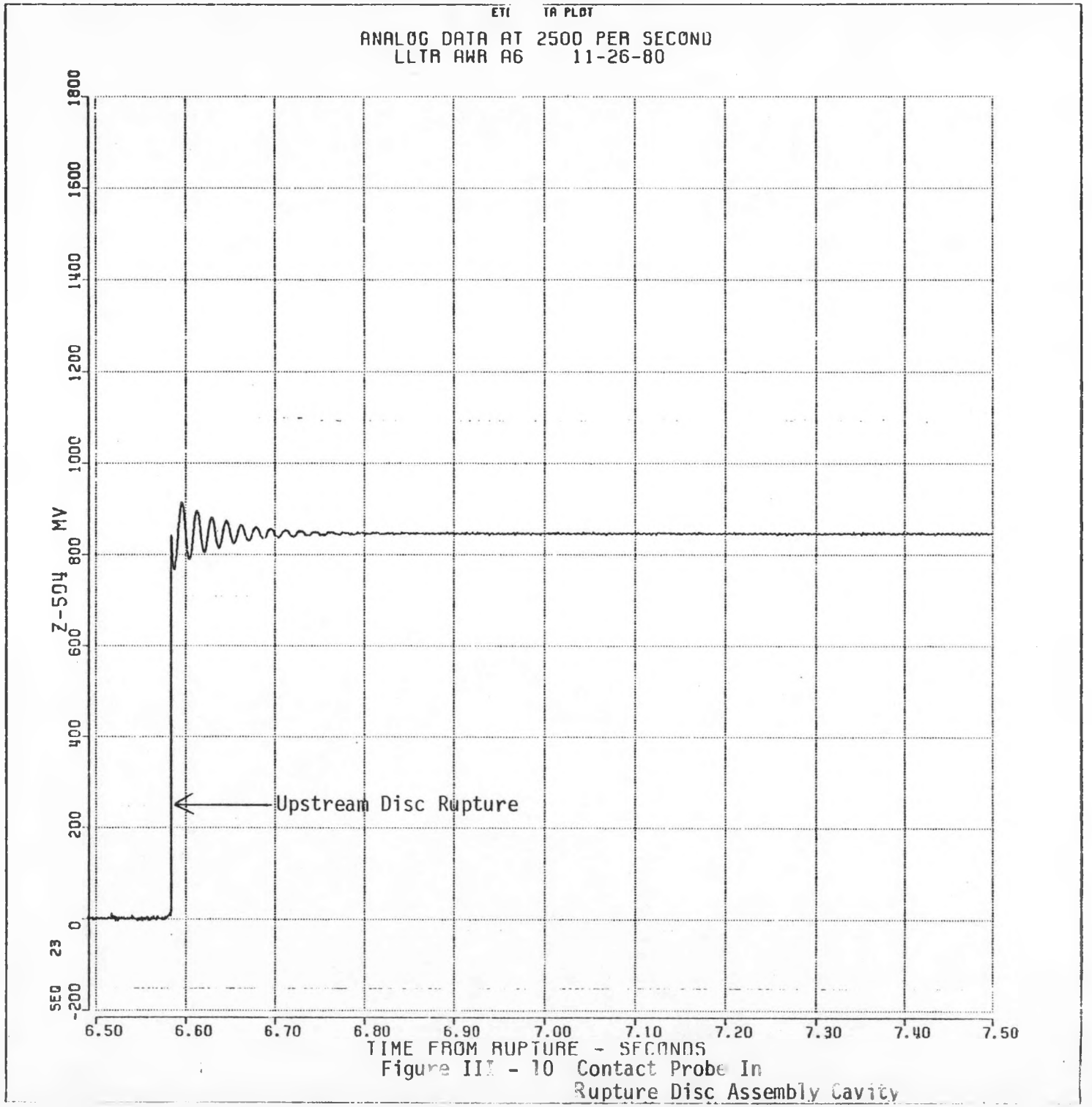

Figure III - 10 Contact Probe In Rupture Disc Assembly Cavity

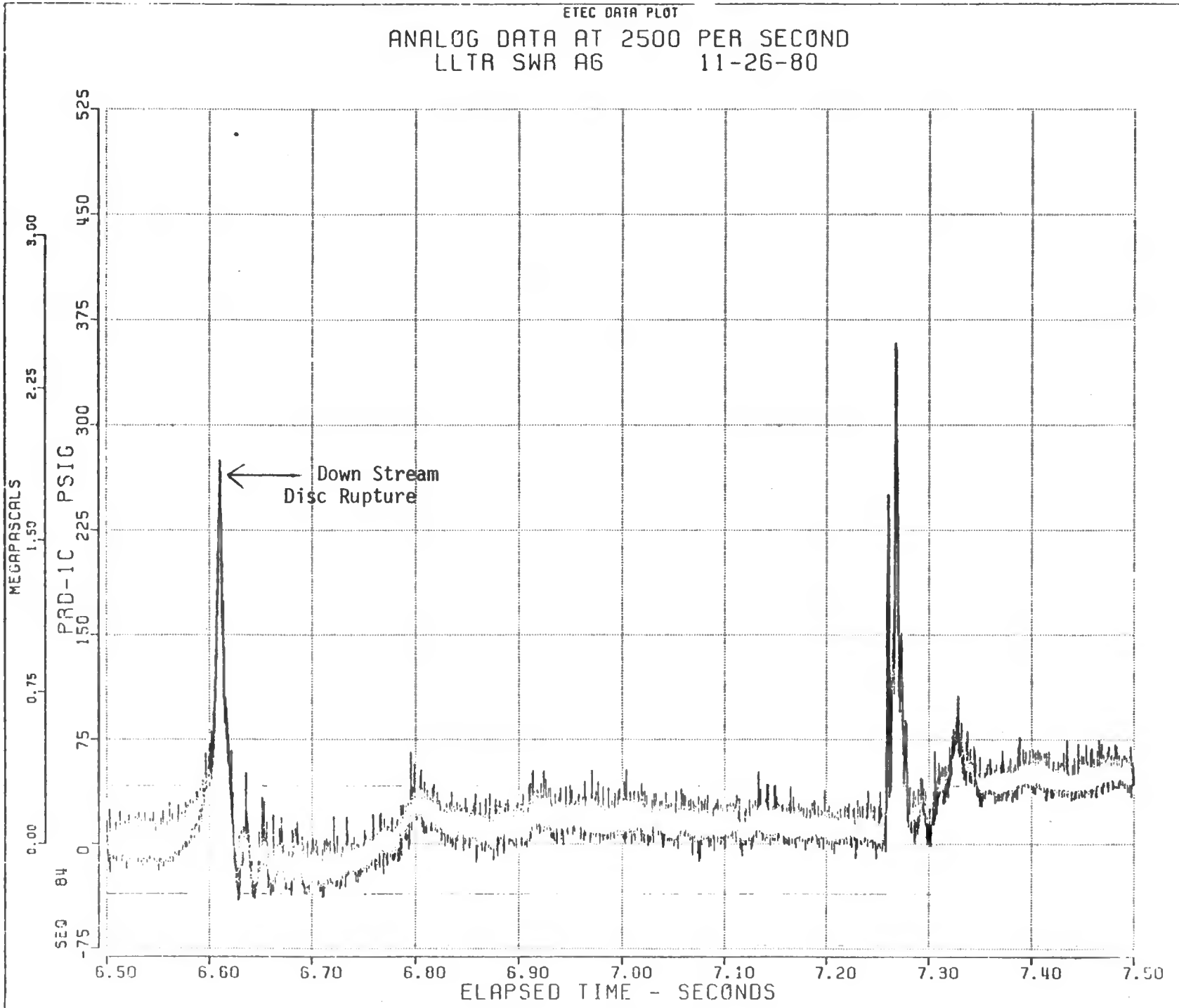

Figure III - 11 Pressure in Rupture Disc Assembly Cavity

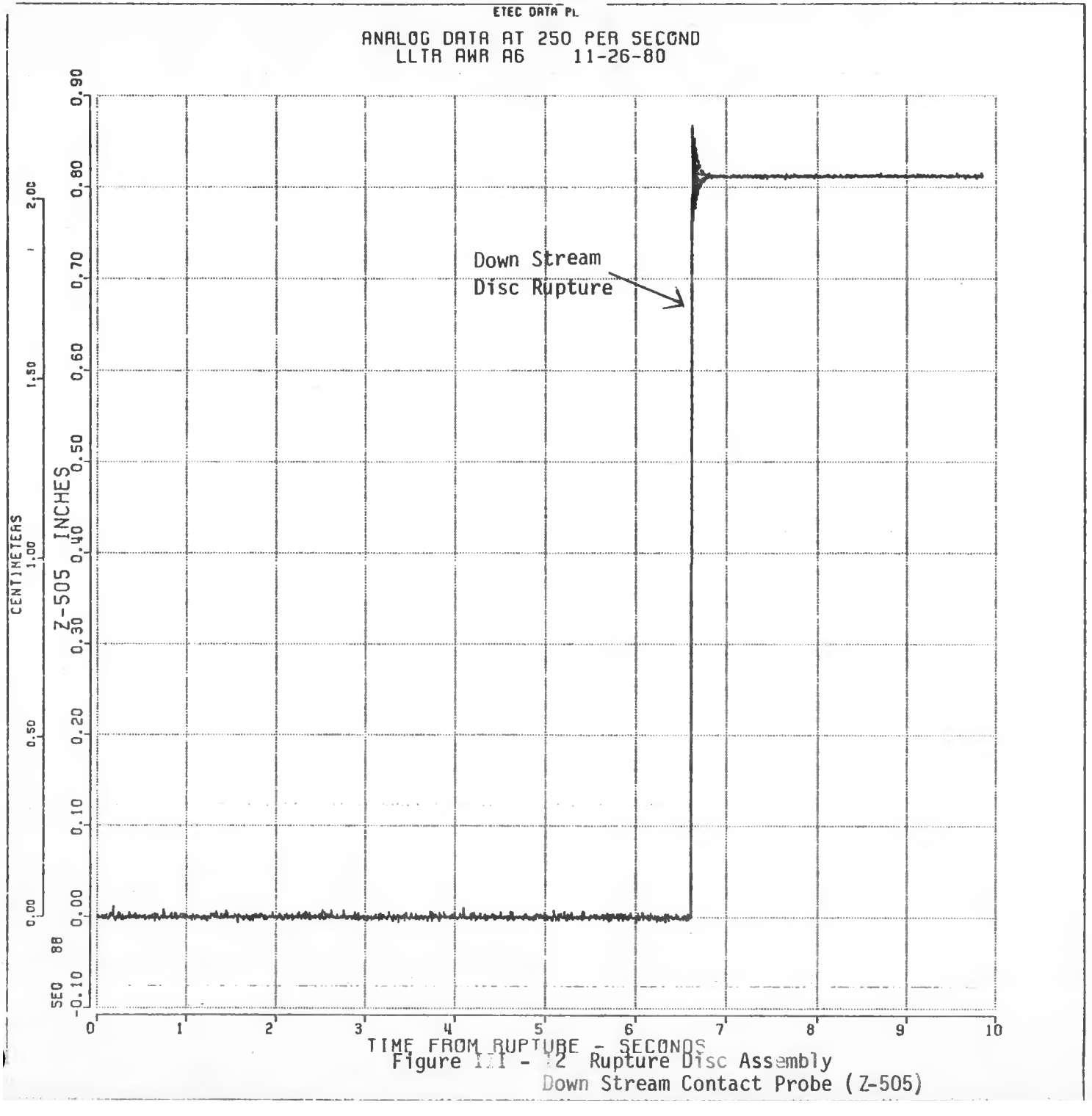

Figure II - 12 Rupture Disc Assembly
Down Stream Contact Probe (Z-505)

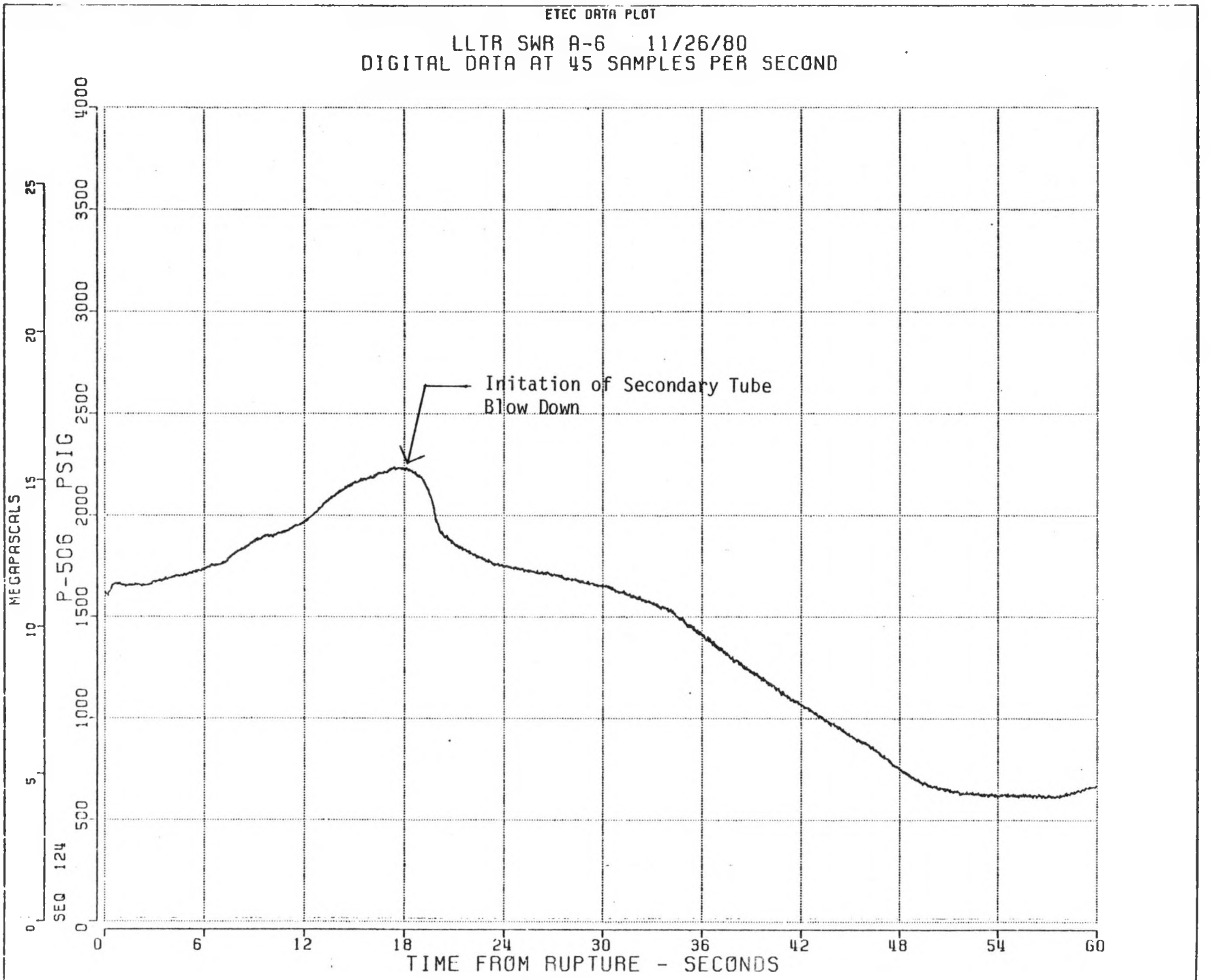

Figure III - 13 Secondary Tube Pressure (P-506)

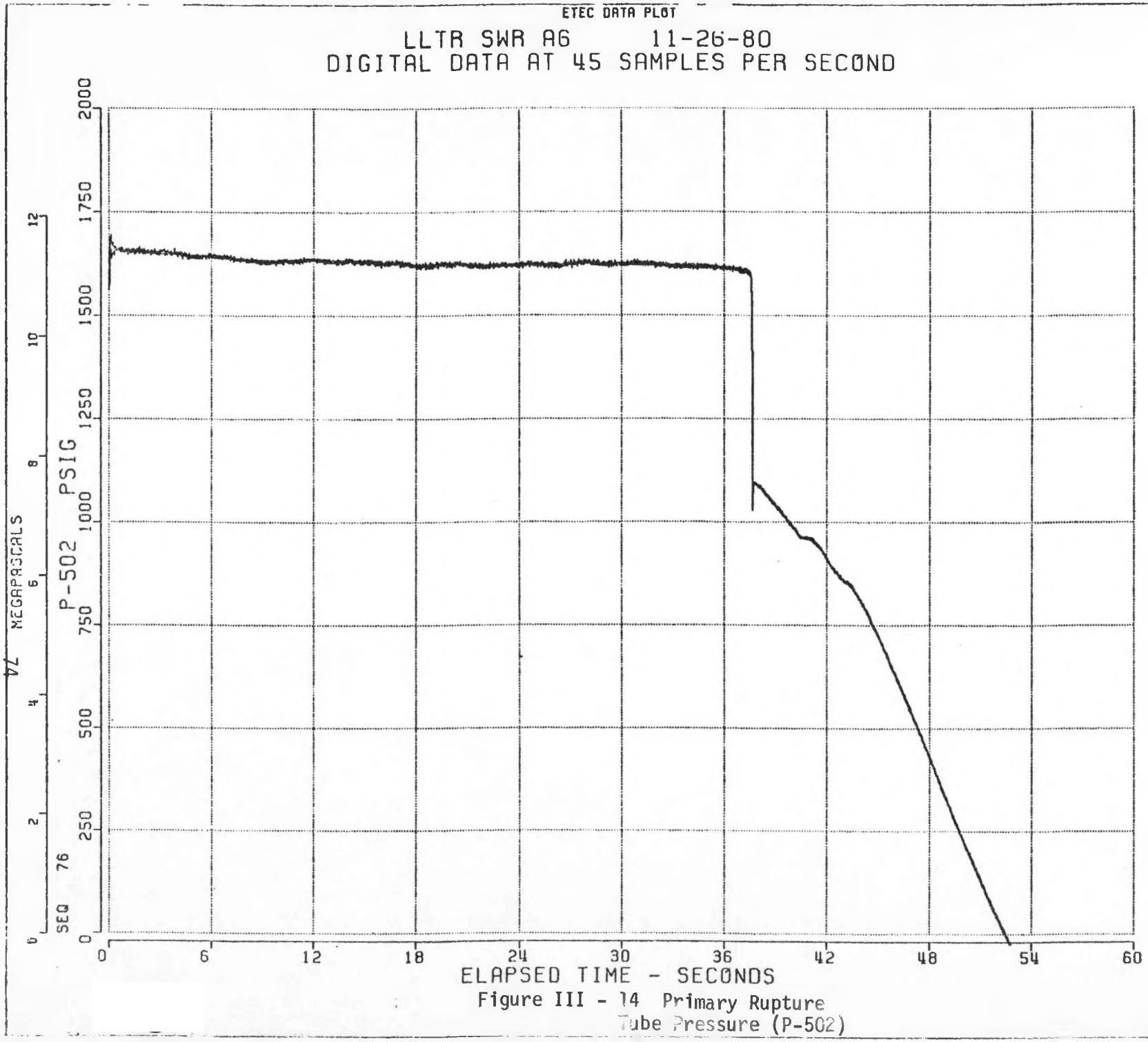

Figure III - 14 Primary Rupture Tube Pressure (P-502)

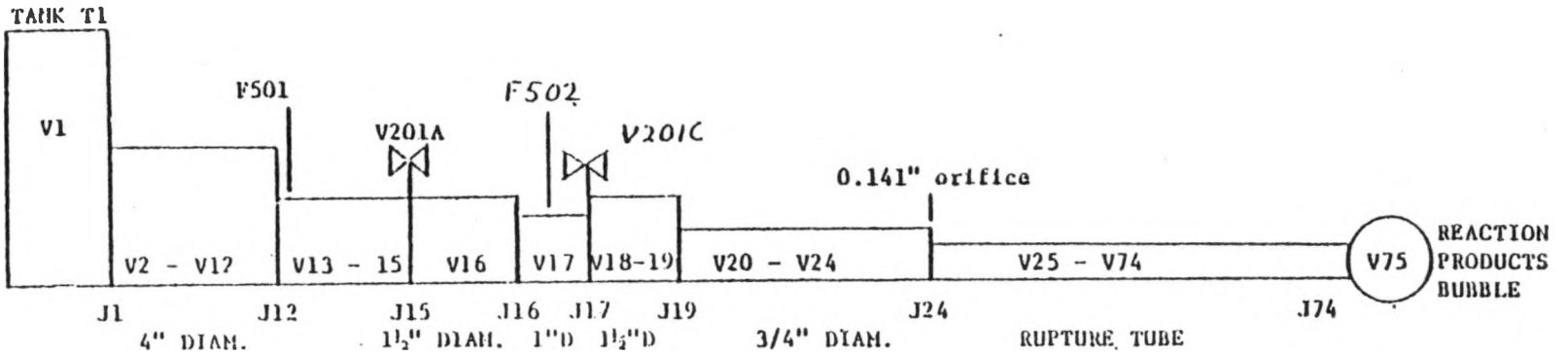

Figure IV-1 RELAP SCHEMATIC FOR TANK T1 SIDE OF RUPTURE TUBE = TEST A6

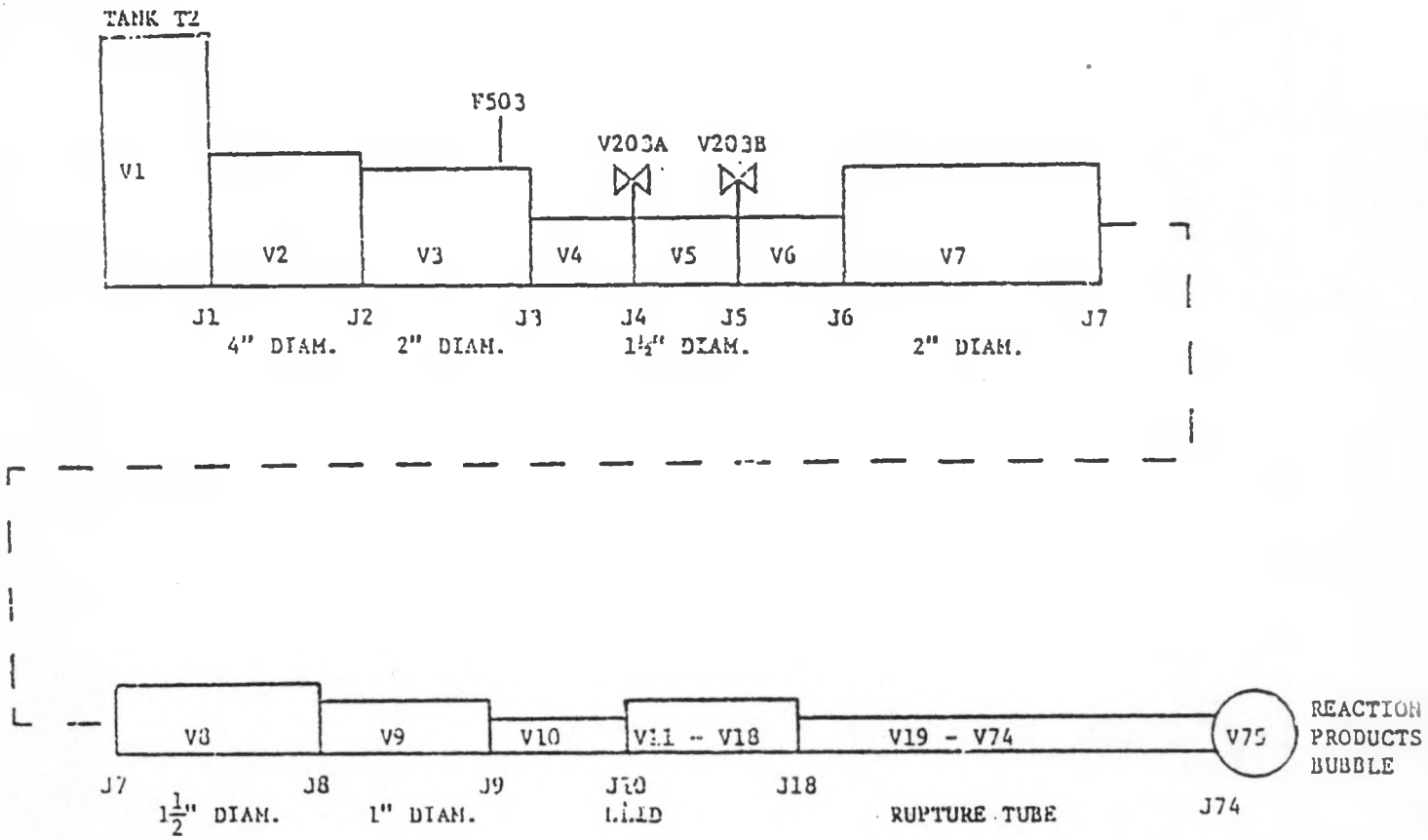

Figure IV-2 RELAP SCHEMATIC FOR TANK T2
SIDE OF RUPTURE TUBE - TEST A-6

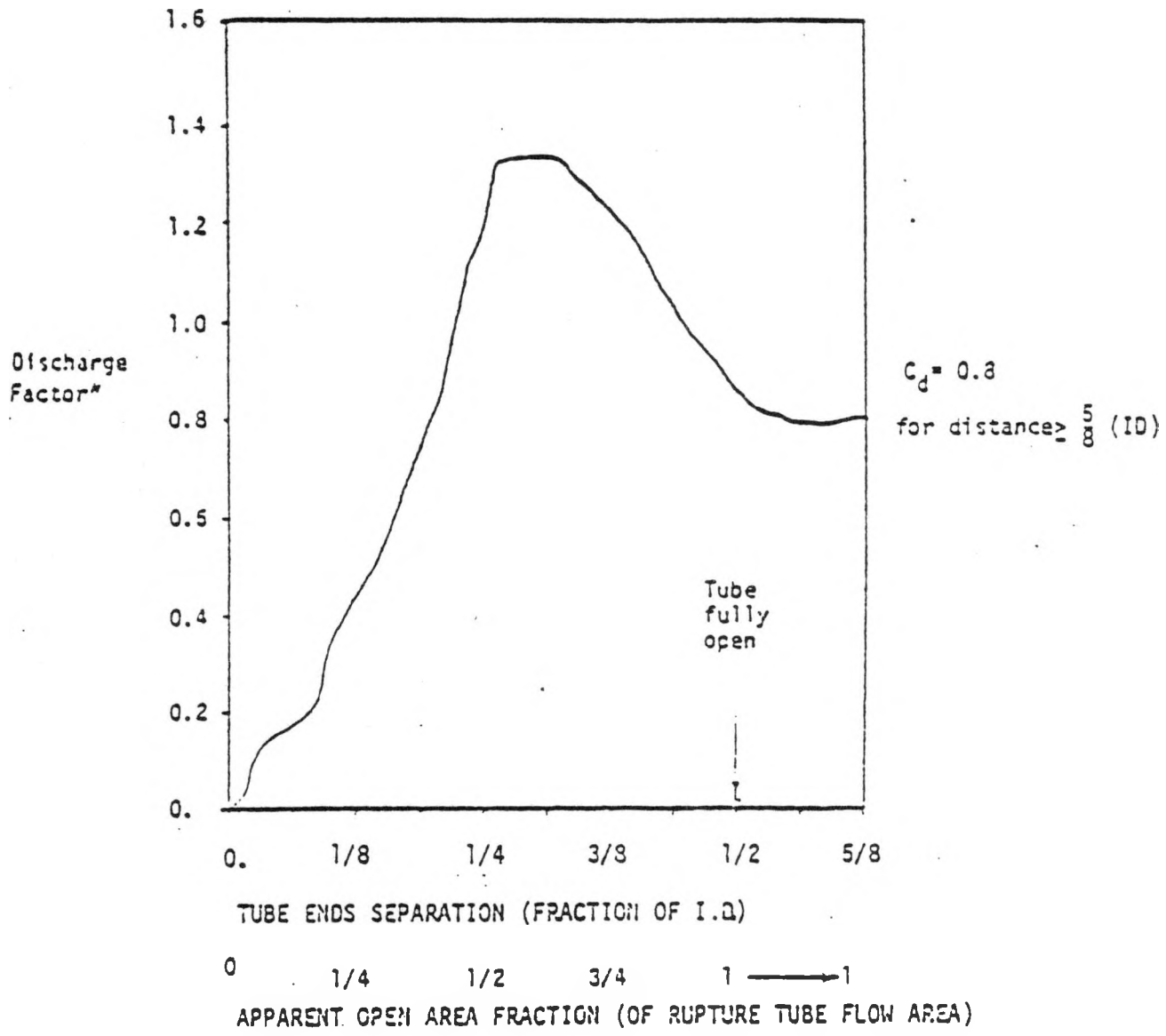

Figure IV-3 EMPIRICALLY-DERIVED DISCHARGE FACTOR FOR SWR-5 LEAKSITE (SERIES I TEST PROGRAM)

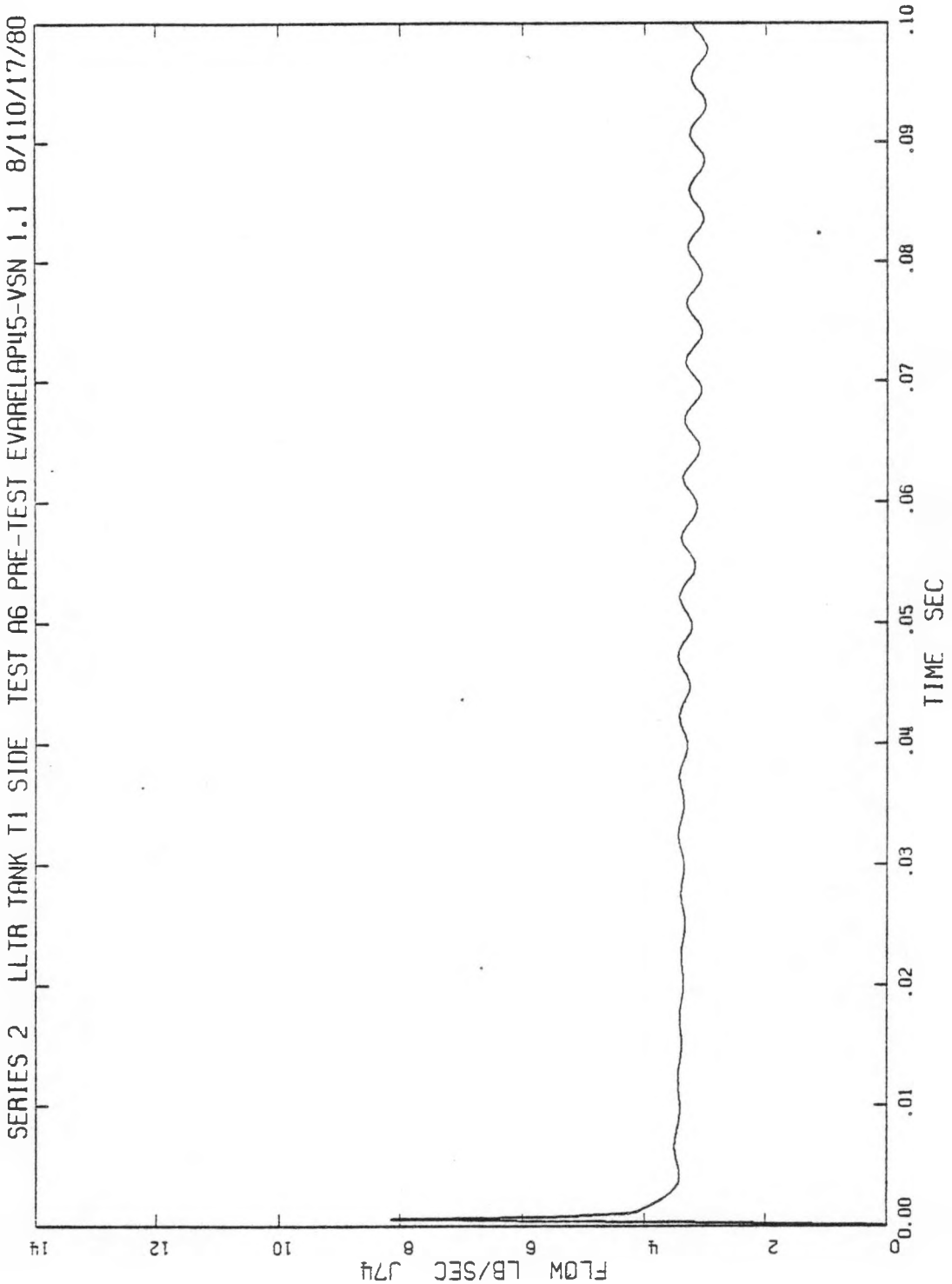

Figure IV-4

Tank T1 Side of Rupture Tube Predicted Flow Rate for Test A-6

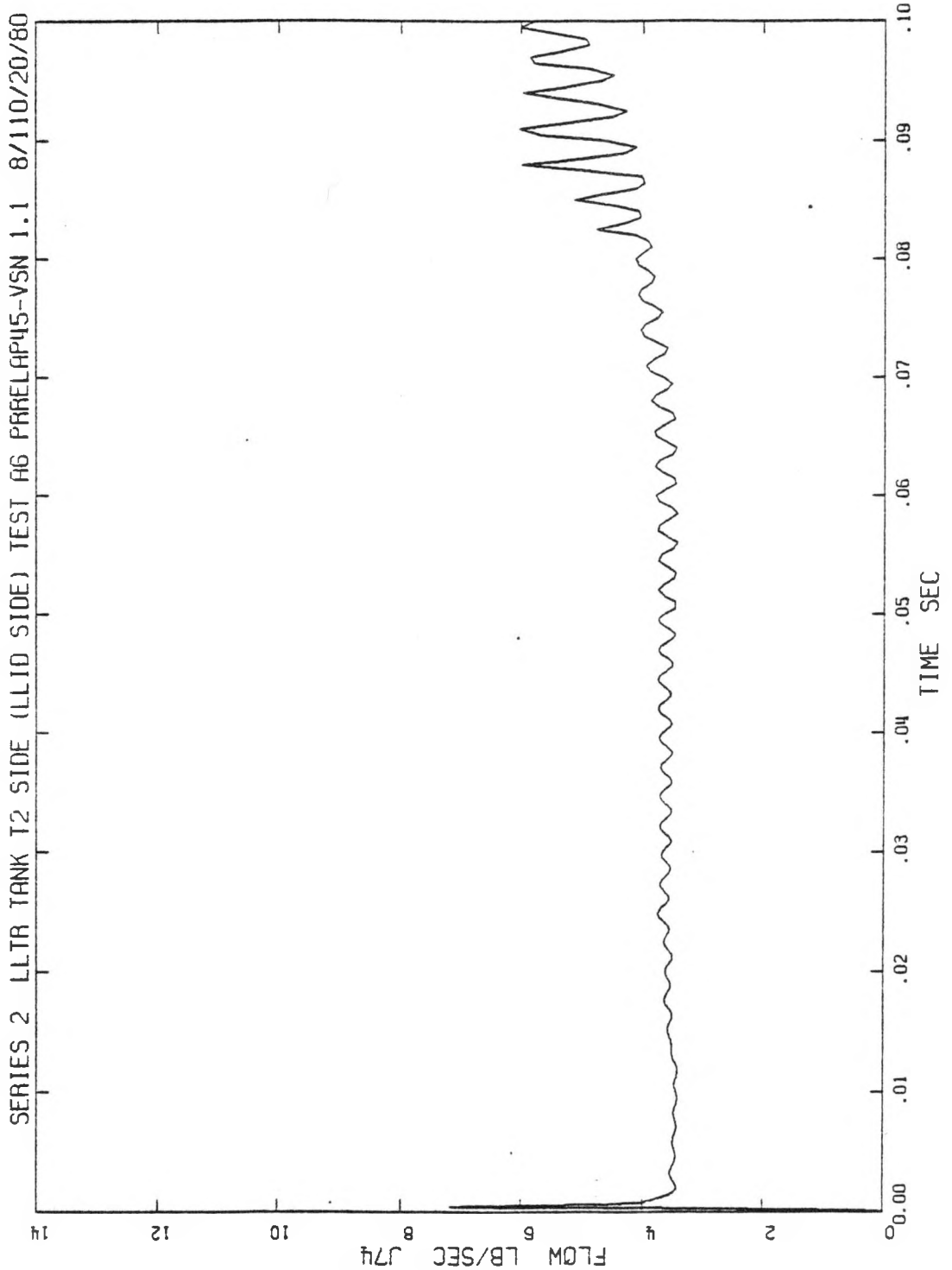

Figure IV-5

TANK T2 Side of Rupture Tube Predicted Flow Rate for Test A-6

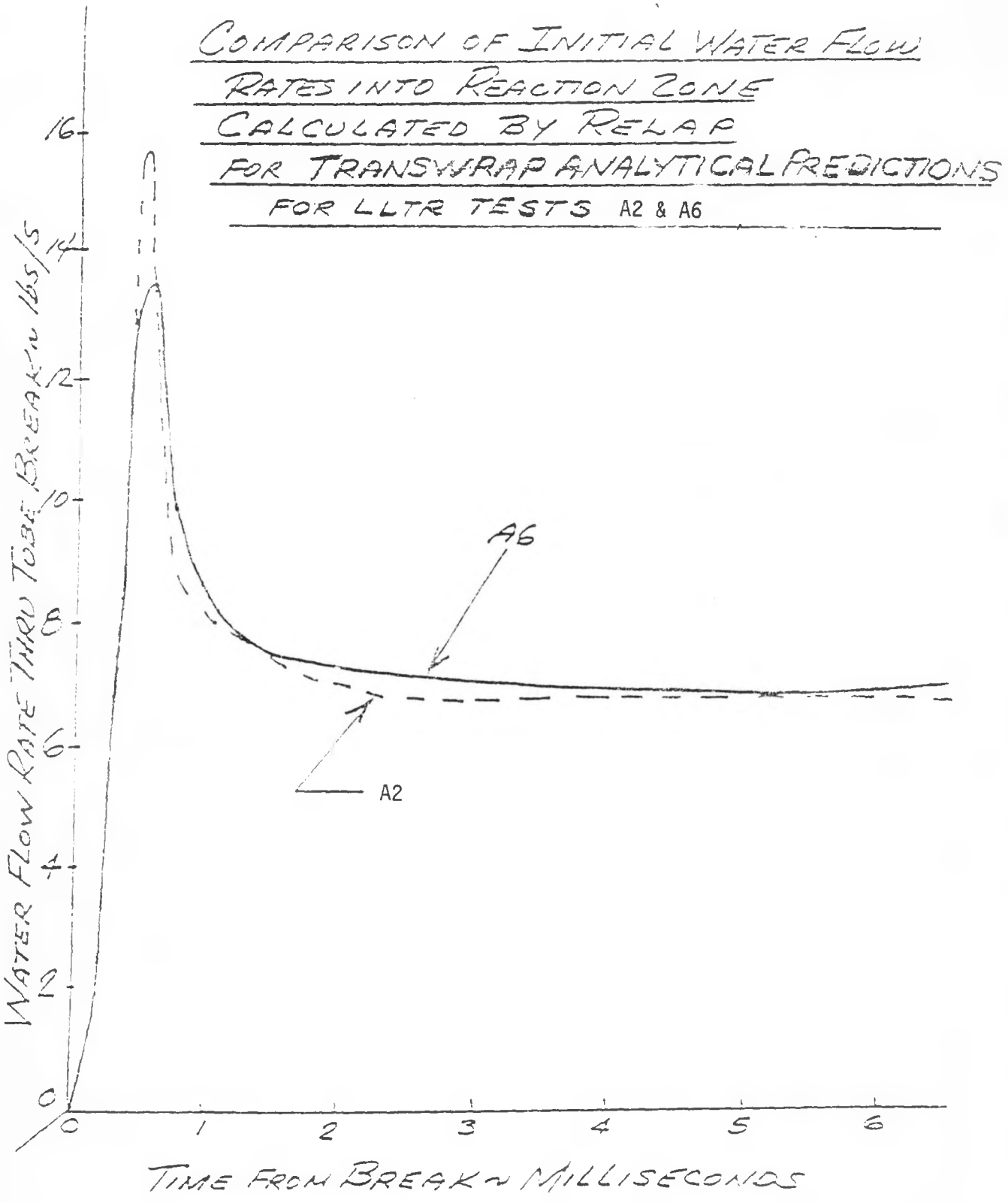
COMPARISON OF INITIAL WATER FLOW RATES INTO REACTION ZONE CALCULATED BY RELAP FOR TRANSWRAP ANALYTICAL PREDICTIONS FOR LLTR TESTS A2 & A6
WATER FLOW RATE THRU TUBE BREAK-lbs/s
0
2
4
6
8
10
12
14
16
A6
A2
0
1
2
3
4
5
6
TIME FROM BREAK-MILLISECONDS

FIGURE IV-6

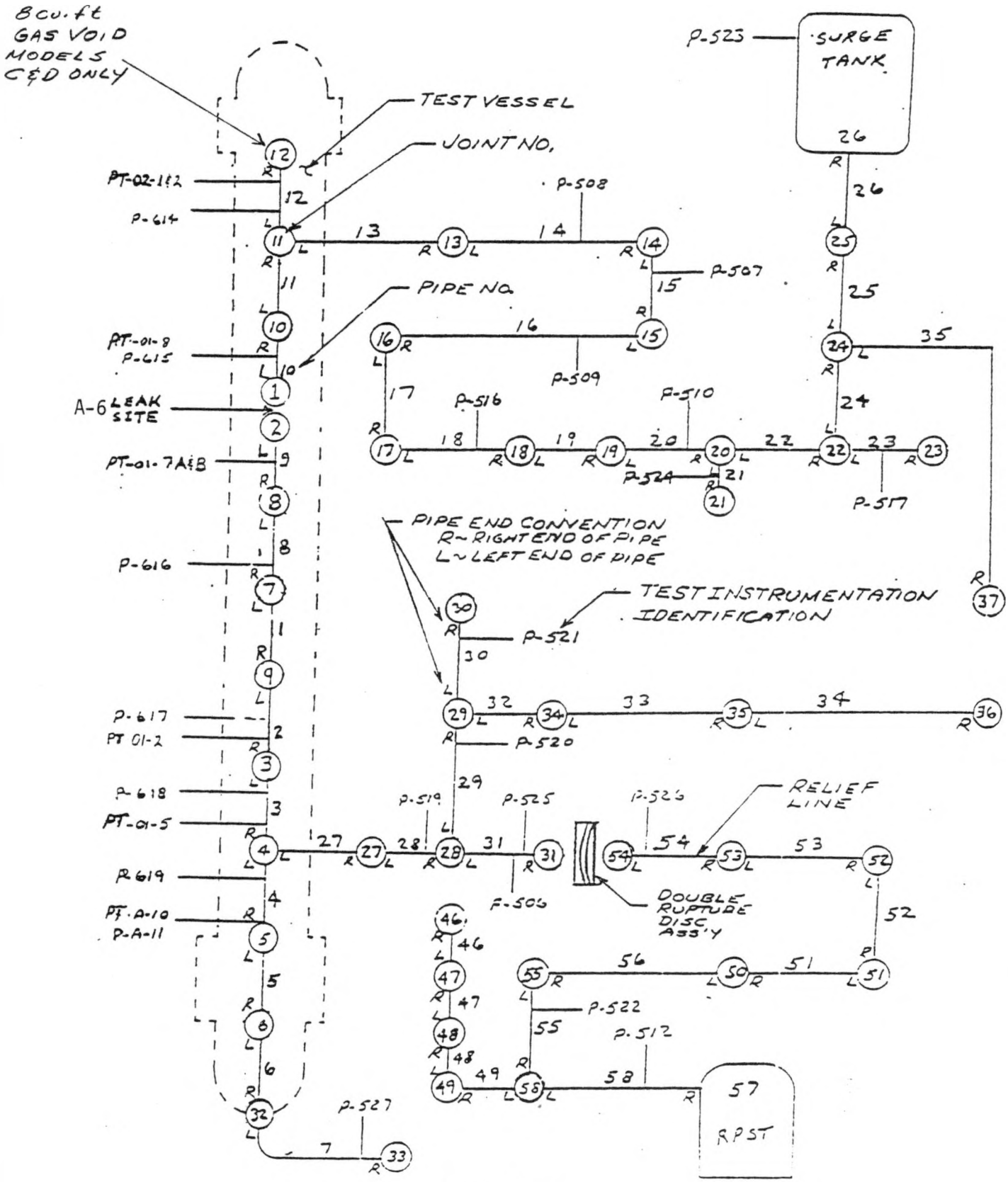

FIGURE IV-7

TRANSWRAP MODEL

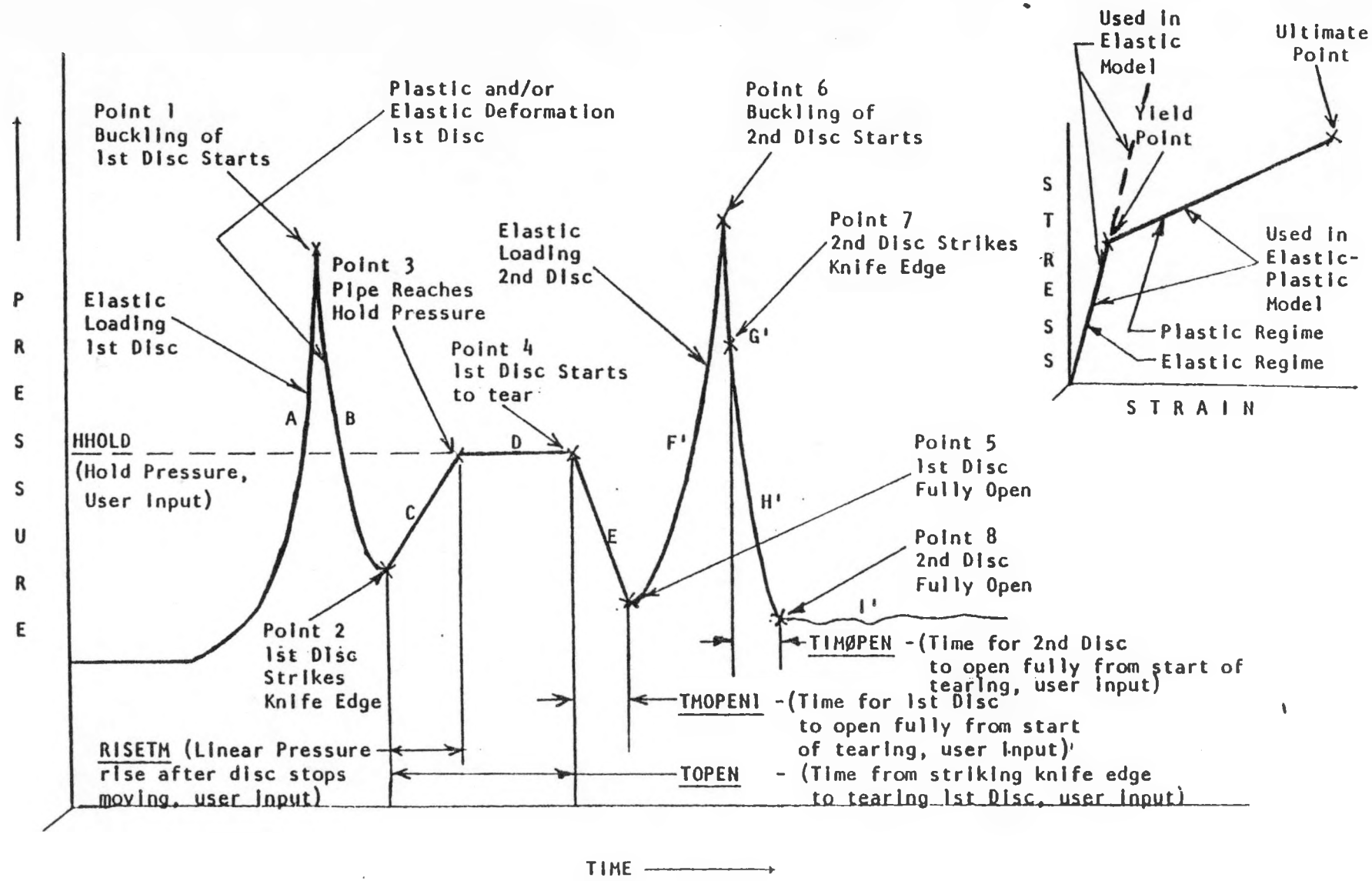

* The behavior of the second disc differs somewhat from that of the first

Figure IV-8

RUPTURE DISC DYNAMIC MODEL

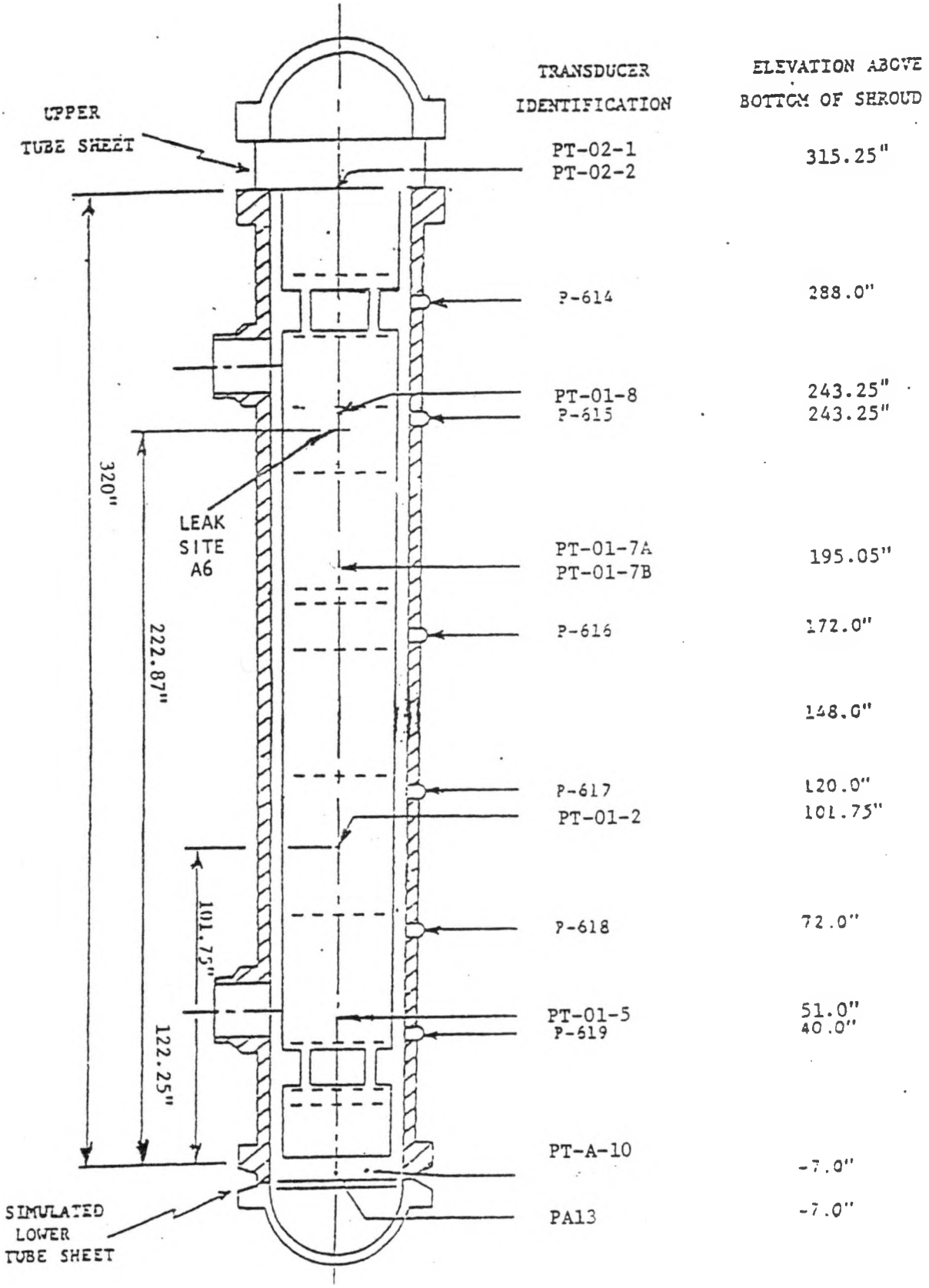

LLTV/LLTI PRESSURE TRANSDUCER LOCATIONS
FIGURE IV-9

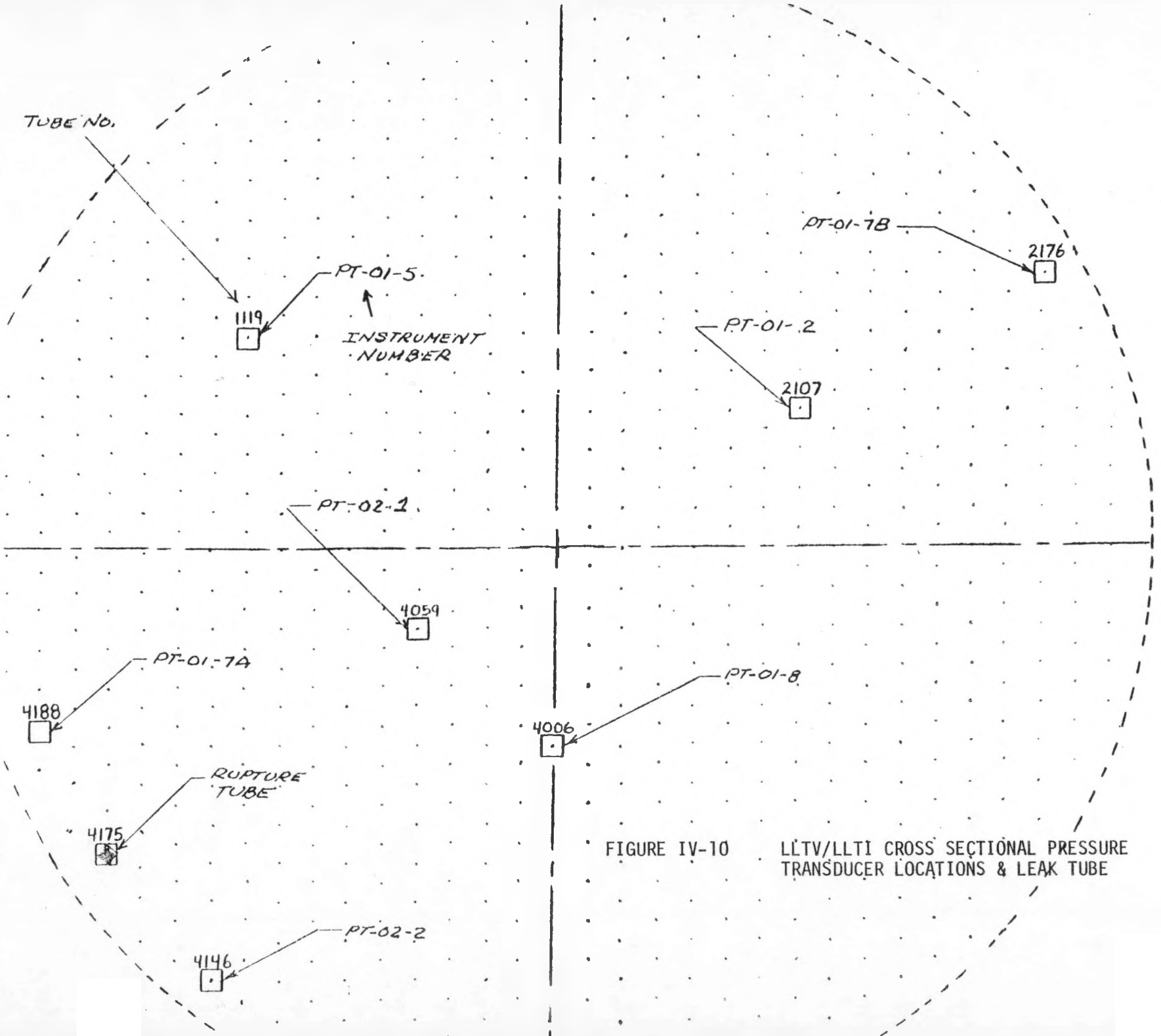

FIGURE IV-10 LLTV/LLTI CROSS SECTIONAL PRESSURE TRANSDUCER LOCATIONS & LEAK TUBE

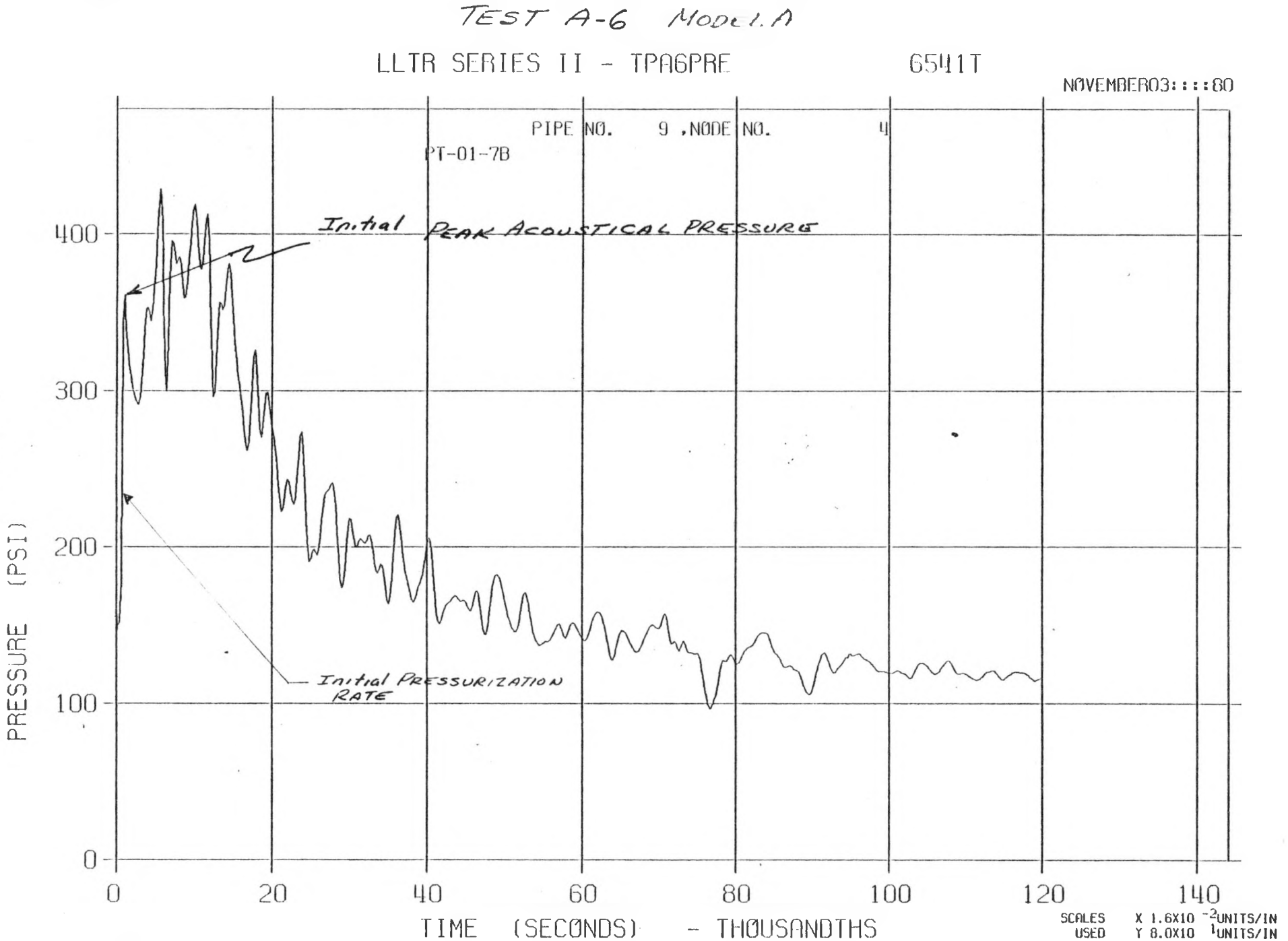

FIGURE V-1 PREDICTED PRESSURE HISTORY NEAR LEAK SITE (TEST A-6 MODEL A)

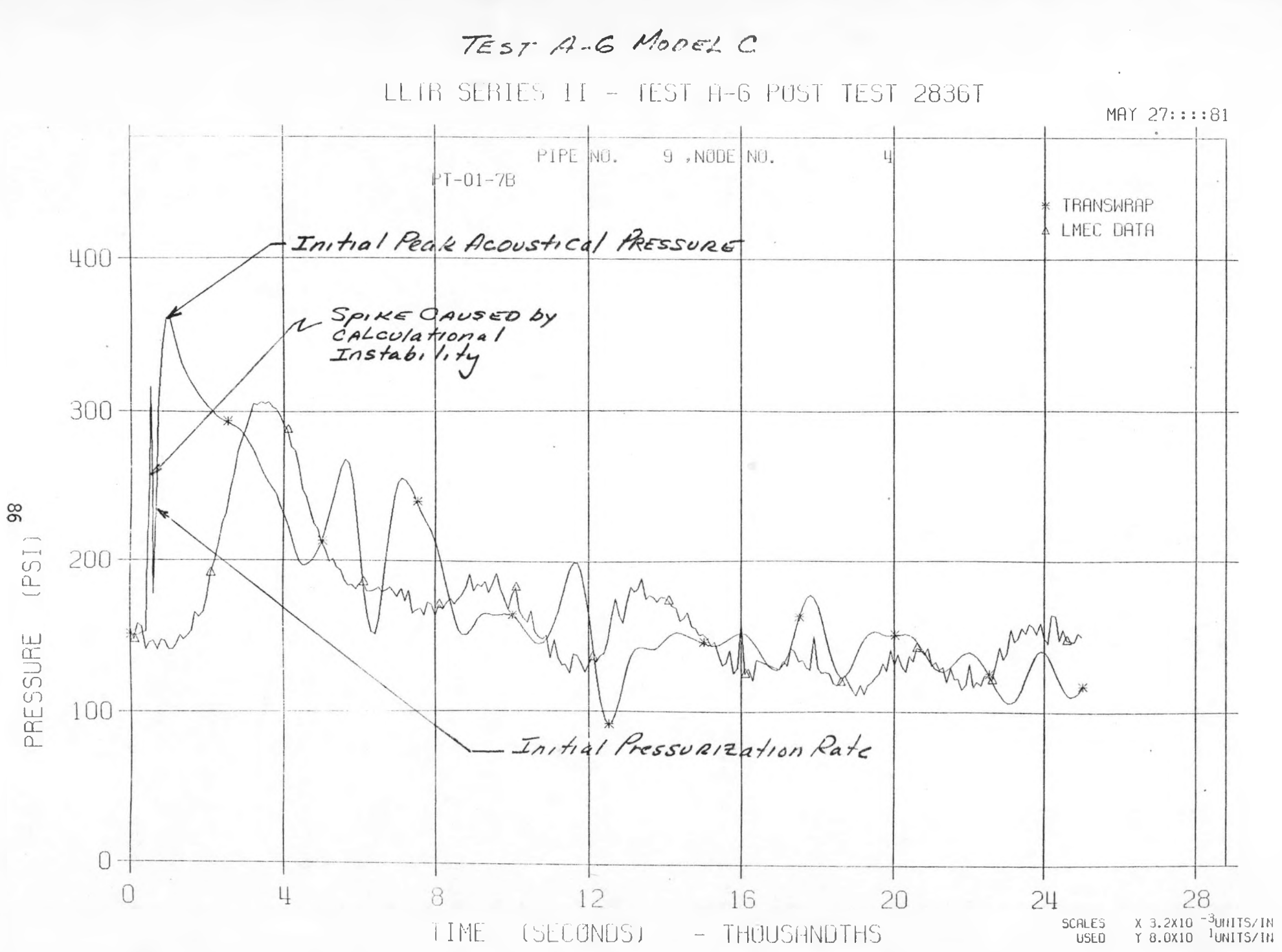

FIGURE V-2 PRESSURE HISTORY NEAR LEAK SITE (TEST A-6 MODEL C PLUS TEST DATA

PL 5

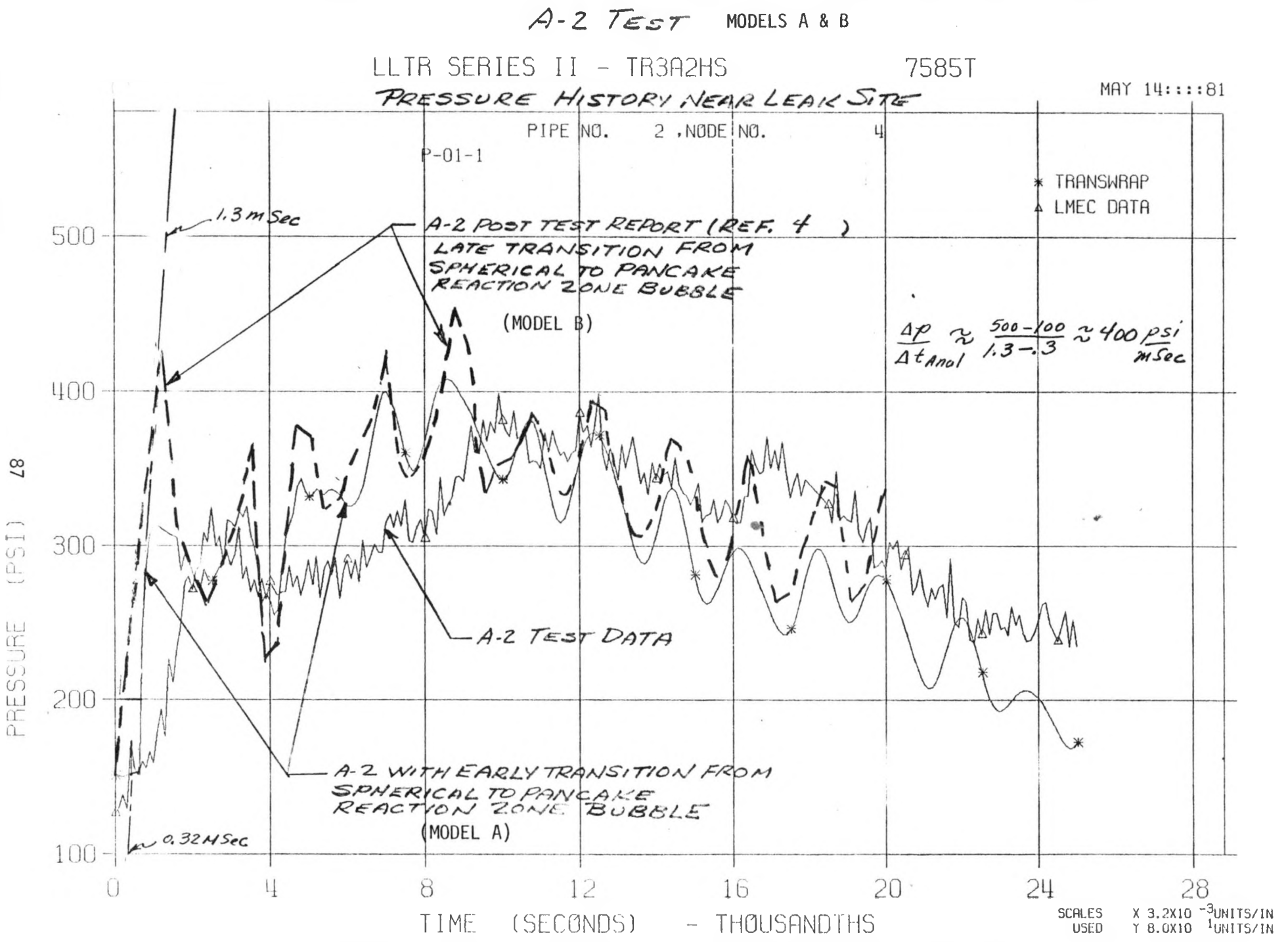

FIGURE V-3 PRESSURE HISTORY NEAR LEAK SITE (TEST A-2 MODEL A & B PLUS TEST DATA)

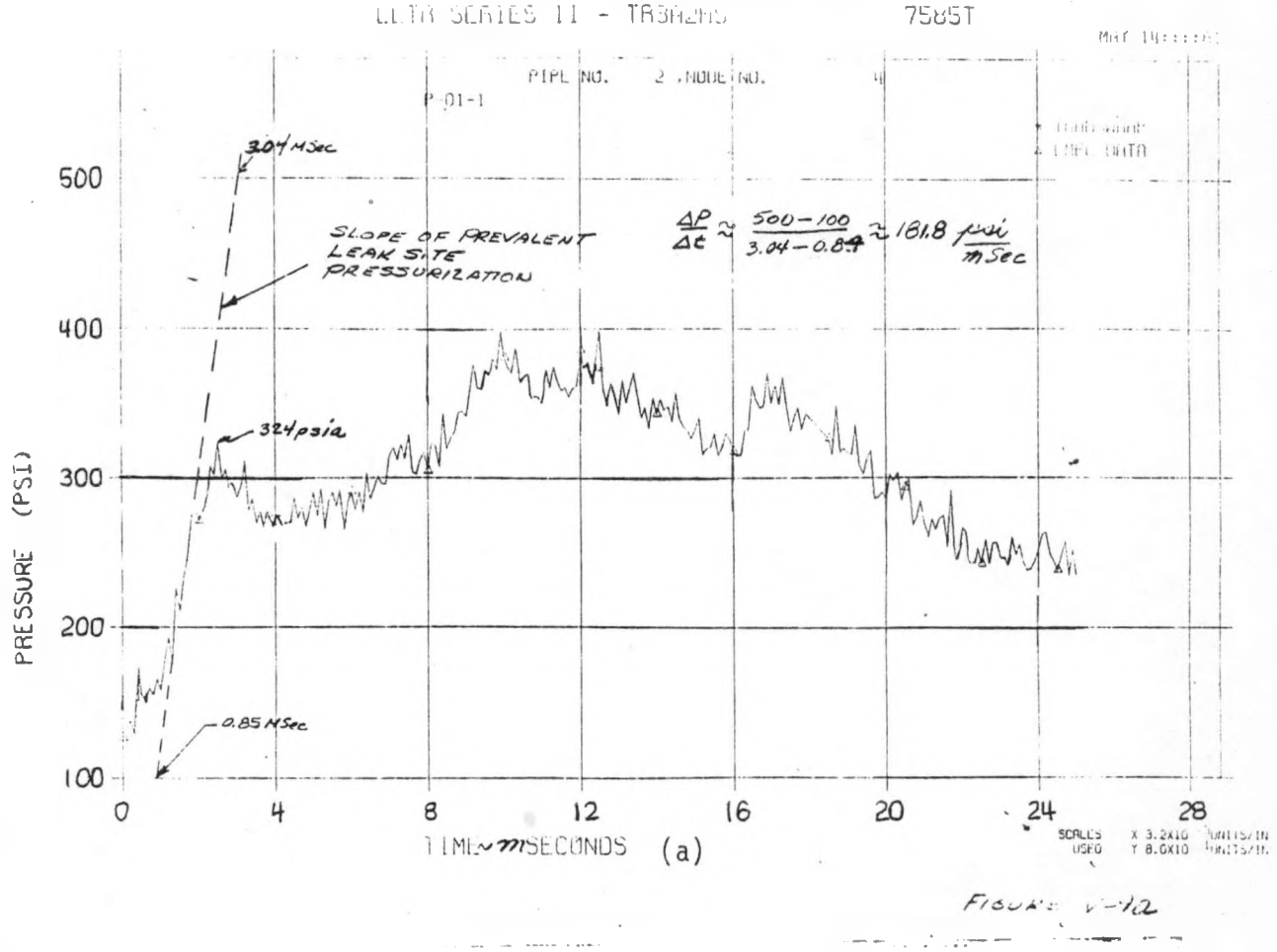

FIGURE V-4a

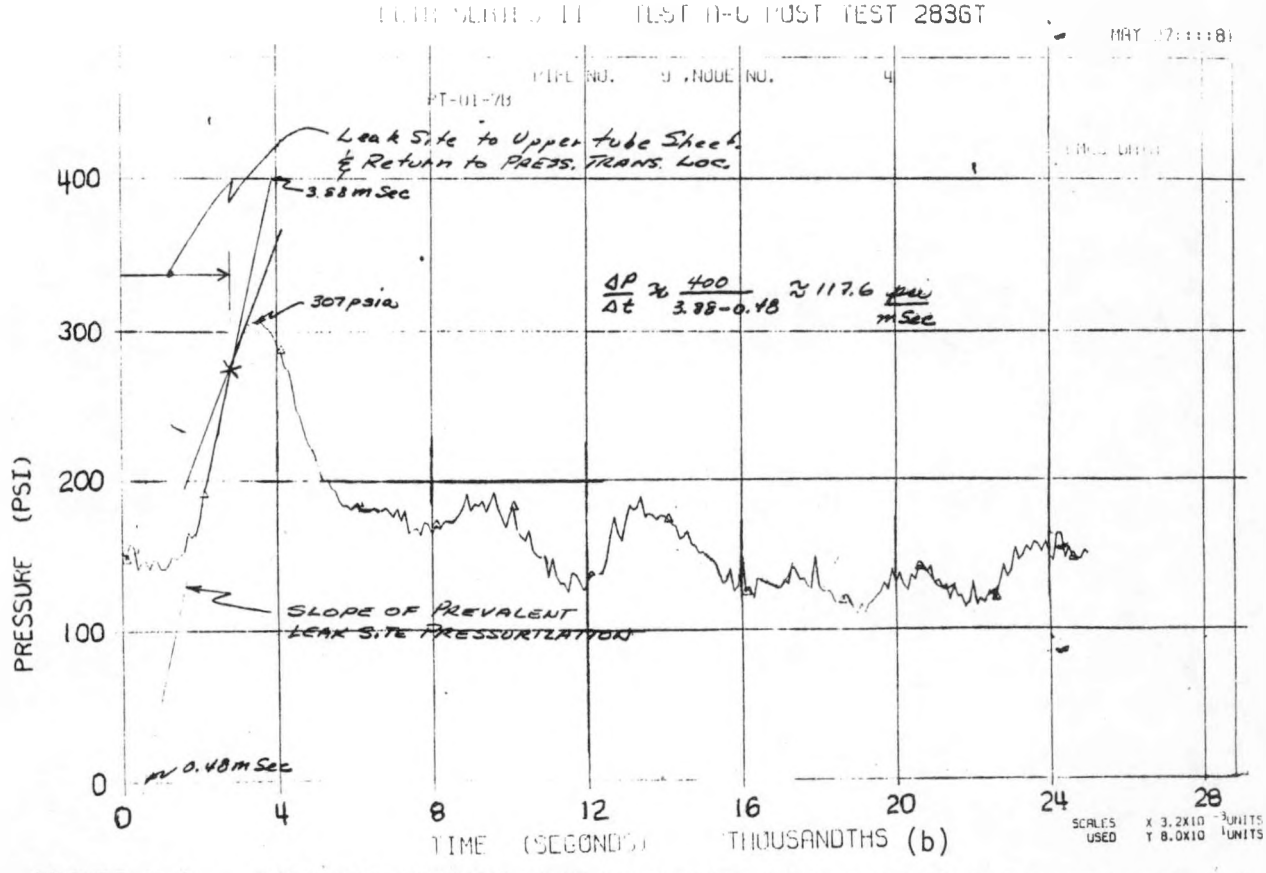

FIGURE V-4 PRESSURE HISTORY NEAR LEAK SITE (TESTS A-2 & A-6 TEST DATA)

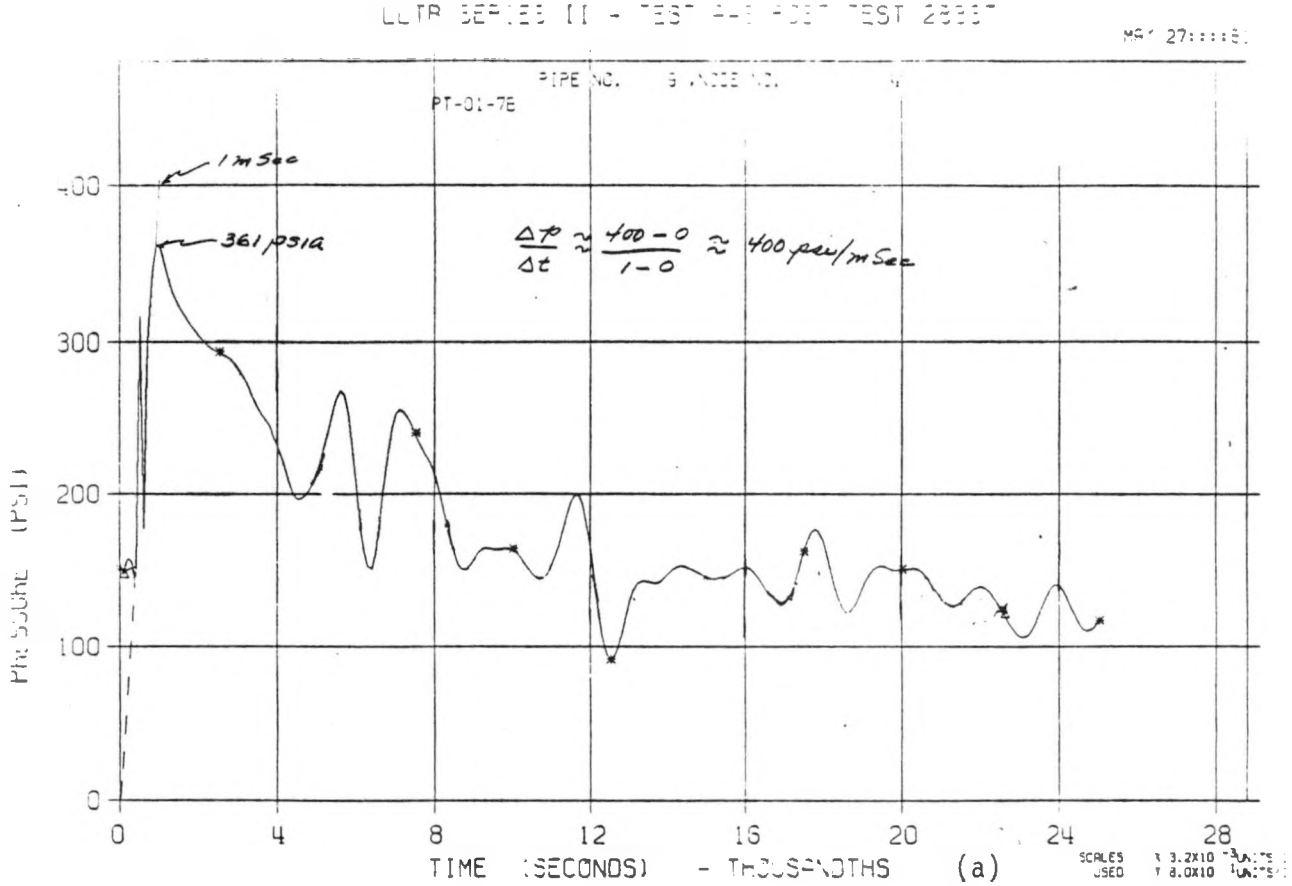

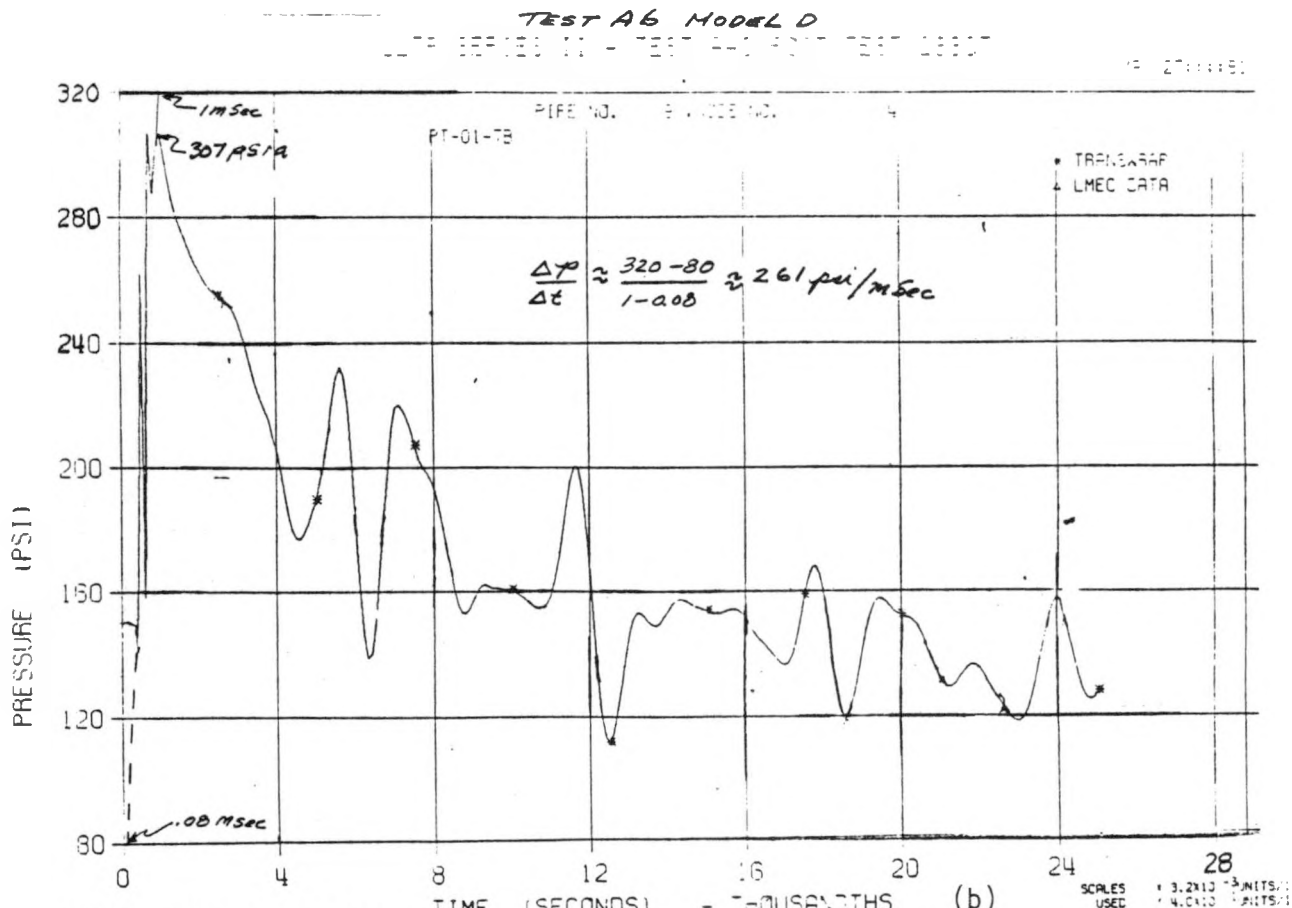

FIGURE V-5 PREDICTED PRESSURE HISTORY NEAR LEAK SITE (TEST A-6 MODEL C & D)

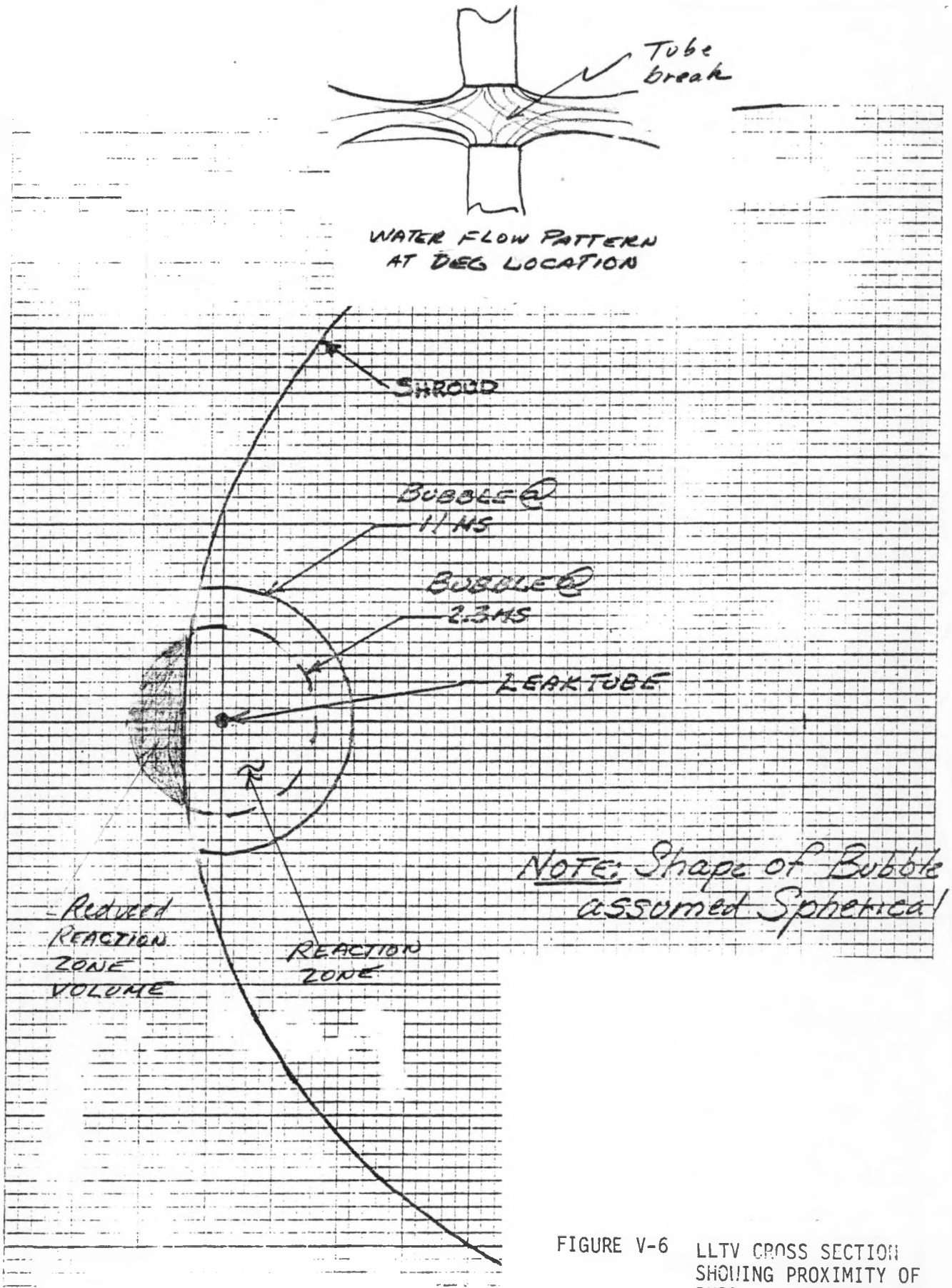

FIGURE V-6 LLTV CROSS SECTION SHOWING PROXIMITY OF BUBBLE TO SHROUD

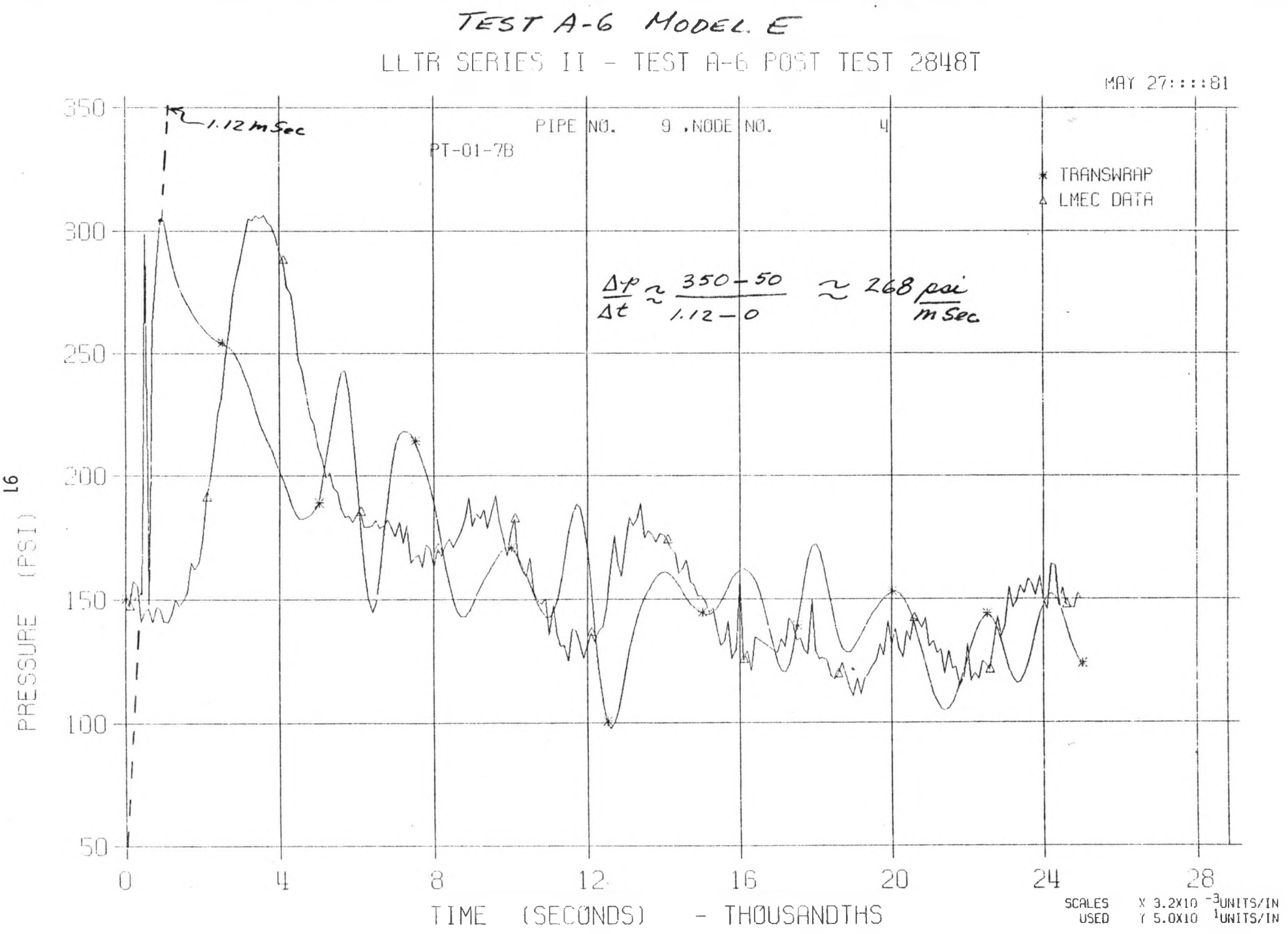

FIGURE V-8 PRESSURE HISTORY NEAR LEAK SITE (TEST A-6 MODEL E PLUS TEST DATA)

PL 5

TEST A-6 MODEL D

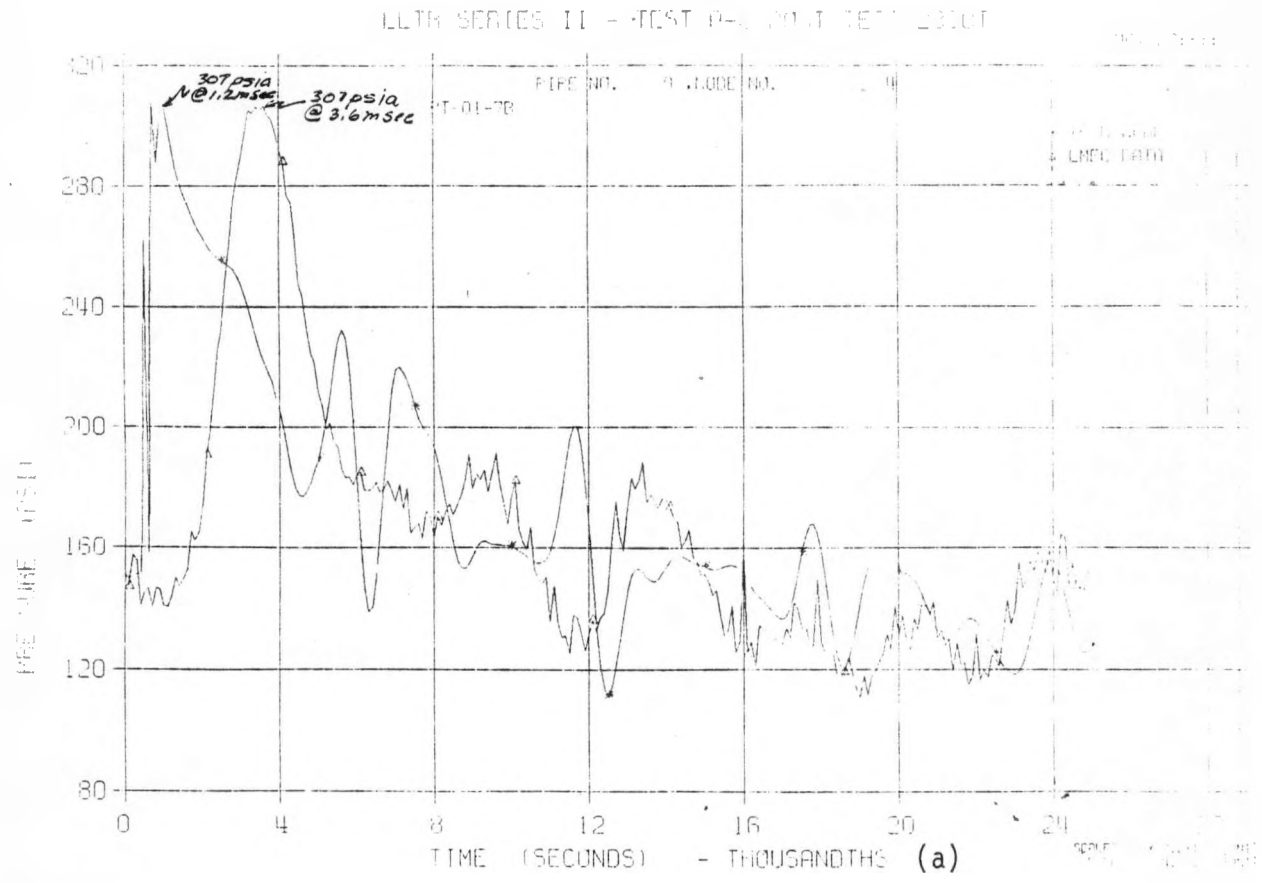

TEST A-6 MODEL D

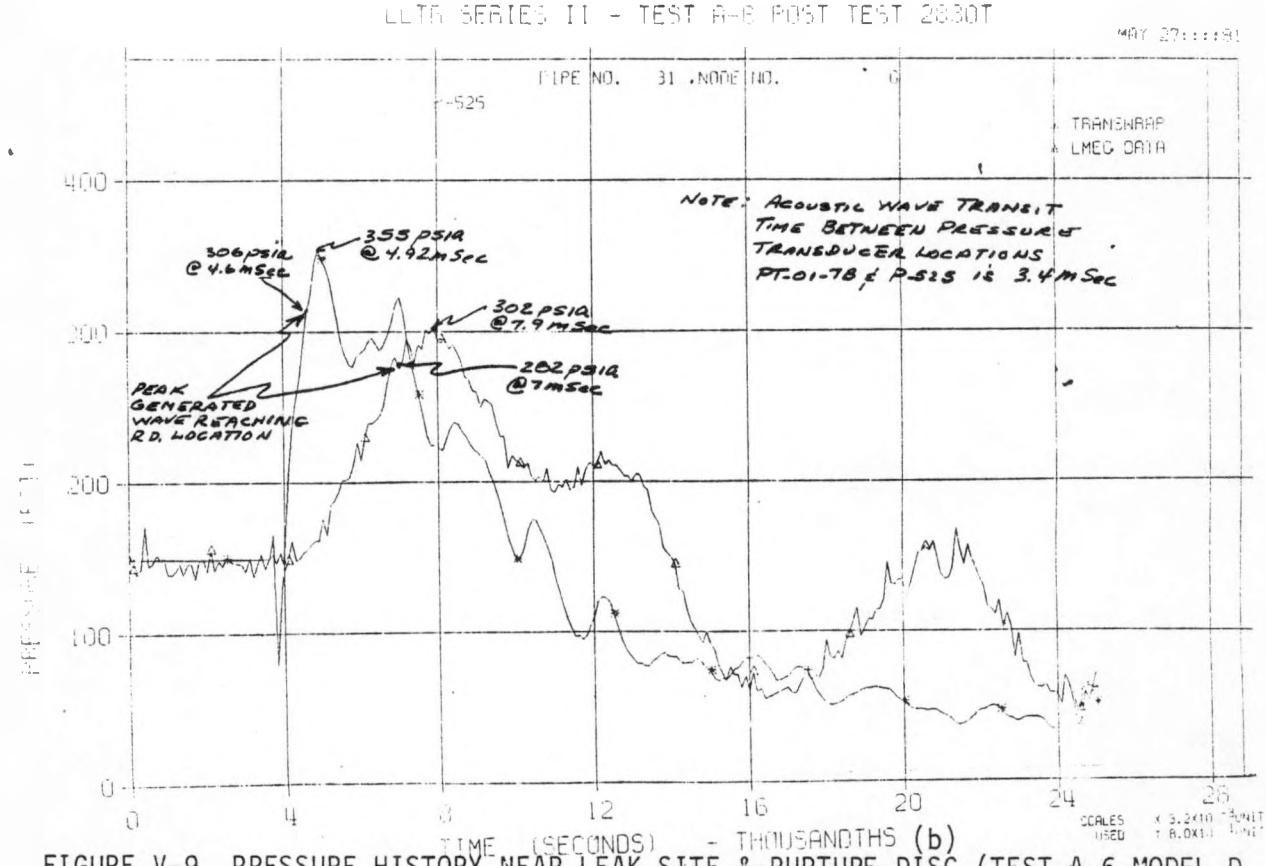

FIGURE V-9 PRESSURE HISTORY NEAR LEAK SITE & RUPTURE DISC (TEST A-6 MODEL D PLUS TEST DATA)

TEST A-6 MODEL F

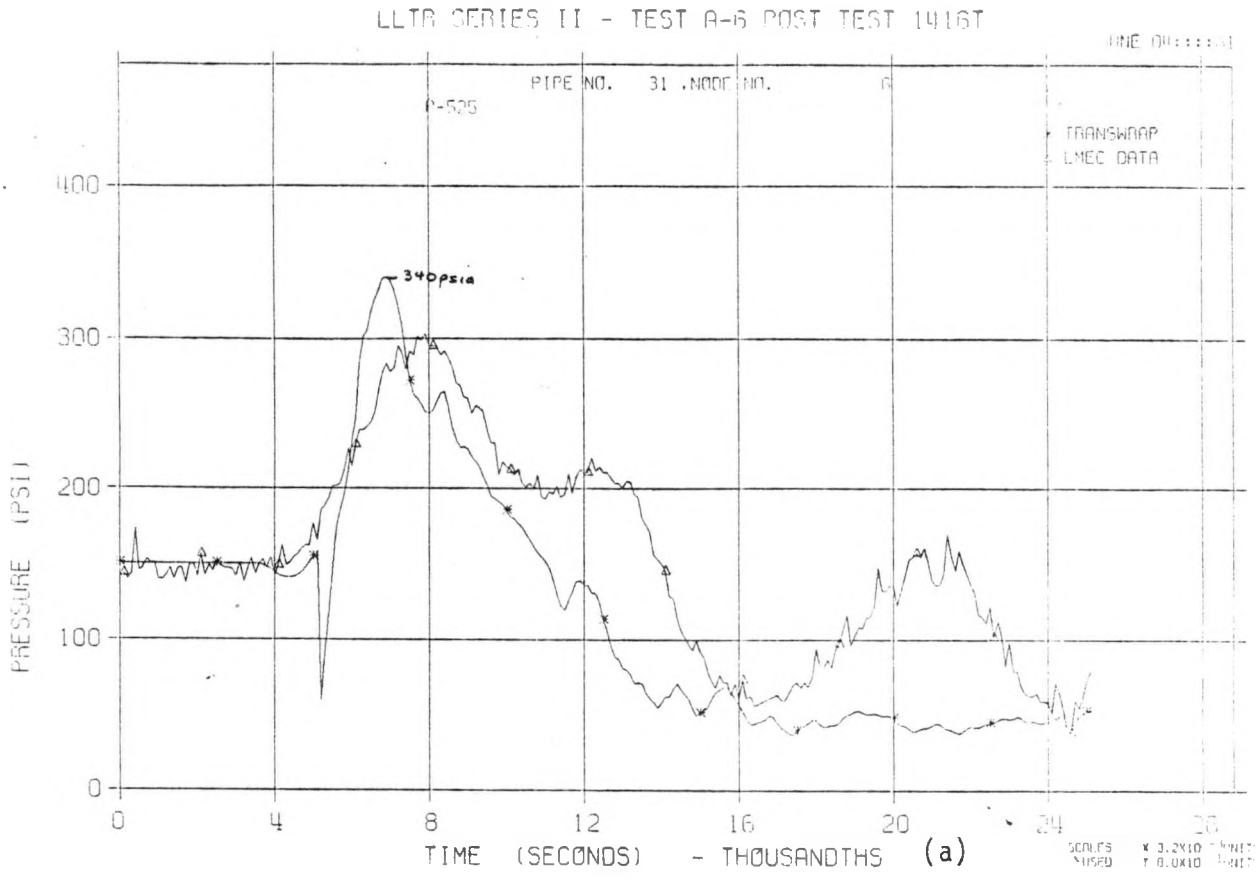

PL 13

TEST A-6 MODEL G

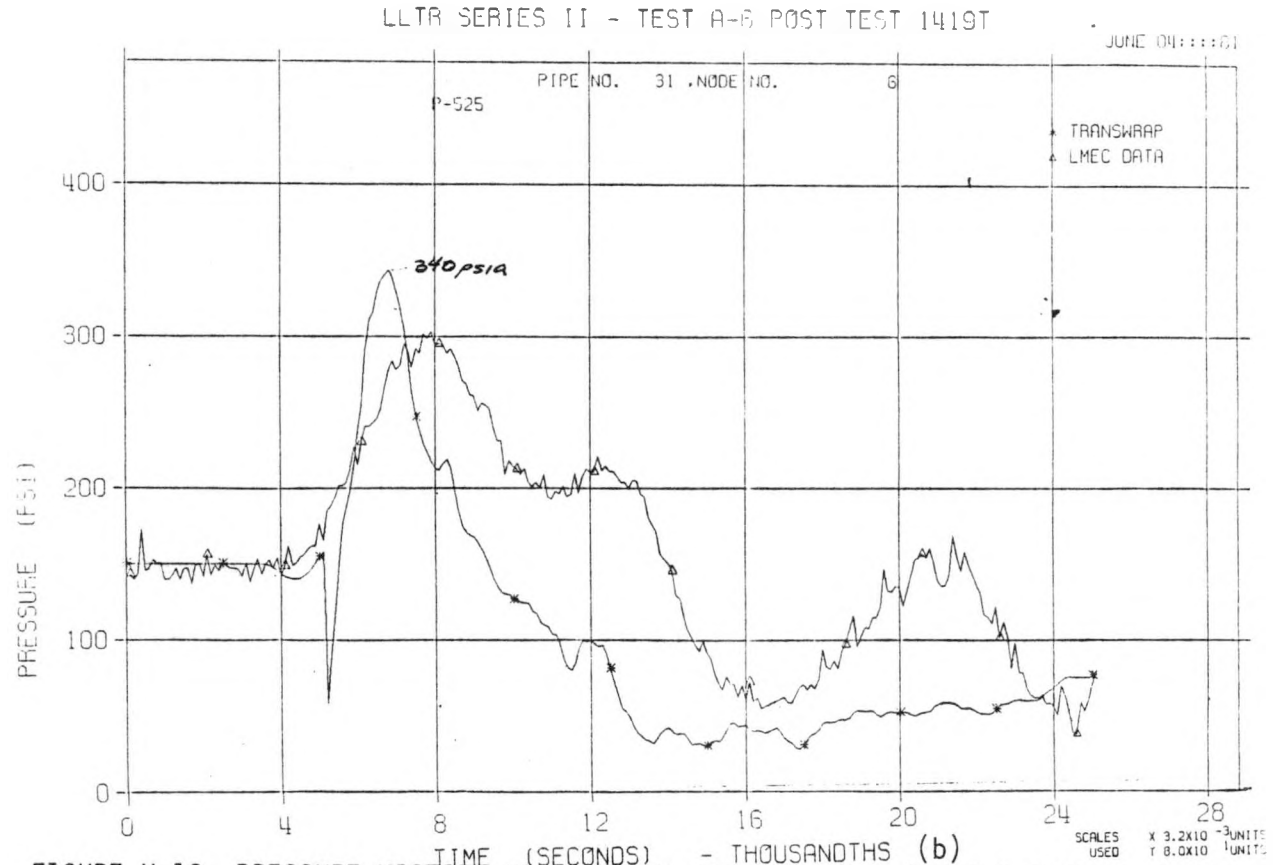

FIGURE V-10 PRESSURE HISTORY UPSTREAM OF RUPTURE DISC (TEST A-6 MODEL F & G PLUS TEST DATA)

PL 19

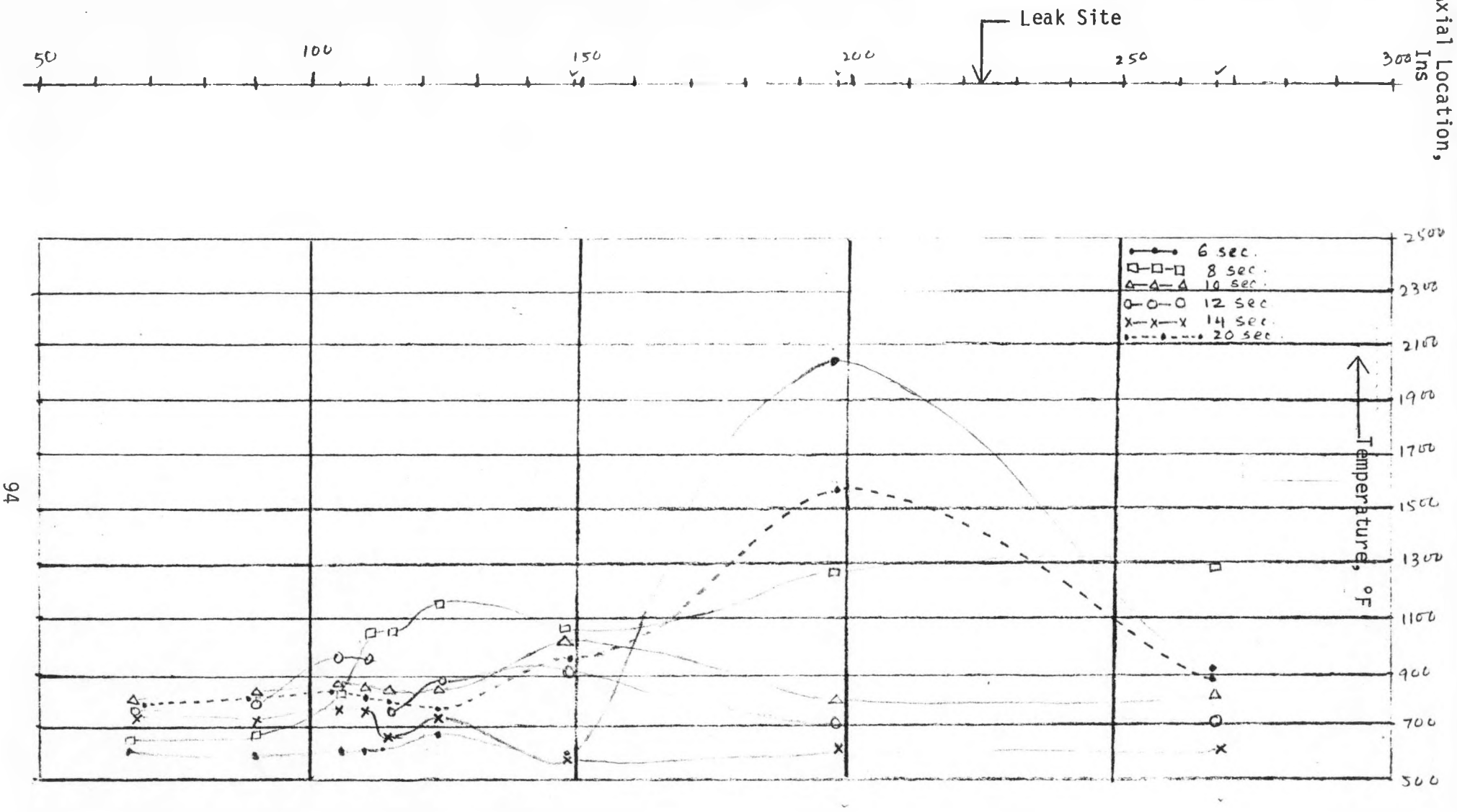

Figure V-11 Temperature Distribution Along Tube 4182
Located 2.11 inches From Rupture Tube

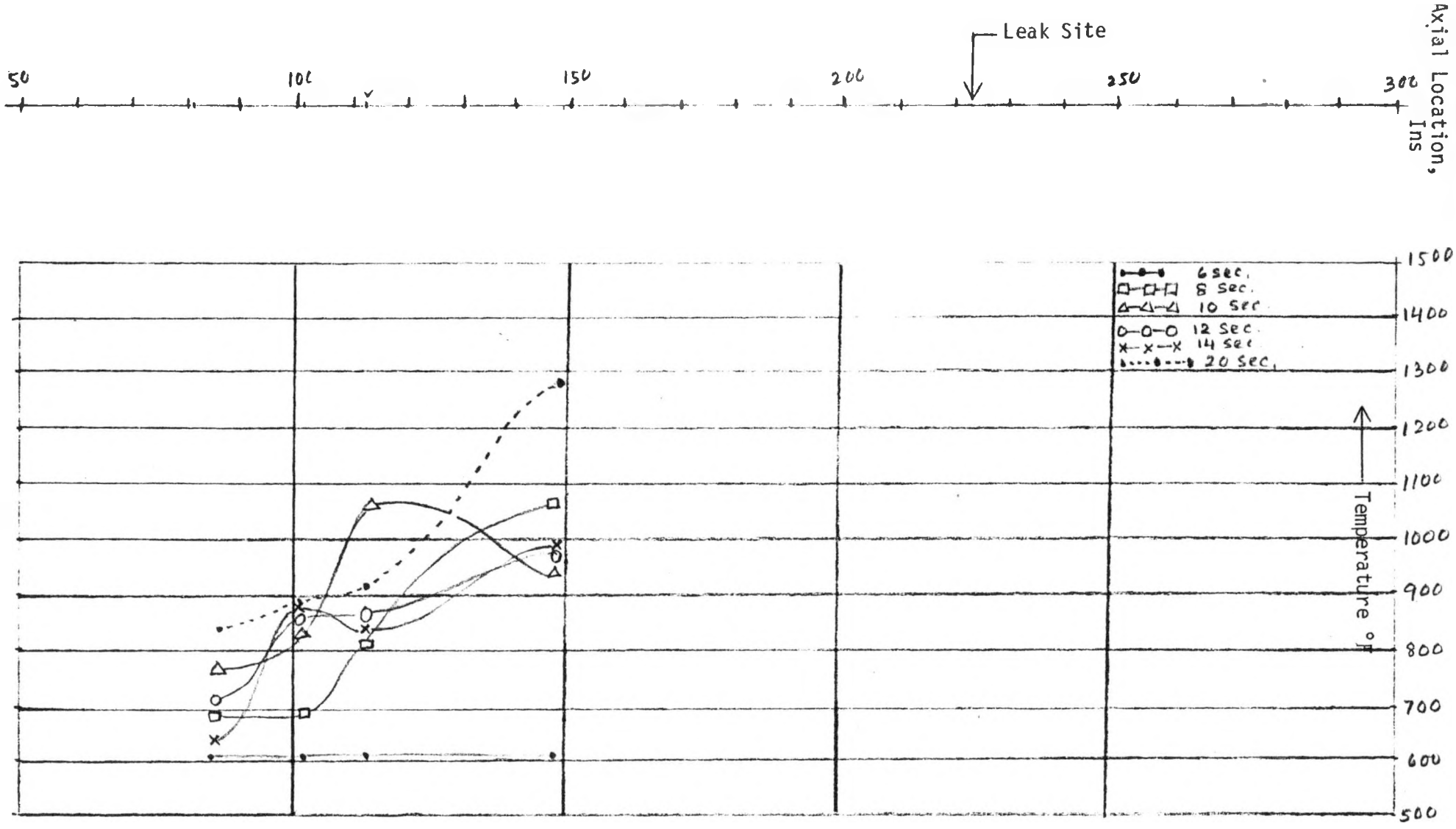

Figure V-2 Temperature Distribution Along Tube 4116
Located 6.11 inches From Rupture Tube

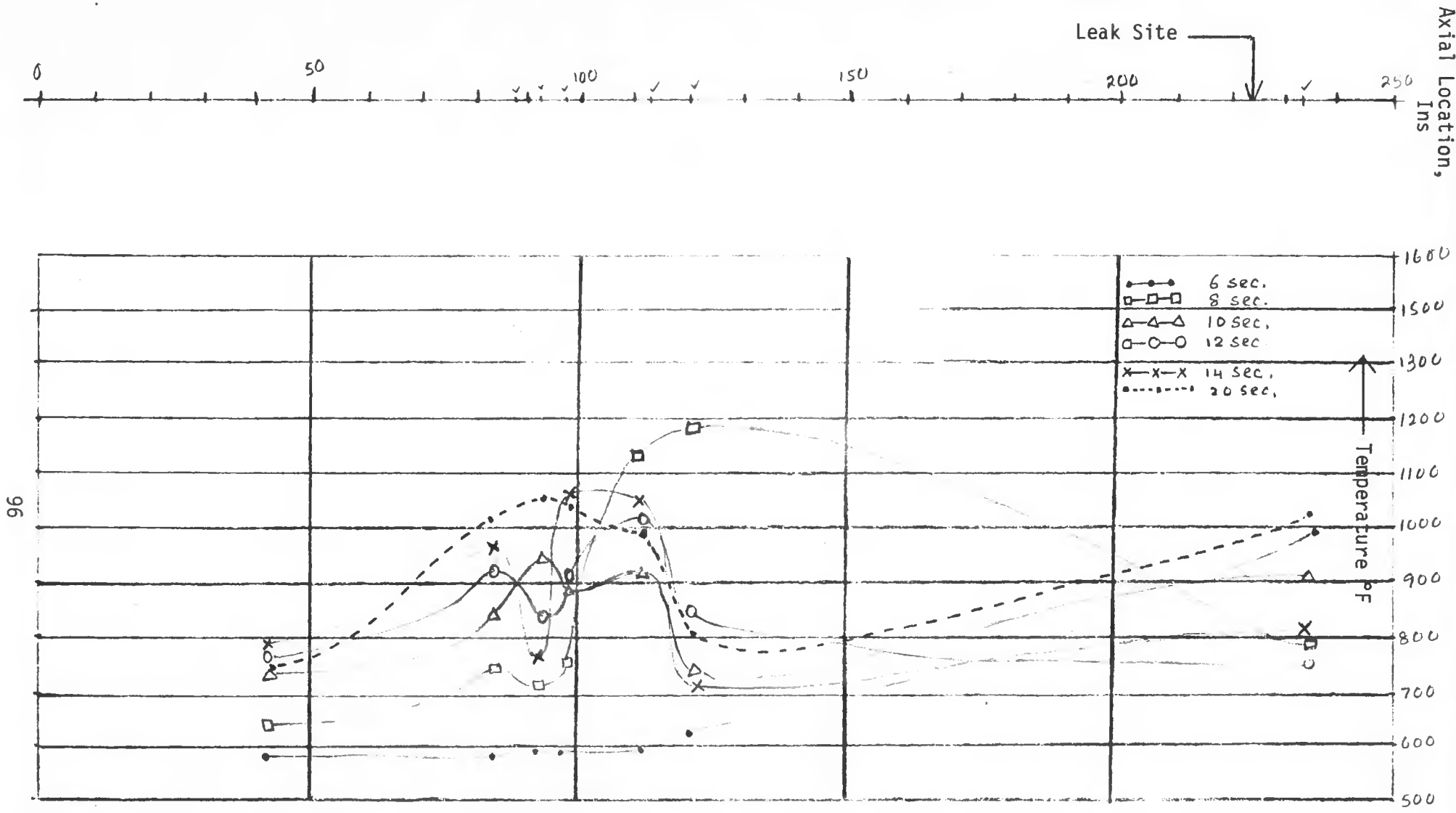

Figure V-13 Temperature Distribution Along Tube 4166
Located 2.11 inches From Tupture Tube

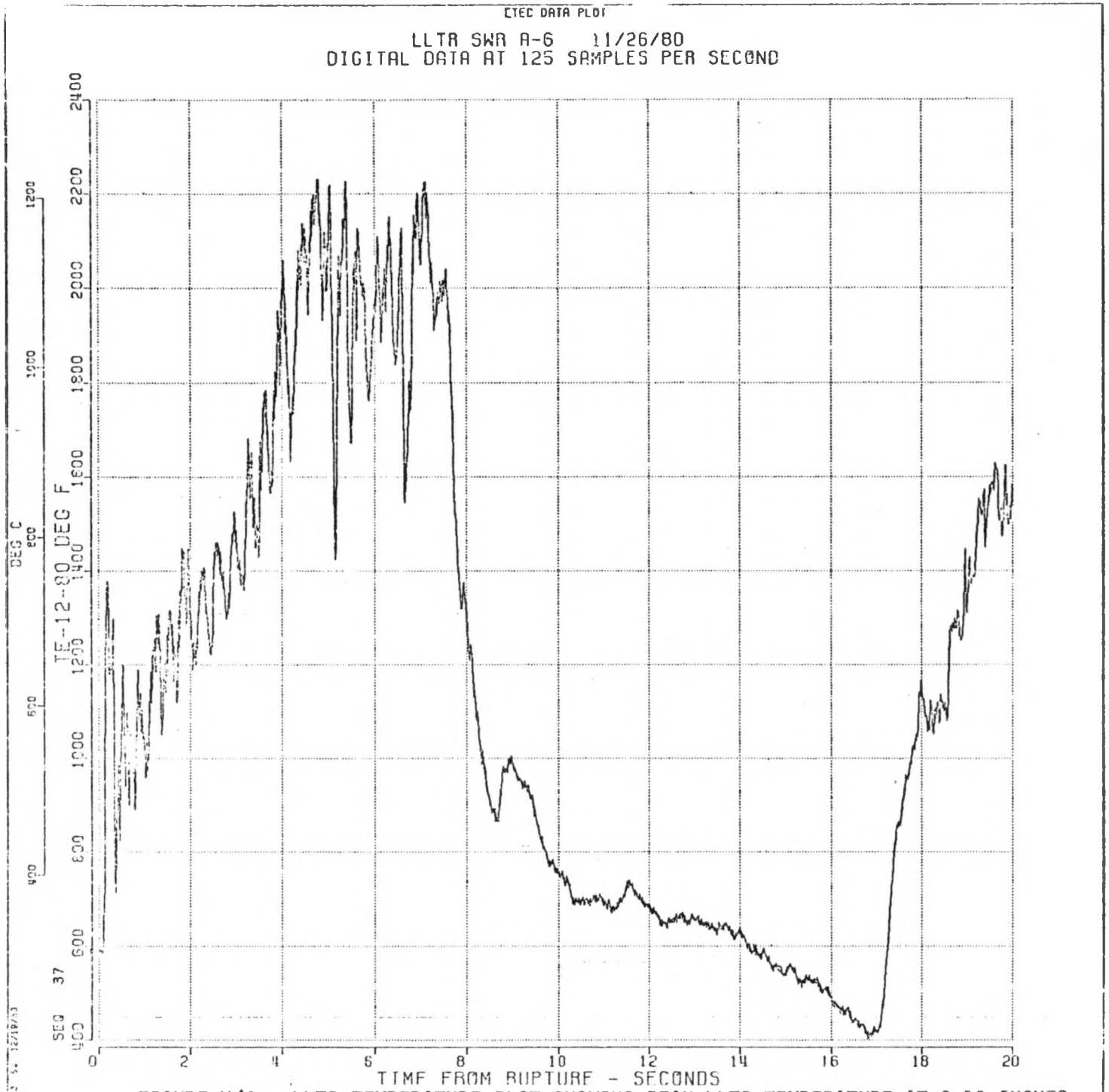

FIGURE V-14 LLTI TEMPERATURE PLOT SHOWING PEAK LLTI TEMPERATURE AT 2.11 INCHES RADIALLY AND 26 INCHES BELOW A-6 LEAK SITE (TE-12-80 TUBE 4182)

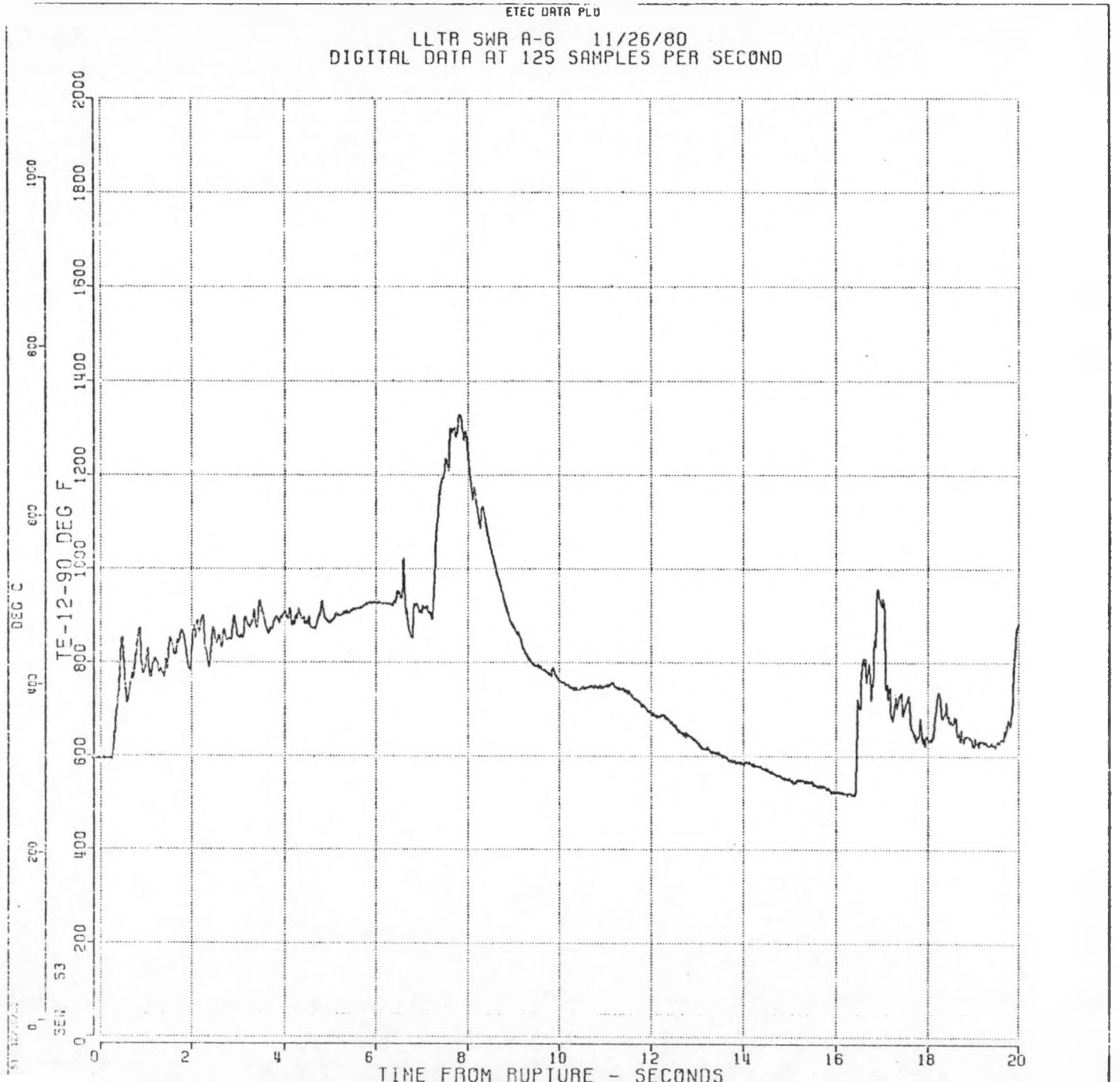

FIGURE V-15 LLTI TEMPERATURE PLOT SHOWING TEMPERATURE AT 2.11 INCHES RADIALLY AND 10 INCHES ABOVE A-6 LEAK SITE (TE-11-90 TUBE 4166)

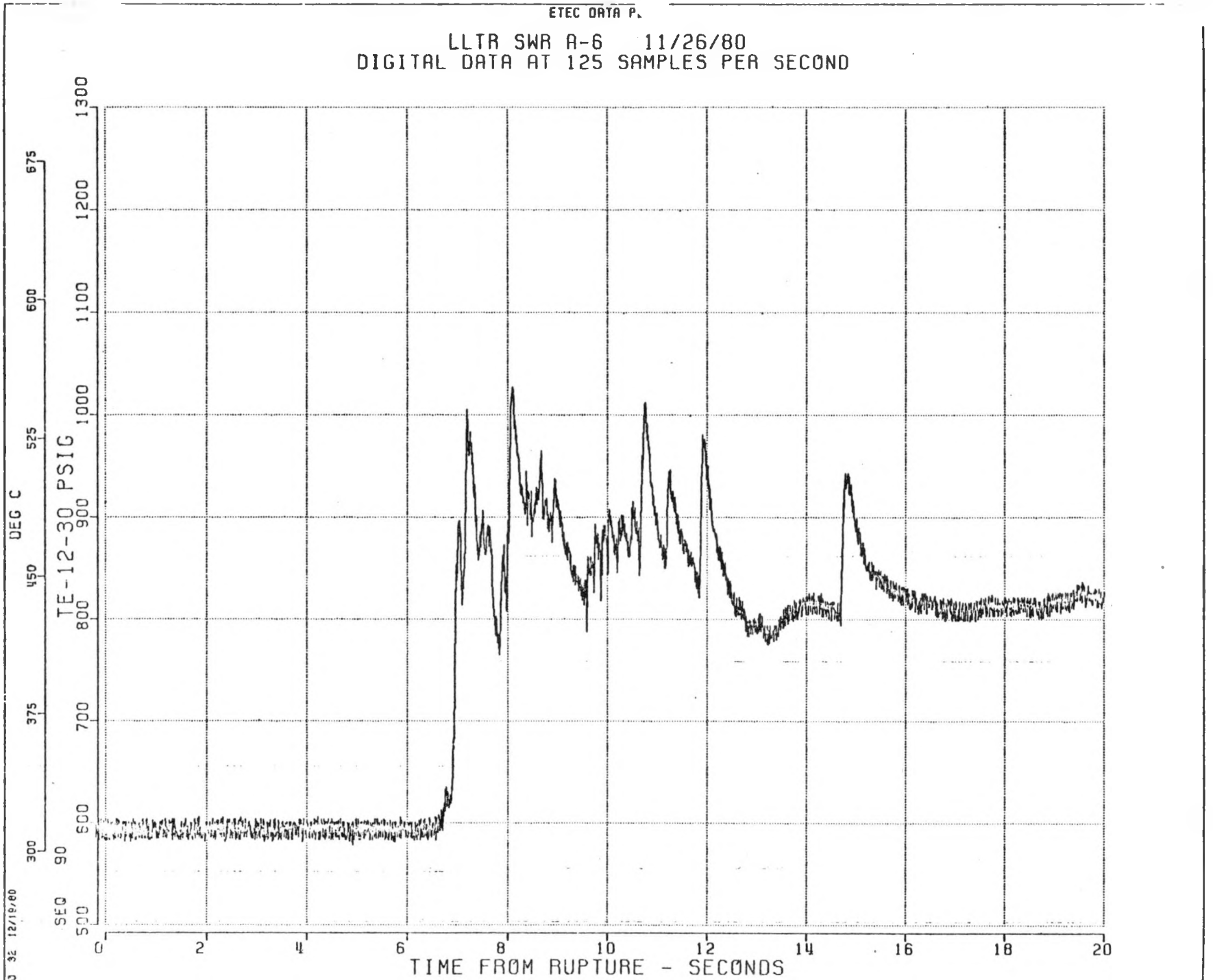

FIGURE V-16 LLTI TEMPERATURE PLOT SHOWING TEMPERATURE 2.11 INCHES RADIALLY AND 118 INCHES BELOW THE A-6 LEAK SITE (TE-12-80 TUBE 4182)

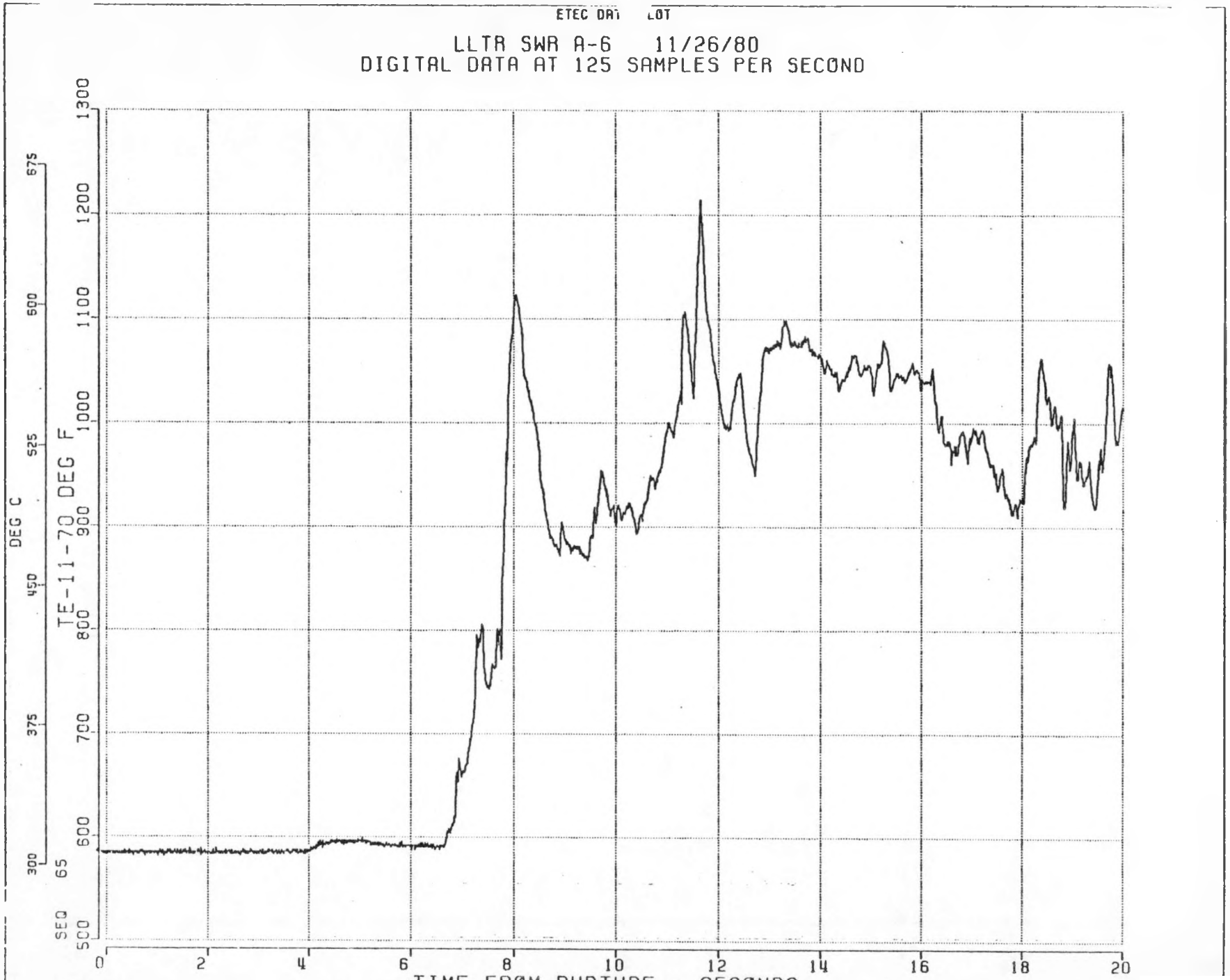

Figure V-7 LLTI Temperature Plot Showing Temperature 2.11 inch Radially and 110 inches Below A-6 Leak Site (TE-11-70, Tube A166)

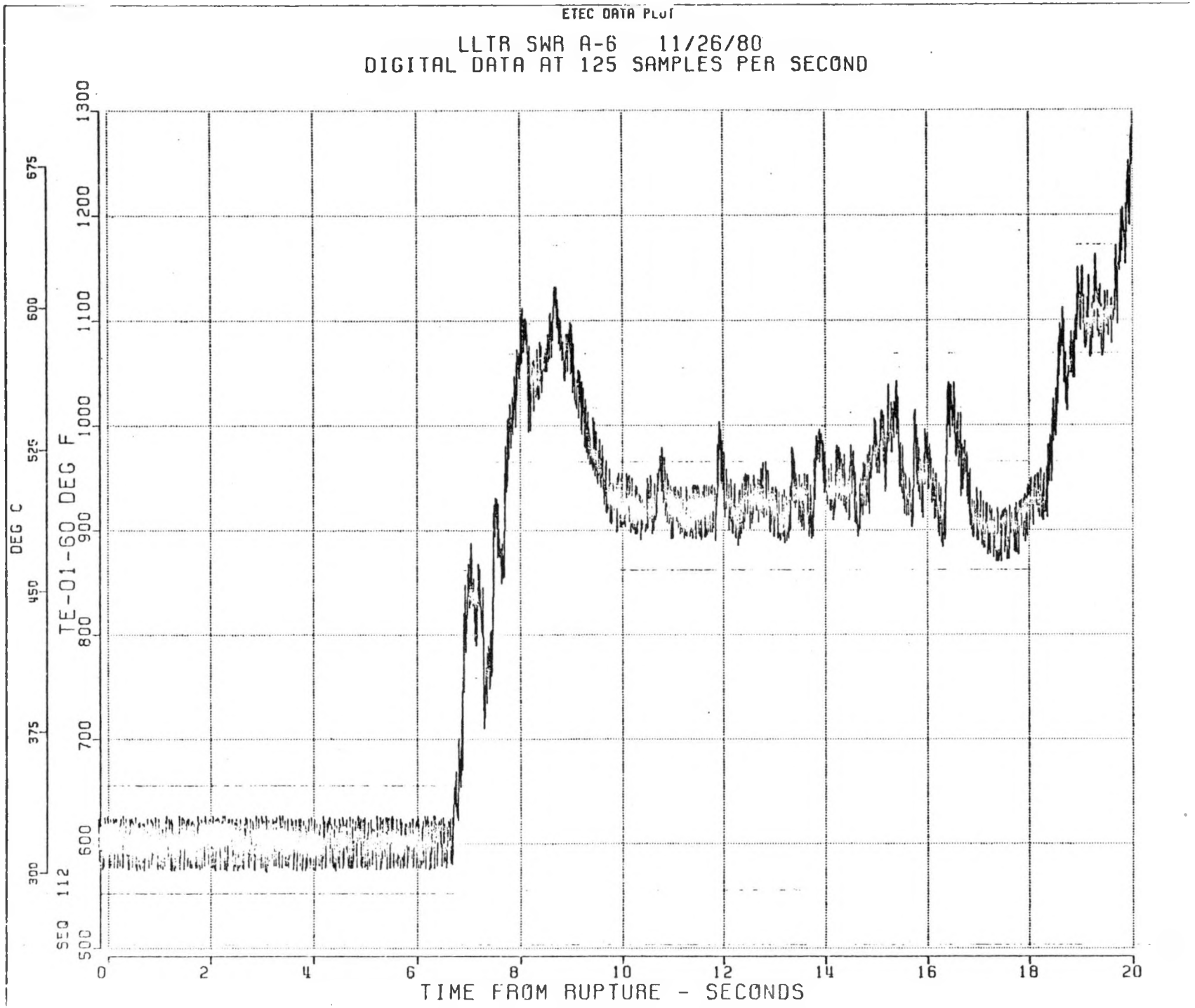

Figure V-18 LLTI Temperature Plot Showing Temperature 6.11 inches Radially and 74 inches Below A-6 Leak Site (TE 01-60, Tube 4116)

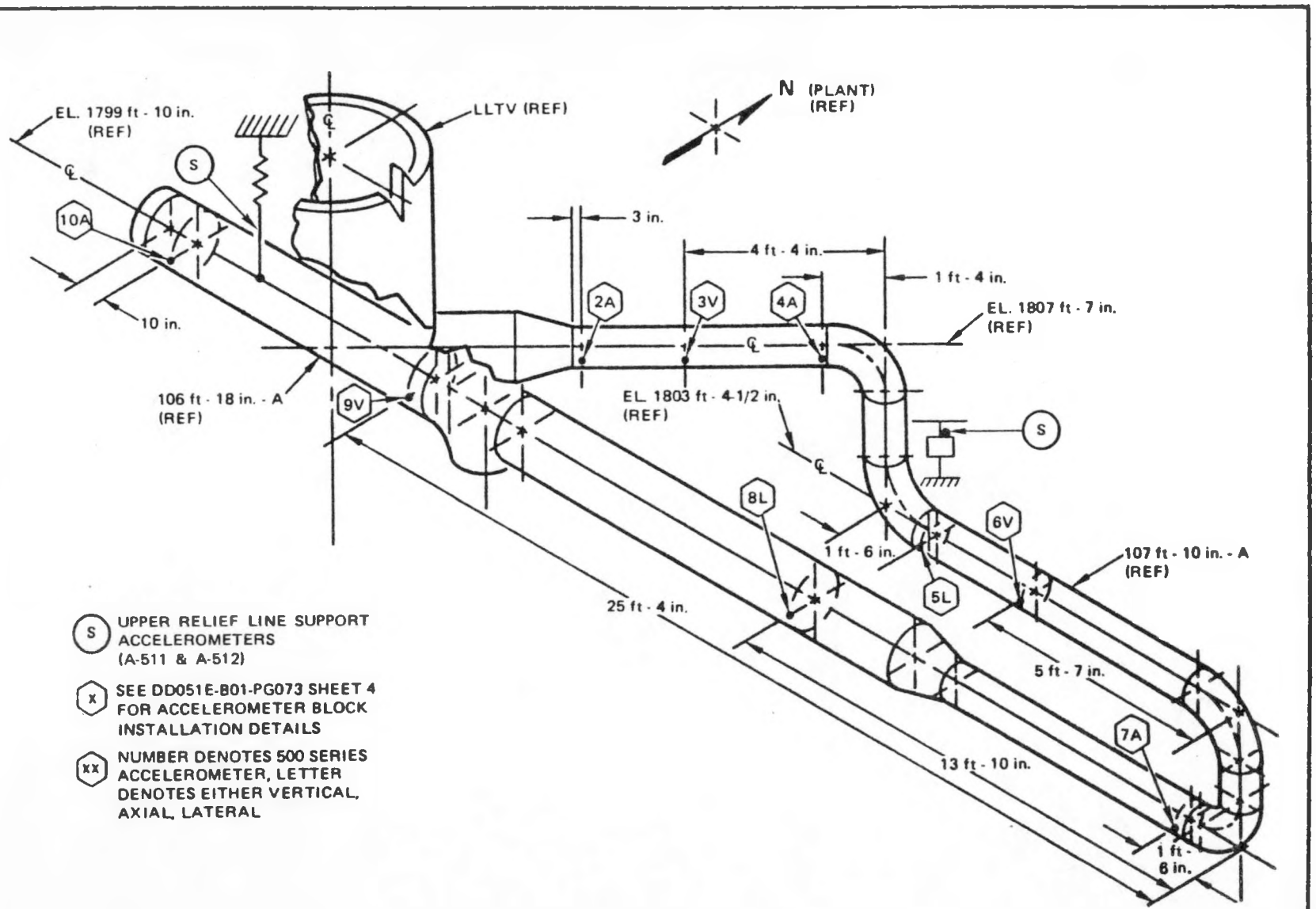

Figure V-19- Location of Load Accelerometers on Secondary Sodium System

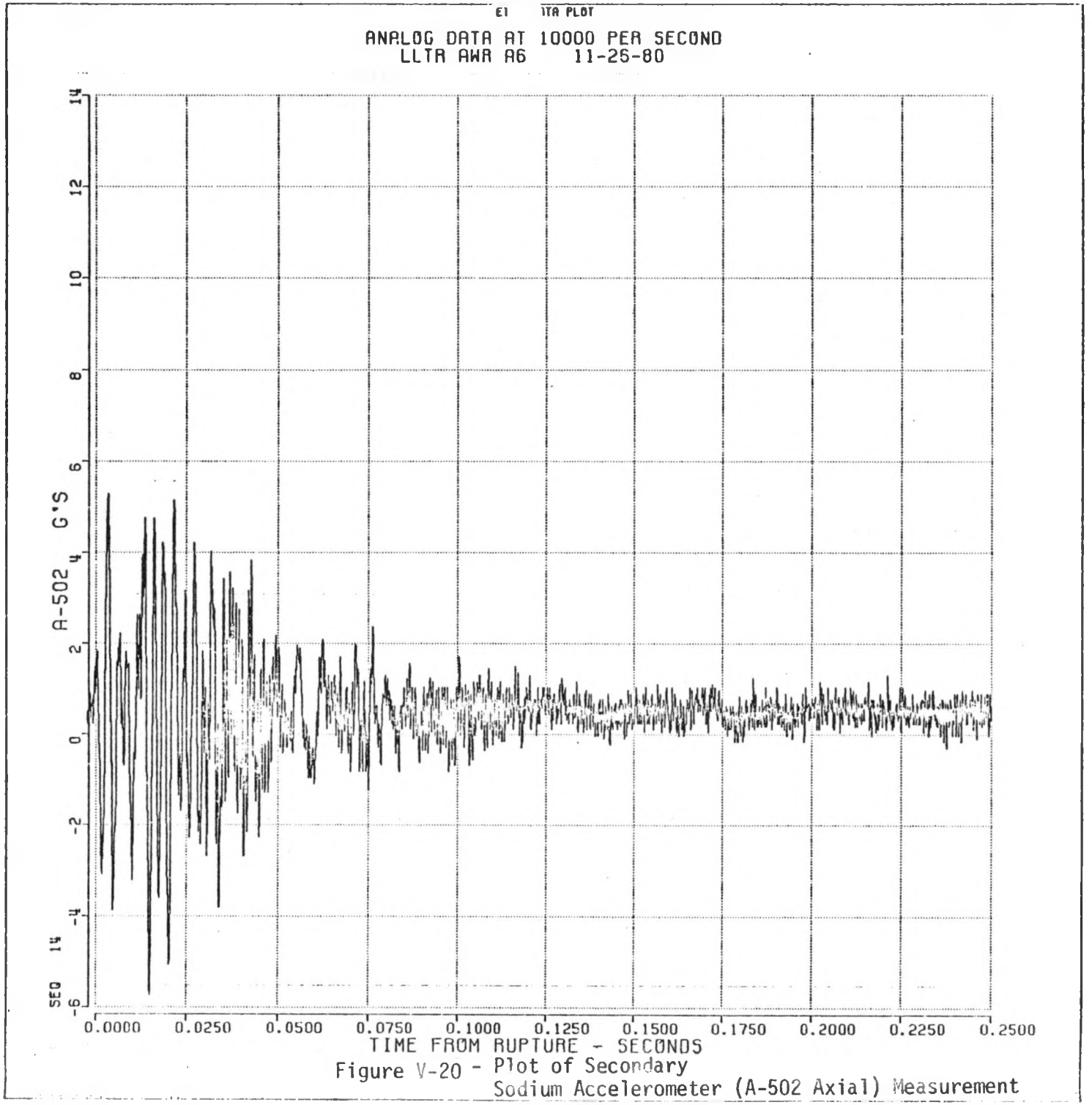

Figure V-20 - Plot of Secondary Sodium Accelerometer (A-502 Axial) Measurement

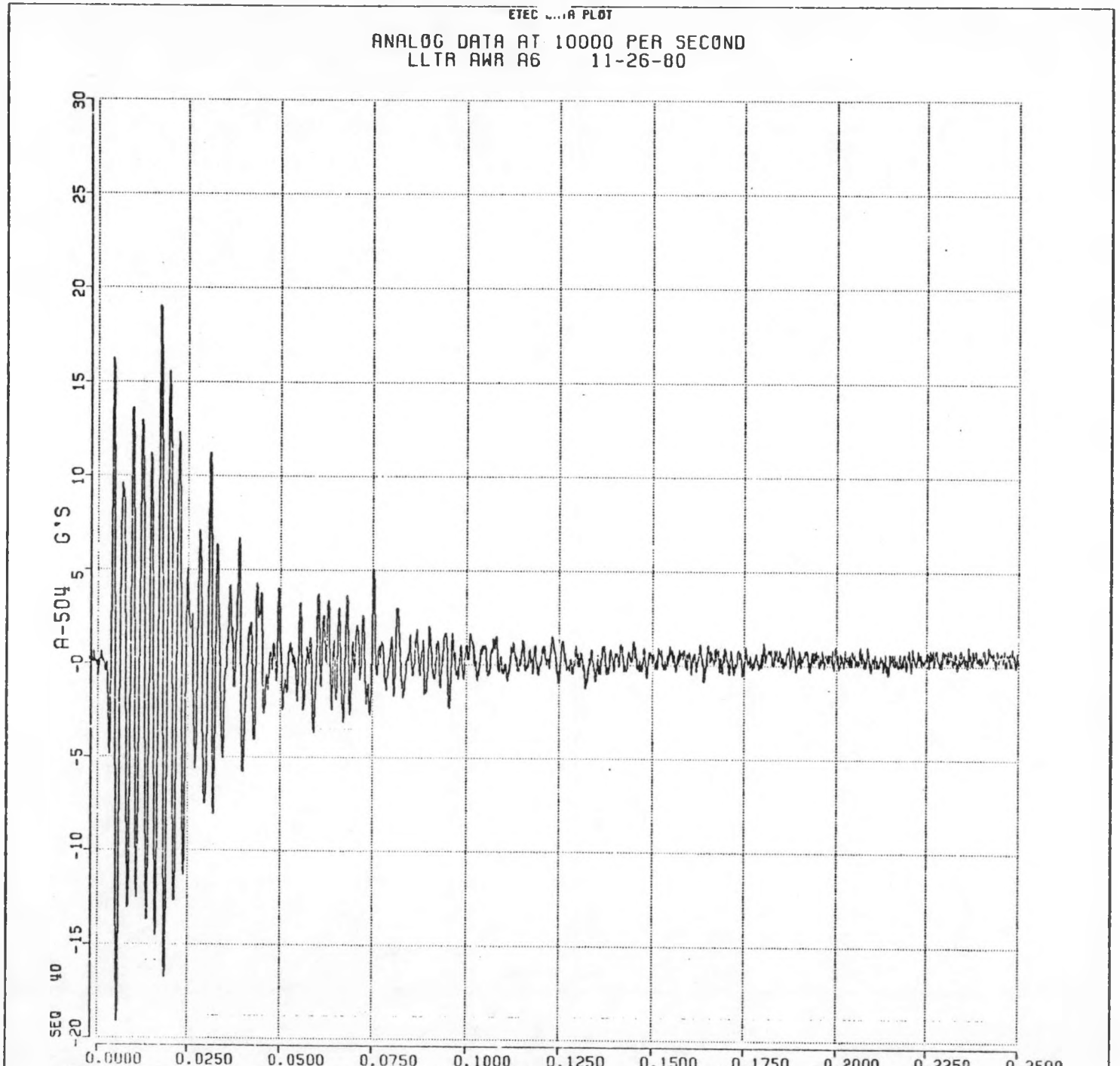

Figure V-21 - Plot of Secondary Sodium Accelerometer (A-504 Axial) Measurement

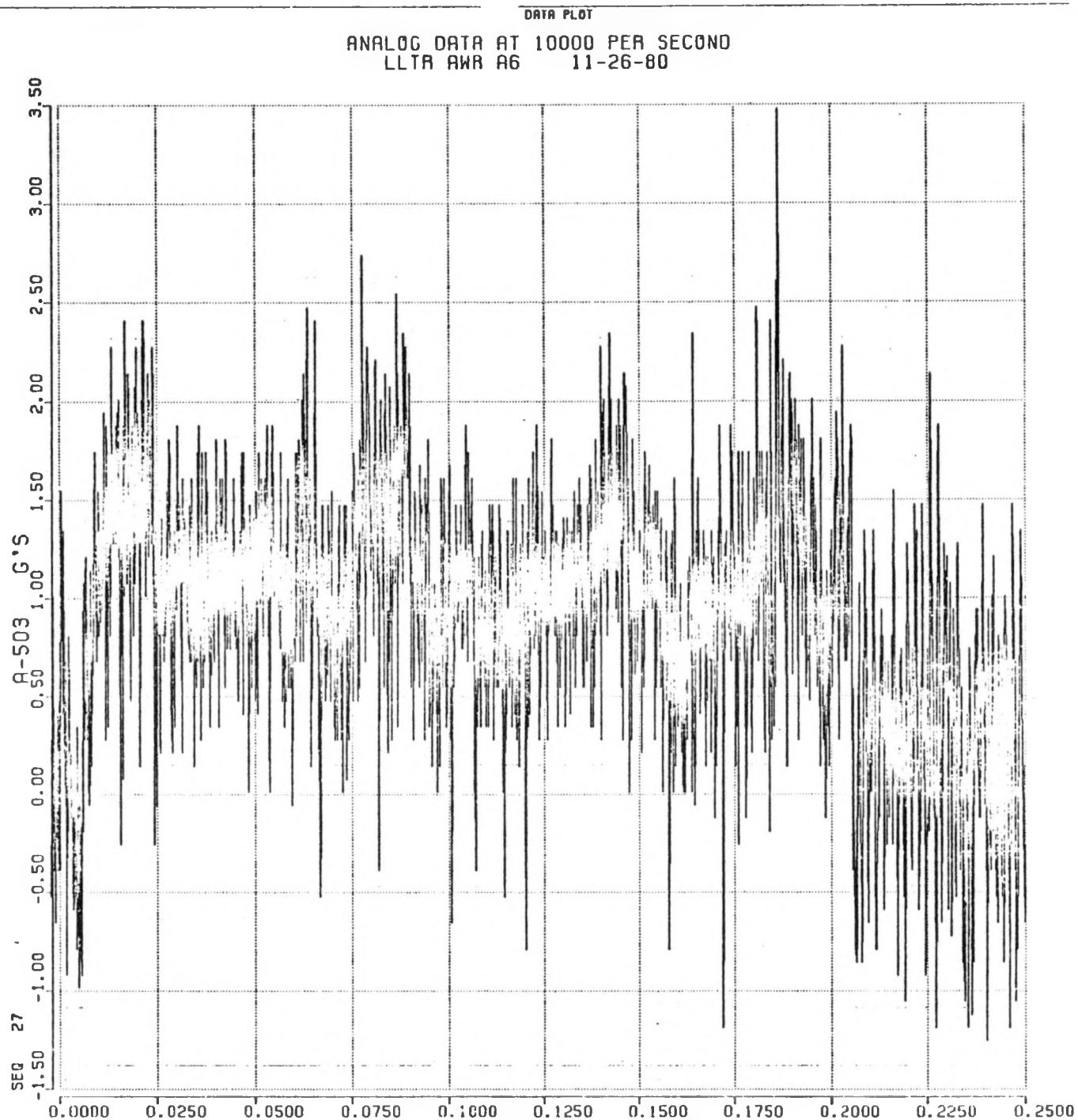

Figure V-22 - Plot of Secondary Sodium System Accelerometer (A-503 Vertical) Measurement

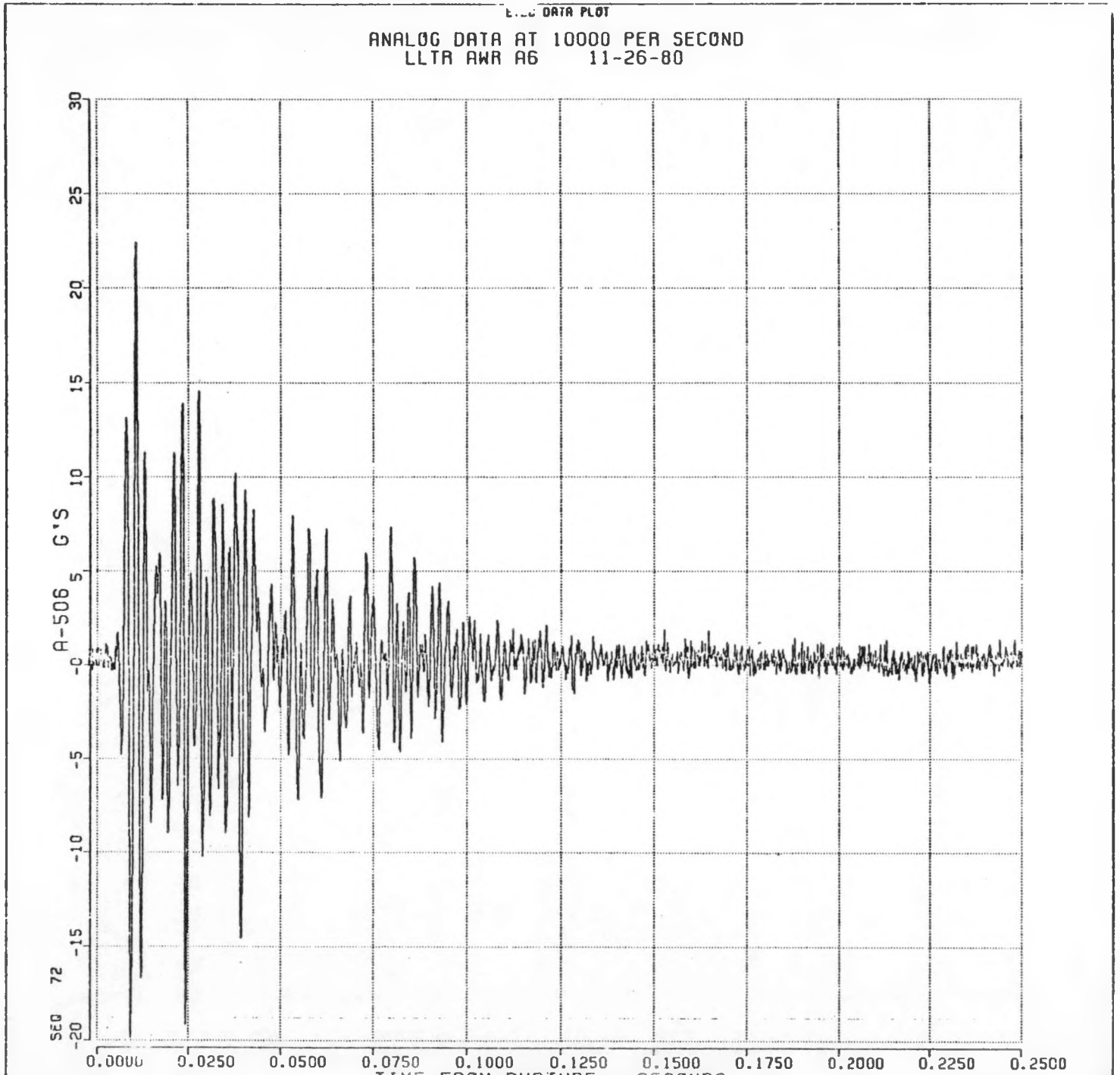

Figure V-23 - Plot of Secondary Sodium System Accelerometer (A-506 Vertical) Measurement

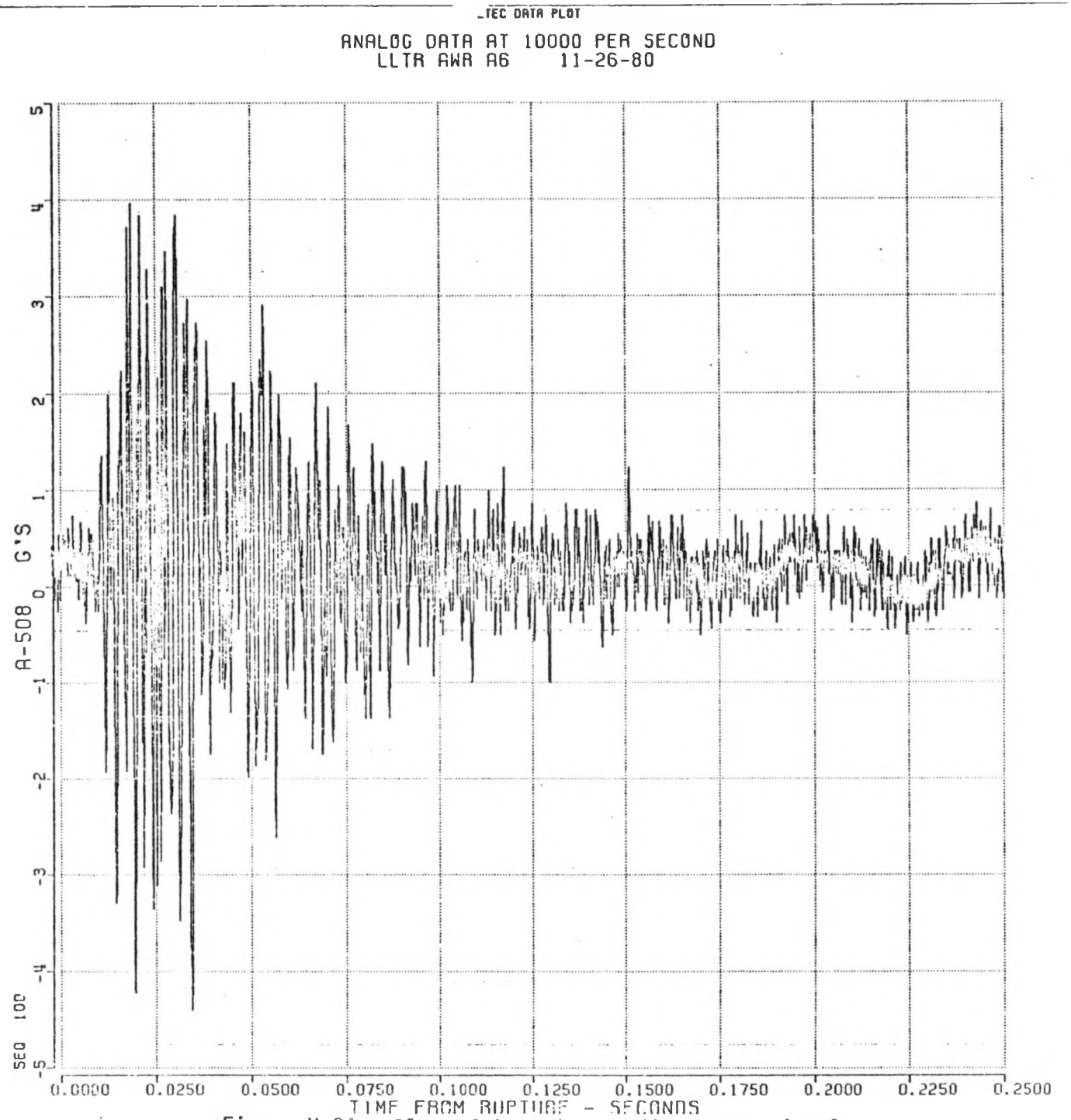

Figure V-24- Plot of Secondary Sodium System Accelerometer (A-508 Lateral) Measurement

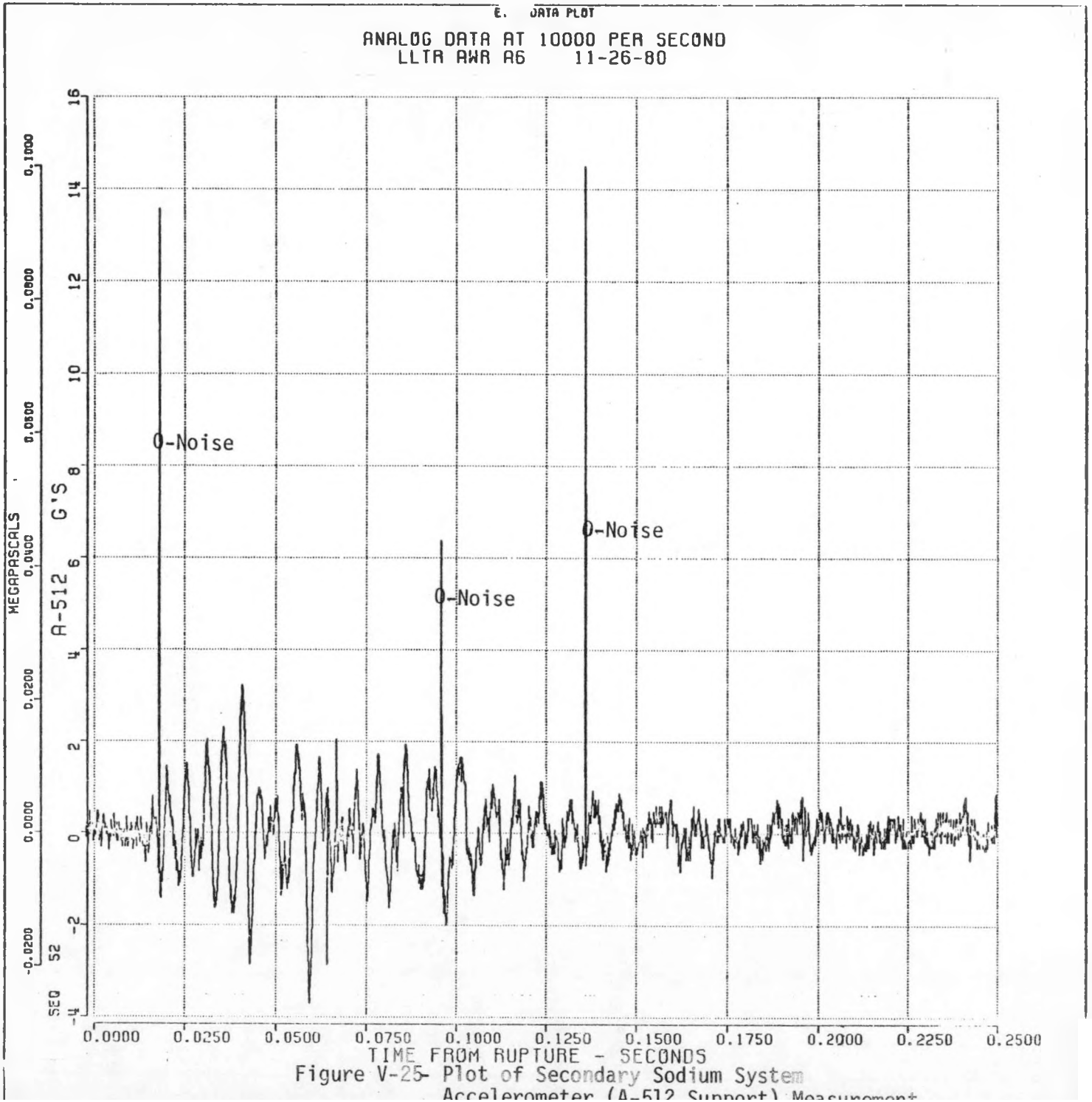

Figure V-25- Plot of Secondary Sodium System Accelerometer (A-512 Support) Measurement

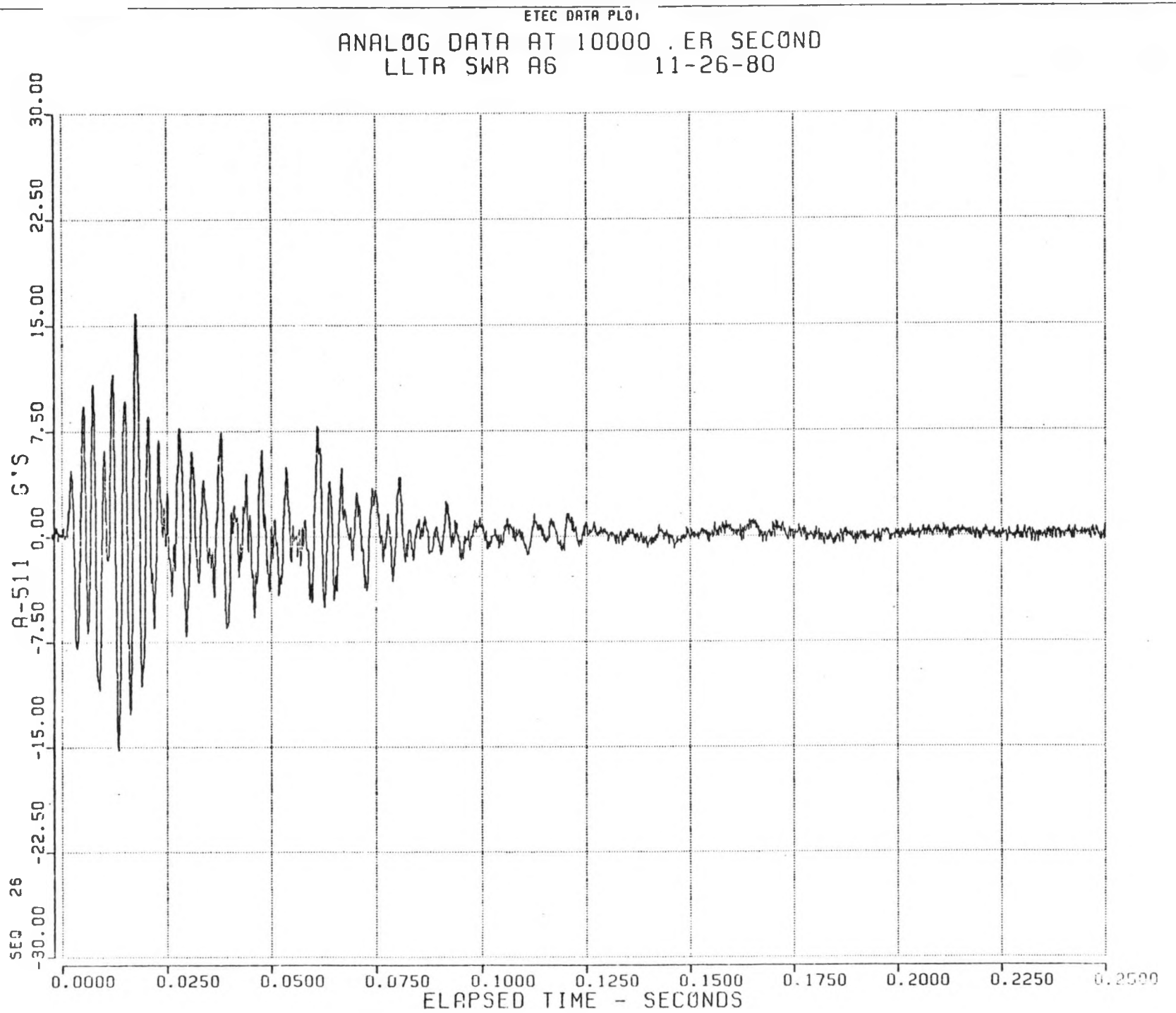

Figure V-26- Plot of Secondary Sodium System Accelerometer (A-511 Support) Measurement.

81-419-04

Figure VI-1. RUPTURE DISC BLADES AFTER TEST A-6

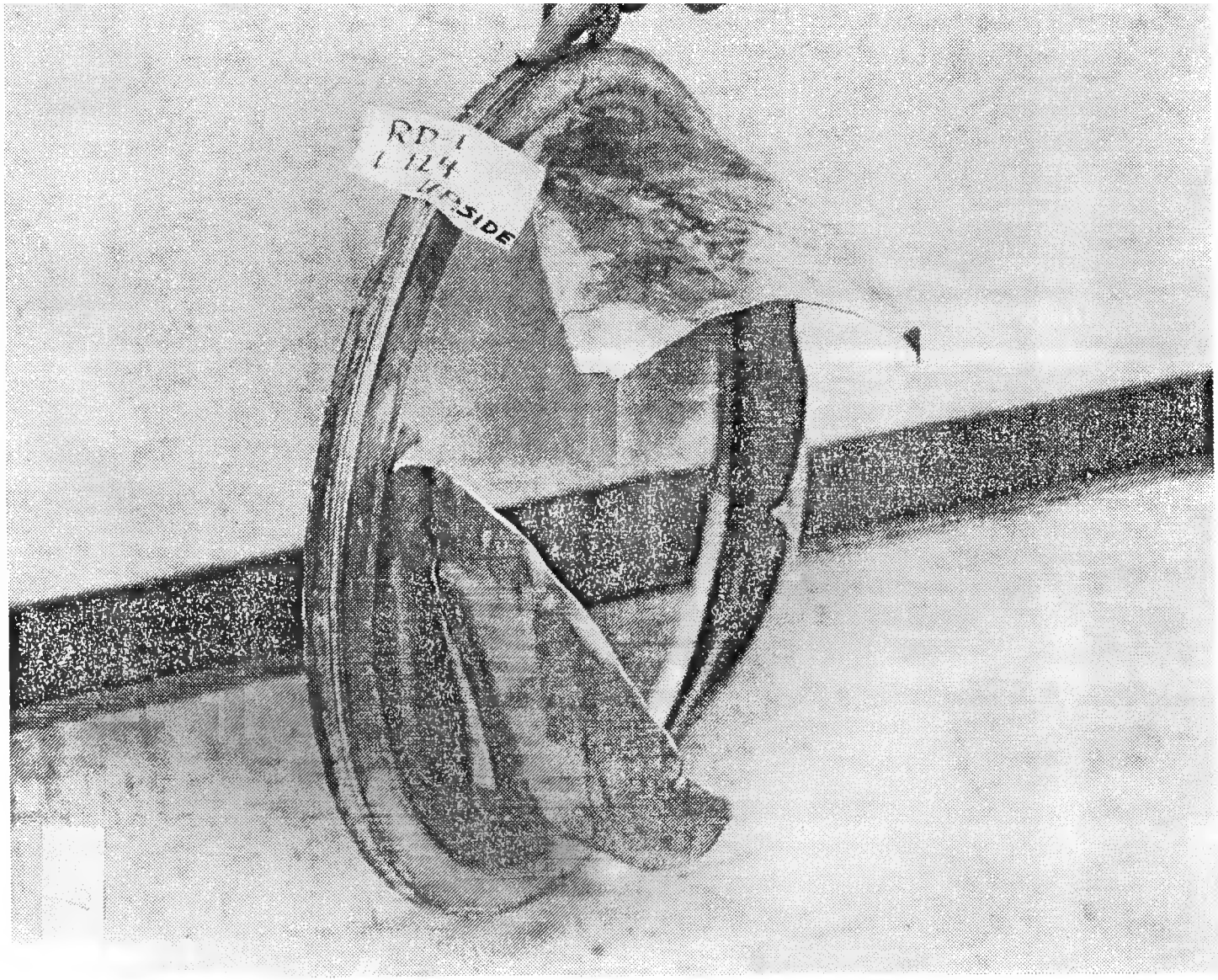

Figure VI-2. RD-1 UPSTREAM RUPTURE DISC AFTER TEST A-6

81-204-22

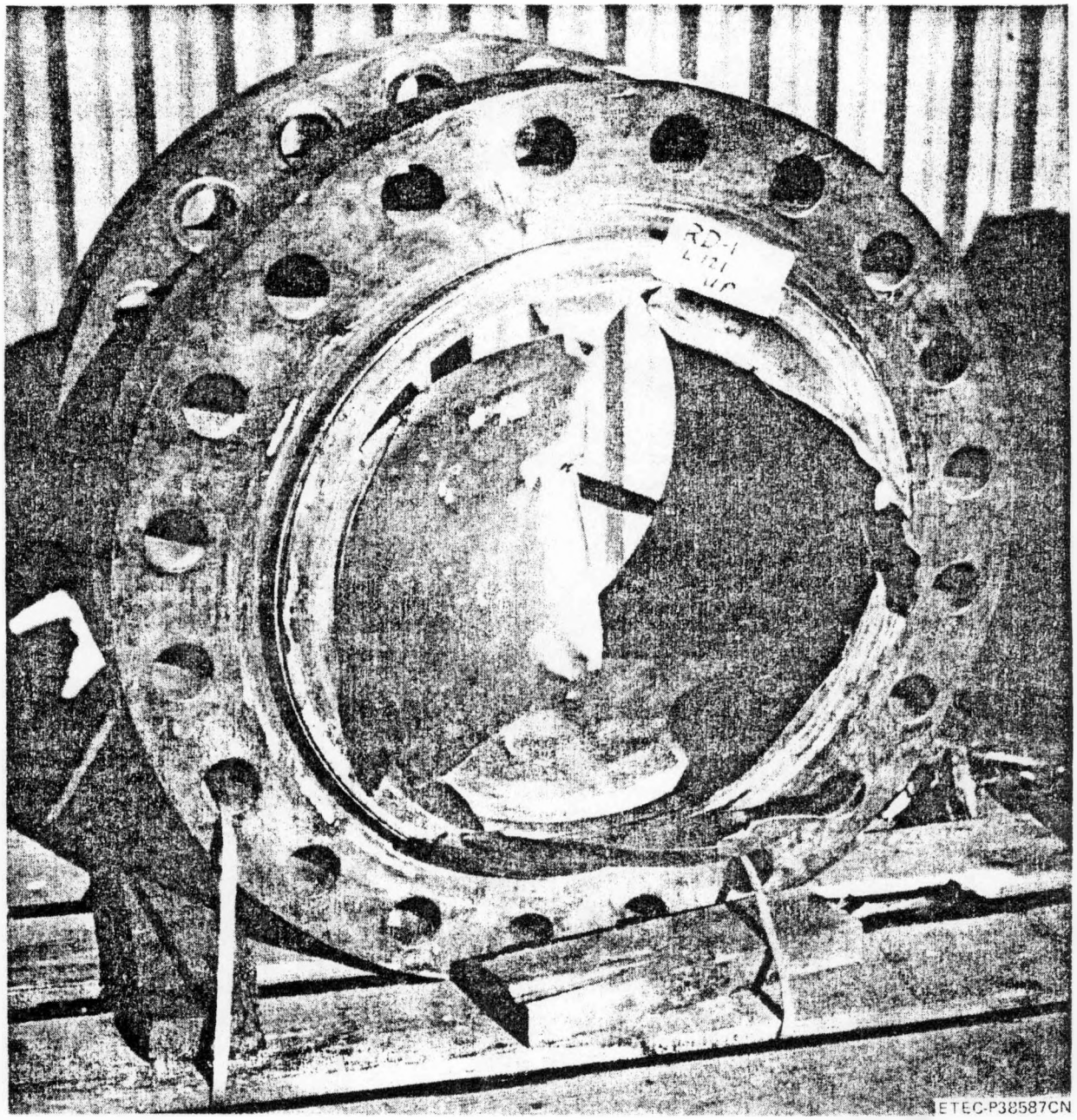

Figure VI-3. The Downstream RD-1 Disc from Another Angle with all Leafs in it

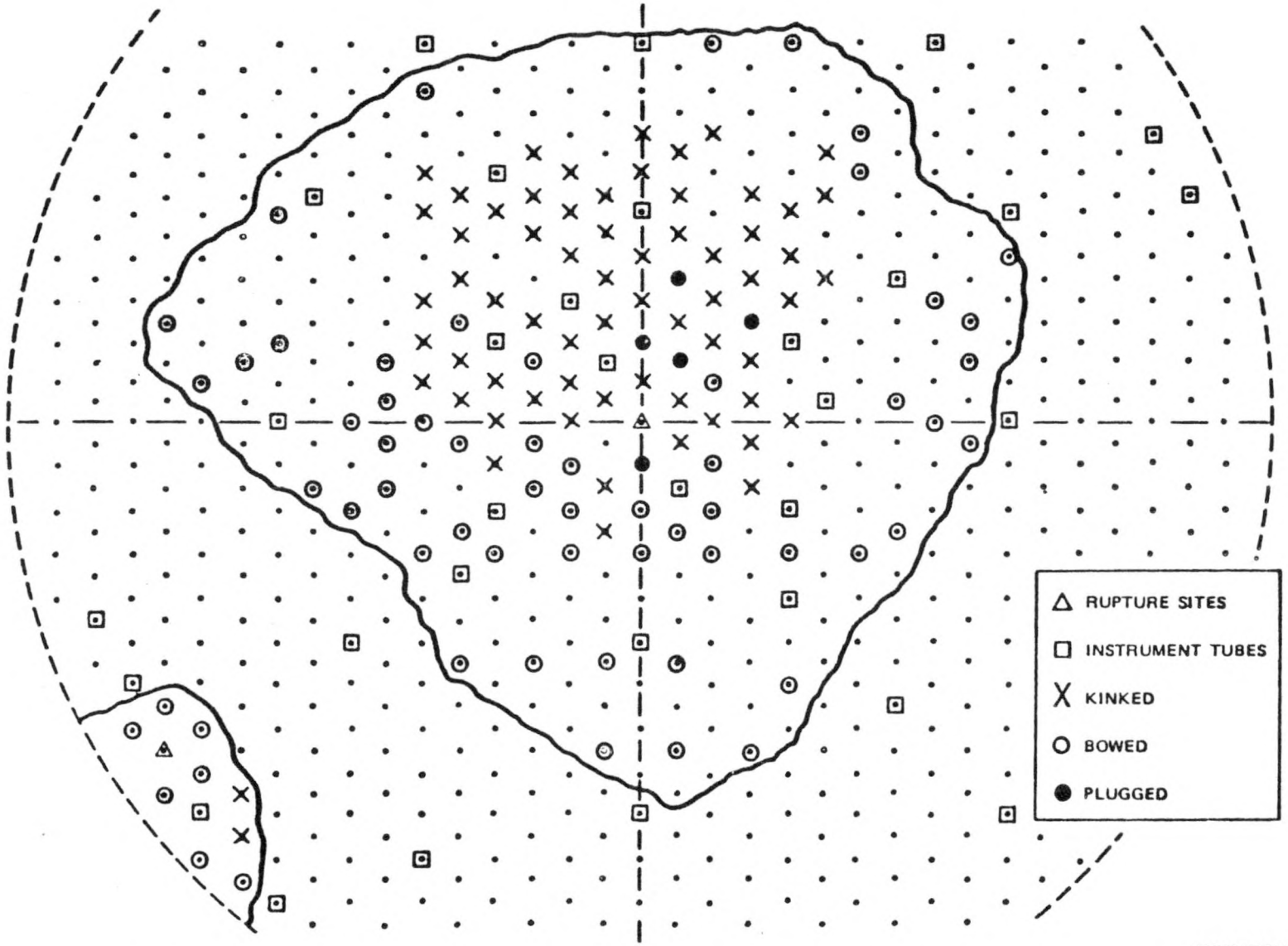

Figure VI-4 The Deformed Areas of SWRs A-3 and A-6; The Central A-3 Area Was Surveyed by Selected Peripheral Measurements That Ascertained Bowing ≥1/2 the Tube Spacing

Figure VI-5 Schematic of LLTR Relief Piping Showing Inspected Welds

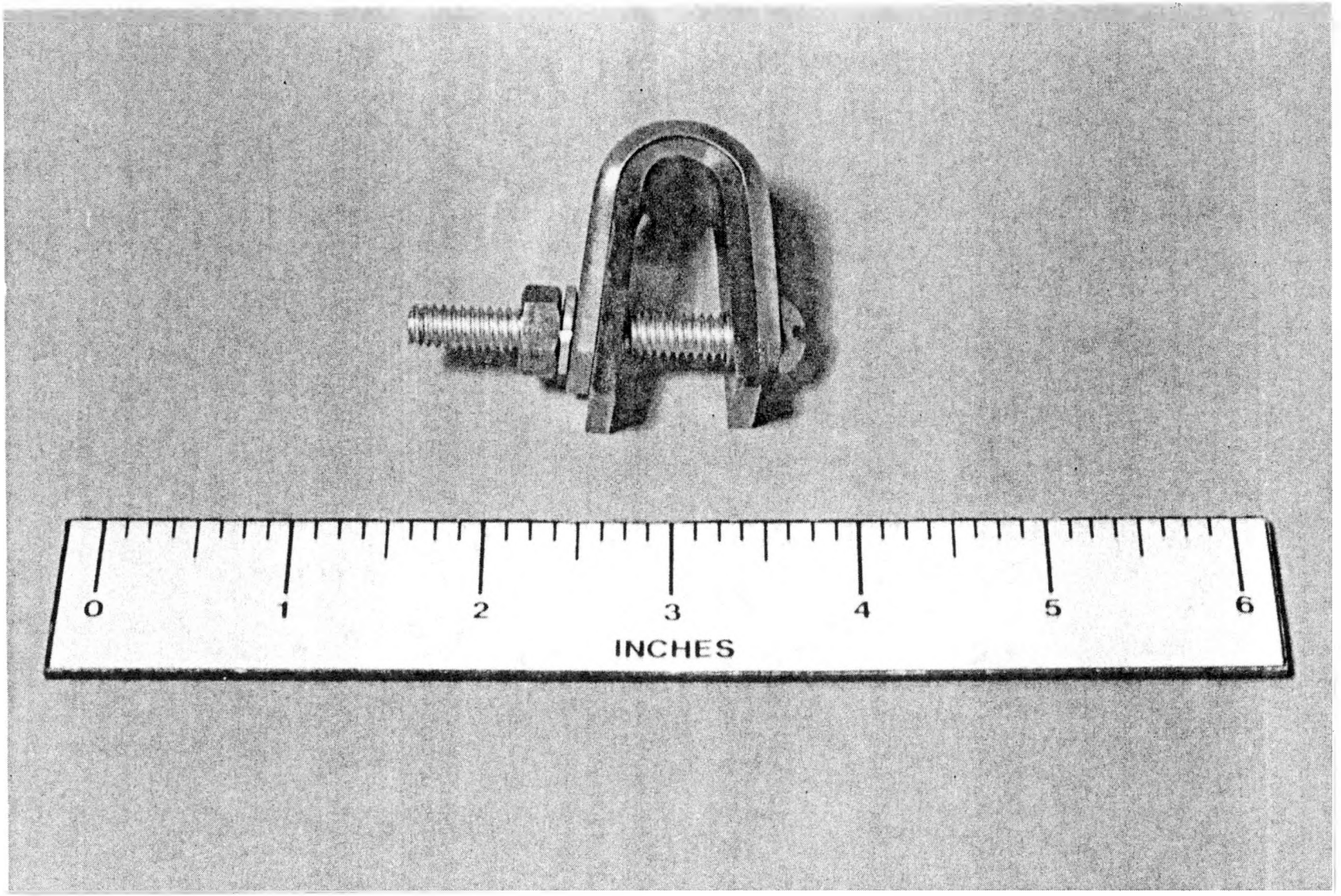

81-419-05

Figure VI-6 CREVICED U-BEND SPECIMEN INSTALLED IN LLTR RELIEF SYSTEM

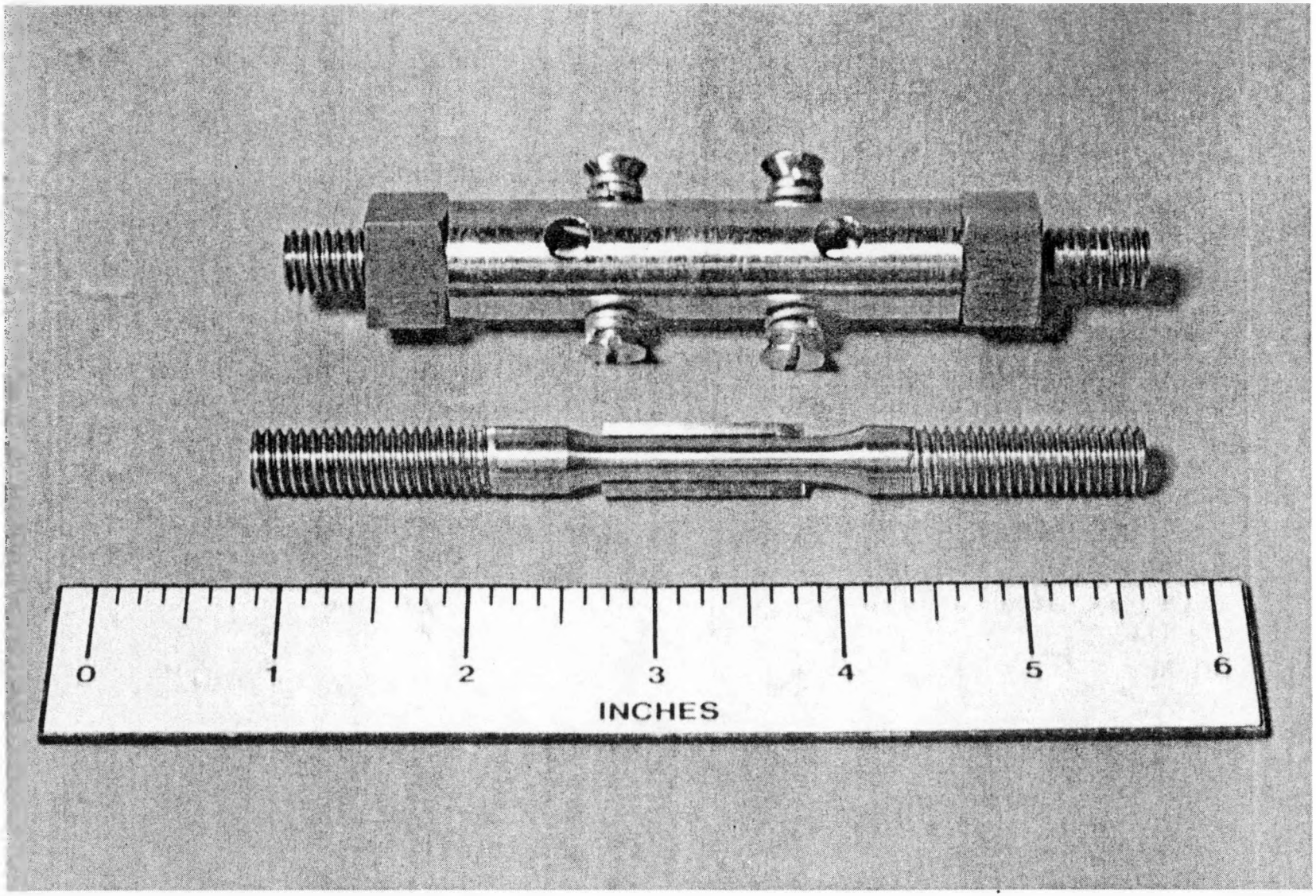

81-419-06

Figure VI-7 STRESSED CREVICED TENSILE BAR SPECIMEN INSTALLED IN LLTR RELIEF SYSTEM

APPENDIX A

TRANSWRAP INPUT LISTING

FOR

MODEL D

```
         1         2         3         4         5         6         7         8
12345678901234567890123456789012345678901234567890123456789012345678901234567890

11                                                                      CARD  1      1
0 999999. 999999. 999999.                                               CARD  2      2
00                                                                      CARD  3      3
   150.0    589.  54.73     43.9                                       CARD  4      4
                                                                        CARD  5      5
1                                                                       CARD  6      6
     1.0     0.0     0.0     0.0     0.0     0.0                        CARD  7      7
                                                                        CARD  8      8
                                                                        CARD  9      9
                                                                        CARD 10     10
                                                                        CARD 11     11
     5.0     2.3     0.0                                                CARD 12     12
   0.001 0.00098          7.5                                           CARD 13     13
T                                                                       CARD 14     14
***** SERIES 2 TEST A6 LLTR POST TEST EVALUATION                        CARD 15     15
***** INJECTION FROM RELAP CASES T2450 +T7506                           CARD 16     16
  71  72   2   2   2   2  69  69   0   0   0                           CARD 17     17
       54.73        43.9        .0010       00.01        0.0        .025 CARD 18     18
     0.00001      0.0001         1.0          1.0        0.1         .02 CARD 19     19
         0.0                                                            CARD 20     20
0.0      .020    10.                                                                 21
.001     .005    .005                                                                22
   1   7   9   6       3.596       2.68        0.0      150.0      150.0 CARD 23     23
    6850.0      0.012                                                   CARD 24     24
   2   9   3   6       3.596       2.68        0.0      150.0      150.0           25
    6650.0      0.012                                                               26
   3   3   4   5       2.877       2.68        0.0      150.0      150.0           27
    6850.0      0.012                                                               28
   4   4   5   7       4.315       2.68        0.0      150.0      150.0           29
    6850.0      0.012                                                               30
   5   5   6   3       1.153       1.368       0.0      150.0      150.0           31
    5492.0      0.012                                                               32
   6   6  32   4       2.315       3.12        0.0      150.0      150.0           33
    7352.0      0.012                                                               34
   7  32  33  13       3.789       .665        0.0      150.0      150.0           35
    6976.0      0.012                                                               36
   8   8   7   3       1.438       2.68        0.0      150.0      150.0           37
    6850.0      0.012                                                               38
   9   2   8   5       3.122       2.68        0.0      150.0      150.0           39
    6950.0      0.012                                                               40
  10   1  10   4       2.631       2.68        0.0      150.0      150.0           41
    6350.0      0.012                                                               42
  11  10  11   3       1.438       2.68        0.0      150.0      150.0           43
    6850.0      0.012                                                               44
  12  11  12   7       4.315       2.68        0.0      150.0      150.0           45
    6850.0      0.012                                                               46
  13  11  13   7       4.315       1.27        0.0      150.0      150.0           47
    6850.0       .012                                                               48
  14  13  14  12       7.552       .797        0.0      150.0      150.0           49
    6539.0      0.012                                                               50

         1         2         3         4         5         6         7         8
12345678901234567890123456789012345678901234567890123456789012345678901234567890
```

```
        1         2         3         4         5         6         7         8
12345678901234567890123456789012345678901234567890123456789012345678901234567890

15  14  15   8        4.806      .797       0.0      150.0     150.0                  51
  6539.0      0.012                                                                  52
16  15  16  16       10.30       0.797      0.0      150.0     150.0                  53
  6539.0      0.012                                                                  54
17  16  17   6        3.432      0.797      0.0      150.0     150.0                  55
  6539.0      0.012                                                                  56
18  17  18  12        7.552      0.797      0.0      150.0     150.0                  57
  6539.0      0.012                                                                  58
19  18  19  12        7.752      1.31       0.0      150.0     150.0                  59
  6712.0      0.012                                                                  60
20  19  20  11        7.047      1.31       0.0      150.0     150.0                  61
  6712.0      0.012                                                                  62
21  20  21   3        1.447      1.27       0.0      150.0     150.0                  63
  6892.0      0.012                                                                  64
22  20  22  14        9.161      1.31       0.0      150.0     150.0                  65
  6712.0      0.012                                                                  66
23  22  23   3        1.409      1.31       0.0      150.0     150.0                  67
  6712.0      0.012                                                                  68
24  22  24   3        1.527      .287       0.0      150.0     150.0                  69
  7273.0      0.012                                                                  70
25  24  25  20        14.51      .287       0.0      150.0     150.0                  71
  7273.0      0.012                                                                  72
26  25  26  20       14.509      .287       0.0      150.0     150.0                  73
  7273.0      0.012                                                                  74
27   4  27   7        4.315      1.75       0.0      150.0     150.0                  75
  6850.0        0.2                                                                  76
28  27  28   5        2.894      1.27       0.0      150.0     150.0                  77
  6892.0      0.012                                                                  78
29  28  29  11        7.236      1.27       0.0      150.0     150.0                  79
  6892.0      0.012                                                                  80
30  29  30  16       10.854      1.27       0.0      150.0     150.0                  81
  6892.0      0.012                                                                  82
31  28  31   7        4.941      1.27       0.0      150.0     150.0                  83
  6892.0      0.012                                                                  84
32  29  34  12        7.752      .287       0.0      150.0     150.0                  85
  6712.0      0.012                                                                  86
33  34  35  12        7.752      .287       0.0      150.0     150.0                  87
  6712.0      0.012                                                                  88
34  35  36  12        7.752      .287       0.0      150.0     150.0                  89
  6712.0      0.012                                                                  90
35  24  37   3        1.409      .287       0.0      150.0     150.0                  91
  6712.0      0.012                                                                  92
36             3          3.0       1.0       0.0      150.0     150.0              93
  6000.0      0.012                                                                  94
37             3          3.0       1.0       0.0      150.0     150.0              95
  6000.0      0.012                                                                  96
38             3          3.0       1.0       0.0      150.0     150.0              97
  6000.0      0.012                                                                  98
39             3          3.0       1.0       0.0      150.0     150.0              99
  6000.0      0.012                                                                 100

        1         2         3         4         5         6         7         8
12345678901234567890123456789012345678901234567890123456789012345678901234567890
```

```
        1         2         3         4         5         6         7         8
12345678901234567890123456789012345678901234567890123456789012345678901234567890

40              3         3.0       1.0       0.0     150.0     150.0                101
  6000.0        0.012                                                              102
41              3         3.0       1.0       0.0     150.0     150.0                103
  6000.0        0.012                                                              104
42              3         3.0       1.0       0.0     150.0     150.0                105
  6000.0        0.012                                                              106
43              3         3.0       1.0       0.0     150.0     150.0                107
  6000.0        0.012                                                              108
44              3         3.0       1.0       0.0     150.0     150.0                109
  6000.0        0.012                                                              110
45              3         3.0       1.0       0.0      15.0      15.0                111
  6000.0        0.012                                                              112
46  47  46  20          12.18       .979      0.0      15.0      15.0                113
  6108.0        0.012                                                              114
47  48  47  20          12.18       .979      0.0      15.0      15.0                115
  6108.0        0.012                                                              116
48  49  48  20          12.18       .979      0.0      15.0      15.0                117
  6108.0        0.012                                                              118
49  58  49  20          12.18       .979      0.0      15.0      15.0                119
  6108.0        0.012                                                              120
50              3         3.0       1.0       0.0      15.0      15.0                121
  6000.0        0.012                                                              122
51  51  50  17          10.895      1.19      0.0      15.0      15.0                123
  6485.0        0.012                                                              124
52  52  51  14          8.852       1.19      0.0      15.0      15.0                125
  6485.0        0.012                                                              126
53  53  52  4           2.042       1.19      0.0      15.0      15.0                127
  6485.0        0.012                                                              128
54  54  53  7           4.342       1.27      0.0      15.0      15.0                129
  6892.0        0.012                                                              130
55  55  58  14          8.852       1.19      0.0      15.0      15.0                131
  6485.0        0.012                                                              132
56  50  55  17          10.895      1.19      0.0      15.0      15.0                133
  6485.0        0.012                                                              134
57              12        7.359       1.19      0.0      15.0      15.0                135
  6370.0        0.012                                                              136
58  58  57  14          8.852       1.19      0.0      15.0      15.0                137
  6485.0        0.012                                                              138
59              3         3.0       1.0       0.0      15.0      15.0                139
  6000.0        0.012                                                              140
60              3         3.0       1.0       0.0      15.0      15.0                141
  6000.0        0.012                                                              142
61              3         3.0       1.0       0.0      15.0      15.0                143
  6000.0        0.012                                                              144
62              3         3.0       1.0       0.0      15.0      15.0                145
  6000.0        0.012                                                              146
63              3         3.0       1.0       0.0      15.0      15.0                147
  6000.0        0.012                                                              148
64              3         3.0       1.0       0.0      15.0      15.0                149
  6000.0        0.012                                                              150

        1         2         3         4         5         6         7         8
12345678901234567890123456789012345678901234567890123456789012345678901234567890
```

```
        1         2         3         4         5         6         7         8
12345678901234567890123456789012345678901234567890123456789012345678901234567890

 65               3       3.0       1.0       0.0      15.0      15.0                151
   6000.0         0.012                                                             152
 66               3       3.0       1.0       0.0      15.0      15.0                153
   6000.0         0.012                                                             154
 67               3       3.0       1.0       0.0      15.0      15.0                155
   6000.0         0.012                                                             156
 68               3       3.0       1.0       0.0      15.0      15.0                157
   6000.0         0.012                                                             158
 69               3       3.0       1.0       0.0      15.0      15.0    CARD 23     159
   6000.0         0.012                                                   CARD 24     160
  1  10           16                                                      CARD 25     161
  2   9           16                                                      CARD 25     162
  3   2    3      10                                                      CARD 25     163
  4   3    4  27   4                                                      CARD 25     164
  5   4    5      10                                                      CARD 25     165
  6   5    6      10                                                      CARD 25     166
  7   1    8      11                                                      CARD 25     167
  8   8    9      11                                                      CARD 25     168
  9   2    1      11                                                      CARD 25     169
 10  10   11      10                                                      CARD 25     170
 11  11   12  13   4                                                      CARD 25     171
 12  12           15       8.0   394.660                                  CARD 25     172
 13  13   14      10                                                      CARD 25     173
 14  14   15      10                                                      CARD 25     174
 15  15   16      10                                                      CARD 25     175
 16  16   17      10                                                      CARD 25     176
 17  17   18      10                                                      CARD 25     177
 18  18   19      10                                                      CARD 25     178
 19  19   20      10                                                      CARD 25     179
 20  20   22  21   4                                                      CARD 25     180
 21  21           14                                                      CARD 25     181
 22  22   23  24   4                                                      CARD 25     182
 23  23           14                                                      CARD 25     183
 24  24   35  25   4                                                      CARD 25     184
 25  25   26      10                                                      CARD 25     185
 26  26           15      47.0   394.660                                  CARD 25     186
 27  27   28      10                                                      CARD 25     187
 28  28   31  29   4                                                      CARD 25     188
 29  29   30  32   4                                                      CARD 25     189
 30  30           14                                                      CARD 25     190
 31  31           14                                                      CARD 25     191
 32   6    7      10                                                      CARD 25     192
 33   7           14                                                      CARD 25     193
 34  32   33      10                                                      CARD 25     194
 35  33   34      10                                                      CARD 25     195
 36  34           14                                                      CARD 25     196
 37  35           14                                                      CARD 25     197
 38               10                                                      CARD 25     198
 39               10                                                      CARD 25     199
 40               10                                                      CARD 25     200

        1         2         3         4         5         6         7         8
12345678901234567890123456789012345678901234567890123456789012345678901234567890
```

```
        1         2         3         4         5         6         7         8
12345678901234567890123456789012345678901234567890123456789012345678901234567890

 41                 10                                                  CARD 25      201
 42                 10                                                  CARD 25      202
 43                 10                                                  CARD 25      203
 44                 10                                                  CARD 25      204
 45                 10                                                  CARD 25      205
 46   46            14                                                  CARD 25      206
 47   47   46       10                                                  CARD 25      207
 48   48   47       10                                                  CARD 25      208
 49   49   48       10                                                  CARD 25      209
 50   51   56       10                                                  CARD 25      210
 51   52   51       10                                                  CARD 25      211
 52   53   52       10                                                  CARD 25      212
 53   54   53       10                                                  CARD 25      213
 54   54            18      24.55       40.4                            CARD 25      214
 55   56   55       10                                                  CARD 25      215
 56                  4                                                  CARD 25      216
 57   58            15    1654.0        40.4                            CARD 25      217
 58   55   58   49   4                                                   CARD 25      218
 59                 13                  40.4                            CARD 25      219
 60                 13                  40.4                            CARD 25      220
 61                 13                  40.4                            CARD 25      221
 62                 13                  40.4                            CARD 25      222
 63                 13                  40.4                            CARD 25      223
 64                 13                  40.4                            CARD 25      224
 65                 13                  40.4                            CARD 25      225
 66                 16                  40.4                            CARD 25      226
 67                 16                  40.4                            CARD 25      227
 68                 16                  40.4                            CARD 25      228
 69                 16                  40.4                            CARD 25      229
$CKKIN                                                                               230
 CKKI(1,3)= 4*1.68,                                                                  231
 CKKI(1,4)= 2.,4.,.5,2.,4.,.5,2.,4.,.5,2.,4.,.5,2.,4.,.5,2.,4.,.5,                   232
 CKKI(1,5)= 4*1.0,                                                                   233
 CKKI(1,6)=4*1.68,                                                                   234
 CKKI(1,7)= 4*1.68,                                                                  235
 CKKI(1,8)= 4*1.68,                                                                  236
 CKKI(1,9)= 4*1.68,                                                                  237
 CKKI(1,10)= 4*1.68,                                                                 238
 CKKI(1,11)= 2.,4.,.5,2.,4.,.5,2.,4.,.5,2.,4.,.5,2.,4.,.5,2.,4.,.5,                  239
 CKKI(3,12)=  8.0,                                                                   240
 CKKI(1,13)= 4*0.14,                                                                 241
 CKKI(1,14)= 4*0.085,                                                                242
 CKKI(1,15)= 4*0.085,                                                                243
 CKKI(1,16)= 4*0.085,                                                                244
 CKKI(1,17)= 4*0.085,                                                                245
 CKKI(1,18)= 4*0.14,                                                                 246
 CKKI(3,26)= 47.0,                                                                   247
 CKKI(1,27)= 4*0.03,                                                                 248
 CKKI(1,51)= 4*0.08,                                                                 249
 CKKI(1,52)= 4*0.08,                                                                 250

        1         2         3         4         5         6         7         8
12345678901234567890123456789012345678901234567890123456789012345678901234567890
```

```
        1         2         3         4         5         6         7         8
12345678901234567890123456789012345678901234567890123456789012345678901234567890

  CKKI(1,55)= 4*0.08,                                                          251
  CKKI(3,54)= 24.55,                                                           252
  CKKI(2,56)=1.,12.,                                                           253
  CKKI(3,57)= 1654.0 $                                                         254
          5          57                                              CARD 27   255
         12         1.4  939470.          .559        650.          CARD 28   256
         26         1.4  939470.          .559        650.          CARD 28   257
         54         1.4  939470.          .559        650.          CARD 28   258
         57         1.4  939470.          .559        650.          CARD 28   259
        169         1.4  939470.          .559        650.          CARD 28   260
    1    1    4    58    3    57    3    4                           CARD 29   261
  170   58                                                           CARD 30   262
        0.0        15.0         5.        400.         1.0      .002 CARD 31   263
       53.0       0.916        1.3       0.01       0.916       1.3CARD 32   264
      827.0        20.0       10.0      0.916       827.0      20.0CARD 33   265
       10.0       0.916                                           CARD 33   266
       20.0        12.0        0.0        0.0        0.0      .375CARD 34   267
        0.5         0.5        0.0        0.0        0.0       0.6 CARD 35   268
      15.0   1500.0                                               CARD 36   269
         45         69         44         69         61         61          CARD 37   270
         58                                                       CARD 38   271
        600.0      0.0075          33  0.650                      CARD 39   272
0.0          .00005      .0001       .0002       .0003       .00035        CARD 40   273
.0004        .00045      .00050      .00055      .00065      .0007         CARD 40   274
.00075   .   .0008       .00125      .0015       .002        .0025         CARD 40   275
.003         .0050       .010        .020        .035        .060          CARD 40   276
.090         .120        .140        .170        .200        .300          CARD 40   277
.400         .500        10.0                                            CARD 40   278
0.0          .168        .330       1.434       3.483       4.826         CARD 41   279
5.719       6.033       6.120       6.236       5.251       4.775         CARD 41   280
4.382       4.210       3.552       3.447       3.319       3.267         CARD 41   281
3.238       3.175       3.151       3.207       3.228       3.184         CARD 41   282
3.600       3.959       3.600       3.854       3.590       3.113         CARD 41   283
3.231       2.677       2.452                                           CARD 41   284
     2650.      .0012          0.      43.9      54.73  0.001805      11.28 CARD 42   285
     9000.       6850.    21600.0   264960.       580.       580.          CARD 43   286
         1          -1         0.1                   1                   CARD 44   287
    150. 99999. 99999. 99999. 99999. 99999. 99999. 99999. 99999. 99999.  CARD 50   288
  70 170   1   2 170  70 170  10   9 170  69  69                        CARD 51   289
  31 170 170 170 170 170 170 170 170 170                                CARD 52   290
  54 170 170 170 170 170 170 170 170 170                                CARD 53   291
  31 170 170 170 170 170 170 170 170 170                                CARD 54   292
  54 170 170 170 170 170 170 170 170 170                                CARD 55   293
   2                                                                    CARD 56   294
15.          15.          2.          1.7                              CARD 57   295
       18.00        .0600      2.92E07        .323       512.0      12.675CARD 58   296
1.5          0.014        0.50        0.025       10 .010       150.       CD 59   297
2.9        E05 5.25     E04 9.3      E04                              CARD 60   298
       18.00        .0600      2.92E07        .323       512.0      12.675CARD 58   299
1.5          0.012        0.60        0.002       10 .003       135.       CD 59   300


        1         2         3         4         5         6         7         8
12345678901234567890123456789012345678901234567890123456789012345678901234567890
```

```
         1         2         3         4         5         6         7         8
12345678901234567890123456789012345678901234567890123456789012345678901234567890

2,9      E05 4.75    E04 9.3     E04                                          CARD 60      301
FT                                                                            CARD 64      302
                                                                              CARD 65      303
 0 0 0 0 0 0 0 0 0 0 0 0 0 0 0 0 0 0 0 0 0 0 0 0 0 0 0 0 0 0 0 0 0 0 0 0 0 1CARD 66      304
 1 1 1 1 1 1 1 1 1 1 1 1 1 1 1 1 1 1 1 1 1 1 1 1 1 1 1 1 1 1 1 1 1 0 0 CARD 66      305
 0 0 0 0 0 0 0 0 0 0 0 0 0 0 0 0 0 0 0 0 0 0 0 0 0 0 0 0 0 0 0 0 0 0 0 0CARD 67      306
 0 1 1 1 1 1 1 1 1 1 1 1 1 1 1 1 1 0 1 1 1 1 1 1 1 1 1 1 1 1 1 1 1 0 0 0CARD 67      307
          0.0      0.00017          0.5    0                               CARD 68      308
    0     0    0    1    0                                                 CARD 69      309
    1     3    1    1                                                      CARD 78      310
0.0    54 53 52                                                           CARD 79      311
5.333      90.         2.0                                                 CARD 80      312
   53 1.25                                                                 CARD 81      313
LLTR SERIES II - TEST A-6 POST TEST EVALUATION                             CARD 82      314
FTTOT                                                                      CARD 83      315
  1 26  1  4  1  0  1  0  0  0  0                                          CARD 84      316
  1 12  6 16 TPT-02-1                                                       CRD 86      317
  2 12  6 42 TPT-02-2                                                       CRD 86      318
  3 10  3107 TPT-01-8                                                       CRD 86      319
  4  9  4 55 TPT-01-7A                                                      CRD 86      320
  5  9  4 81 TPT-01-7B                                                      CRD 86      321
  6  2  4 29 TPT-01-2                                                       CRD 86      322
  7  3  4 68 TPT-01-5                                                       CRD 86      323
  8  4  6 75 TPT-A-10                                                       CRD 86      324
  9 15  4 14 TP-507                                                         CRD 86      325
 10 14  6 27 TP-508                                                         CRD 86      326
 11 16  7 40 TP-509                                                         CRD 86      327
 12 20  7 66 TP-510                                                         CRD 86      328
 13 18  7 53 TP-516                                                         CRD 86      329
 14 23  2 79 TP-517                                                         CRD 86      330
 15 28  3112 TP-519                                                         CRD 86      331
 16 29  9 86 TP-520                                                         CRD 86      332
 17 30 11 99 TP-521                                                         CRD 86      333
 18 21  2 20 TP-524                                                         CRD 86      334
 19 31  6 59 TP-525                                                         CRD 86      335
    31  7 59 TRUPTURE DISC                                                  CRD 86      336
 20 12  4 41 TP-614                                                         CRD 86      337
 21 10  3 54 TP-615                                                         CRD 86      338
 22  8  1 67 TP-616                                                         CRD 86      339
 23  2  2 80 TP-617                                                         CRD 86      340
 24  3  2 93 TP-618                                                         CRD 86      341
 25  4  2106 TP-619                                                         CRD 86      342
 26          TRUPTURE DISC CAVITY                                           CRD 87      343
    31  7 72 TRUPTURE DISC VEL                                              CRD 88      344
 27 31  5 76 TF-506                                                         CRD 88      345
 28 51 11 72 TF-510                                                         CRD 88      346
 29 55  8 85 TF-511                                                         CRD 88      347
 29          TRUPTURE DISC DISP                                             CRD 89      348
 30          TFX RELIEF ELBOW 1                                             CRD 91      349
 31          TFY RELIEF ELBOW 1                                             CRD 91      350

         1         2         3         4         5         6         7         8
12345678901234567890123456789012345678901234567890123456789012345678901234567890
```

```
        1         2         3         4         5         6         7         8
12345678901234567890123456789012345678901234567890123456789012345678901234567890

 32           TRELIEF REDUCER 1                                          CRD 91      351
    1                                                                    CRD 94      352
          1.         0.5        36.5        0.0        -1.0            CRD 95      353
TFTTFFF   57.969                                                       CRD 96      354
.001      0.                                                           CRD 97      355
```

APPENDIX B

TRANSWRAP MODEL A

0-25 M sec

100% Std Methodology

SWR Rate

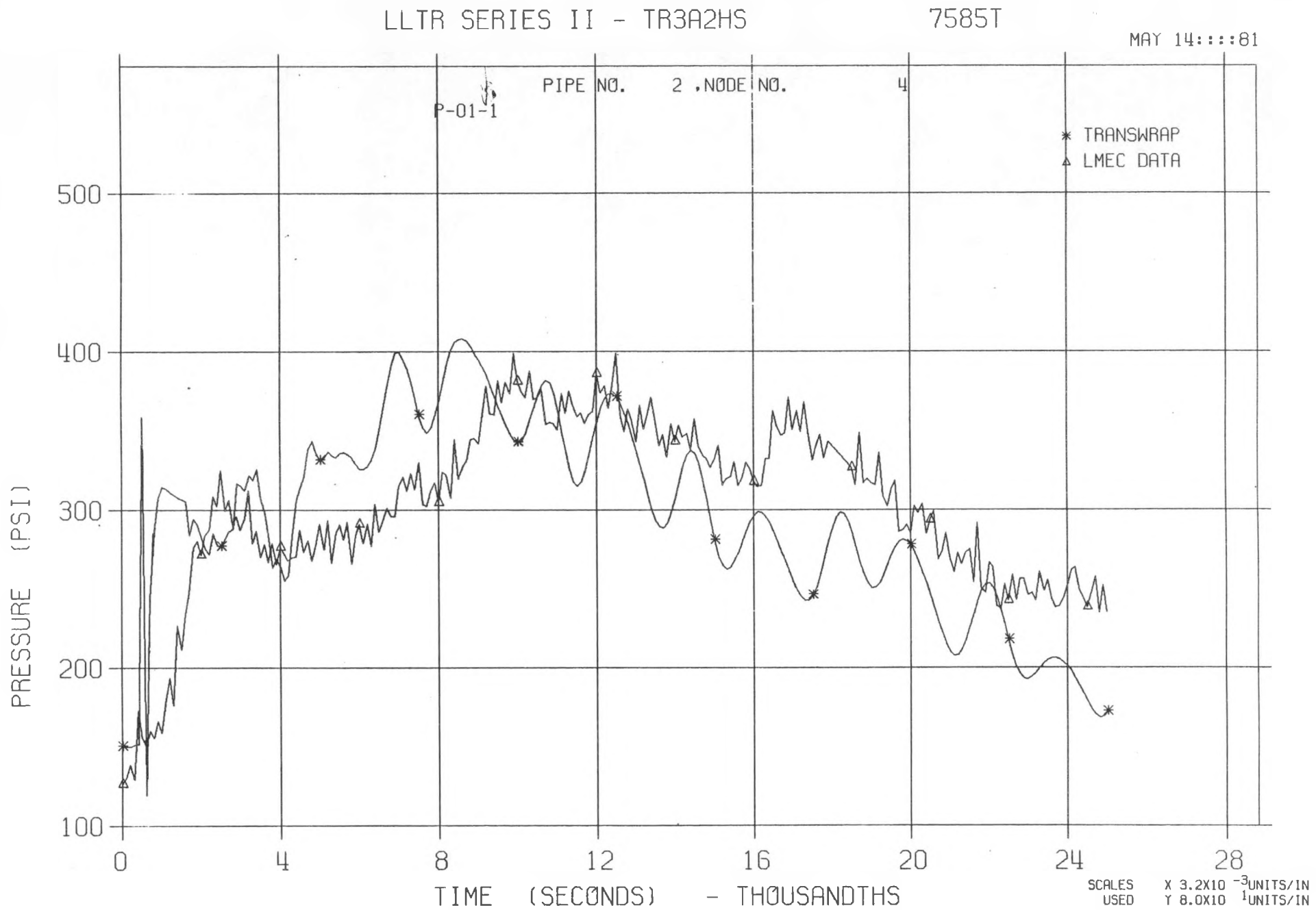
LLTR SERIES II - TR3A2HS
7585T
MAY 14::::81
PIPE NO. 2 ,NODE NO. 4
P-01-1
TRANSWRAP
LMEC DATA
500
400
300
200
100
PRESSURE (PSI)
0
4
8
12
16
20
24
28
TIME (SECONDS) - THOUSANDTHS
SCALES USED
X 3.2X10 -3 UNITS/IN
Y 8.0X10 1 UNITS/IN

B-1

PL 1

B.1

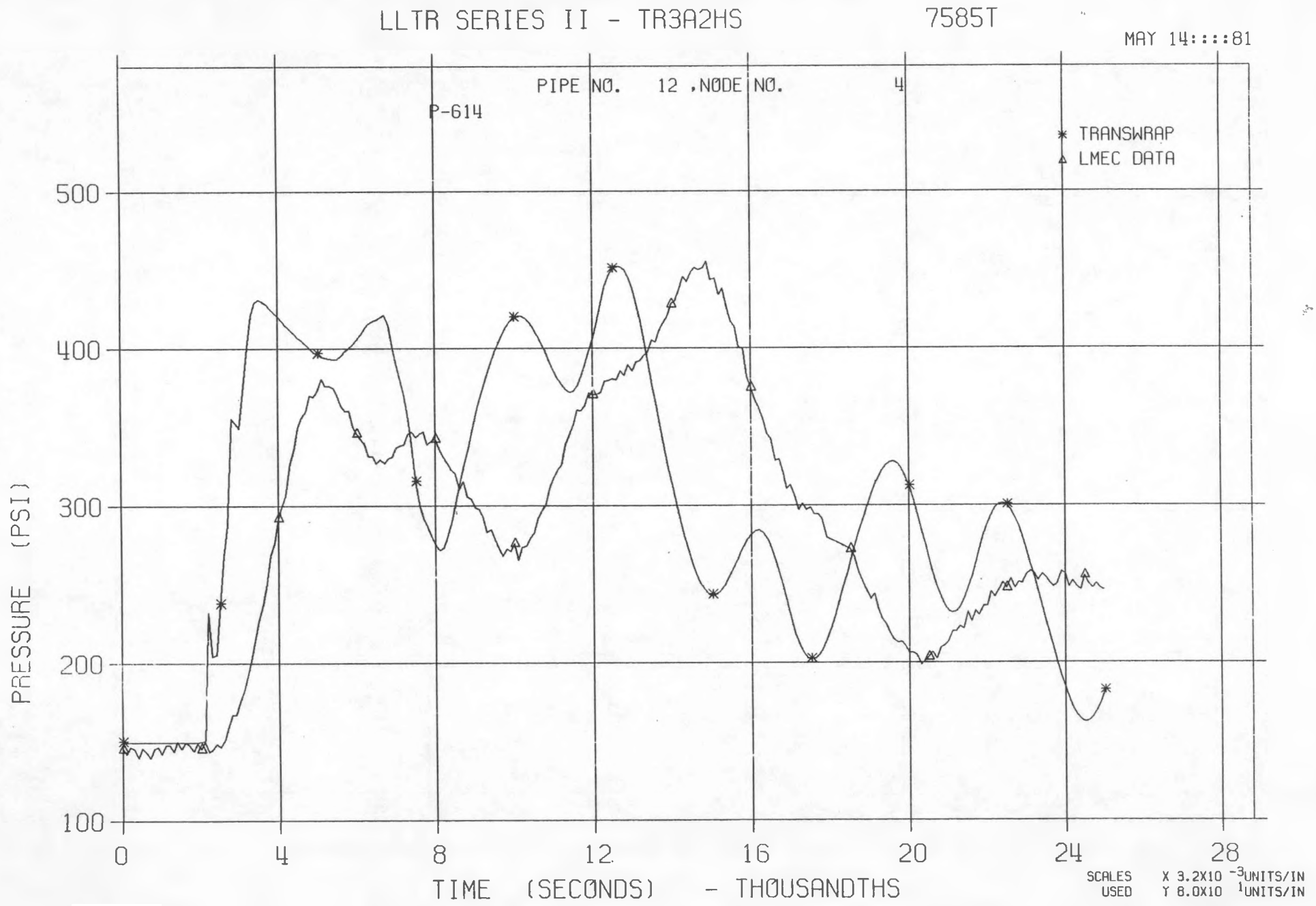
LLTR SERIES II - TR3A2HS
7585T
MAY 14::::81
PIPE NO. 12 ,NODE NO. 4
P-614
TRANSWRAP
LMEC DATA
500
400
300
200
100
PRESSURE (PSI)
0
4
8
12
16
20
24
28
TIME (SECONDS) - THOUSANDTHS
SCALES USED
X 3.2X10 -3 UNITS/IN
Y 8.0X10 1 UNITS/IN

B-2

PL 6

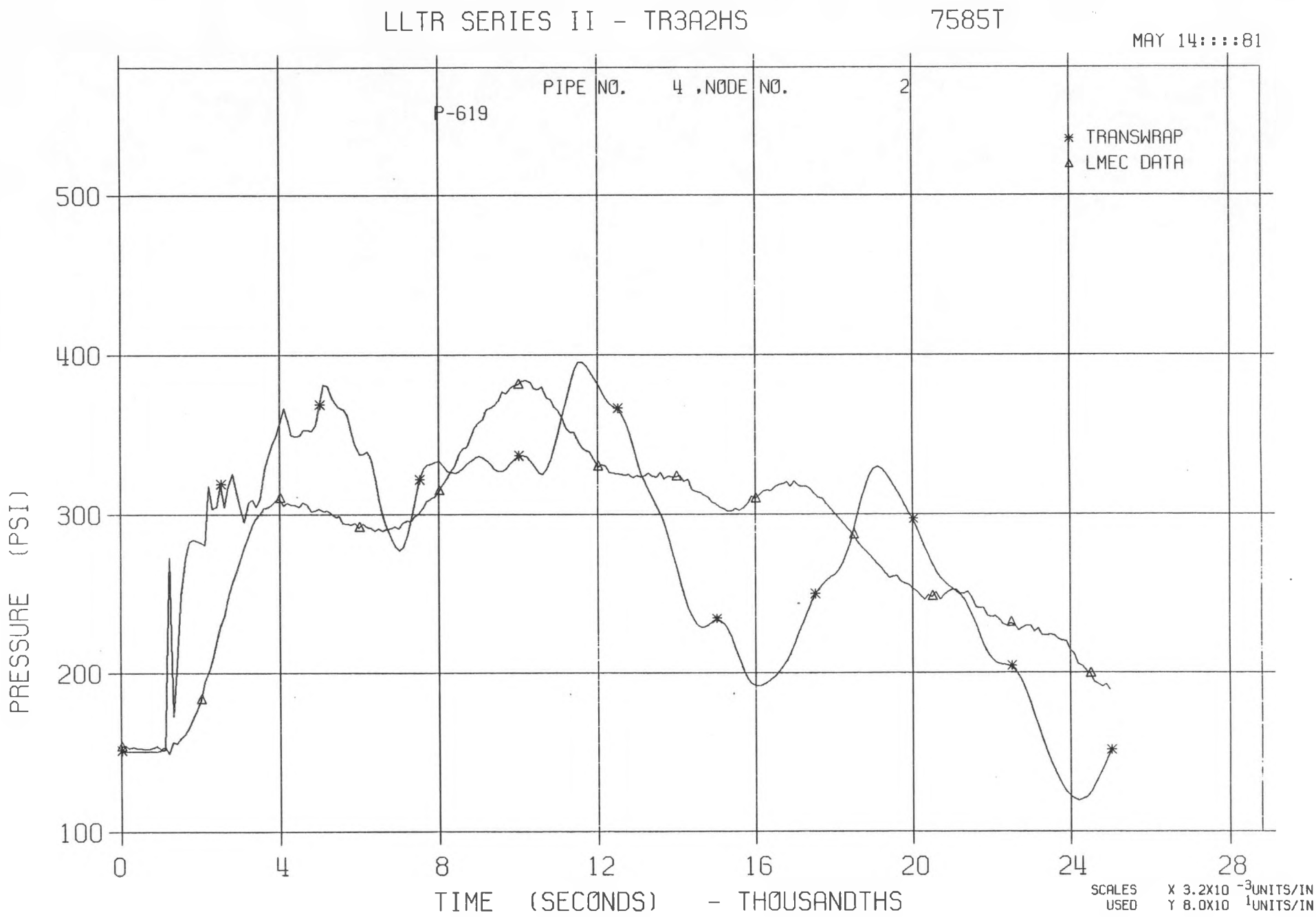
LLTR SERIES II - TR3A2HS
7585T
MAY 14::::81
PIPE NØ. 4 ,NØDE NØ. 2
P-619
TRANSWRAP
LMEC DATA
500
400
300
200
100
PRESSURE (PSI)
0
4
8
12
16
20
24
28
TIME (SECØNDS) - THØUSANDTHS
SCALES USED
X 3.2X10 -3 UNITS/IN
Y 8.0X10 1 UNITS/IN

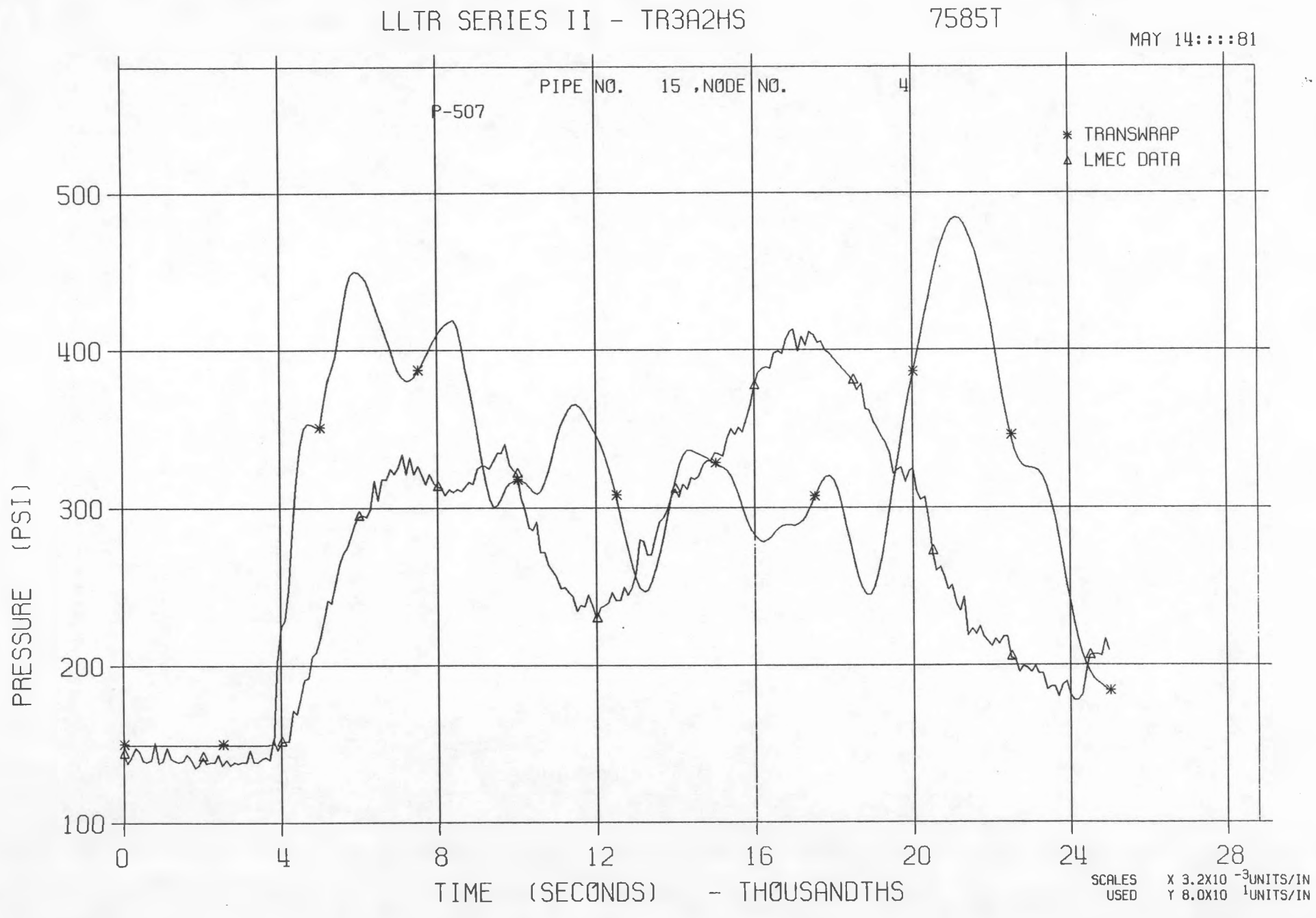
LLTR SERIES II - TR3A2HS
7585T
MAY 14::::81
PIPE NO. 15 ,NODE NO. 4
P-507
TRANSWRAP
LMEC DATA
500
400
300
200
100
PRESSURE (PSI)
0
4
8
12
16
20
24
28
TIME (SECONDS) - THOUSANDTHS
SCALES USED
X 3.2X10 -3 UNITS/IN
Y 8.0X10 1 UNITS/IN

4.0

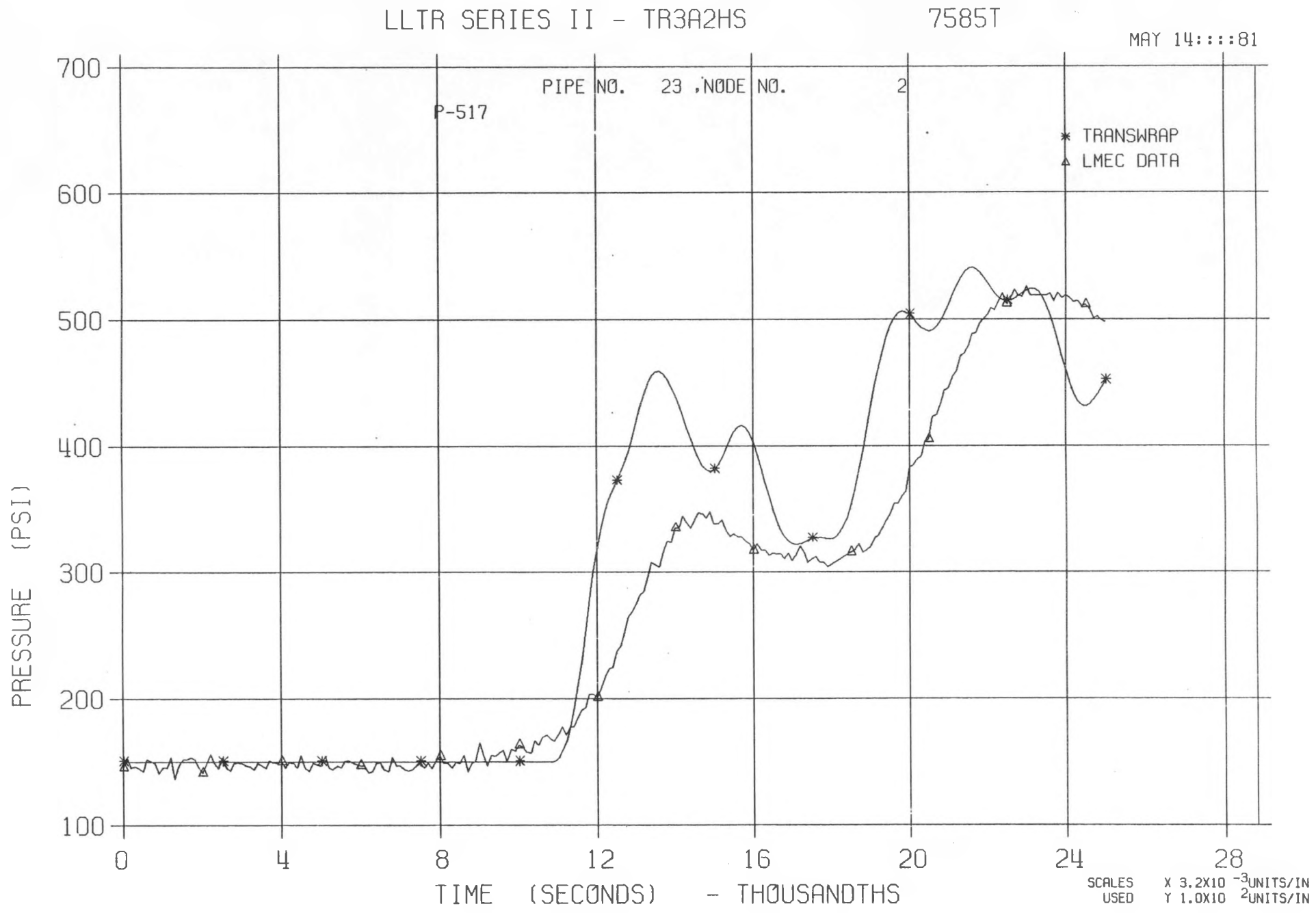
LLTR SERIES II - TR3A2HS 7585T
MAY 14::::81
PIPE NO. 23 ,NODE NO. 2
P-517
TRANSWRAP
LMEC DATA
700
600
500
400
300
200
100
PRESSURE (PSI)
0
4
8
12
16
20
24
28
TIME (SECONDS) - THOUSANDTHS
SCALES USED
X 3.2X10 -3 UNITS/IN
Y 1.0X10 2 UNITS/IN

PL 3

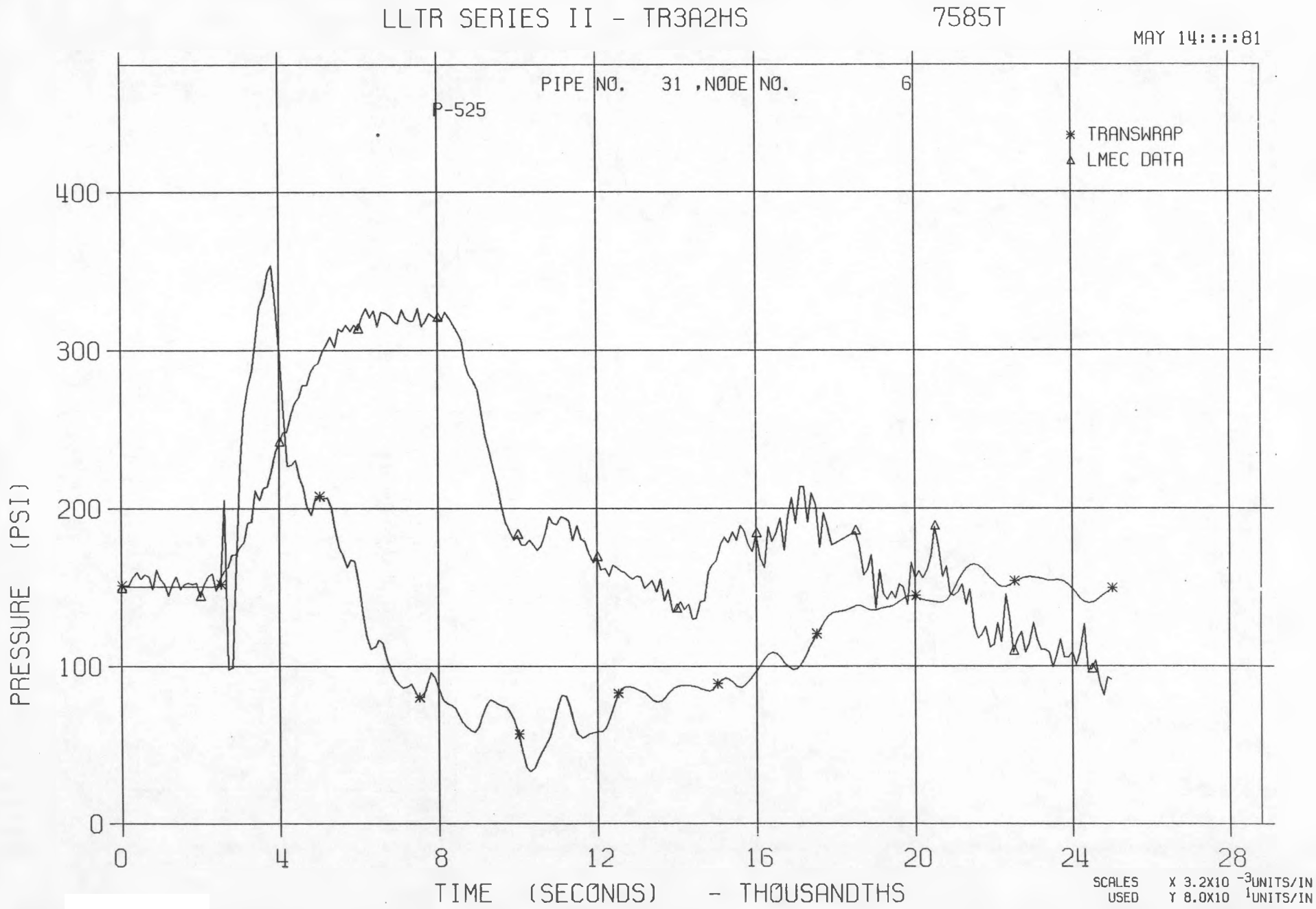
LLTR SERIES II - TR3A2HS
7585T
MAY 14::::81
PIPE NO. 31 ,NODE NO. 6
P-525
TRANSWRAP
LMEC DATA
400
300
200
100
0
PRESSURE (PSI)
0
4
8
12
16
20
24
28
TIME (SECONDS) - THOUSANDTHS
SCALES USED
X 3.2X10 -3 UNITS/IN
Y 8.0X10 1 UNITS/IN

B-6

PL 4

B.6

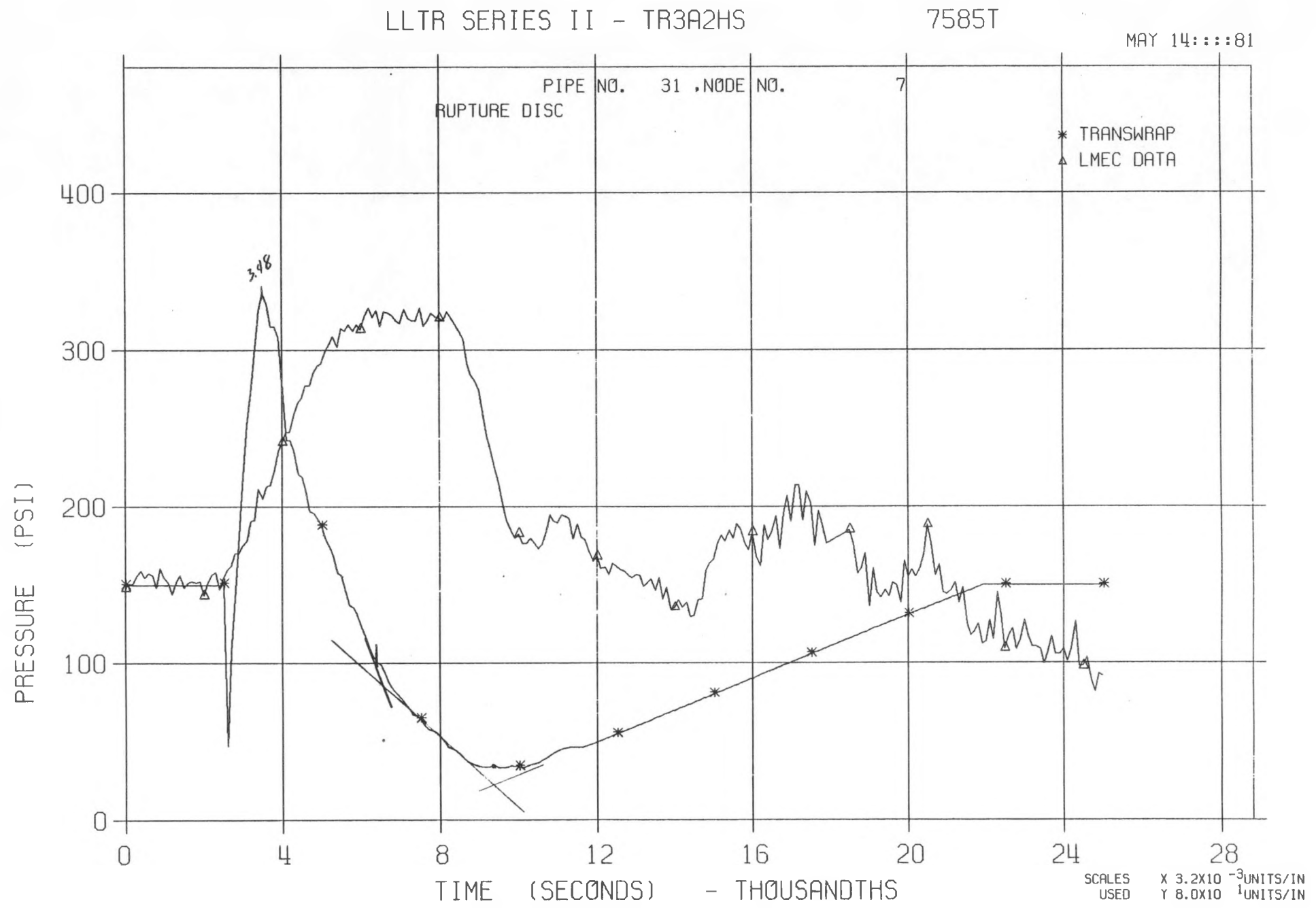
LLTR SERIES II - TR3A2HS 7585T
MAY 14::::81
PIPE NO. 31 ,NODE NO. 7
RUPTURE DISC
TRANSWRAP
LMEC DATA
3.48
400
300
200
100
0
PRESSURE (PSI)
0
4
8
12
16
20
24
28
TIME (SECONDS) - THOUSANDTHS
SCALES USED
X 3.2X10 -3 UNITS/IN
Y 8.0X10 1 UNITS/IN

8-7

PL 5

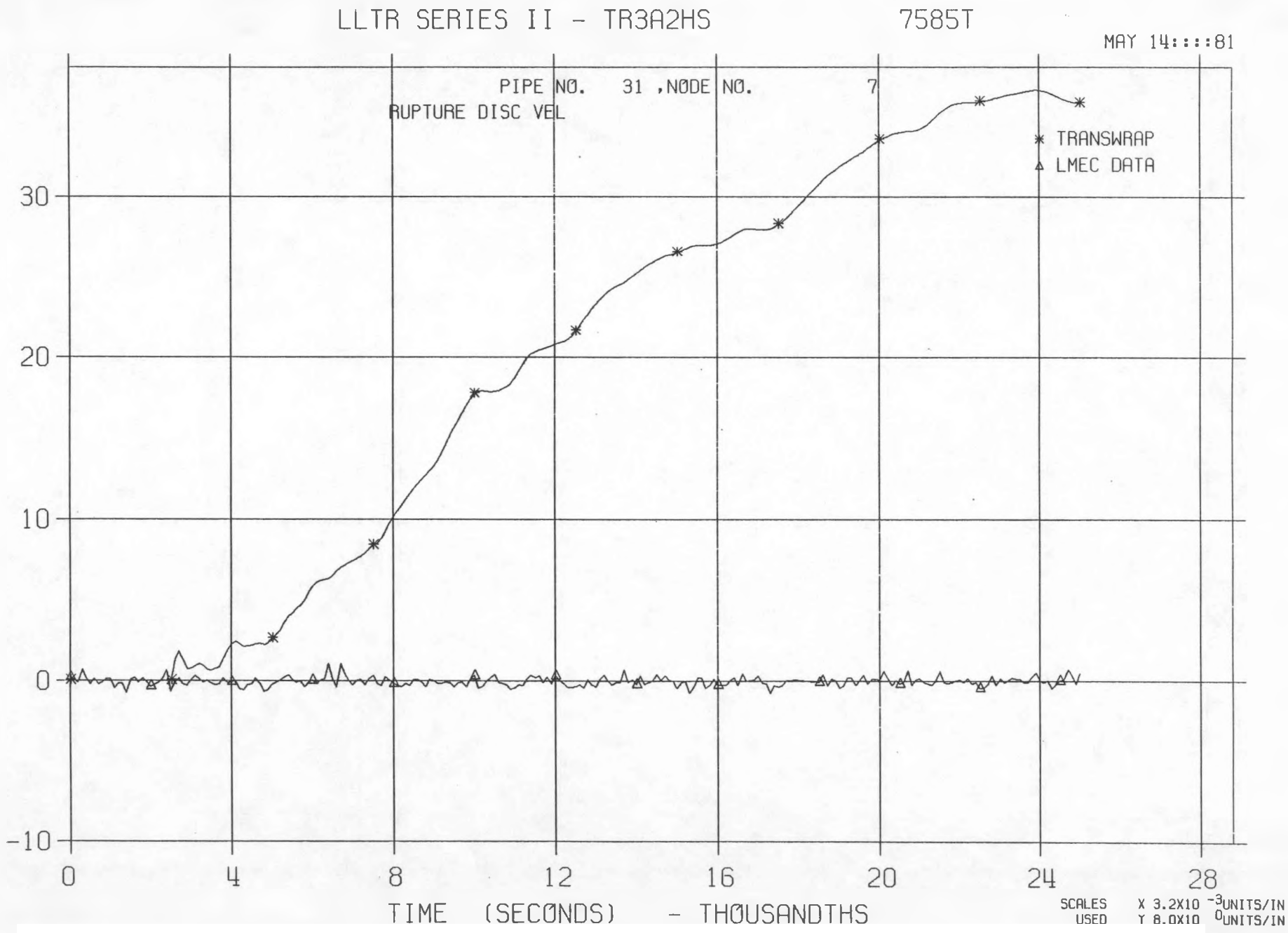
LLTR SERIES II - TR3A2HS 7585T
MAY 14::::81
PIPE NO. 31 ,NODE NO. 7
RUPTURE DISC VEL
TRANSWRAP
LMEC DATA
30
20
10
0
-10
VELOCITY (FT/SEC)
0
4
8
12
16
20
24
28
TIME (SECONDS) - THOUSANDTHS
SCALES USED
X 3.2X10 -3 UNITS/IN
Y 8.0X10 0 UNITS/IN

B-8

PL 9

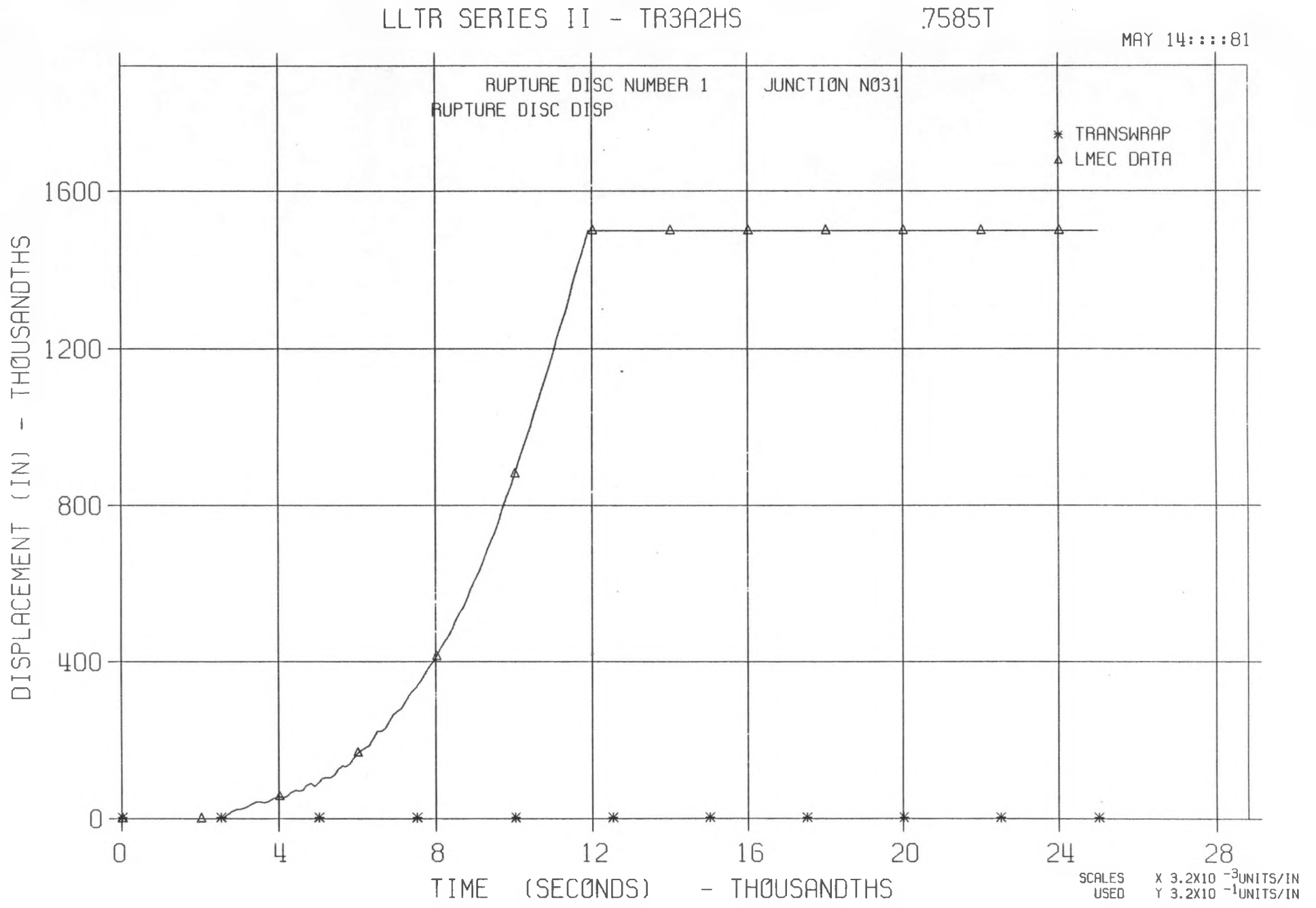
LLTR SERIES II - TR3A2HS .7585T
MAY 14::::81
RUPTURE DISC NUMBER 1
RUPTURE DISC DISP
JUNCTION N031
TRANSWRAP
LMEC DATA
DISPLACEMENT (IN) - THOUSANDTHS
0
400
800
1200
1600
0
4
8
12
16
20
24
28
TIME (SECONDS) - THOUSANDTHS
SCALES USED
X 3.2X10 -3 UNITS/IN
Y 3.2X10 -1 UNITS/IN

PL 10

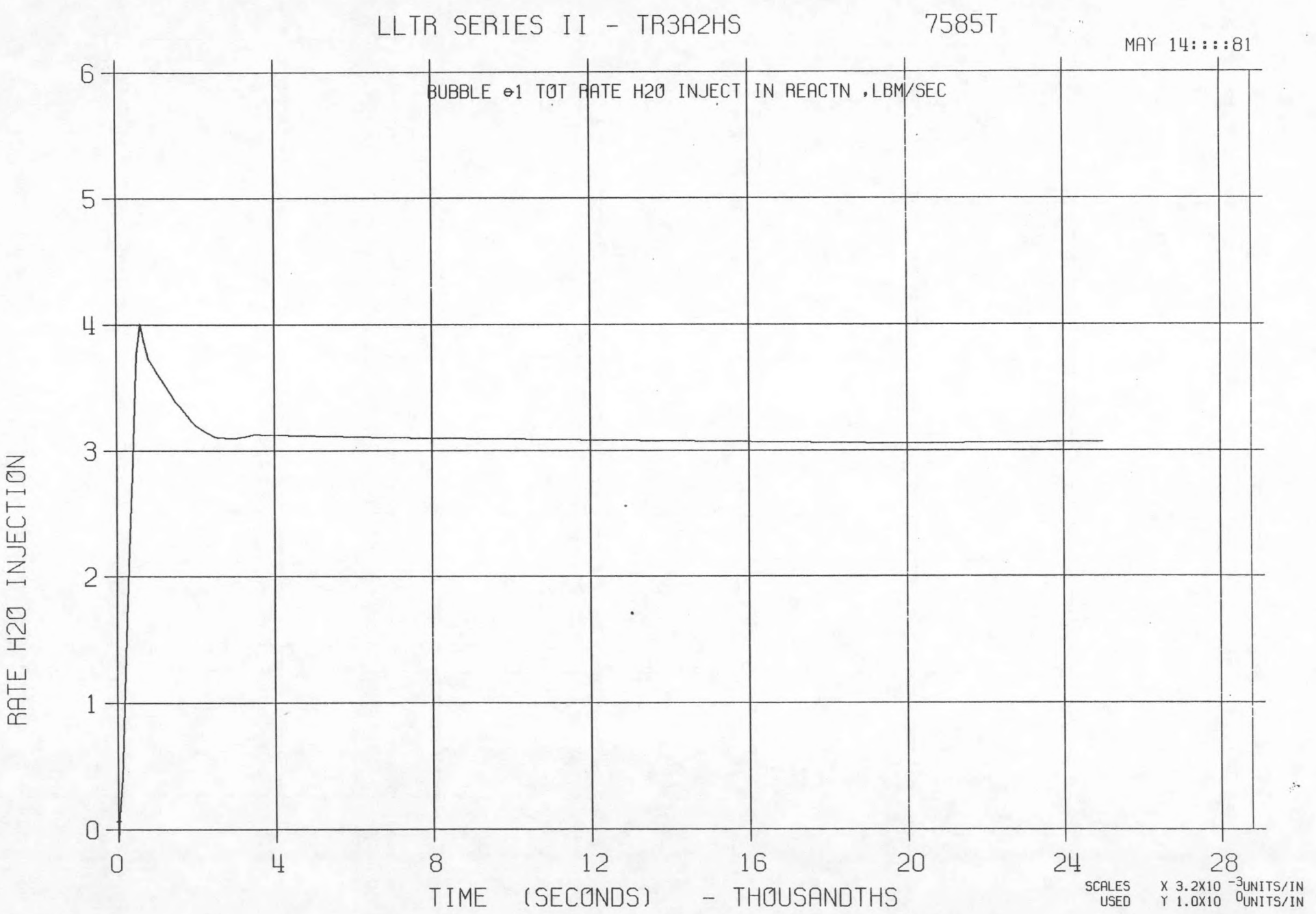
LLTR SERIES II - TR3A2HS 7585T
MAY 14::::81
BUBBLE ⊖1 TØT RATE H20 INJECT IN REACTN ,LBM/SEC
RATE H20 INJECTIØN
0
1
2
3
4
5
6
0
4
8
12
16
20
24
28
TIME (SECØNDS) - THØUSANDTHS
SCALES USED
X 3.2X10 -3 UNITS/IN
Y 1.0X10 0 UNITS/IN

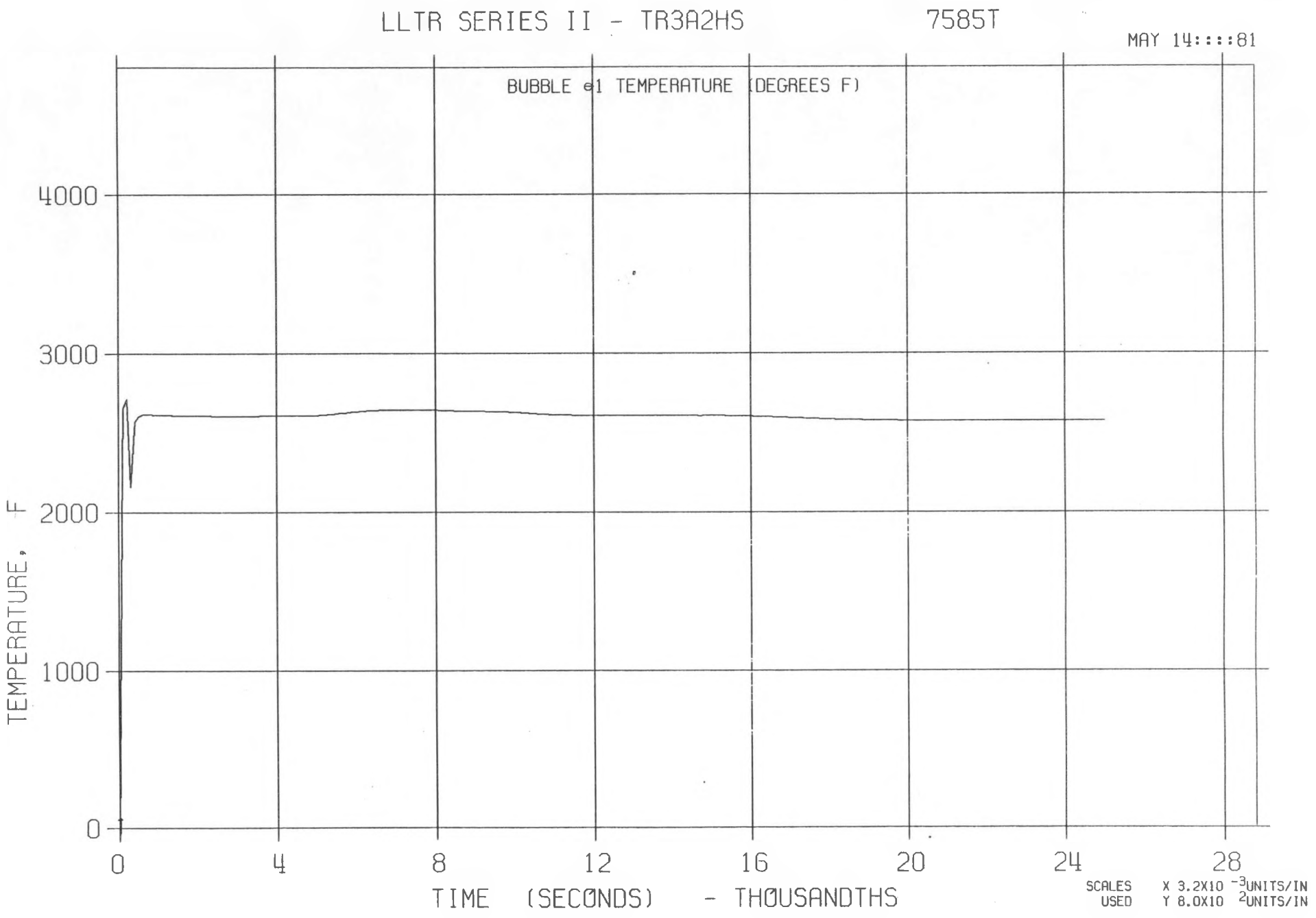
LLTR SERIES II - TR3A2HS
7585T
MAY 14::::81
BUBBLE #1 TEMPERATURE (DEGREES F)
4000
3000
2000
1000
0
TEMPERATURE, F
0
4
8
12
16
20
24
28
TIME (SECONDS) - THOUSANDTHS
SCALES USED
X 3.2X10 -3 UNITS/IN
Y 8.0X10 2 UNITS/IN

B-11

PL 14

B,11

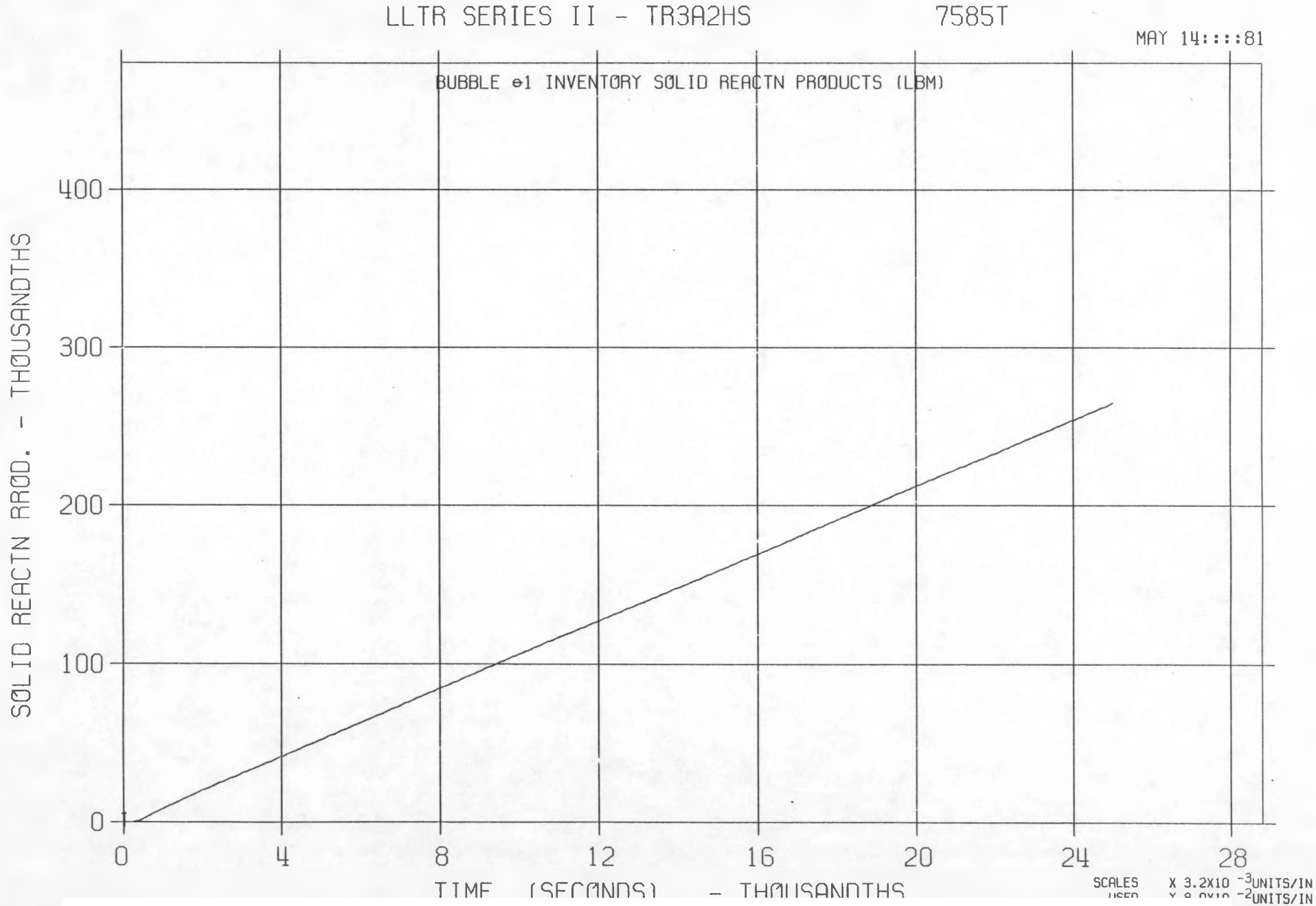
LLTR SERIES II - TR3A2HS 7585T
MAY 14::::81
BUBBLE e1 INVENTORY SOLID REACTN PRODUCTS (LBM)
SOLID REACTN RROD. - THOUSANDTHS
400
300
200
100
0
0
4
8
12
16
20
24
28
TIME (SECONDS) - THOUSANDTHS
SCALES X 3.2X10 -3UNITS/IN
X 8.0X10 -2UNITS/IN

B-12

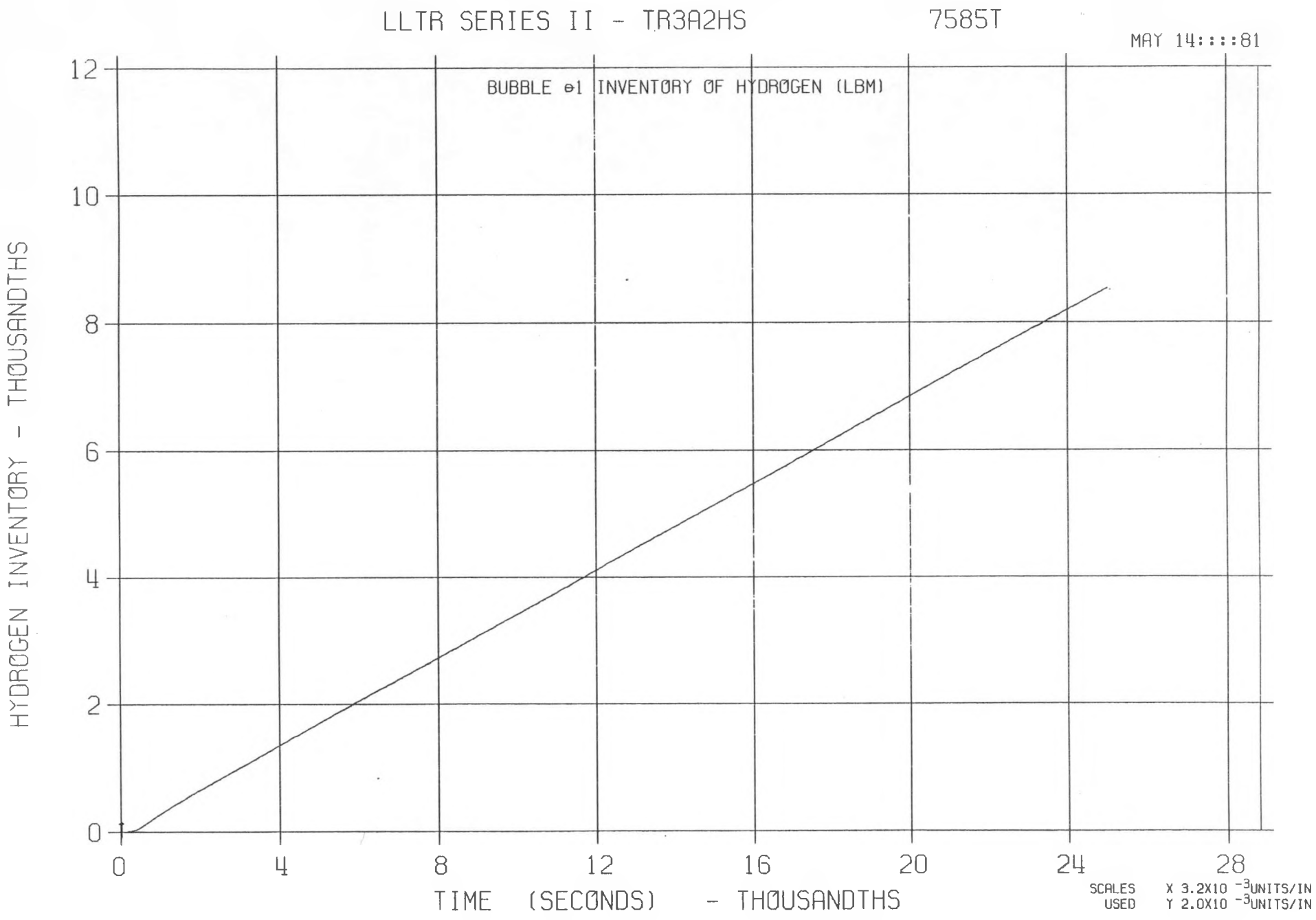
LLTR SERIES II - TR3A2HS 7585T
MAY 14::::81
BUBBLE el INVENTORY OF HYDROGEN (LBM)
HYDROGEN INVENTORY - THOUSANDTHS
TIME (SECONDS) - THOUSANDTHS
0
2
4
6
8
10
12
0
4
8
12
16
20
24
28
SCALES USED
X 3.2X10 -3 UNITS/IN
Y 2.0X10 -3 UNITS/IN

B-13

PL 16

B, 13

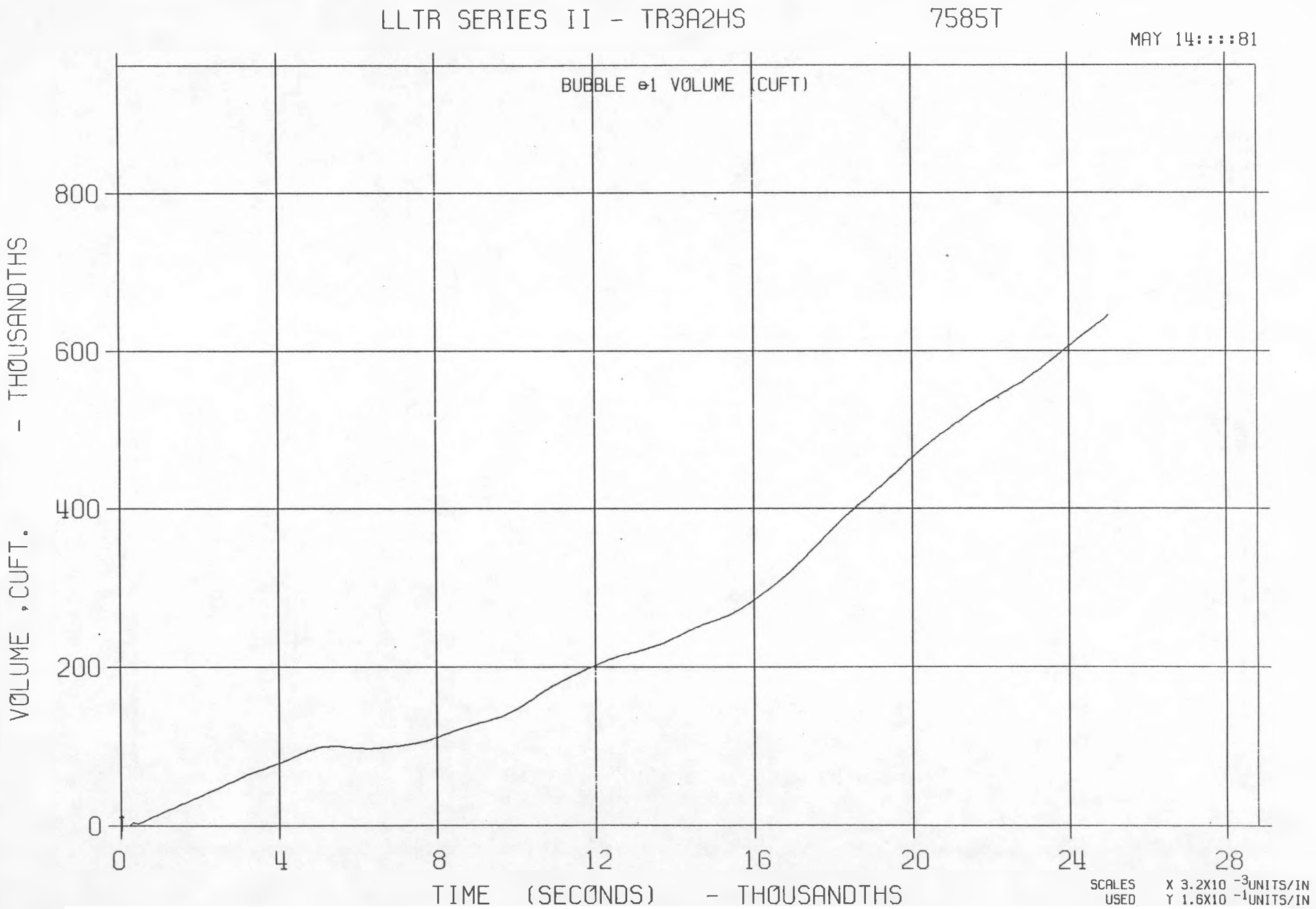
LLTR SERIES II - TR3A2HS
7585T
MAY 14::::81
BUBBLE #1 VOLUME (CUFT)
VOLUME , CUFT. - THOUSANDTHS
800
600
400
200
0
0
4
8
12
16
20
24
28
TIME (SECONDS) - THOUSANDTHS
SCALES USED
X 3.2X10 -3 UNITS/IN
Y 1.6X10 -1 UNITS/IN

41-8

PL 17

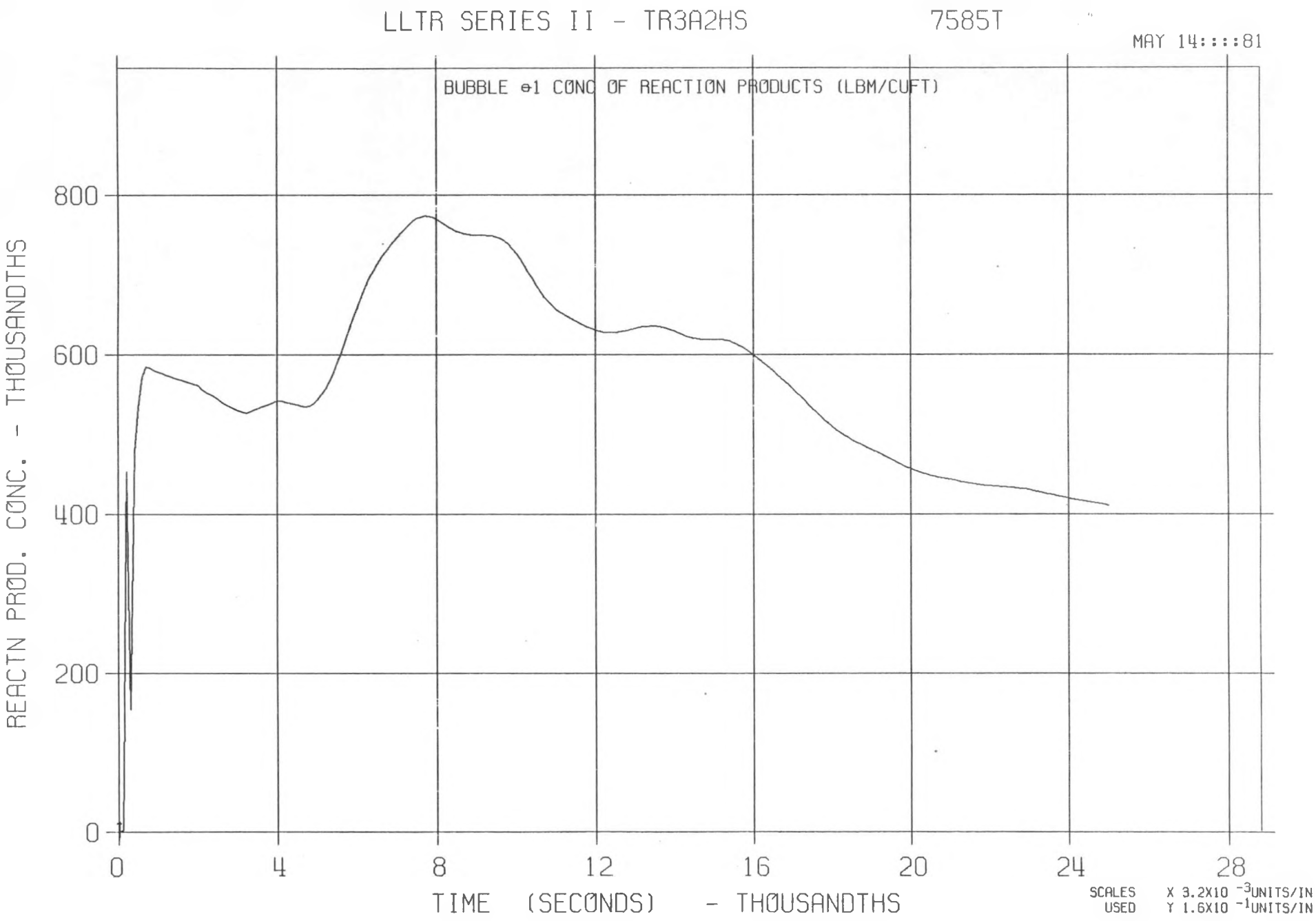
LLTR SERIES II - TR3A2HS 7585T
MAY 14::::81
BUBBLE ⊖1 CØNC ØF REACTIØN PRØDUCTS (LBM/CUFT)
REACTN PRØD. CØNC. - THØUSANDTHS
0
200
400
600
800
0
4
8
12
16
20
24
28
TIME (SECØNDS) - THØUSANDTHS
SCALES USED
X 3.2X10 -3 UNITS/IN
Y 1.6X10 -1 UNITS/IN

```
*EOJ***
DEVICE ....        T4
CHC .......      V313
TAPE ......     46444
FORMS .....        NO
FUNCTION ..        47
RECORDS ...        16
USER ......       DEK
DIST ......     S3S31
SNUMB/ACT . 7585T-01
```

APPENDIX C

TRANSWRAP MODEL.C

A-6 TEST

1 X SWR

GAS VOID AT TOP OF LLTV

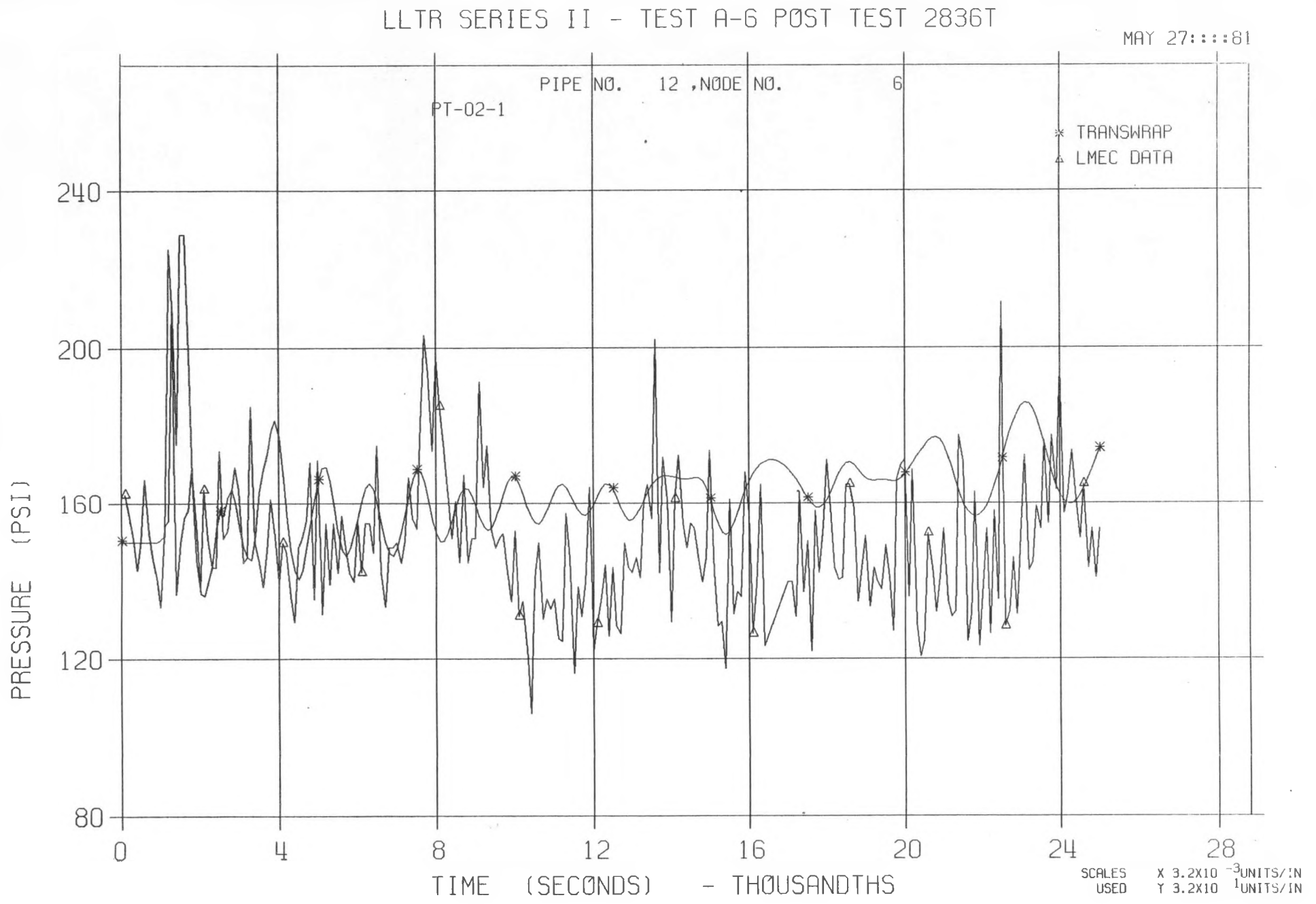
LLTR SERIES II - TEST A-6 POST TEST 2836T
MAY 27::::81
PIPE NO. 12 ,NODE NO. 6
PT-02-1
* TRANSWRAP
Δ LMEC DATA
240
200
160
120
80
PRESSURE (PSI)
0
4
8
12
16
20
24
28
TIME (SECONDS) - THOUSANDTHS
SCALES USED
X 3.2X10 -3 UNITS/IN
Y 3.2X10 1 UNITS/IN

C-1

PL 1

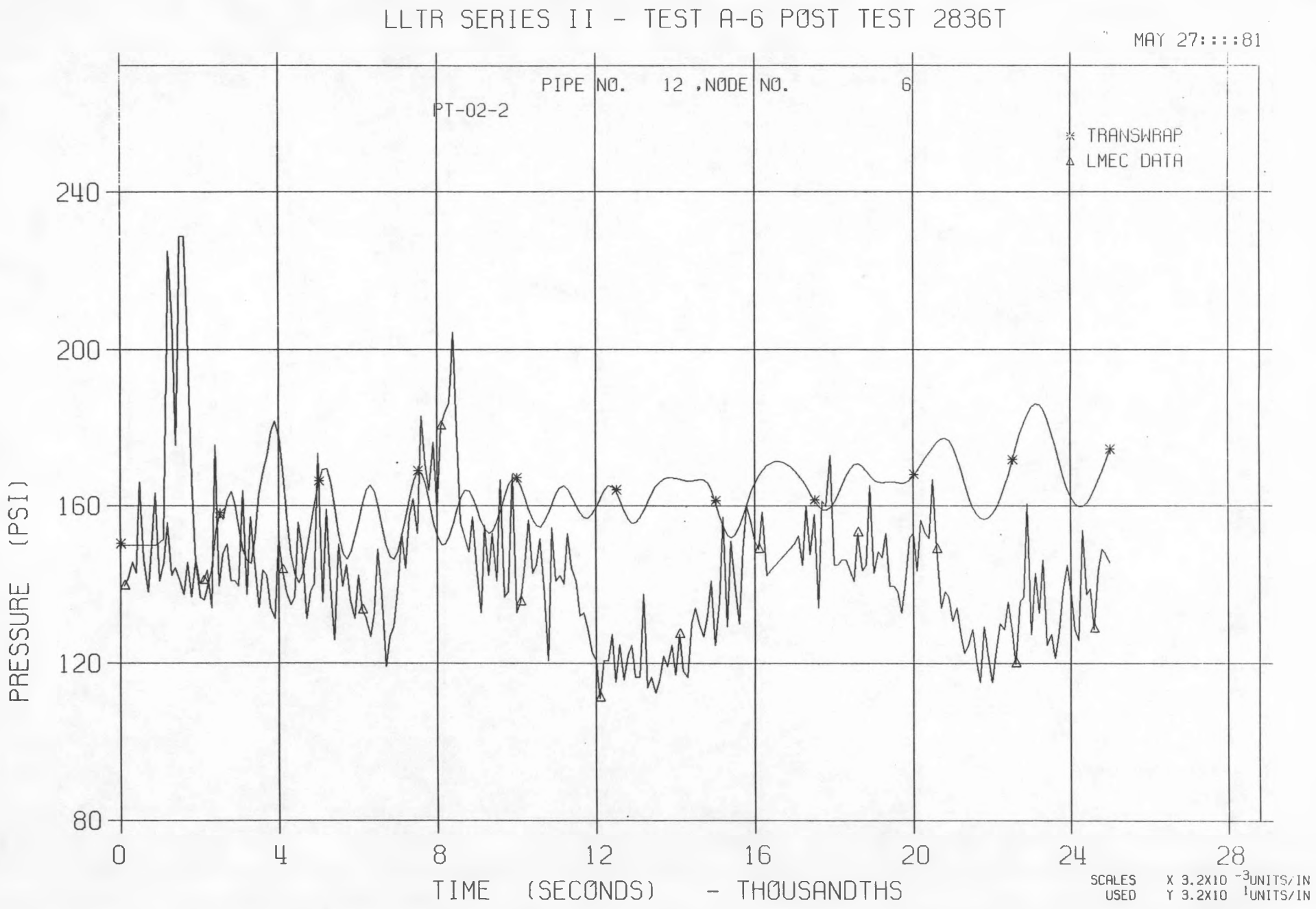
LLTR SERIES II - TEST A-6 POST TEST 2836T
MAY 27::::81
PIPE NO. 12 ,NODE NO. 6
PT-02-2
* TRANSWRAP
Δ LMEC DATA
240
200
160
120
80
PRESSURE (PSI)
0
4
8
12
16
20
24
28
TIME (SECONDS) - THOUSANDTHS
SCALES USED
X 3.2X10 -3 UNITS/IN
Y 3.2X10 1 UNITS/IN

C-2

PL 2

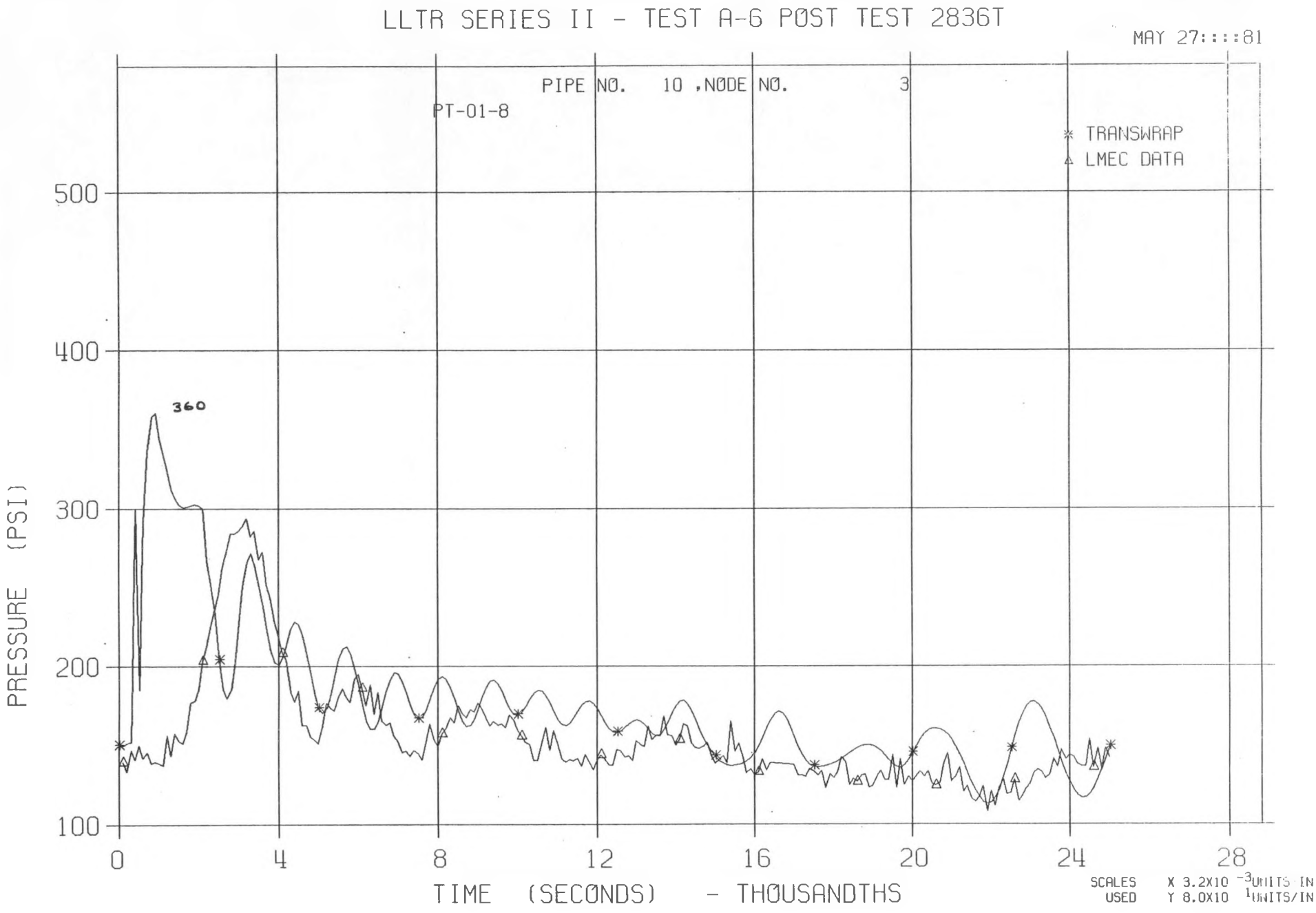
LLTR SERIES II - TEST A-6 POST TEST 2836T
MAY 27::::81
PIPE NO. 10 ,NODE NO. 3
PT-01-8
* TRANSWRAP
Δ LMEC DATA
360
PRESSURE (PSI)
500
400
300
200
100
0
4
8
12
16
20
24
28
TIME (SECONDS) - THOUSANDTHS
SCALES USED
X 3.2X10 -3 UNITS IN
Y 8.0X10 1 UNITS/IN

C-3

PL 3

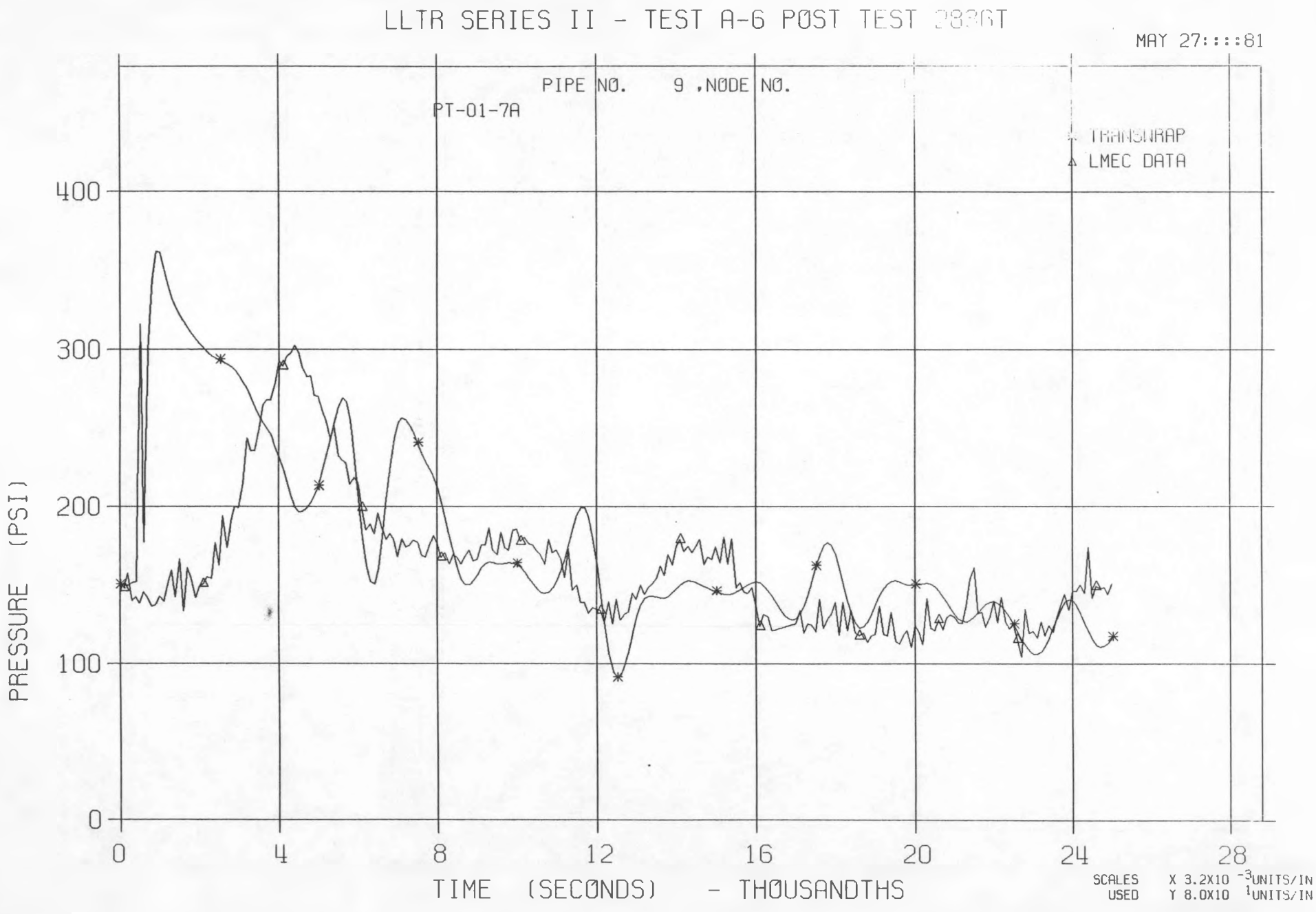
LLTR SERIES II - TEST A-6 PØST TEST 283GT
MAY 27::::81
PIPE NØ. 9 ,NØDE NØ.
PT-01-7A
TRANSWRAP
LMEC DATA
400
300
200
100
0
PRESSURE (PSI)
0
4
8
12
16
20
24
28
TIME (SECØNDS) - THØUSANDTHS
SCALES USED
X 3.2X10 -3 UNITS/IN
Y 8.0X10 1 UNITS/IN

A-2

PL 4

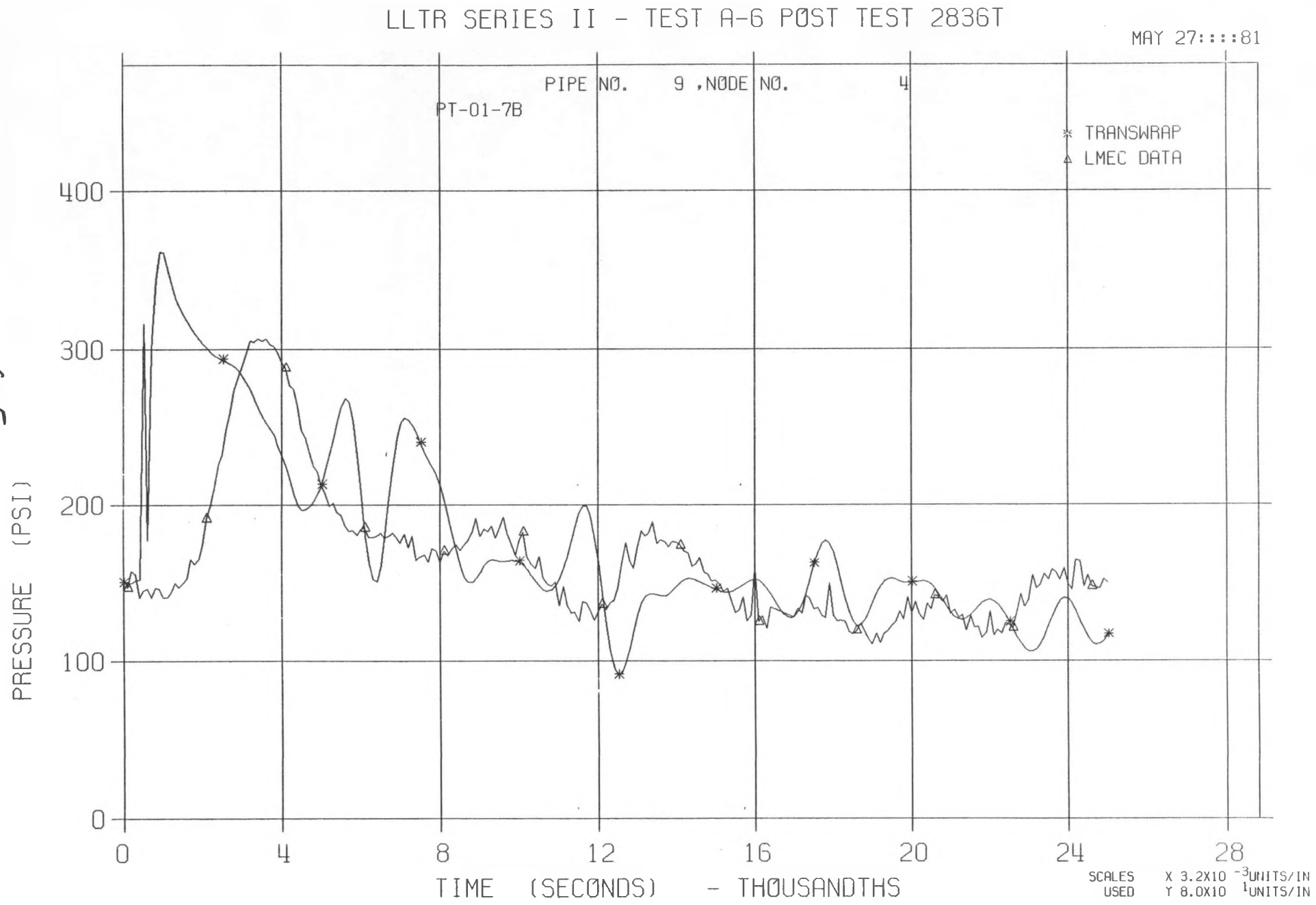
LLTR SERIES II - TEST A-6 PØST TEST 2836T
MAY 27::::81
PIPE NØ. 9 ,NØDE NØ. 4
PT-01-7B
TRANSWRAP
LMEC DATA
400
300
200
100
0
PRESSURE (PSI)
0
4
8
12
16
20
24
28
TIME (SECØNDS) - THØUSANDTHS
SCALES USED
X 3.2X10 -3 UNITS/IN
Y 8.0X10 1 UNITS/IN

C-5

PL 5

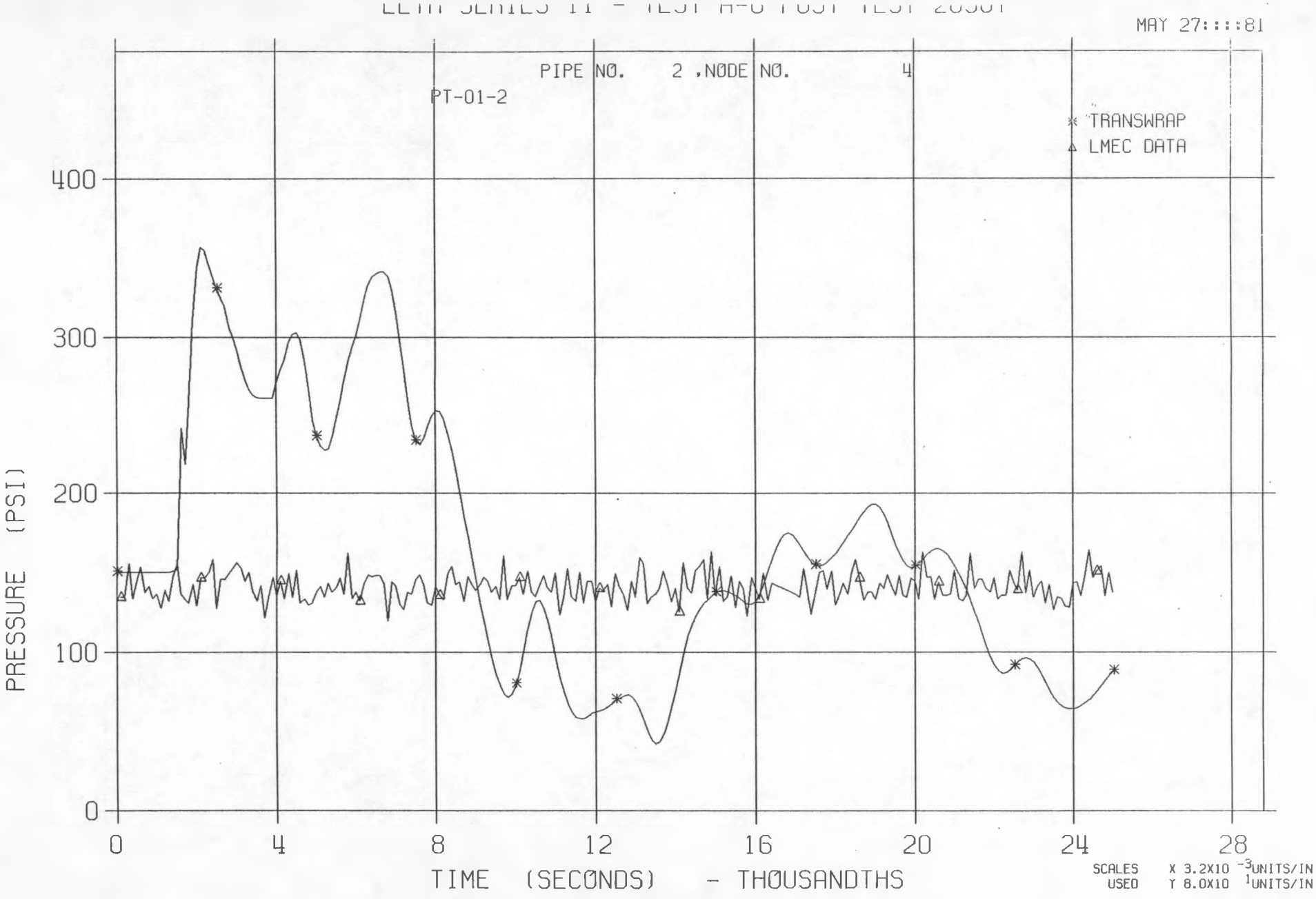
MAY 27::::81
PIPE NØ. 2 ,NØDE NØ. 4
PT-01-2
TRANSWRAP
LMEC DATA
400
300
200
100
0
PRESSURE (PSI)
0
4
8
12
16
20
24
28
TIME (SECØNDS) - THØUSANDTHS
SCALES USED
X 3.2X10 -3 UNITS/IN
Y 8.0X10 1 UNITS/IN

PL 6

PL 8

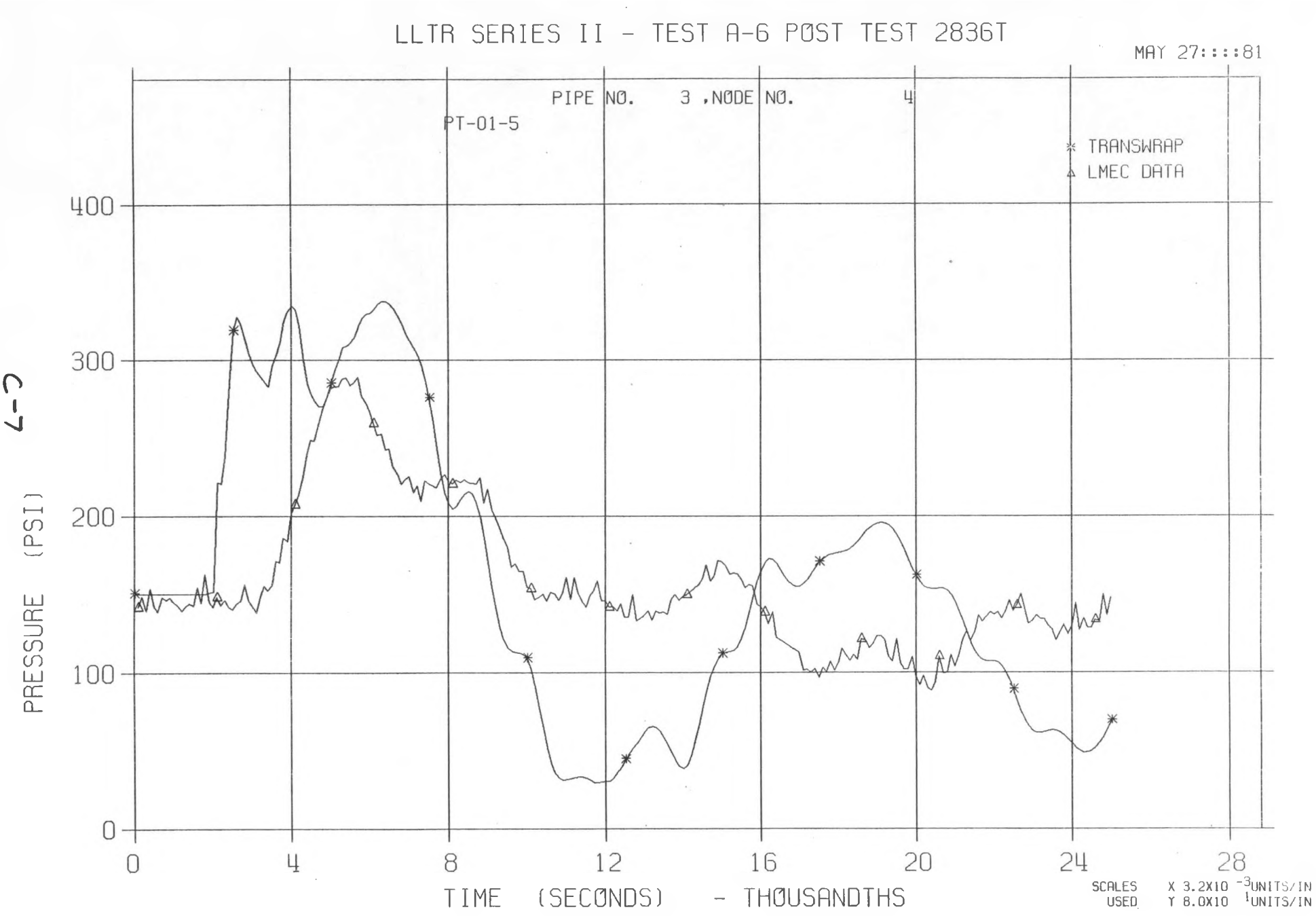
LLTR SERIES II - TEST A-6 POST TEST 2836T
MAY 27::::81
PIPE NO. 3 ,NODE NO. 4
PT-01-5
TRANSWRAP
LMEC DATA
PRESSURE (PSI)
400
300
200
100
0
0
4
8
12
16
20
24
28
TIME (SECONDS) - THOUSANDTHS
SCALES USED
X 3.2X10 -3 UNITS/IN
Y 8.0X10 1 UNITS/IN

PL 7

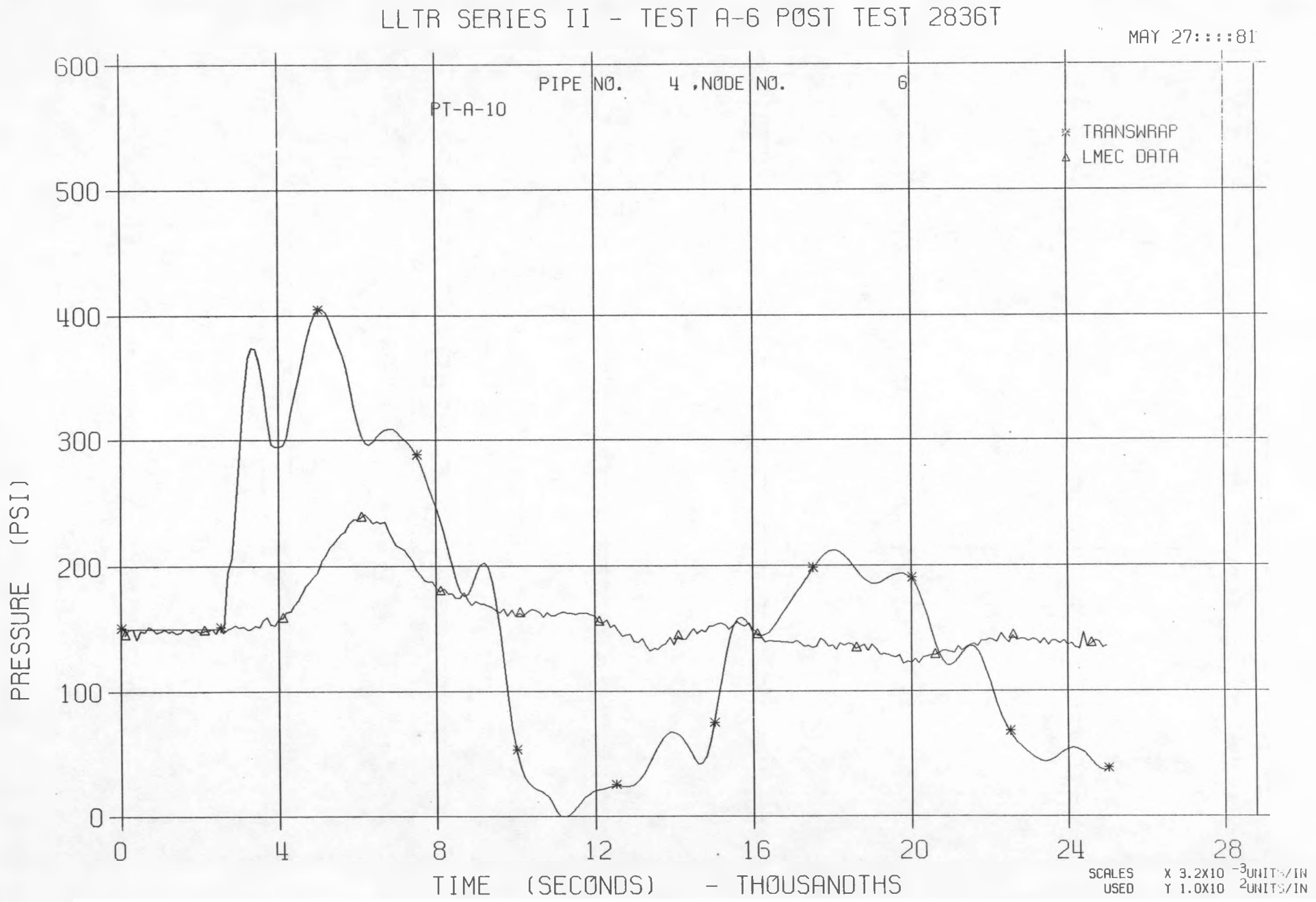
LLTR SERIES II - TEST A-6 POST TEST 2836T
MAY 27::::81
PIPE NO. 4 ,NODE NO. 6
PT-A-10
TRANSWRAP
LMEC DATA
PRESSURE (PSI)
600
500
400
300
200
100
0
0
4
8
12
16
20
24
28
TIME (SECONDS) - THOUSANDTHS
SCALES USED
X 3.2X10 -3 UNITS/IN
Y 1.0X10 2 UNITS/IN

8-7

PL 8

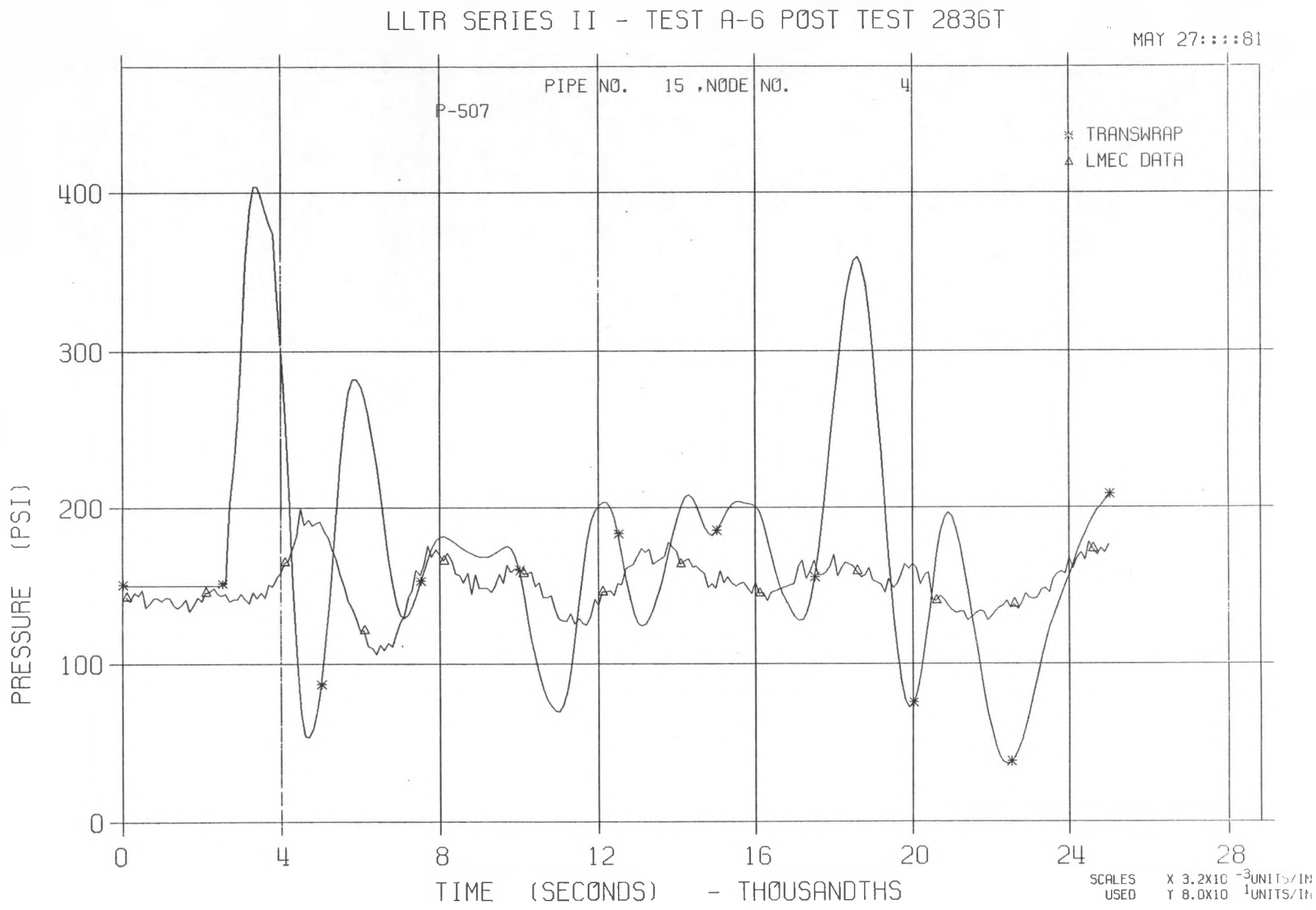
LLTR SERIES II - TEST A-6 POST TEST 2836T
MAY 27::::81
PIPE NO. 15 ,NODE NO. 4
P-507
TRANSWRAP
LMEC DATA
400
300
200
100
0
PRESSURE (PSI)
0
4
8
12
16
20
24
28
TIME (SECONDS) - THOUSANDTHS
SCALES USED
X 3.2X10 -3 UNITS/IN
Y 8.0X10 1 UNITS/IN

C-9

PL 9

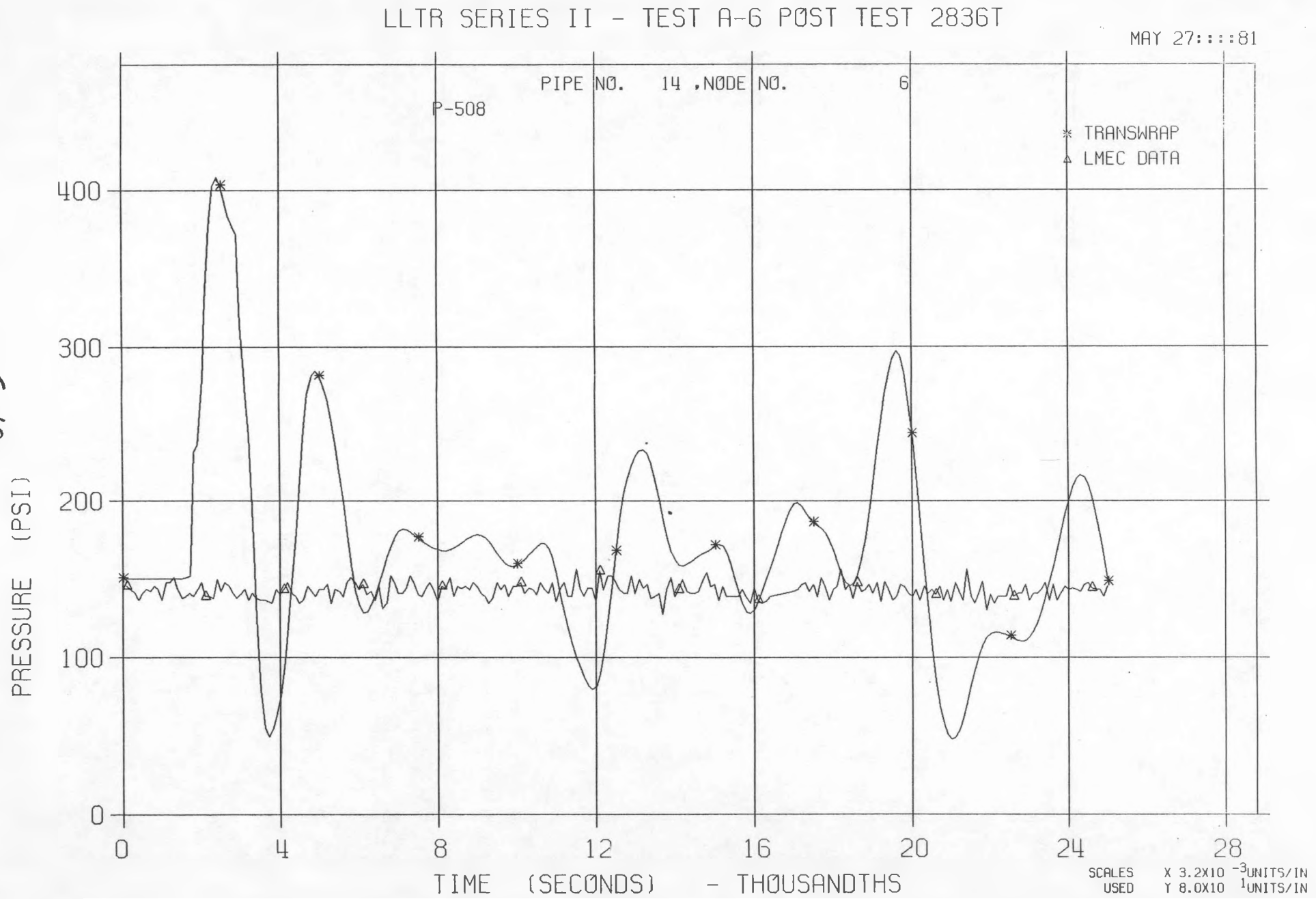
LLTR SERIES II - TEST A-6 POST TEST 2836T
MAY 27::::81
PIPE NO. 14 ,NODE NO. 6
P-508
TRANSWRAP
LMEC DATA
PRESSURE (PSI)
0
100
200
300
400
0
4
8
12
16
20
24
28
TIME (SECONDS) - THOUSANDTHS
SCALES USED
X 3.2X10 -3 UNITS/IN
Y 8.0X10 1 UNITS/IN

01-2

PL 10

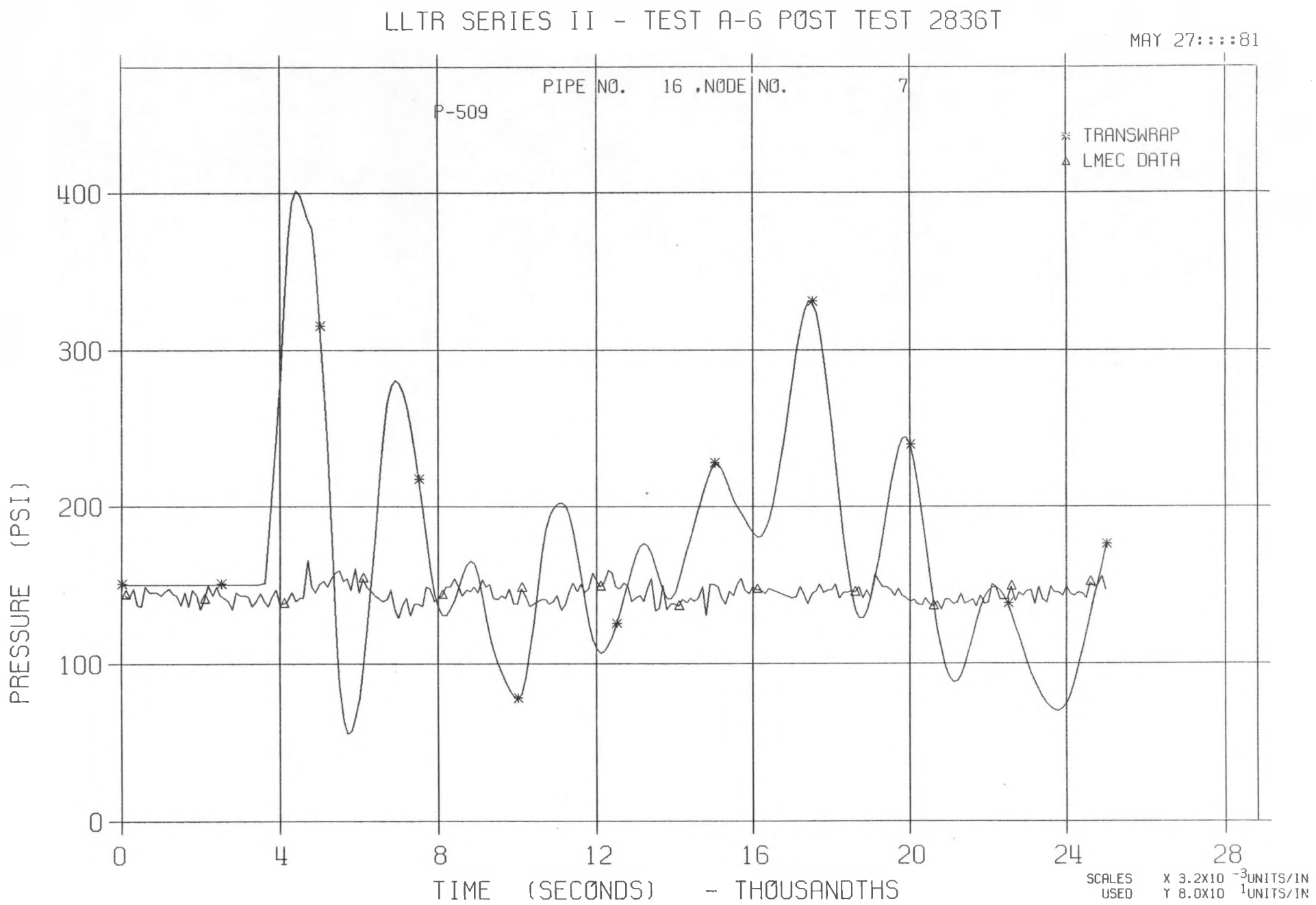
LLTR SERIES II - TEST A-6 PØST TEST 2836T
MAY 27::::81
PIPE NØ. 16 ,NØDE NØ. 7
P-509
TRANSWRAP
LMEC DATA
PRESSURE (PSI)
0
100
200
300
400
0
4
8
12
16
20
24
28
TIME (SECØNDS) - THØUSANDTHS
SCALES USED
X 3.2X10 -3 UNITS/IN
Y 8.0X10 1 UNITS/IN

II-2

PL 11

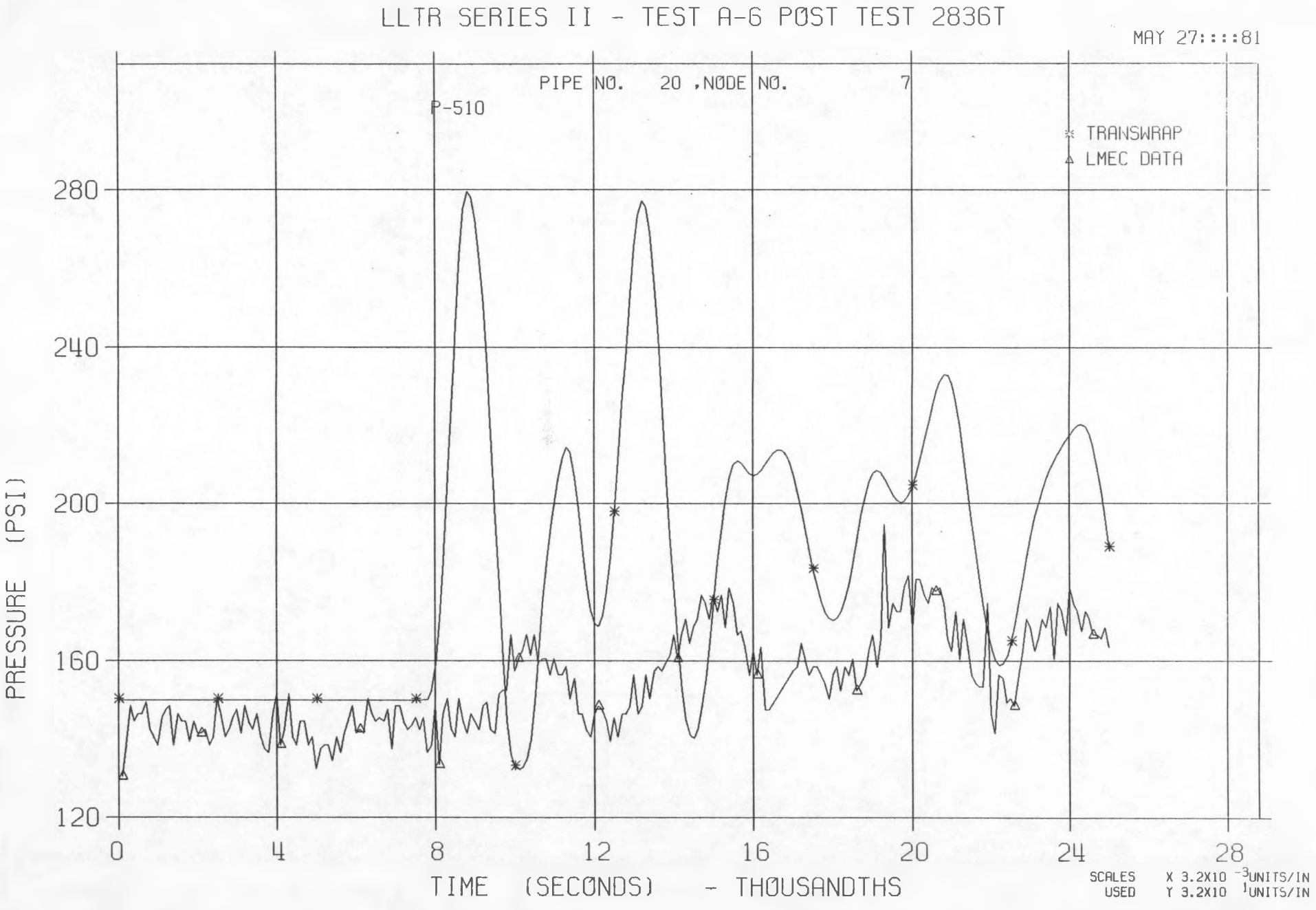
LLTR SERIES II - TEST A-6 POST TEST 2836T
MAY 27::::81
PIPE NO. 20 ,NODE NO. 7
P-510
TRANSWRAP
LMEC DATA
280
240
200
160
120
PRESSURE (PSI)
0
4
8
12
16
20
24
28
TIME (SECONDS) - THOUSANDTHS
SCALES USED
X 3.2X10 -3 UNITS/IN
Y 3.2X10 1 UNITS/IN

C-12

PL 12

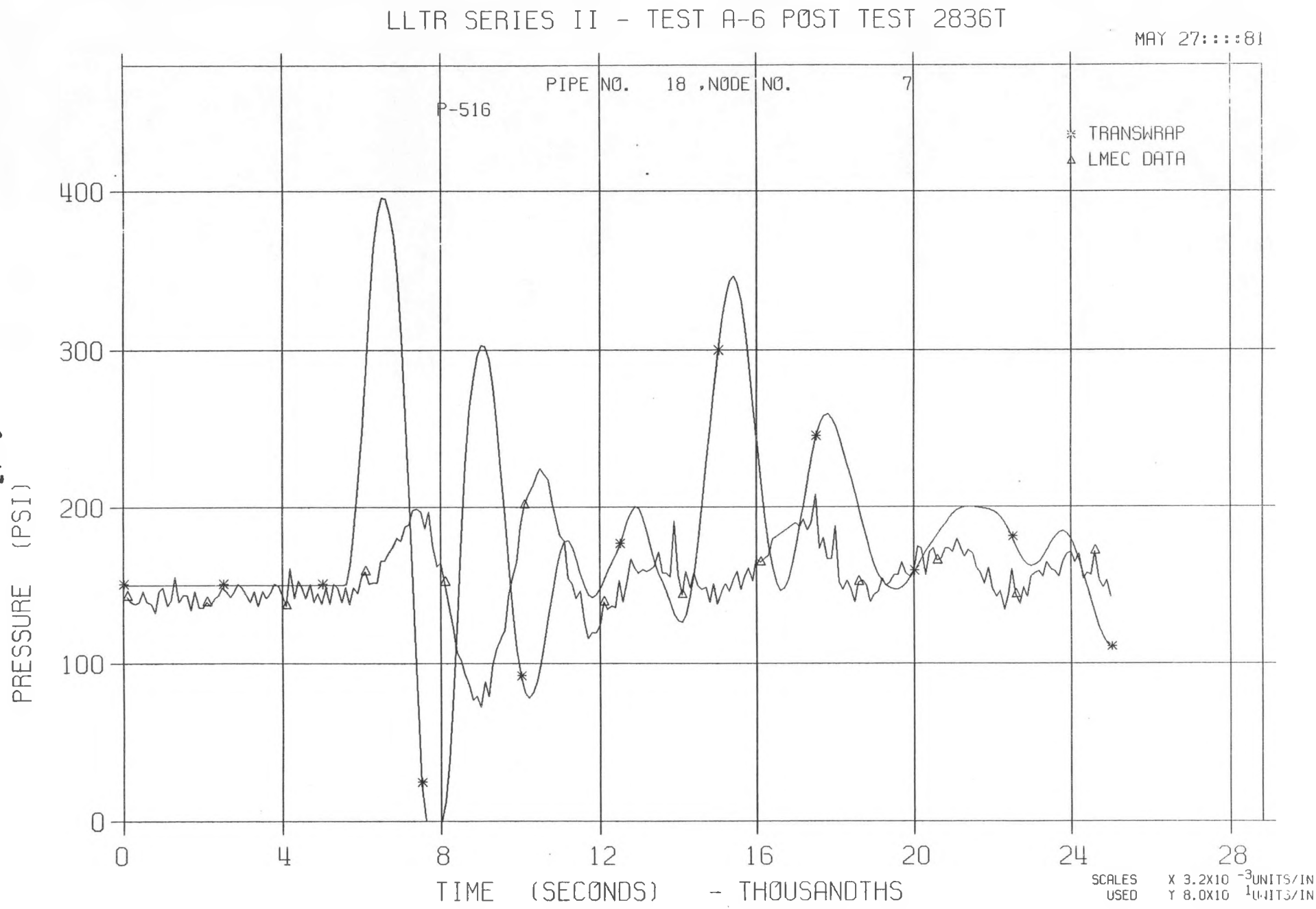
LLTR SERIES II - TEST A-6 POST TEST 2836T
MAY 27::::81
PIPE NO. 18 ,NODE NO. 7
P-516
TRANSWRAP
LMEC DATA
400
300
200
100
0
PRESSURE (PSI)
0
4
8
12
16
20
24
28
TIME (SECONDS) - THOUSANDTHS
SCALES USED
X 3.2X10 -3 UNITS/IN
Y 8.0X10 1 UNITS/IN

C-13

PL 13

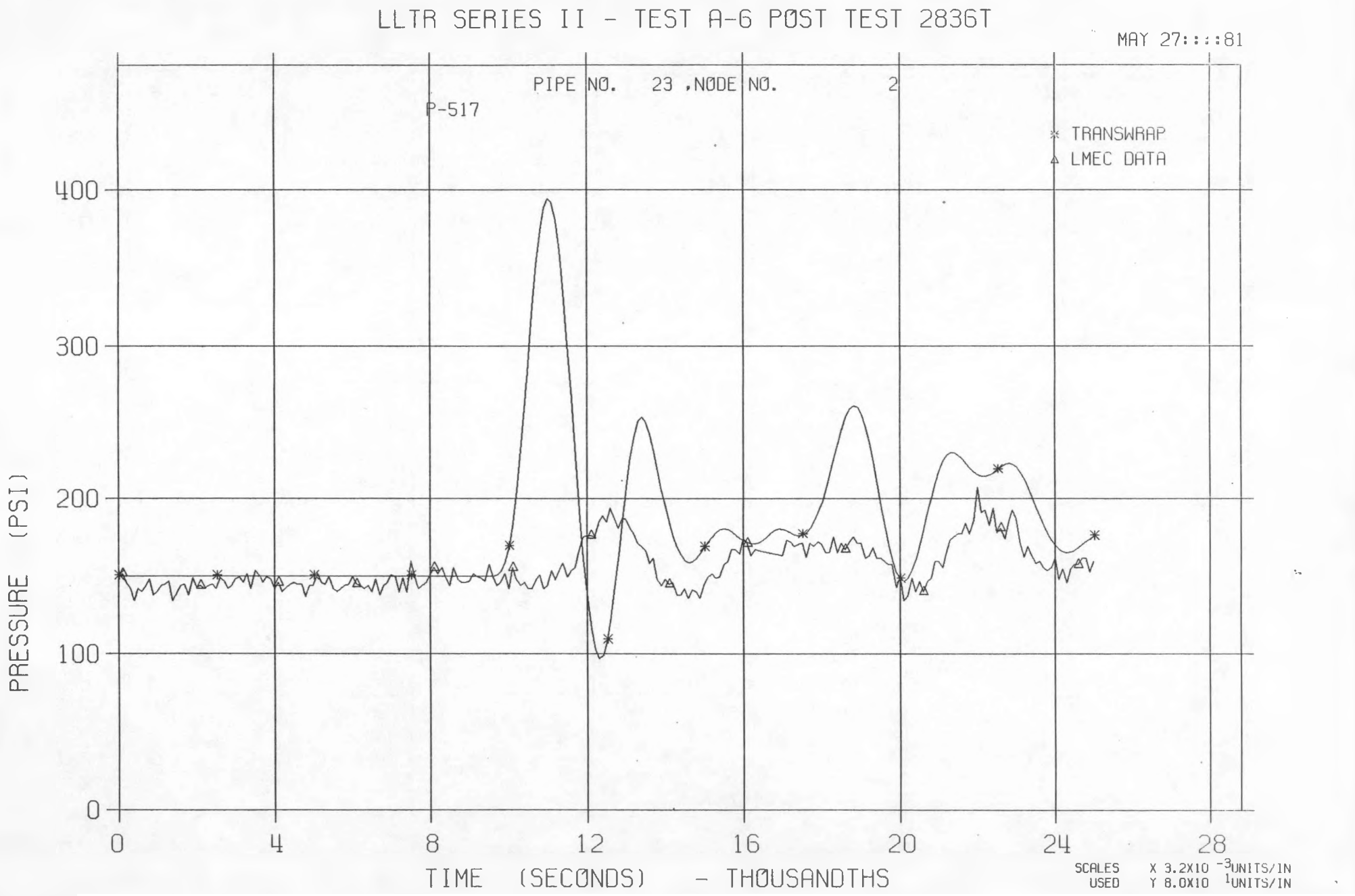
LLTR SERIES II - TEST A-6 POST TEST 2836T
MAY 27::::81
PIPE NO. 23 ,NODE NO. 2
P-517
TRANSWRAP
LMEC DATA
400
300
200
100
0
PRESSURE (PSI)
0
4
8
12
16
20
24
28
TIME (SECONDS) - THOUSANDTHS
SCALES USED
X 3.2X10 -3 UNITS/IN
Y 8.0X10 1 UNITS/IN

41-2

PL 14

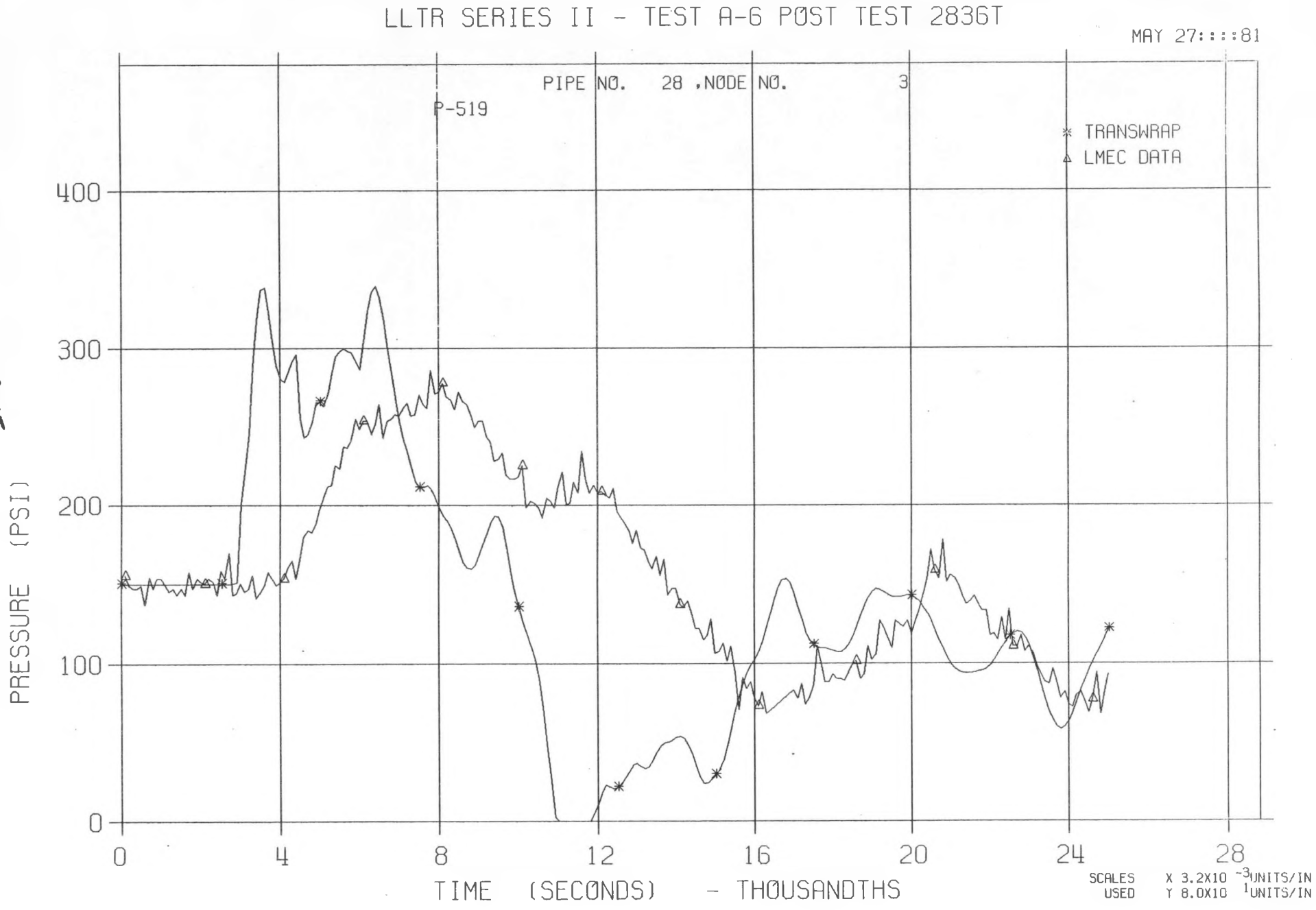
LLTR SERIES II - TEST A-6 PØST TEST 2836T
MAY 27::::81
PIPE NØ. 28 ,NØDE NØ. 3
P-519
* TRANSWRAP
Δ LMEC DATA
PRESSURE (PSI)
0
100
200
300
400
0
4
8
12
16
20
24
28
TIME (SECØNDS) - THØUSANDTHS
SCALES USED
X 3.2X10 -3 UNITS/IN
Y 8.0X10 1 UNITS/IN

C-15

PL 15

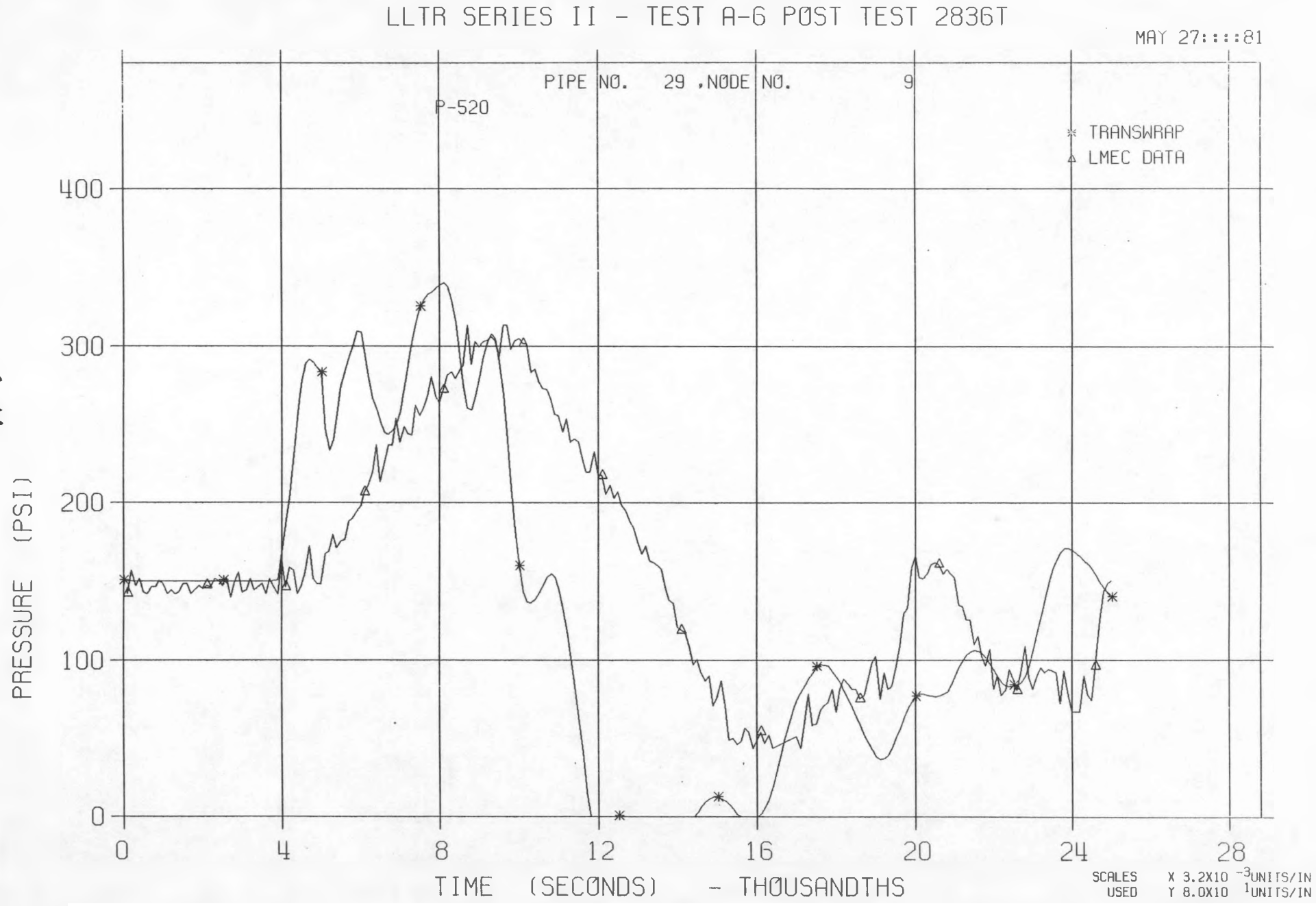
LLTR SERIES II - TEST A-6 POST TEST 2836T
MAY 27::::81
PIPE NO. 29 ,NODE NO. 9
P-520
TRANSWRAP
LMEC DATA
PRESSURE (PSI)
0
100
200
300
400
0
4
8
12
16
20
24
28
TIME (SECONDS) - THOUSANDTHS
SCALES USED
X 3.2X10 -3 UNITS/IN
Y 8.0X10 1 UNITS/IN

C-16

PL 16

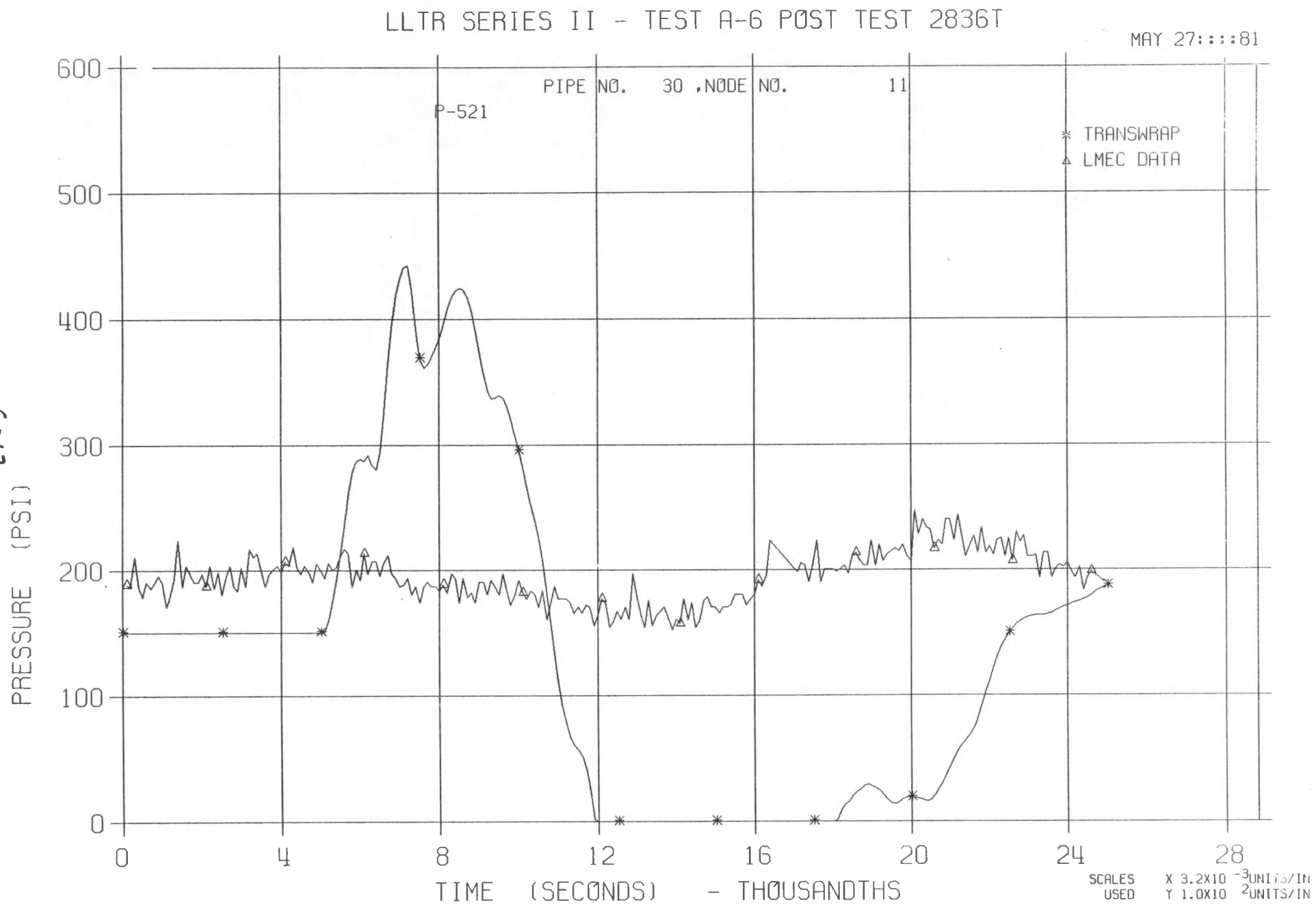
LLTR SERIES II - TEST A-6 POST TEST 2836T
MAY 27::::81
PIPE NO. 30 ,NODE NO. 11
P-521
TRANSWRAP
LMEC DATA
PRESSURE (PSI)
600
500
400
300
200
100
0
0
4
8
12
16
20
24
28
TIME (SECONDS) - THOUSANDTHS
SCALES USED
X 3.2X10 -3 UNITS/IN
Y 1.0X10 2 UNITS/IN

C-17

PL 17

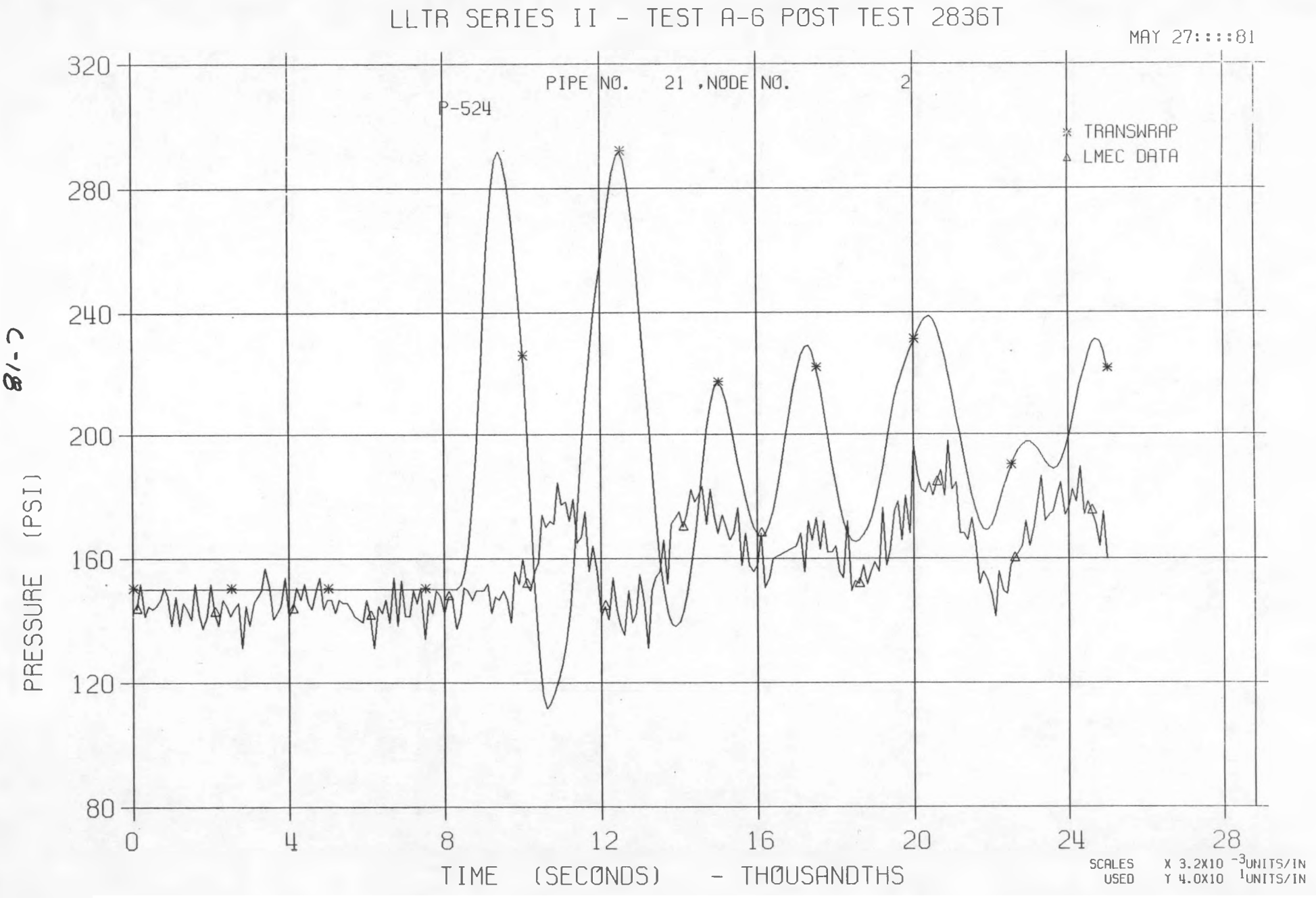
LLTR SERIES II - TEST A-6 POST TEST 2836T
MAY 27::::81
PIPE NO. 21 ,NODE NO. 2
P-524
TRANSWRAP
LMEC DATA
320
280
240
200
160
120
80
PRESSURE (PSI)
0
4
8
12
16
20
24
28
TIME (SECONDS) - THOUSANDTHS
SCALES USED
X 3.2X10 -3 UNITS/IN
Y 4.0X10 1 UNITS/IN

C-18

PL 18

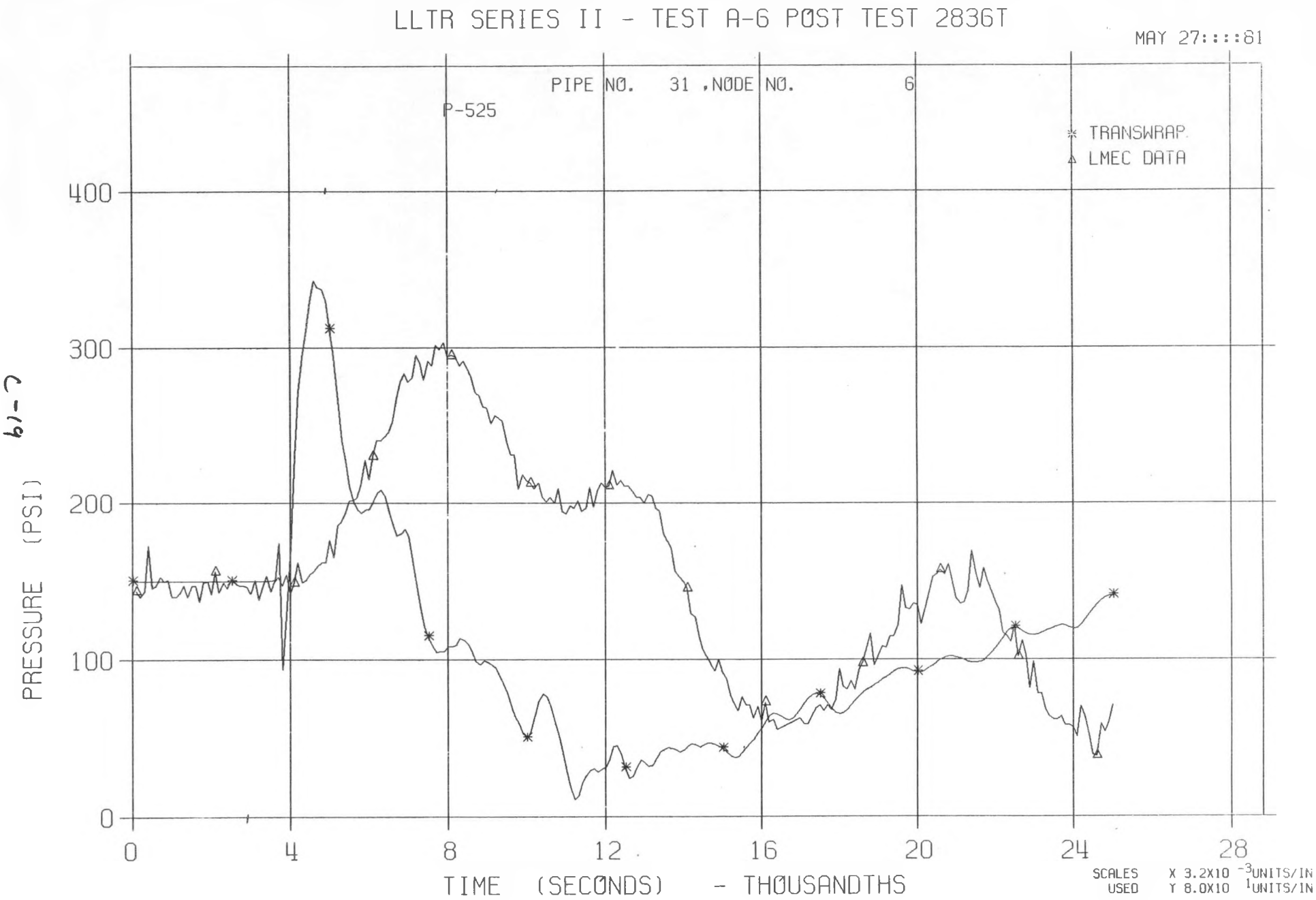
LLTR SERIES II - TEST A-6 POST TEST 2836T
MAY 27::::81
PIPE NO. 31 ,NODE NO. 6
P-525
TRANSWRAP
LMEC DATA
PRESSURE (PSI)
400
300
200
100
0
0
4
8
12
16
20
24
28
TIME (SECONDS) - THOUSANDTHS
SCALES USED
X 3.2X10 -3 UNITS/IN
Y 8.0X10 1 UNITS/IN

C-19

PL 19

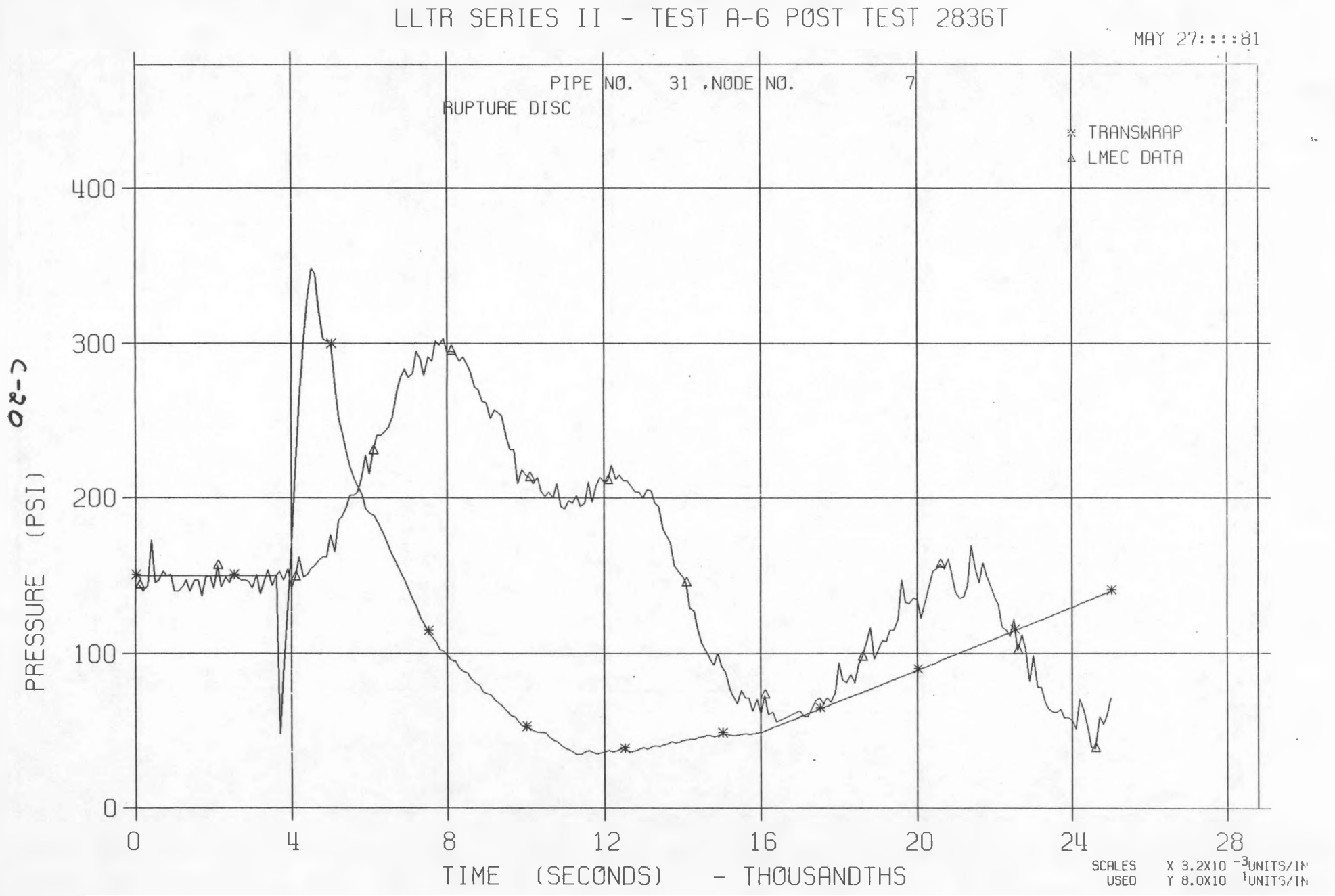
LLTR SERIES II - TEST A-6 POST TEST 2836T
MAY 27::::81
PIPE NO. 31 ,NODE NO. 7
RUPTURE DISC
TRANSWRAP
LMEC DATA
PRESSURE (PSI)
0
100
200
300
400
0
4
8
12
16
20
24
28
TIME (SECONDS) - THOUSANDTHS
SCALES USED
X 3.2X10 -3 UNITS/IN
Y 8.0X10 1 UNITS/IN

C-20

PL 20

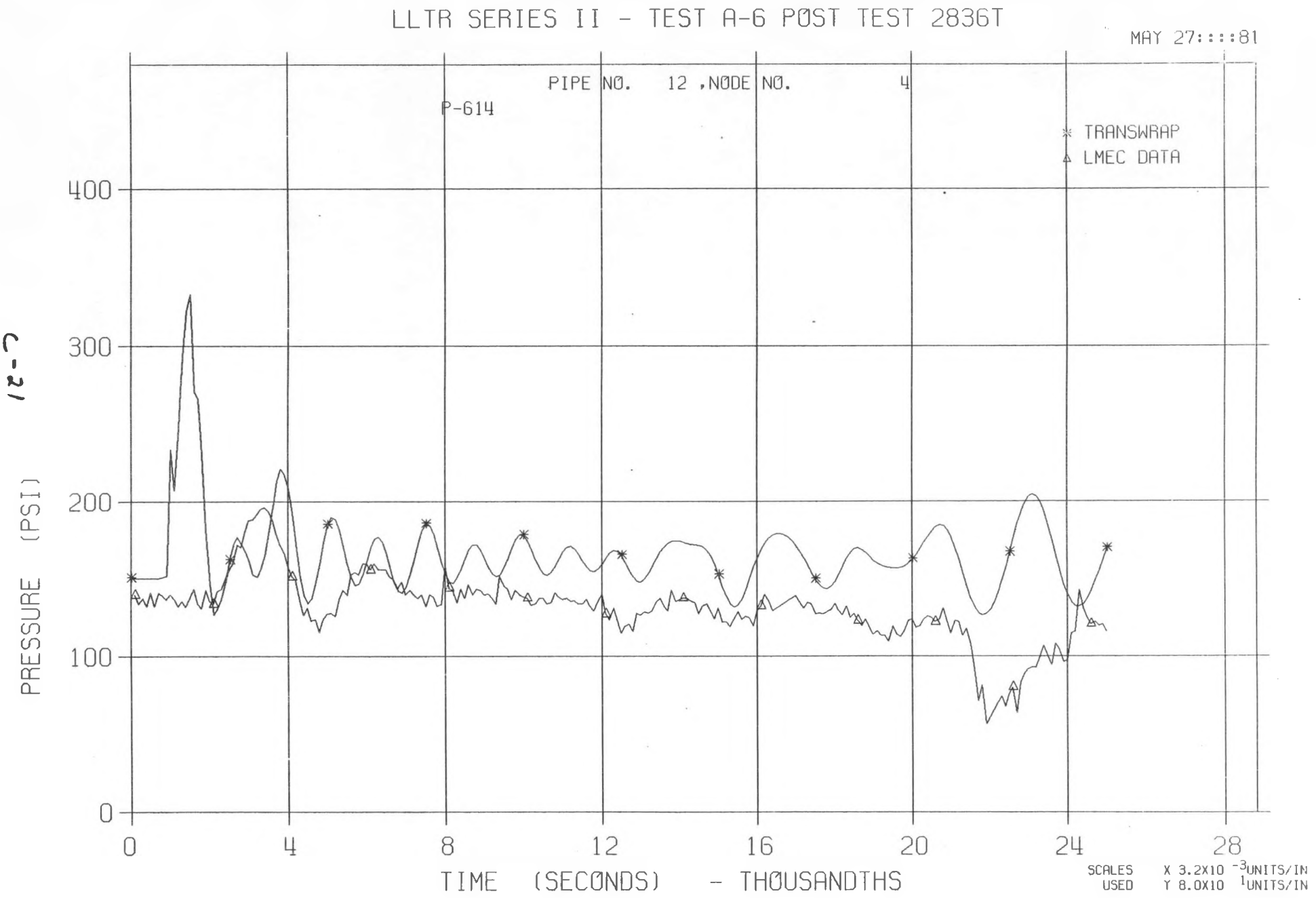
LLTR SERIES II - TEST A-6 POST TEST 2836T
MAY 27::::81
PIPE NO. 12 ,NODE NO. 4
P-614
* TRANSWRAP
Δ LMEC DATA
PRESSURE (PSI)
400
300
200
100
0
0
4
8
12
16
20
24
28
TIME (SECONDS) - THOUSANDTHS
SCALES USED
X 3.2X10 -3 UNITS/IN
Y 8.0X10 1 UNITS/IN

12-7

PL 21

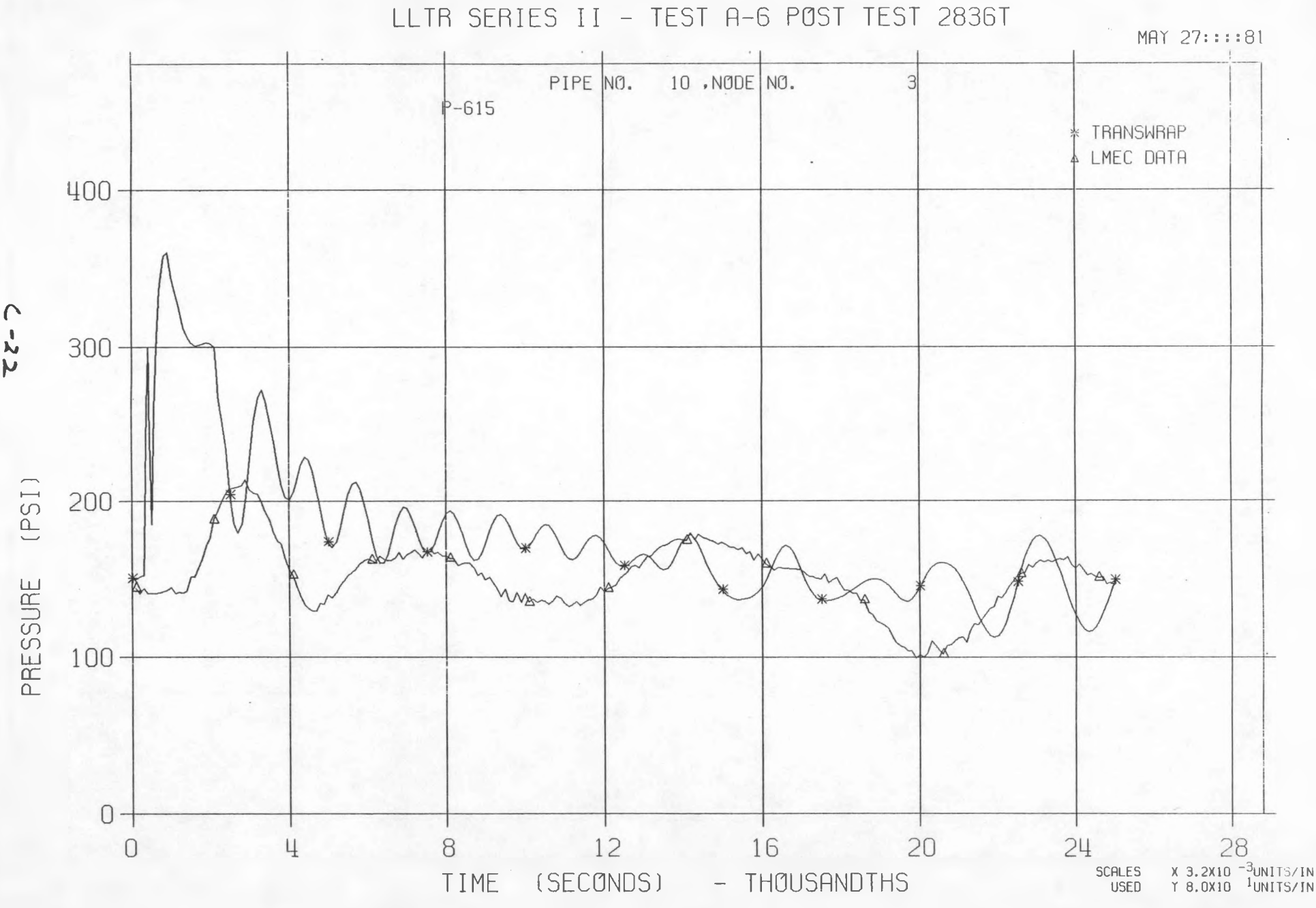
LLTR SERIES II - TEST A-6 POST TEST 2836T
MAY 27::::81
PIPE NO. 10 ,NODE NO. 3
P-615
TRANSWRAP
LMEC DATA
400
300
200
100
0
PRESSURE (PSI)
0
4
8
12
16
20
24
28
TIME (SECONDS) - THOUSANDTHS
SCALES USED
X 3.2X10 -3 UNITS/IN
Y 8.0X10 1 UNITS/IN

C-22

PL 22

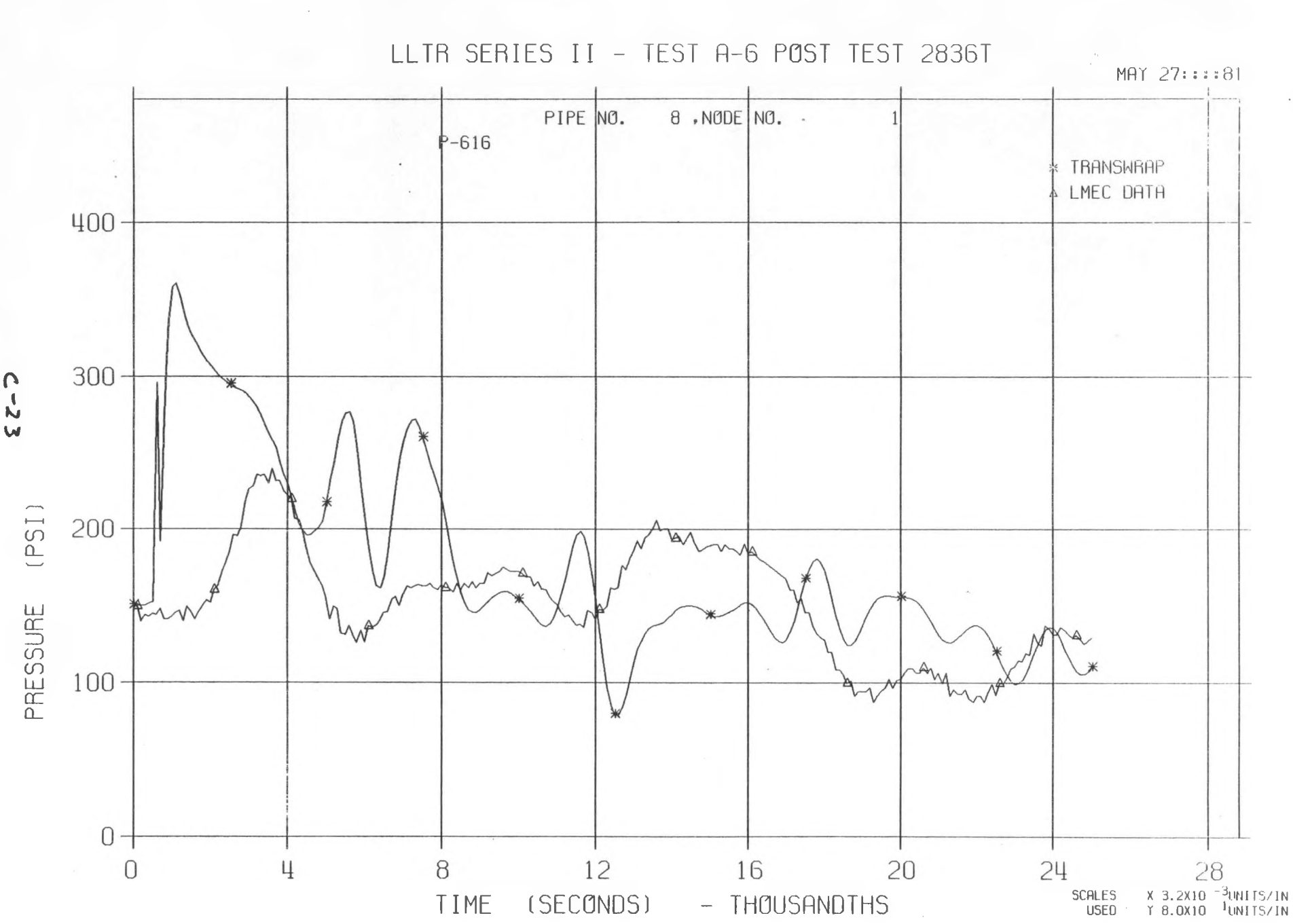
LLTR SERIES II - TEST A-6 POST TEST 2836T
MAY 27::::81
PIPE NO. 8 ,NODE NO. 1
P-616
* TRANSWRAP
Δ LMEC DATA
PRESSURE (PSI)
0
100
200
300
400
0
4
8
12
16
20
24
28
TIME (SECONDS) - THOUSANDTHS
SCALES USED
X 3.2X10 -3 UNITS/IN
Y 8.0X10 1 UNITS/IN

C-23

PL 23

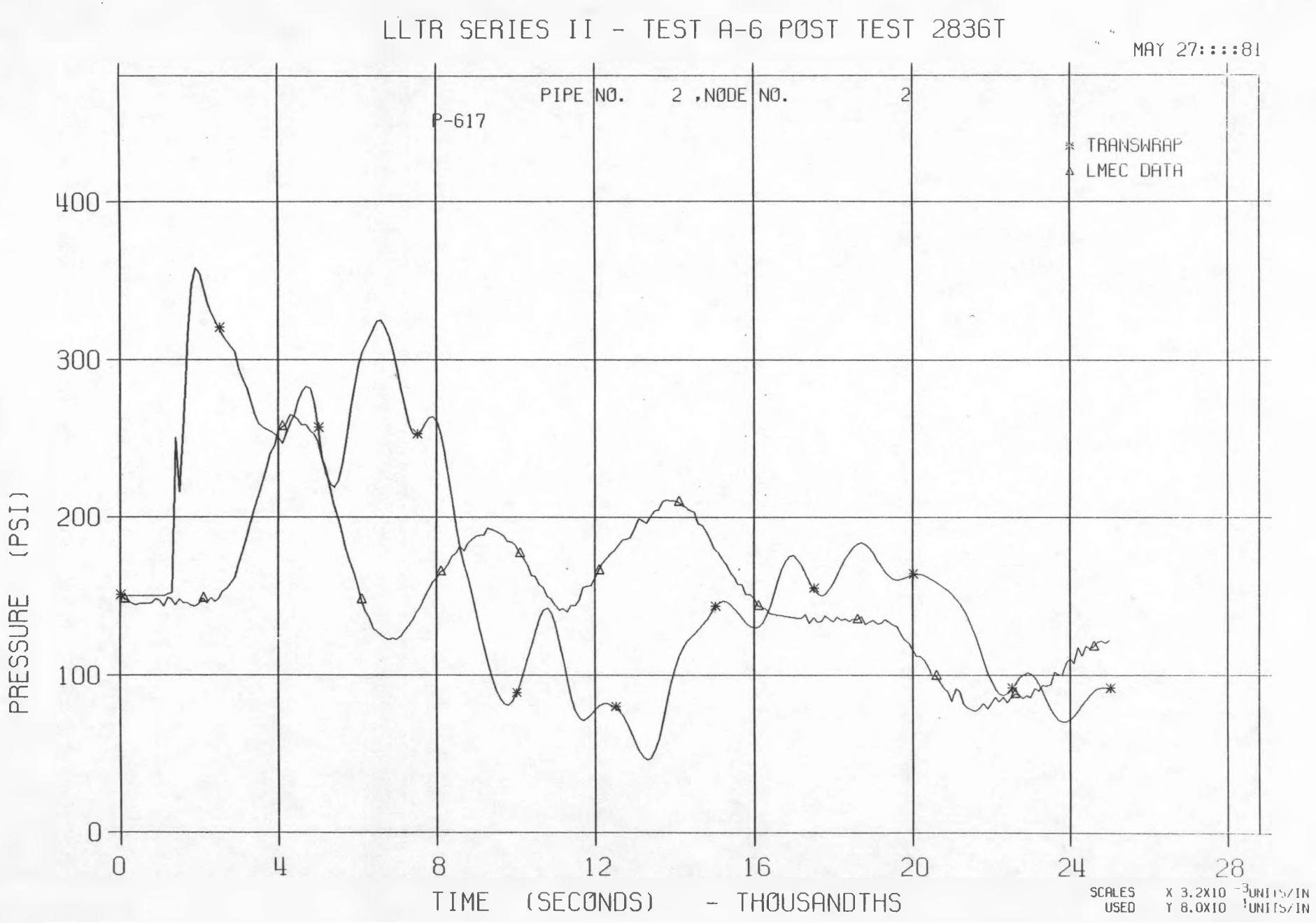
LLTR SERIES II - TEST A-6 POST TEST 2836T
MAY 27::::81
PIPE NO. 2 ,NODE NO. 2
P-617
* TRANSWRAP
Δ LMEC DATA
PRESSURE (PSI)
0
100
200
300
400
0
4
8
12
16
20
24
28
TIME (SECONDS) - THOUSANDTHS
SCALES USED
X 3.2X10 -3 UNITS/IN
Y 8.0X10 1 UNITS/IN

42-2

PL 24

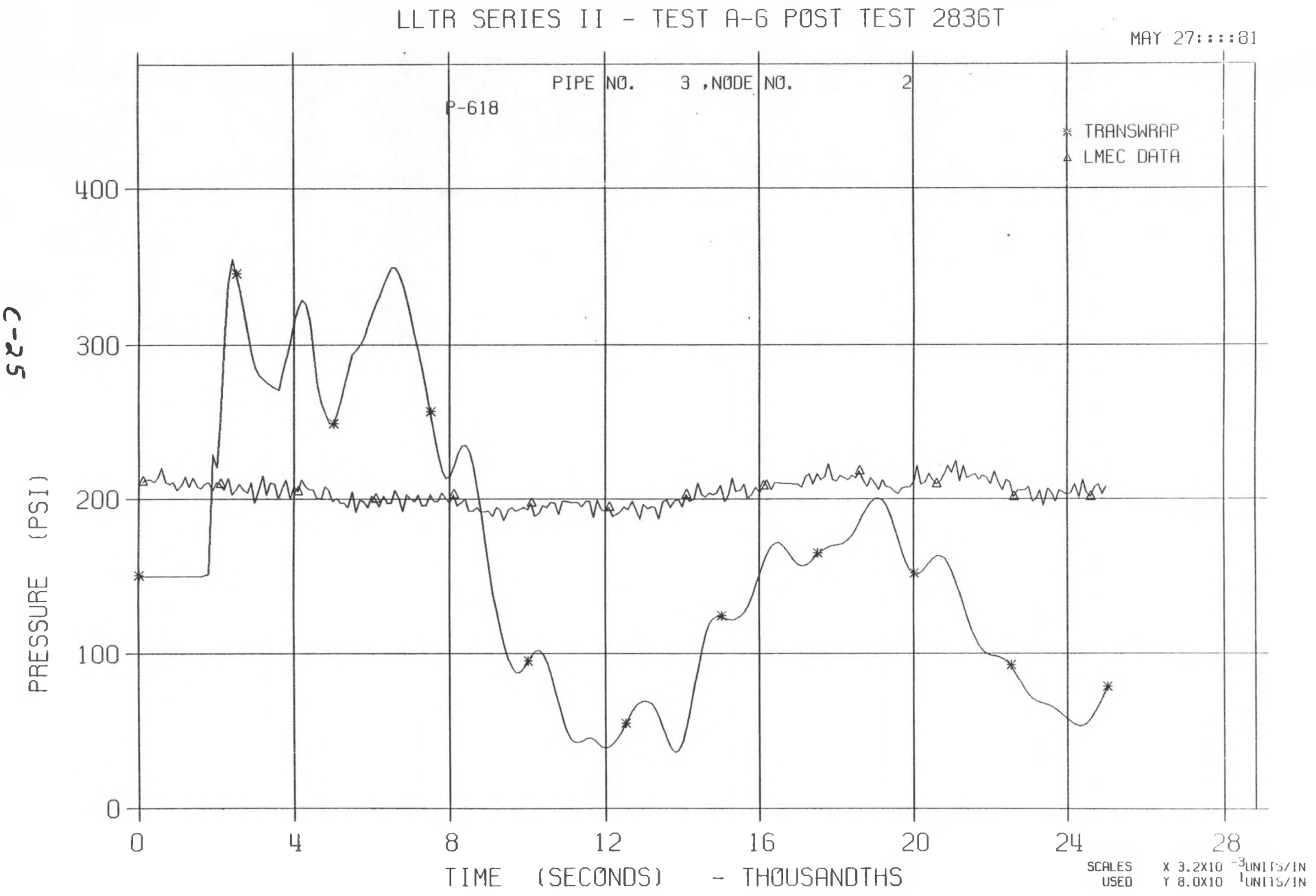
LLTR SERIES II - TEST A-6 POST TEST 2836T
MAY 27::::81
PIPE NO. 3 ,NODE NO. 2
P-618
TRANSWRAP
LMEC DATA
400
300
200
100
0
PRESSURE (PSI)
0
4
8
12
16
20
24
28
TIME (SECONDS) - THOUSANDTHS
SCALES USED
X 3.2X10 -3 UNITS/IN
Y 8.0X10 1 UNITS/IN

C-25

PL 25

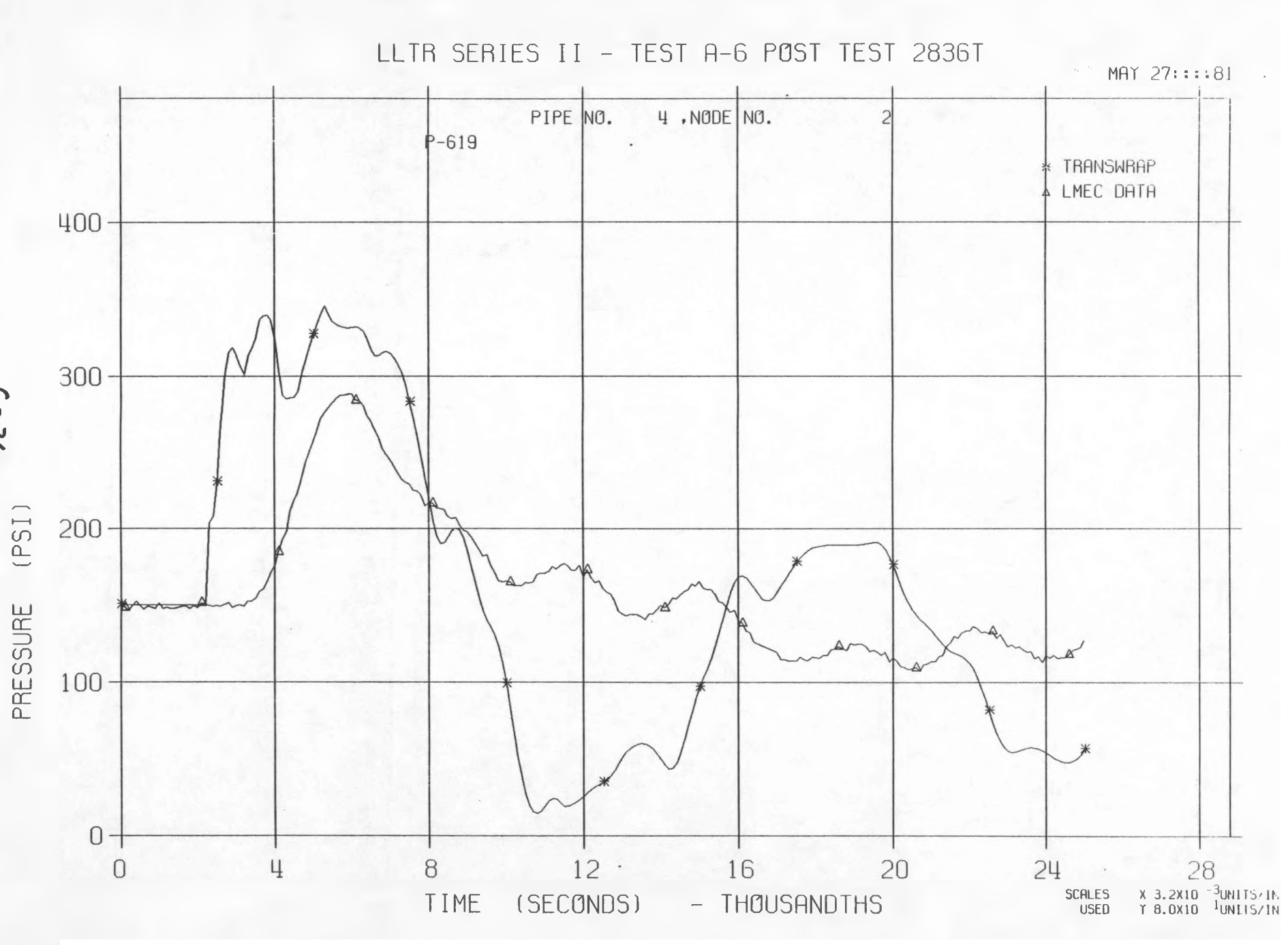
LLTR SERIES II - TEST A-6 PØST TEST 2836T
MAY 27::::81
PIPE NØ. 4 ,NØDE NØ. 2
P-619
TRANSWRAP
LMEC DATA
400
300
200
100
0
PRESSURE (PSI)
0
4
8
12
16
20
24
28
TIME (SECONDS) - THØUSANDTHS
SCALES USED
X 3.2X10 -3 UNITS/IN
Y 8.0X10 1 UNITS/IN

C-26

PL 26

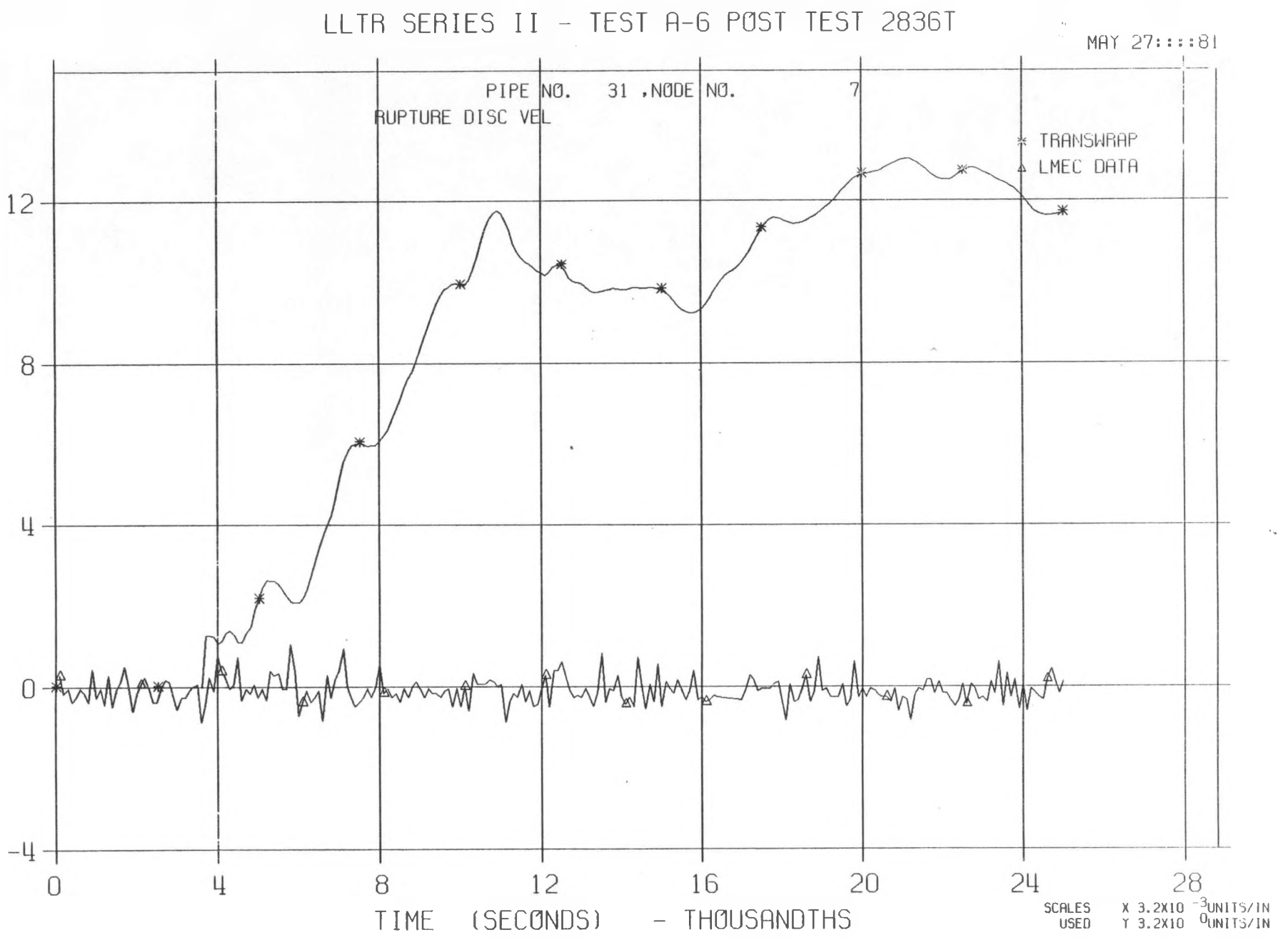
LLTR SERIES II - TEST A-6 POST TEST 2836T
MAY 27::::81
PIPE NO. 31 ,NODE NO. 7
RUPTURE DISC VEL
TRANSWRAP
LMEC DATA
12
8
4
0
-4
VELOCITY (FT/SEC)
0
4
8
12
16
20
24
28
TIME (SECONDS) - THOUSANDTHS
SCALES USED
X 3.2X10 -3 UNITS/IN
Y 3.2X10 0 UNITS/IN

PL 28

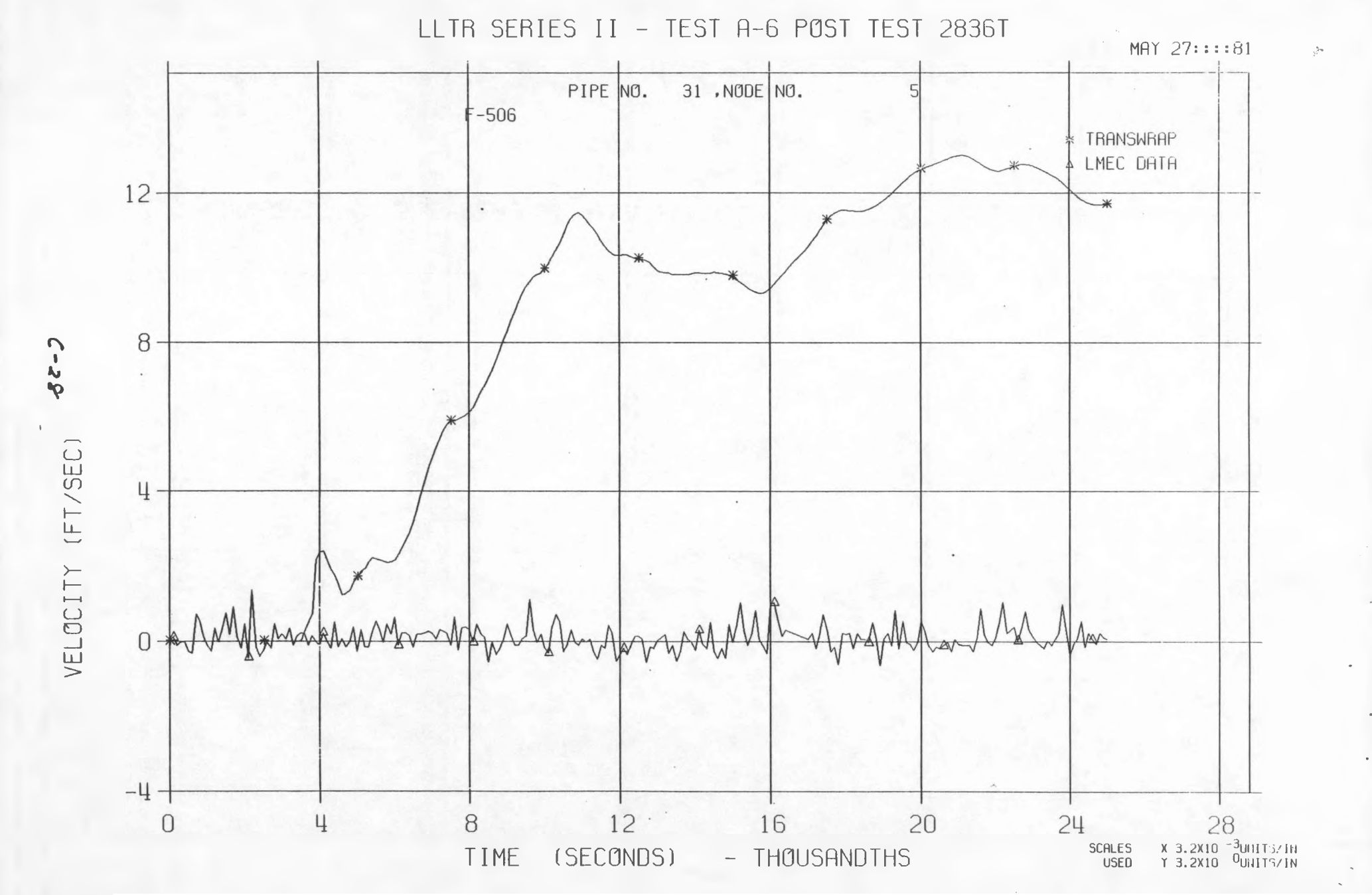
LLTR SERIES II - TEST A-6 POST TEST 2836T
MAY 27::::81
PIPE NO. 31 ,NODE NO. 5
F-506
TRANSWRAP
LMEC DATA
VELOCITY (FT/SEC)
12
8
4
0
-4
0
4
8
12
16
20
24
28
TIME (SECONDS) - THOUSANDTHS
SCALES USED
X 3.2X10 -3 UNITS/IN
Y 3.2X10 0 UNITS/IN

C-28

PL 29

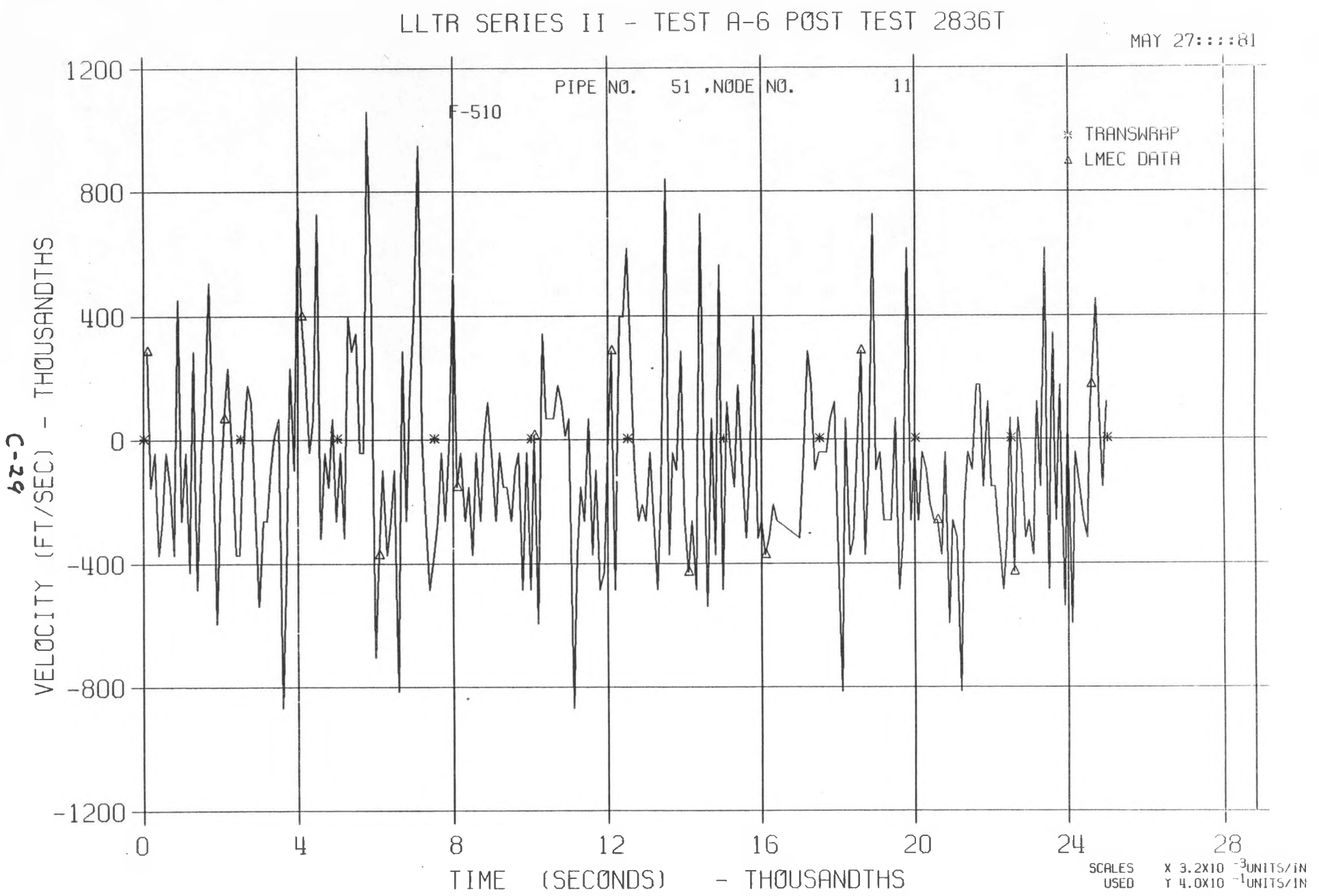
LLTR SERIES II - TEST A-6 POST TEST 2836T
MAY 27::::81
PIPE NO. 51 ,NODE NO. 11
F-510
TRANSWRAP
LMEC DATA
1200
800
400
0
-400
-800
-1200
VELOCITY (FT/SEC) - THOUSANDTHS
0
4
8
12
16
20
24
28
TIME (SECONDS) - THOUSANDTHS
SCALES USED
X 3.2X10 -3 UNITS/IN
Y 4.0X10 -1 UNITS/IN

C-29

PL 30

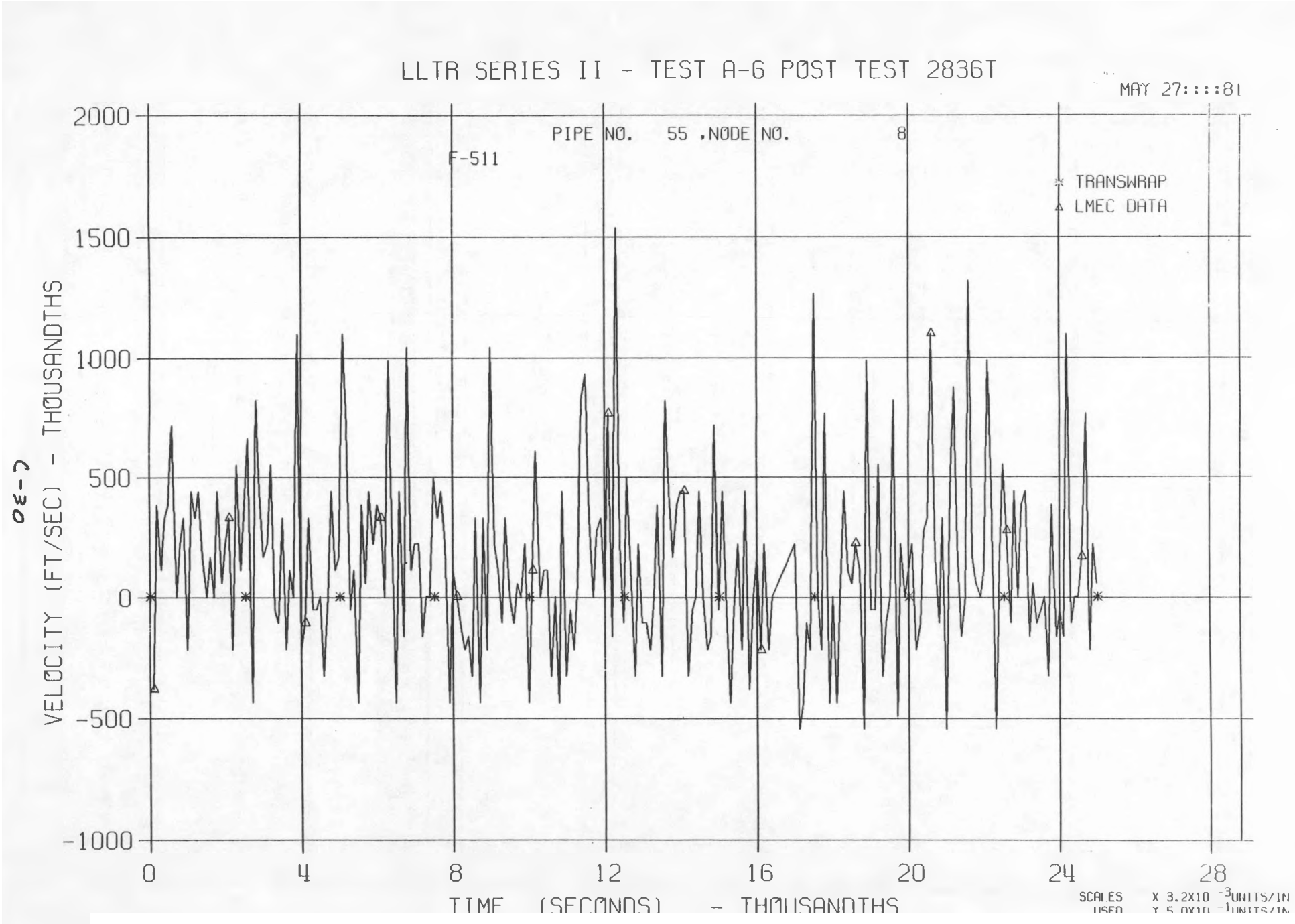
LLTR SERIES II - TEST A-6 POST TEST 2836T
MAY 27::::81
PIPE NO. 55 .NODE NO. 8
F-511
TRANSWRAP
LMEC DATA
VELOCITY (FT/SEC) - THOUSANDTHS
2000
1500
1000
500
0
-500
-1000
0
4
8
12
16
20
24
28
TIME (SECONDS) - THOUSANDTHS
SCALES USED
X 3.2X10 -3 UNITS/IN
Y 5.0X10 -1 UNITS/IN

C-30

PL 31

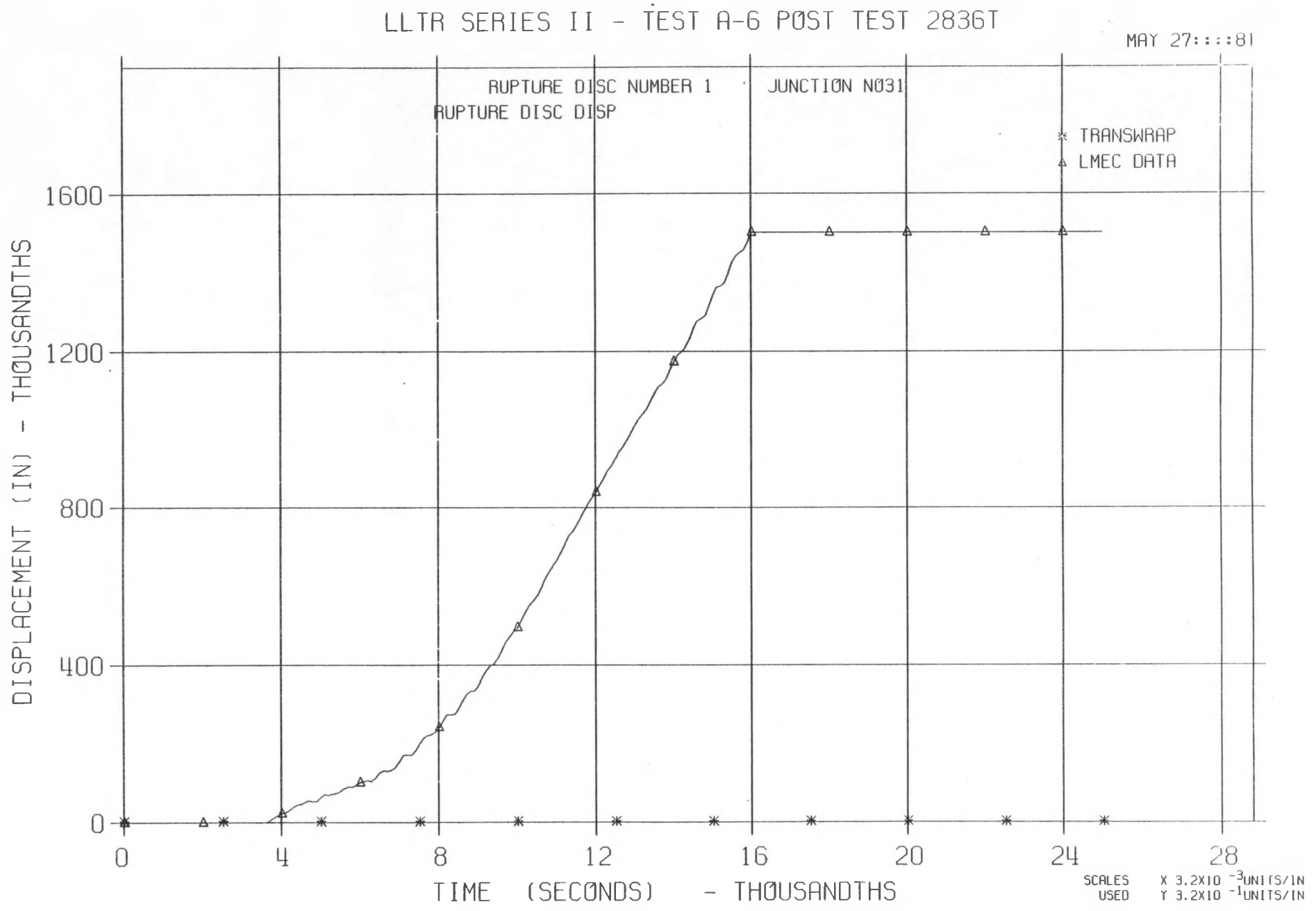
LLTR SERIES II - TEST A-6 POST TEST 2836T
MAY 27::::81
RUPTURE DISC NUMBER 1
RUPTURE DISC DISP
JUNCTION N031
TRANSWRAP
LMEC DATA
DISPLACEMENT (IN) - THOUSANDTHS
1600
1200
800
400
0
0
4
8
12
16
20
24
28
TIME (SECONDS) - THOUSANDTHS
SCALES USED
X 3.2X10 -3 UNITS/IN
Y 3.2X10 -1 UNITS/IN

C-31

PL 32

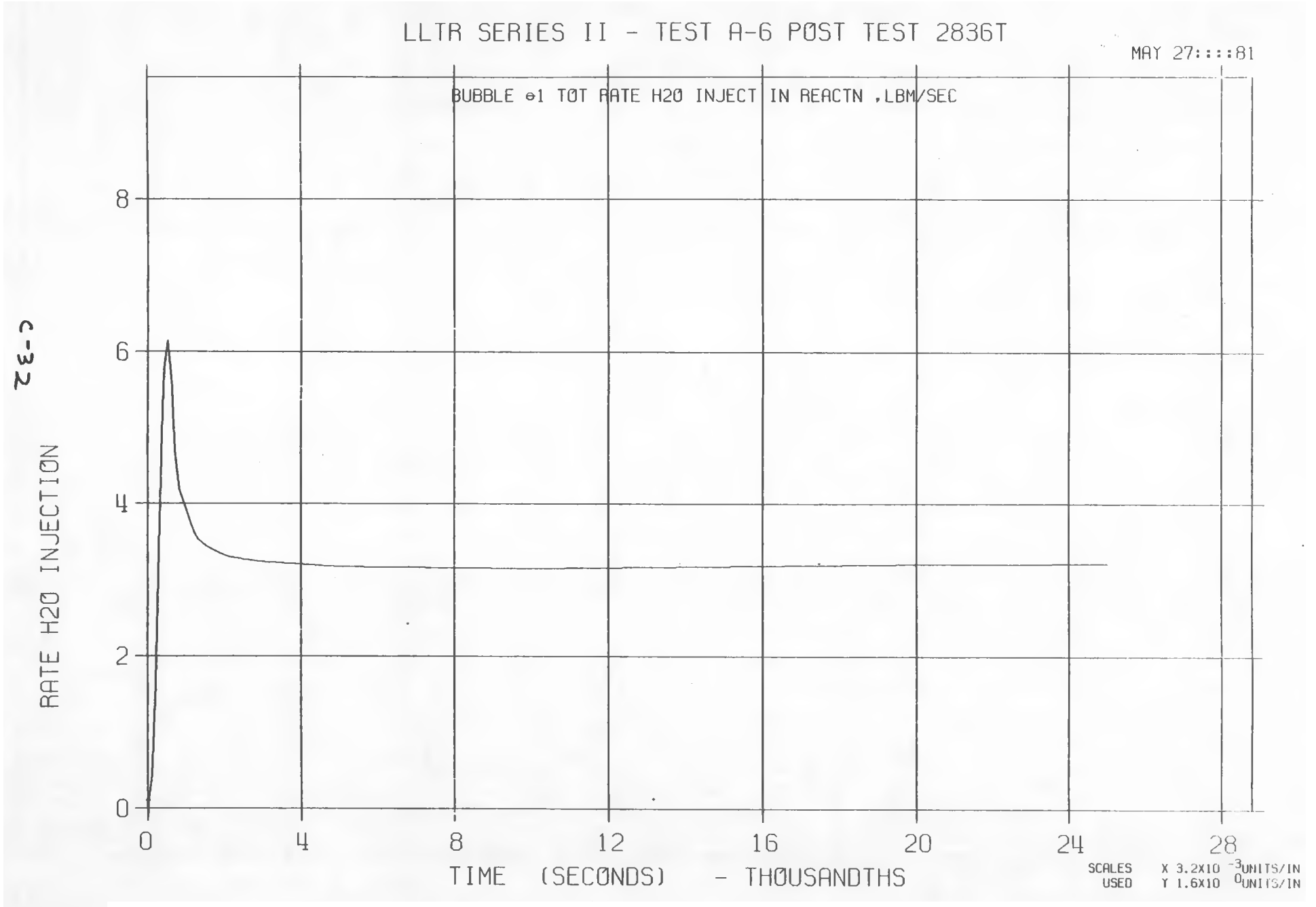
LLTR SERIES II - TEST A-6 POST TEST 2836T
MAY 27::::81
BUBBLE e1 TOT RATE H20 INJECT IN REACTN ,LBM/SEC
8
6
4
2
0
0
4
8
12
16
20
24
28
TIME (SECONDS) - THOUSANDTHS
RATE H20 INJECTION
SCALES USED
X 3.2X10 -3 UNITS/IN
Y 1.6X10 0 UNITS/IN

PL 37

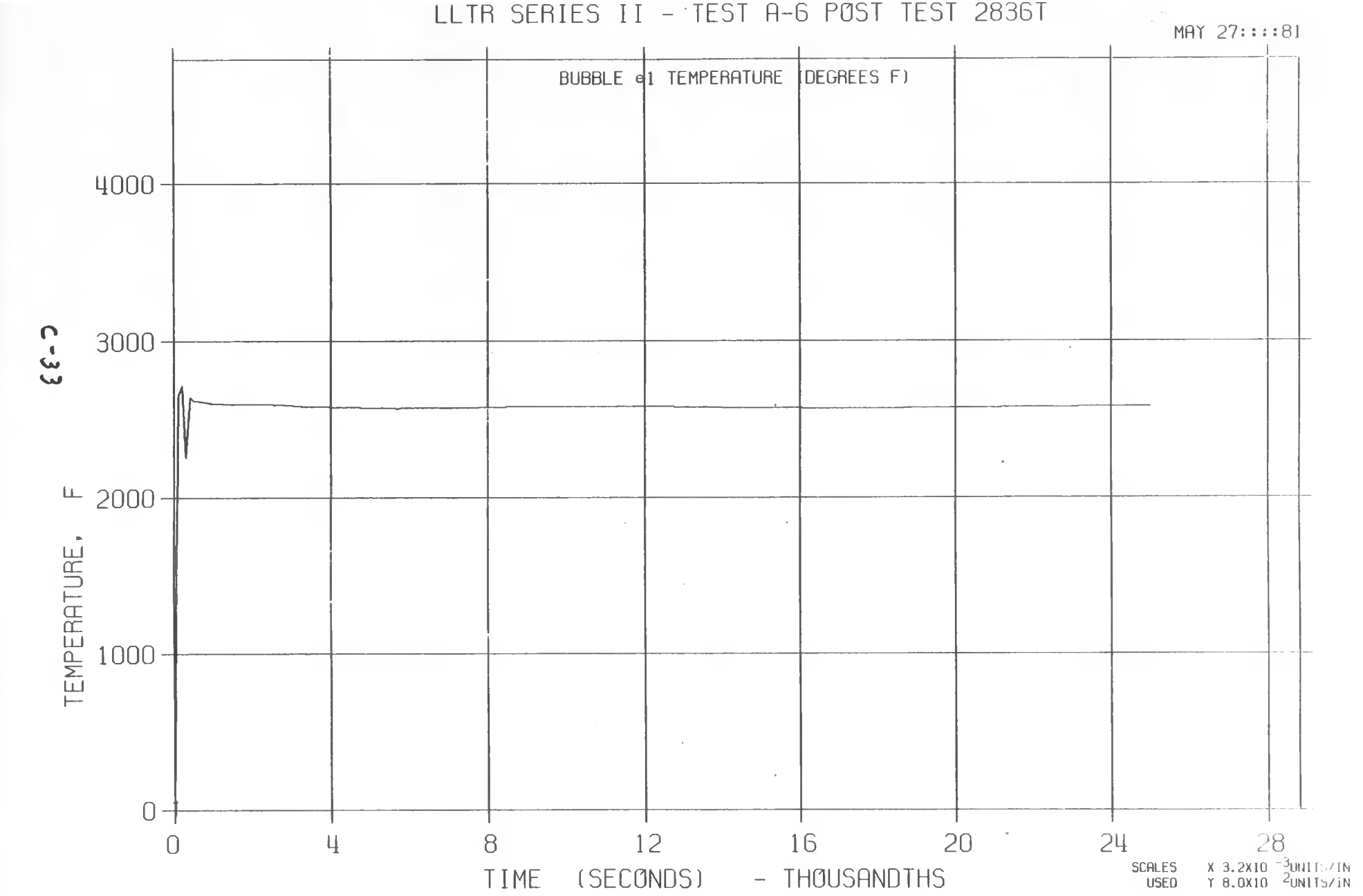
LLTR SERIES II - TEST A-6 POST TEST 2836T
MAY 27::::81
BUBBLE e1 TEMPERATURE (DEGREES F)
4000
3000
2000
1000
0
TEMPERATURE, F
0
4
8
12
16
20
24
28
TIME (SECONDS) - THOUSANDTHS
SCALES USED
X 3.2X10 -3 UNITS/IN
Y 8.0X10 2 UNITS/IN

PL 38

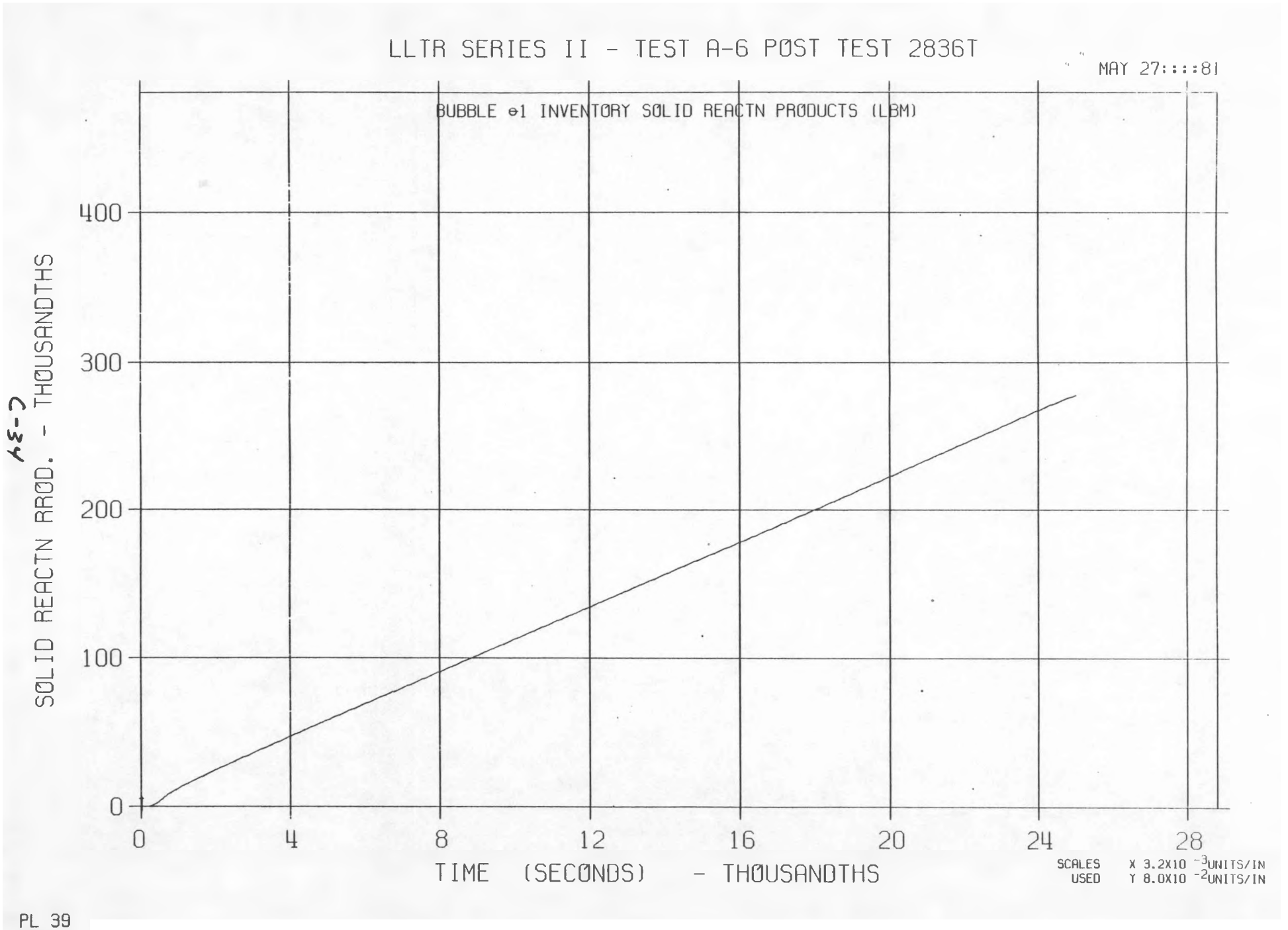
LLTR SERIES II - TEST A-6 POST TEST 2836T
MAY 27::::81
BUBBLE #1 INVENTORY SOLID REACTN PRODUCTS (LBM)
SOLID REACTN PROD. - THOUSANDTHS
400
300
200
100
0
0
4
8
12
16
20
24
28
TIME (SECONDS) - THOUSANDTHS
SCALES USED
X 3.2X10 -3 UNITS/IN
Y 8.0X10 -2 UNITS/IN

C-34

PL 39

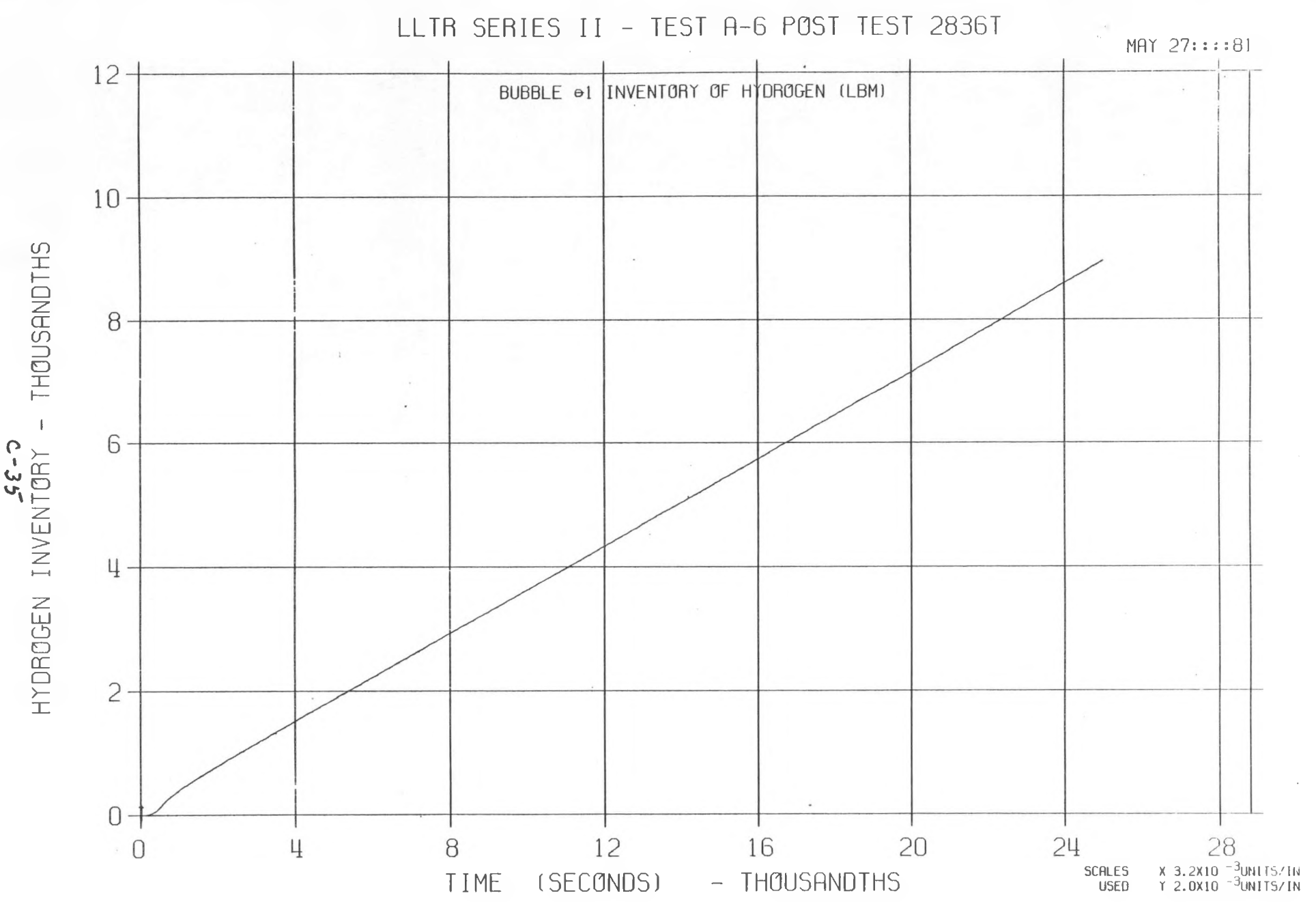
LLTR SERIES II - TEST A-6 POST TEST 2836T
MAY 27::::81
BUBBLE el INVENTORY OF HYDROGEN (LBM)
HYDROGEN INVENTORY - THOUSANDTHS
0
2
4
6
8
10
12
0
4
8
12
16
20
24
28
TIME (SECONDS) - THOUSANDTHS
SCALES USED
X 3.2X10 -3 UNITS/IN
Y 2.0X10 -3 UNITS/IN

PL 40

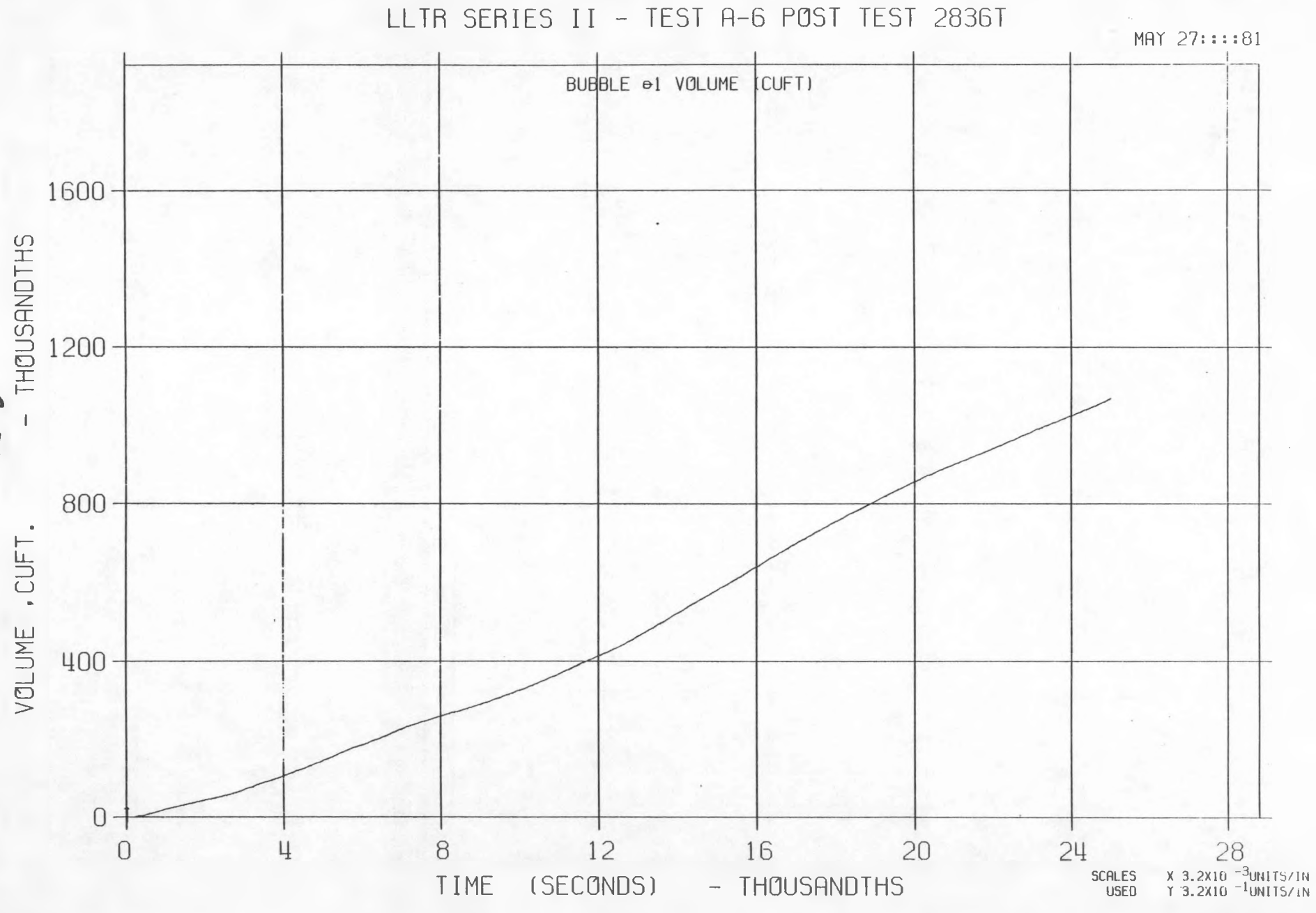
LLTR SERIES II - TEST A-6 POST TEST 2836T
MAY 27::::81
BUBBLE #1 VOLUME (CUFT)
VOLUME , CUFT. - THOUSANDTHS
1600
1200
800
400
0
0
4
8
12
16
20
24
28
TIME (SECONDS) - THOUSANDTHS
SCALES USED
X 3.2X10 -3 UNITS/IN
Y 3.2X10 -1 UNITS/IN

C-34

PL 41

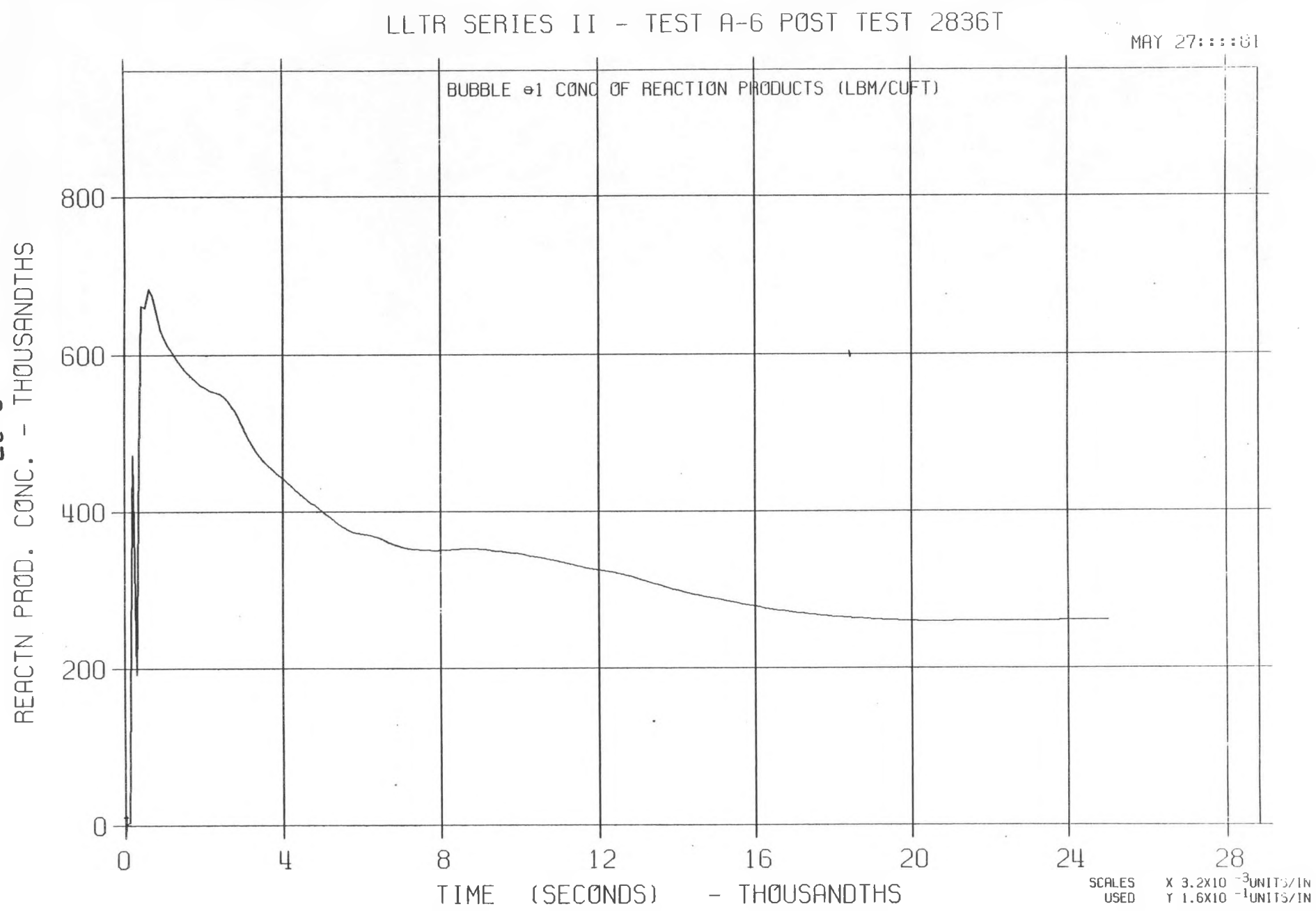
LLTR SERIES II - TEST A-6 POST TEST 2836T
MAY 27::::81
BUBBLE θ1 CONC OF REACTION PRODUCTS (LBM/CUFT)
REACTN PROD. CONC. - THOUSANDTHS
800
600
400
200
0
0
4
8
12
16
20
24
28
TIME (SECONDS) - THOUSANDTHS
SCALES USED
X 3.2X10 -3 UNITS/IN
Y 1.6X10 -1 UNITS/IN

C-37

PL 42

[illegible]	
[illegible]	74
[illegible]	V313
[illegible]	38345
[illegible]	NO
[illegible]	47
[illegible]	38
[illegible]	DEK
[illegible]	SSS31
[illegible]	2836T-01

APPENDIX D

TRANSWRAP MODEL D

A-6 TEST

0.65 X SWR

GAS VOID AT TOP OF LLTV

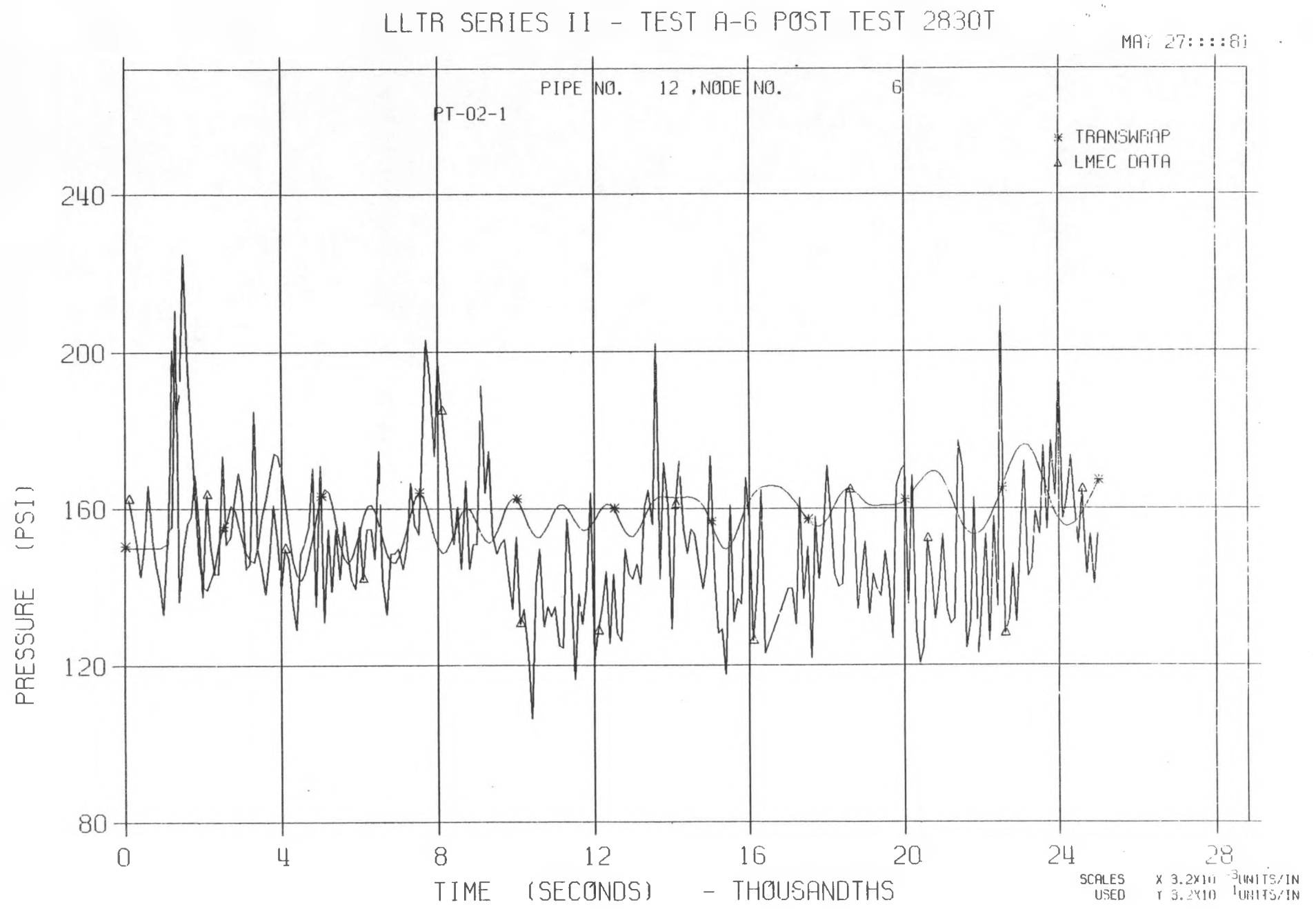
LLTR SERIES II - TEST A-6 POST TEST 2830T
MAY 27::::81
PIPE NO. 12 ,NODE NO. 6
PT-02-1
* TRANSWRAP
Δ LMEC DATA
240
200
160
120
80
PRESSURE (PSI)
0
4
8
12
16
20
24
28
TIME (SECONDS) - THOUSANDTHS
SCALES USED
X 3.2X10 -3 UNITS/IN
Y 3.2X10 1 UNITS/IN

PL 1

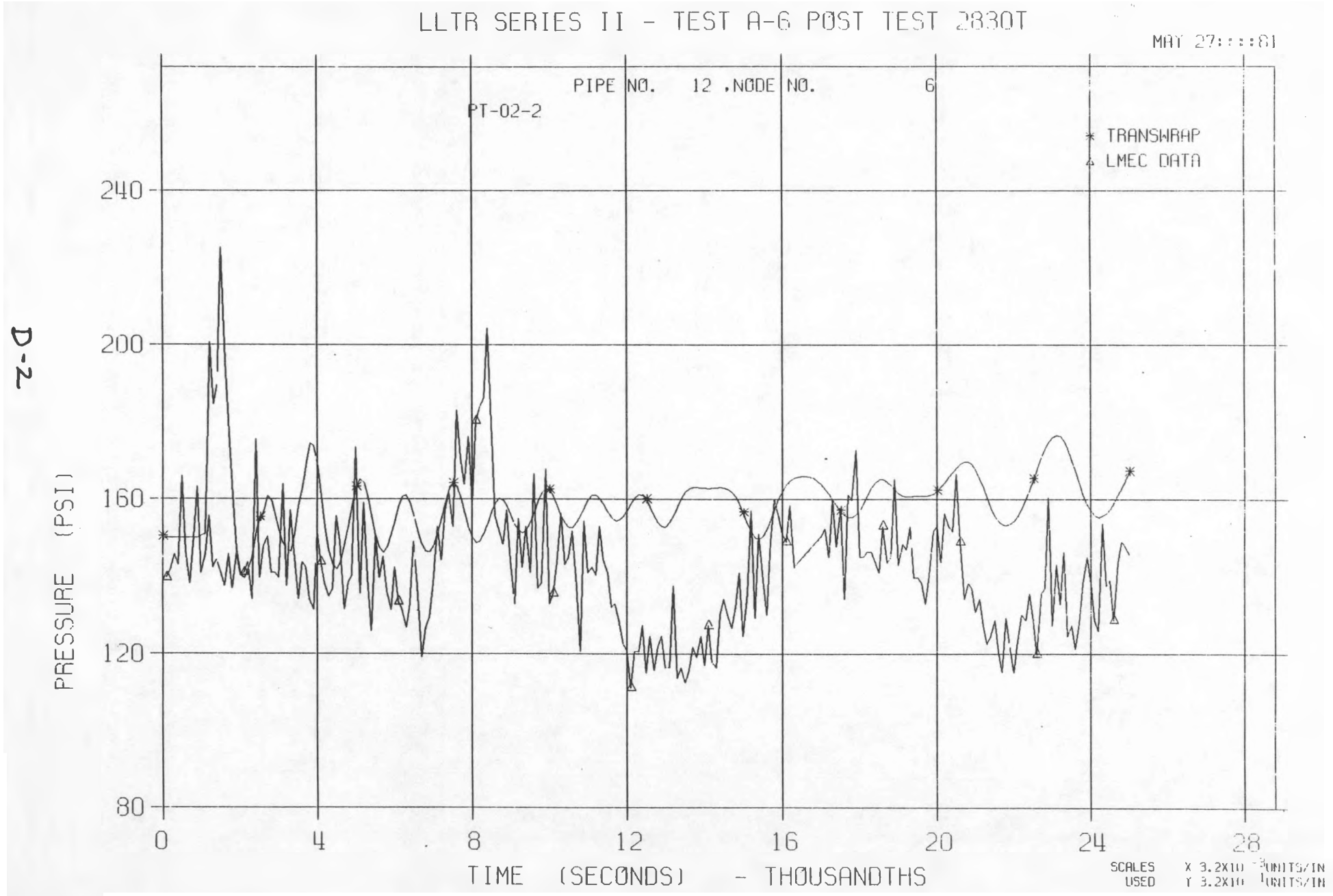
LLTR SERIES II - TEST A-6 POST TEST 2830T
MAY 27::::81
PIPE NO. 12 ,NODE NO. 6
PT-02-2
* TRANSWRAP
Δ LMEC DATA
240
200
160
120
80
PRESSURE (PSI)
0
4
8
12
16
20
24
28
TIME (SECONDS) - THOUSANDTHS
SCALES USED
X 3.2X10 -3 UNITS/IN
Y 3.2X10 1 UNITS/IN

D-2

PL 2

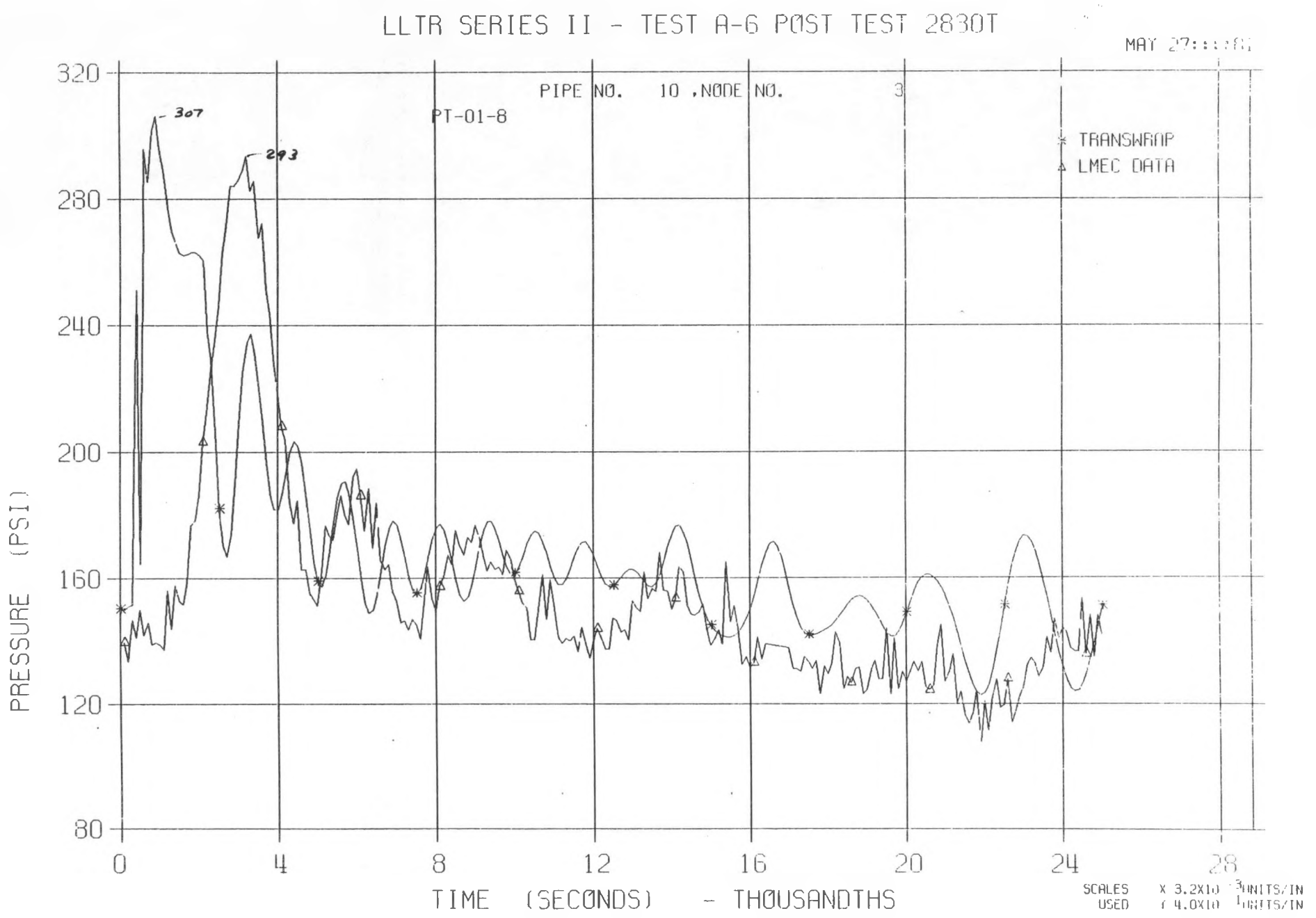
LLTR SERIES II - TEST A-6 POST TEST 2830T
MAY 27
PIPE NO. 10 , NODE NO. 3
PT-01-8
307
293
TRANSWRAP
LMEC DATA
320
280
240
200
160
120
80
PRESSURE (PSI)
0
4
8
12
16
20
24
28
TIME (SECONDS) - THOUSANDTHS
SCALES USED
X 3.2X10 -3 UNITS/IN
Y 4.0X10 UNITS/IN

D-3

PL 3

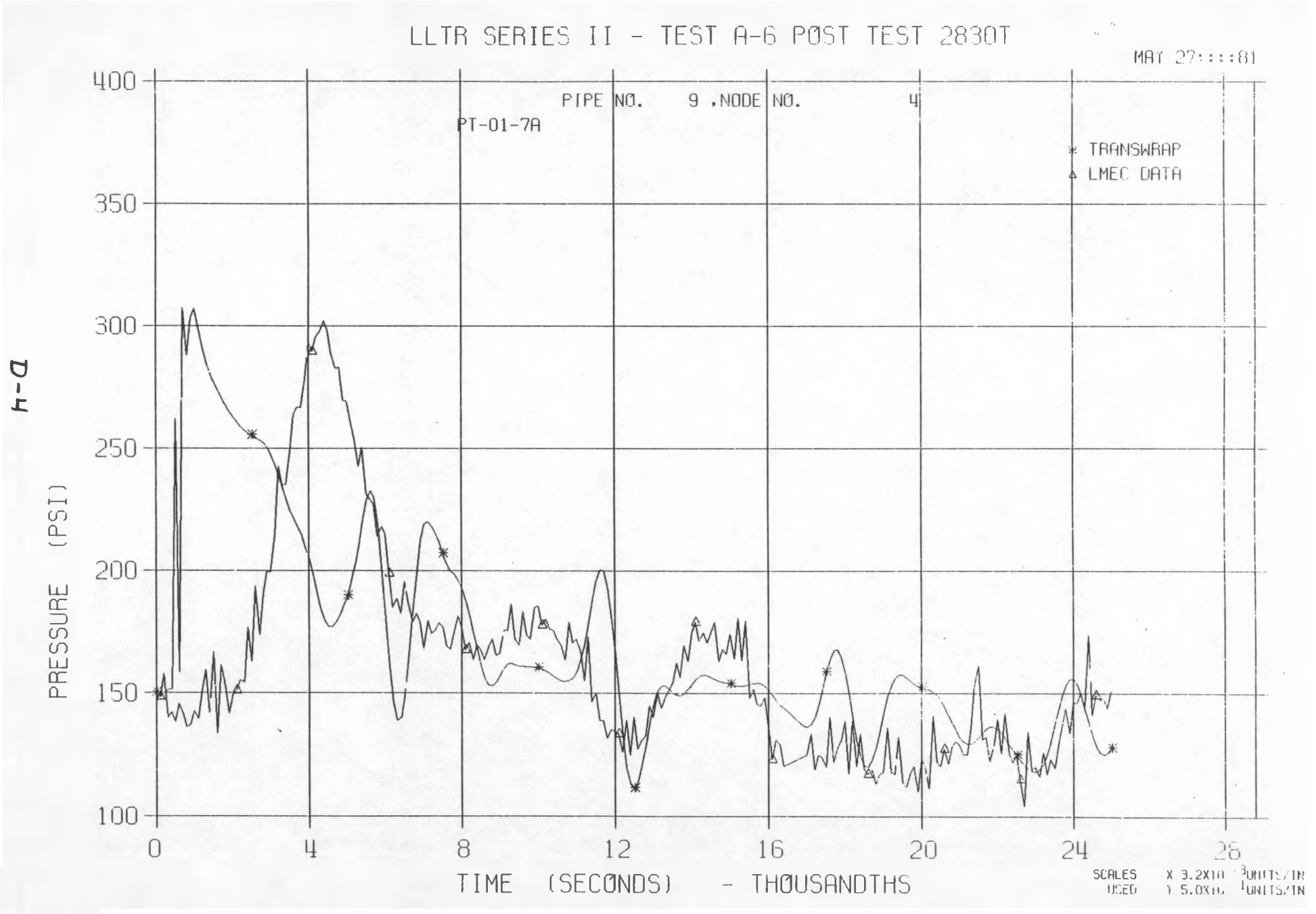
LLTR SERIES II - TEST A-6 POST TEST 2830T
MAY 27::::81
PIPE NO. 9 .NODE NO. 4
PT-01-7A
* TRANSWRAP
Δ LMEC DATA
400
350
300
250
200
150
100
PRESSURE (PSI)
0
4
8
12
16
20
24
28
TIME (SECONDS) - THOUSANDTHS
SCALES USED
X 3.2X10 -3 UNITS/IN
Y 5.0X10 1 UNITS/IN

D-4

PL 4

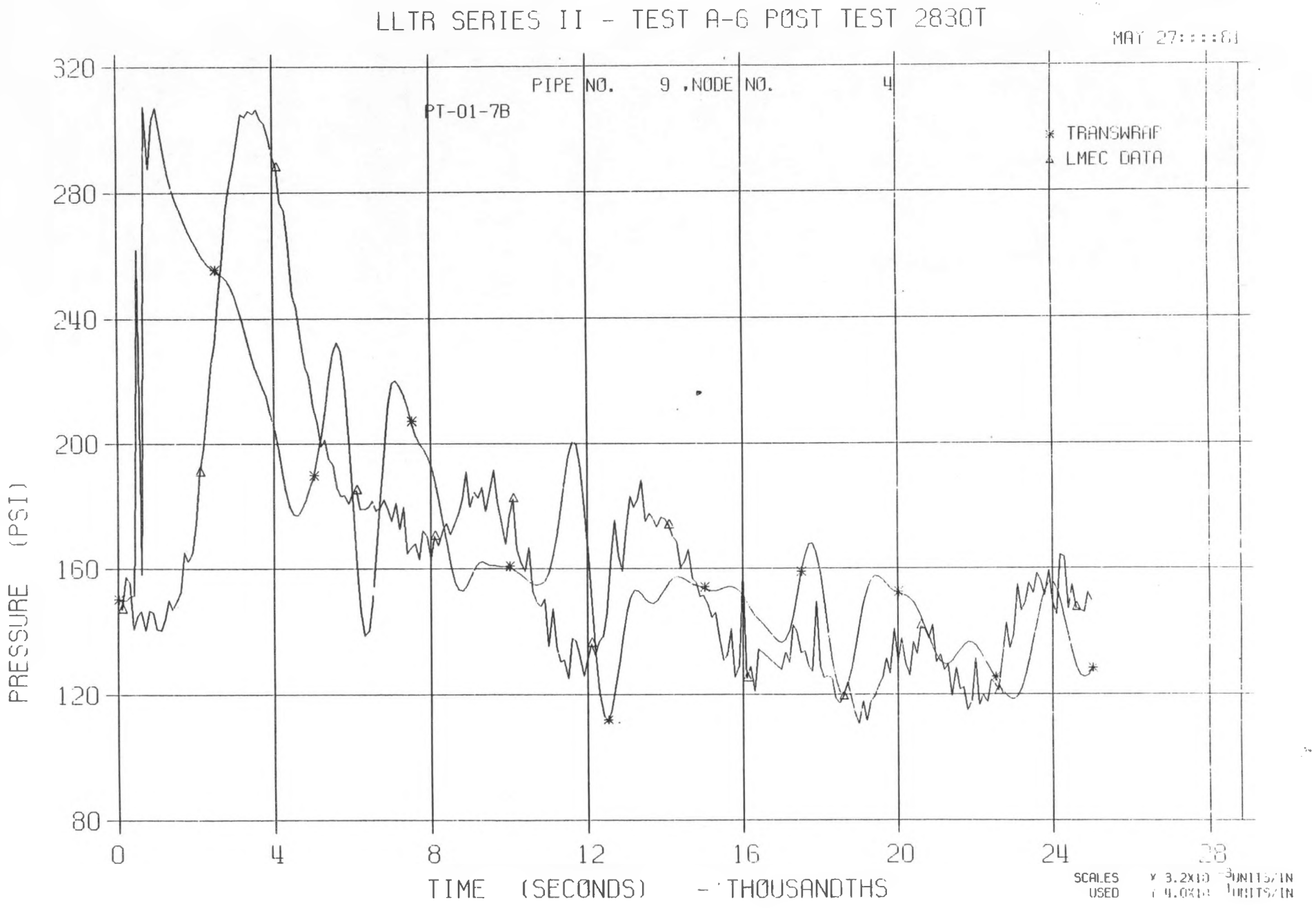
LLTR SERIES II - TEST A-6 POST TEST 2830T
MAY 27::::81
PIPE NO. 9 ,NODE NO. 4
PT-01-7B
TRANSWRAP
LMEC DATA
PRESSURE (PSI)
320
280
240
200
160
120
80
0
4
8
12
16
20
24
28
TIME (SECONDS) - THOUSANDTHS
SCALES USED
UNITS/IN
UNITS/IN

A-5

PL 5

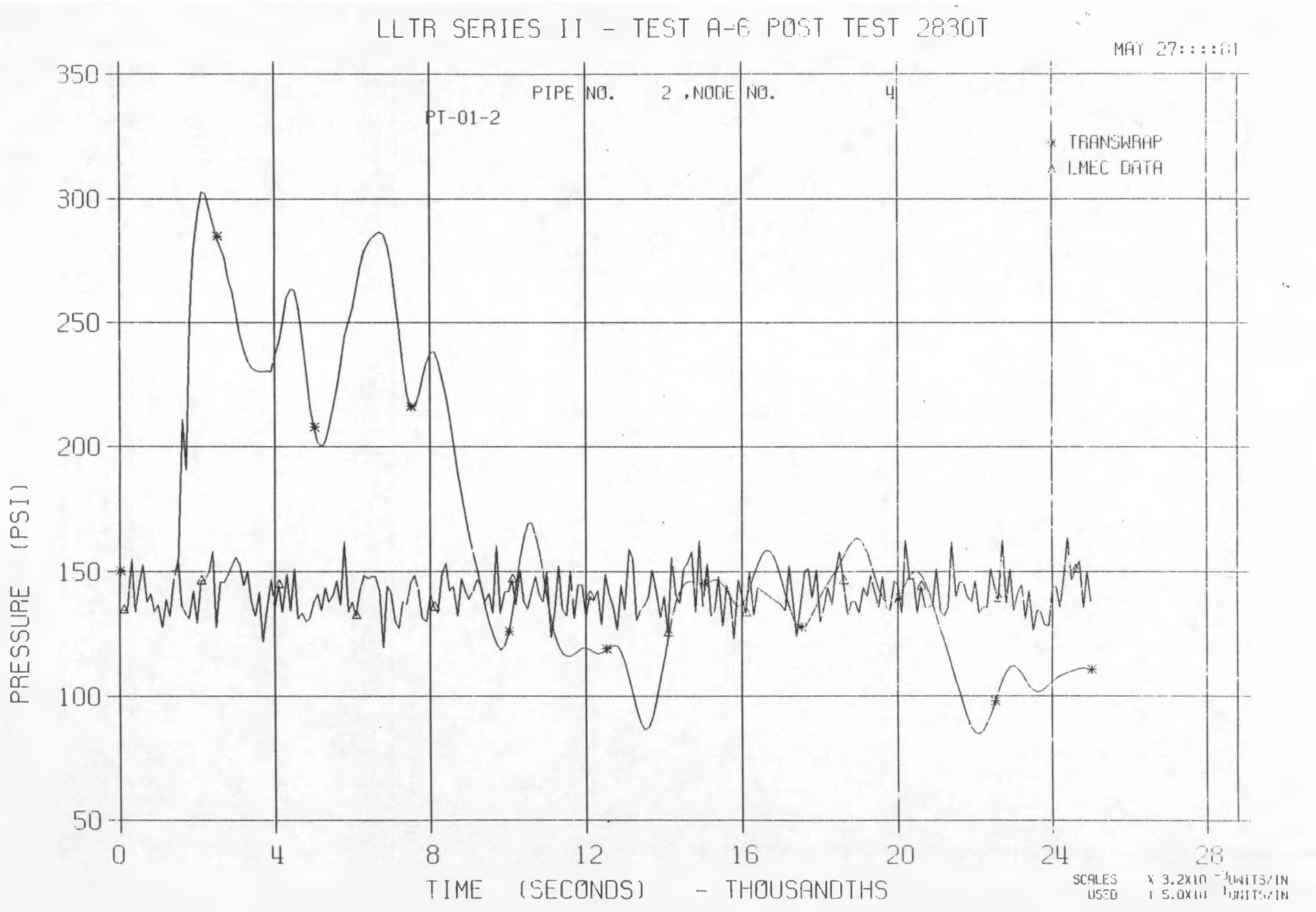
LLTR SERIES II - TEST A-6 POST TEST 2830T
MAY 27::::81
PIPE NO. 2 ,NODE NO. 4
PT-01-2
TRANSWRAP
LMEC DATA
PRESSURE (PSI)
350
300
250
200
150
100
50
0
4
8
12
16
20
24
28
TIME (SECONDS) - THOUSANDTHS
SCALES USED
X 3.2X10 UNITS/IN
Y 5.0X10 UNITS/IN

PL 6

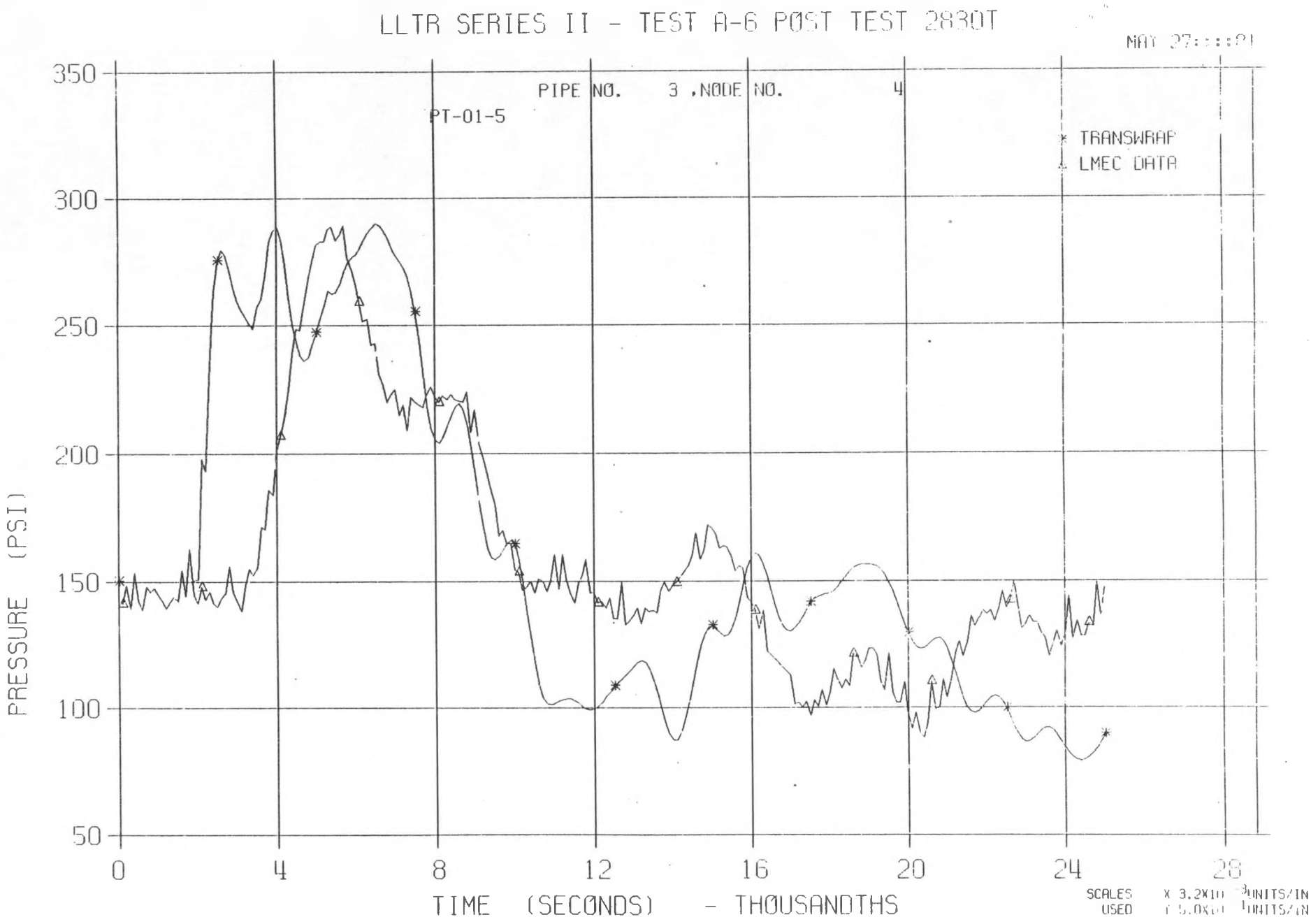
LLTR SERIES II - TEST A-6 POST TEST 2830T
MAY 27::::21
PIPE NO. 3 ,NODE NO. 4
PT-01-5
TRANSWRAP
LMEC DATA
350
300
250
200
150
100
50
PRESSURE (PSI)
0
4
8
12
16
20
24
28
TIME (SECONDS) - THOUSANDTHS
SCALES USED
X 3.2X10^3 UNITS/IN
Y 5.0X10^1 UNITS/IN

D-7

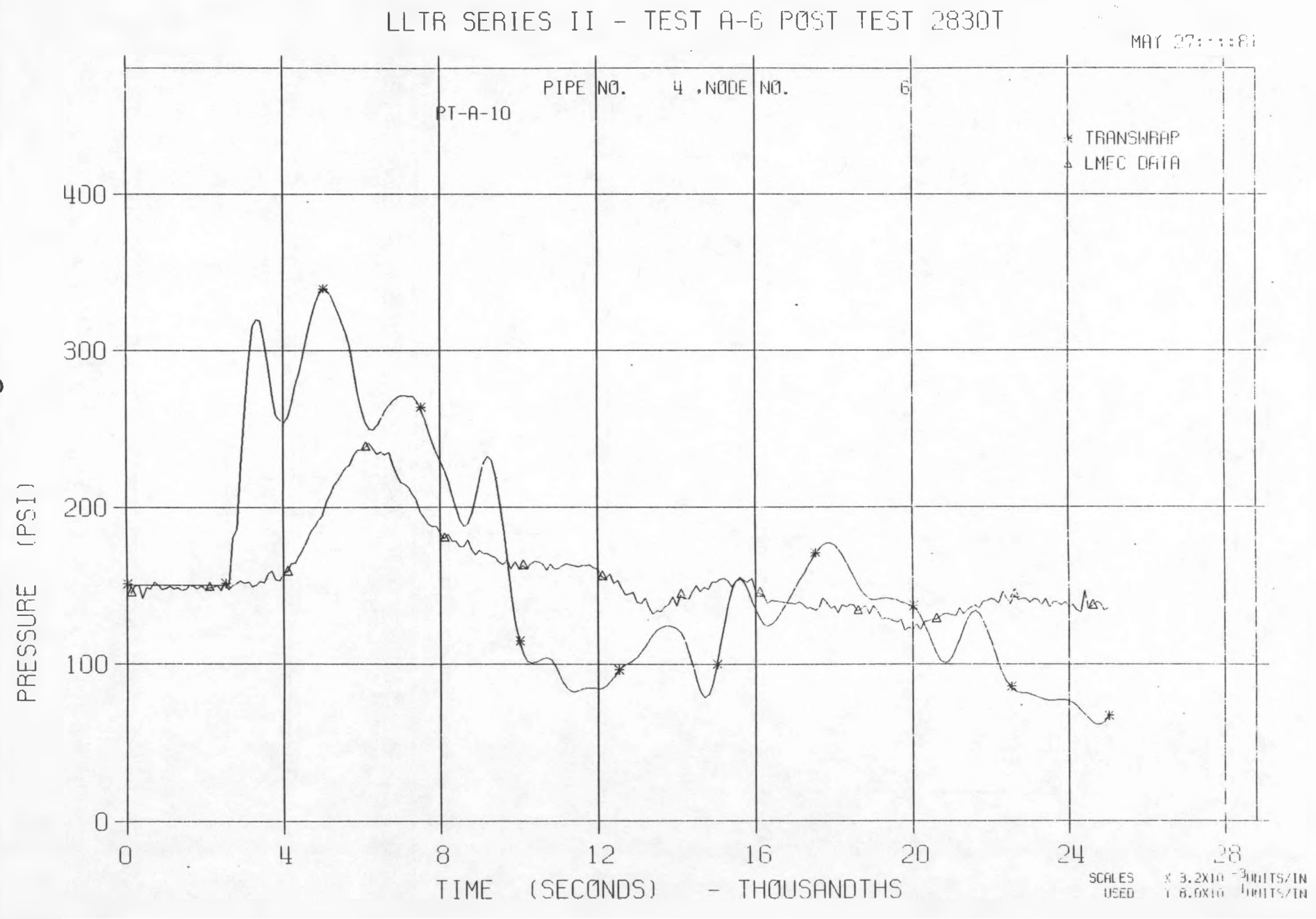
LLTR SERIES II - TEST A-6 POST TEST 2830T
MAY 27:::81
PIPE NO. 4 ,NODE NO. 6
PT-A-10
* TRANSWRAP
Δ LMEC DATA
400
300
200
100
0
PRESSURE (PSI)
0
4
8
12
16
20
24
28
TIME (SECONDS) - THOUSANDTHS
SCALES USED
X 3.2X10 -3 UNITS/IN
Y 8.0X10 1 UNITS/IN

PL 8

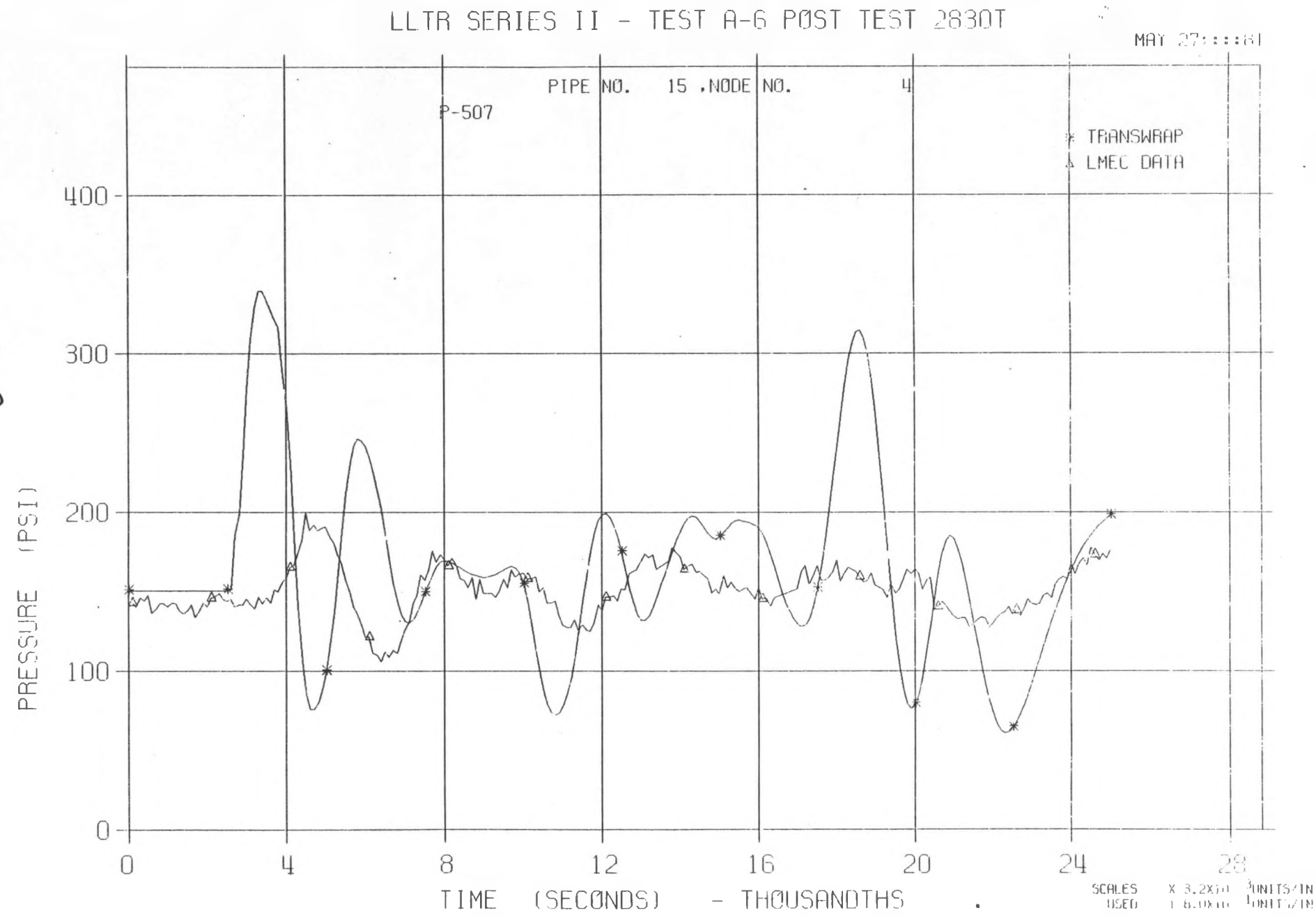
LLTR SERIES II - TEST A-6 POST TEST 2830T
MAY 27
PIPE NO. 15 ,NODE NO. 4
P-507
* TRANSWRAP
Δ LMEC DATA
400
300
200
100
0
PRESSURE (PSI)
0
4
8
12
16
20
24
28
TIME (SECONDS) - THOUSANDTHS
SCALES USED
X 3.2X10
Y 6.0X10
3UNITS/IN
4UNITS/IN

PL 9

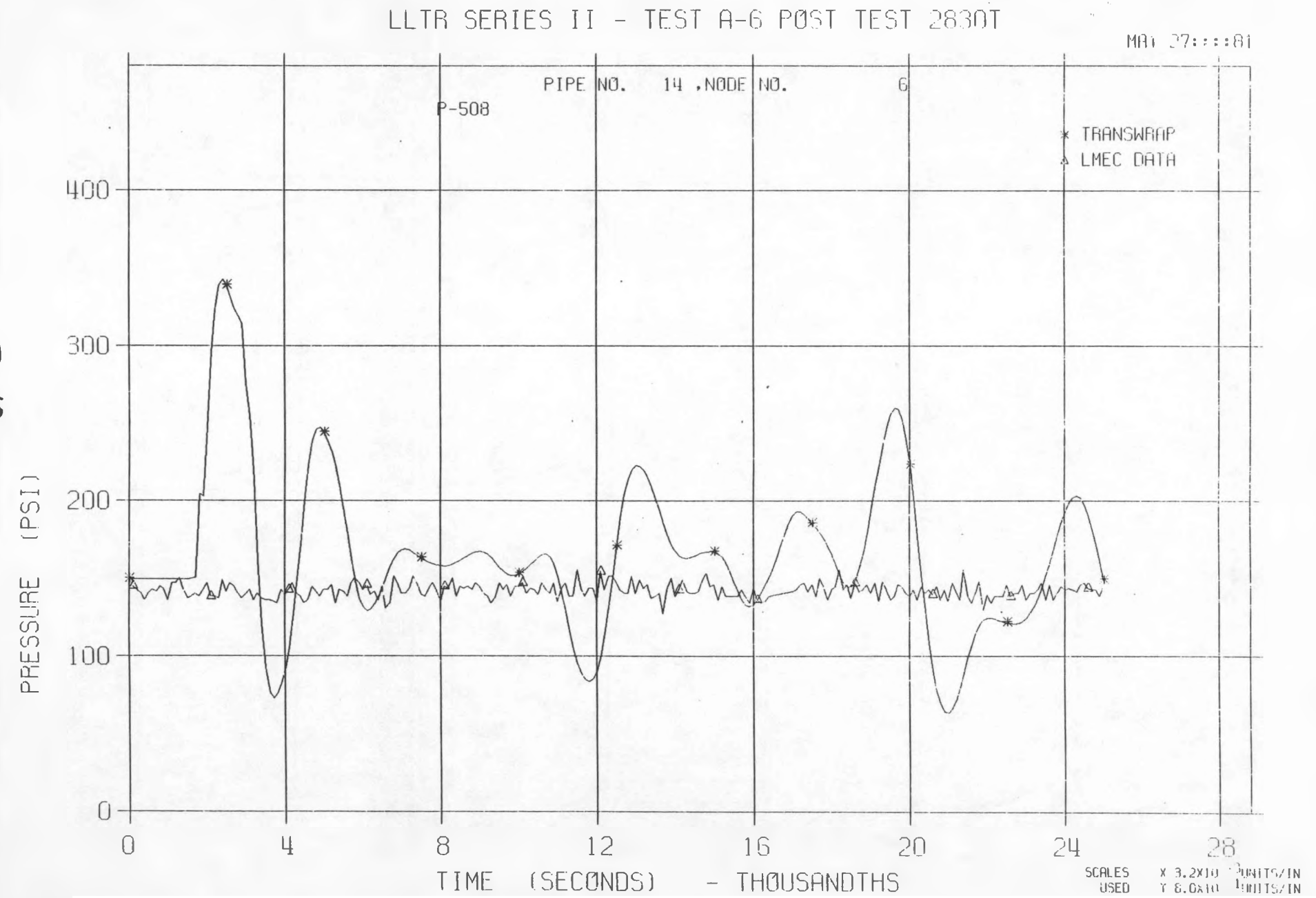
LLTR SERIES II - TEST A-6 POST TEST 2830T
MAY 27::::81
PIPE NO. 14 ,NODE NO. 6
P-508
TRANSWRAP
LMEC DATA
400
300
200
100
0
PRESSURE (PSI)
0
4
8
12
16
20
24
28
TIME (SECONDS) - THOUSANDTHS
SCALES USED
X 3.2X10 UNITS/IN
Y 8.0X10 UNITS/IN

D-10

PL 10

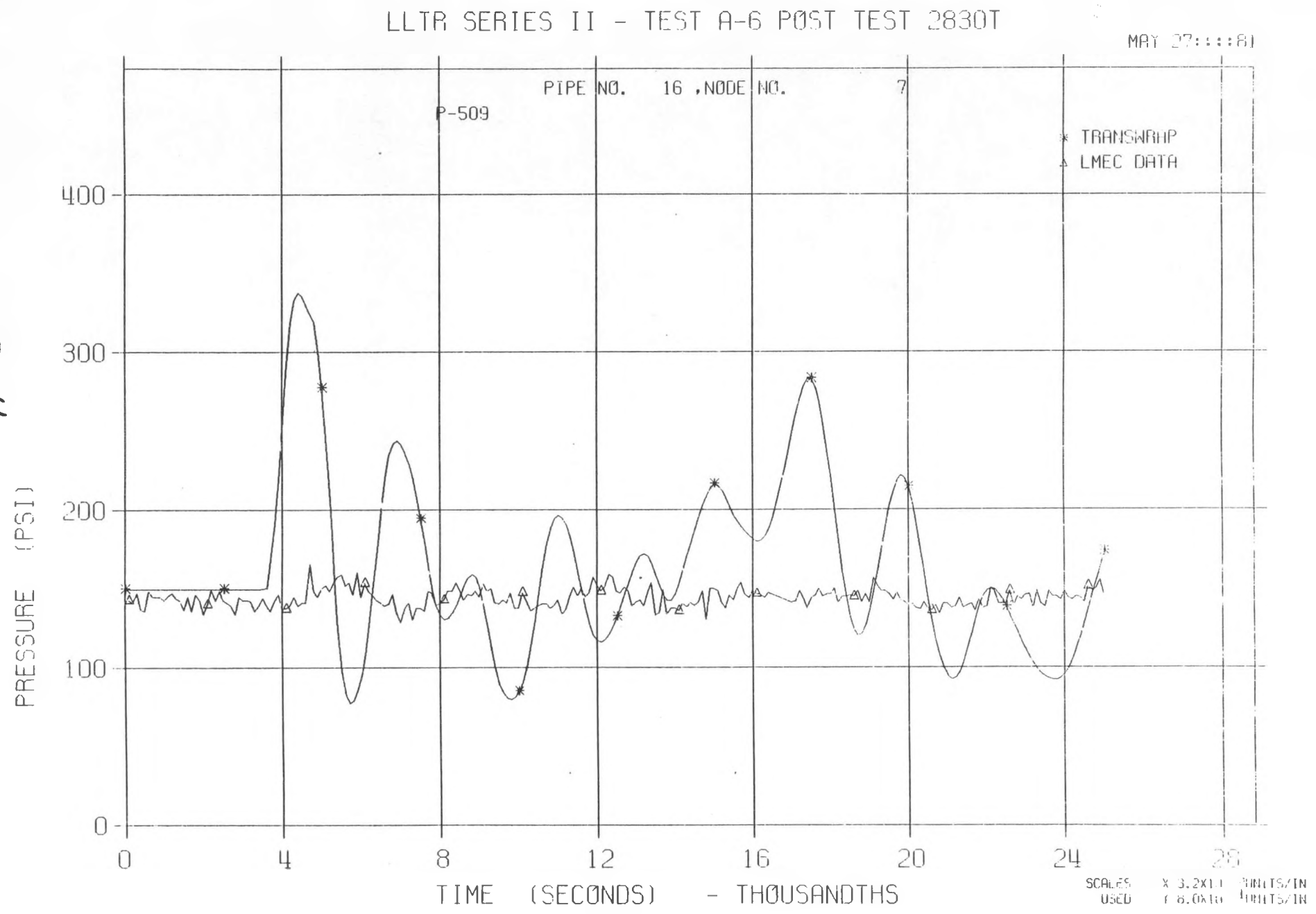
LLTR SERIES II - TEST A-6 POST TEST 2830T
MAY 27::::81
PIPE NO. 16 ,NODE NO. 7
P-509
TRANSWRAP
LMEC DATA
400
300
200
100
0
PRESSURE (PSI)
0
4
8
12
16
20
24
TIME (SECONDS) - THOUSANDTHS
SCALES USED

D-11

PL 11

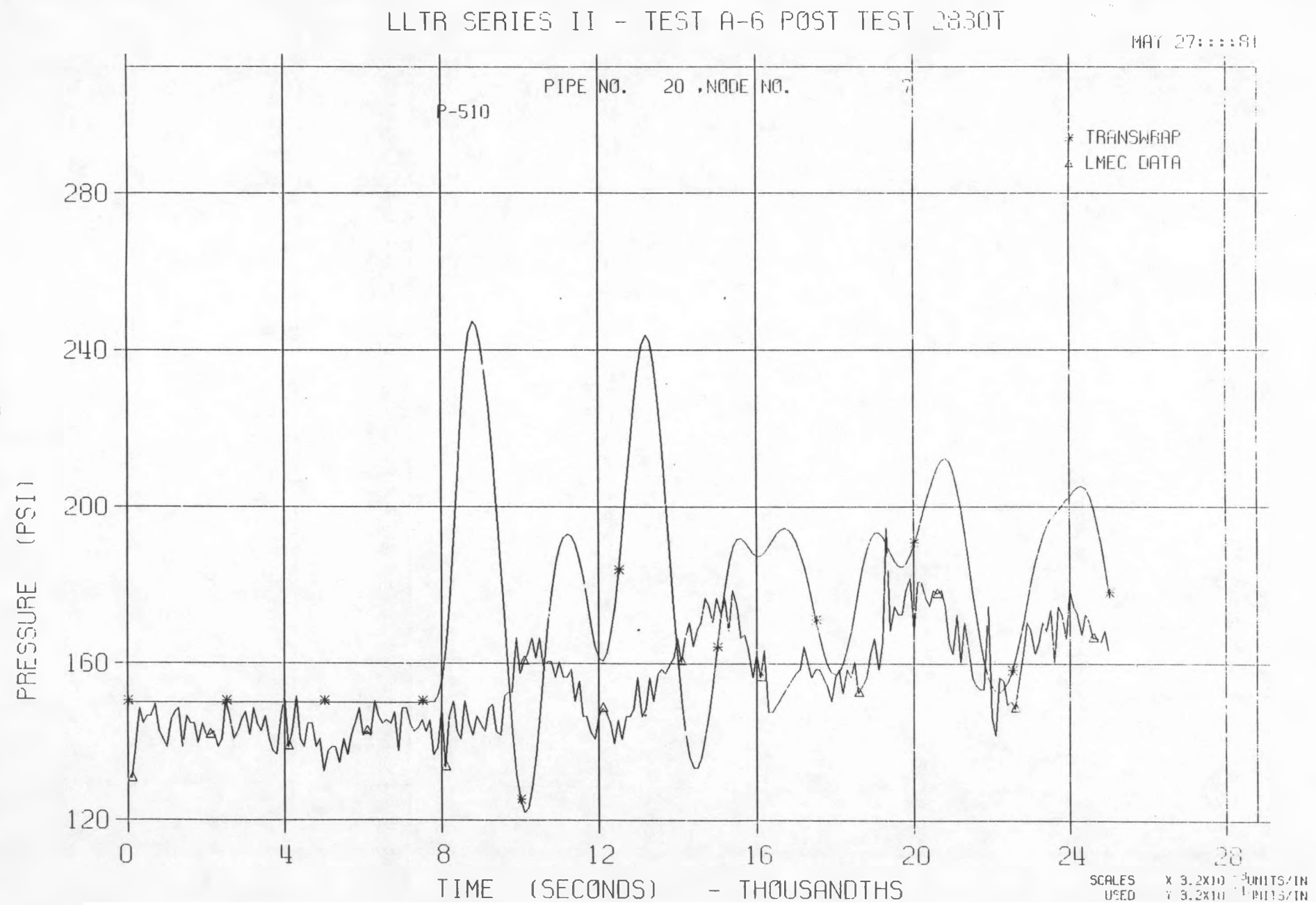
LLTR SERIES II - TEST A-6 POST TEST 2830T
MAY 27::::81
PIPE NO. 20 ,NODE NO. 7
P-510
TRANSWRAP
LMEC DATA
280
240
200
160
120
PRESSURE (PSI)
0
4
8
12
16
20
24
28
TIME (SECONDS) - THOUSANDTHS
SCALES USED
X 3.2X10 -3 UNITS/IN
Y 3.2X10 1 UNITS/IN

D-12

PL 12

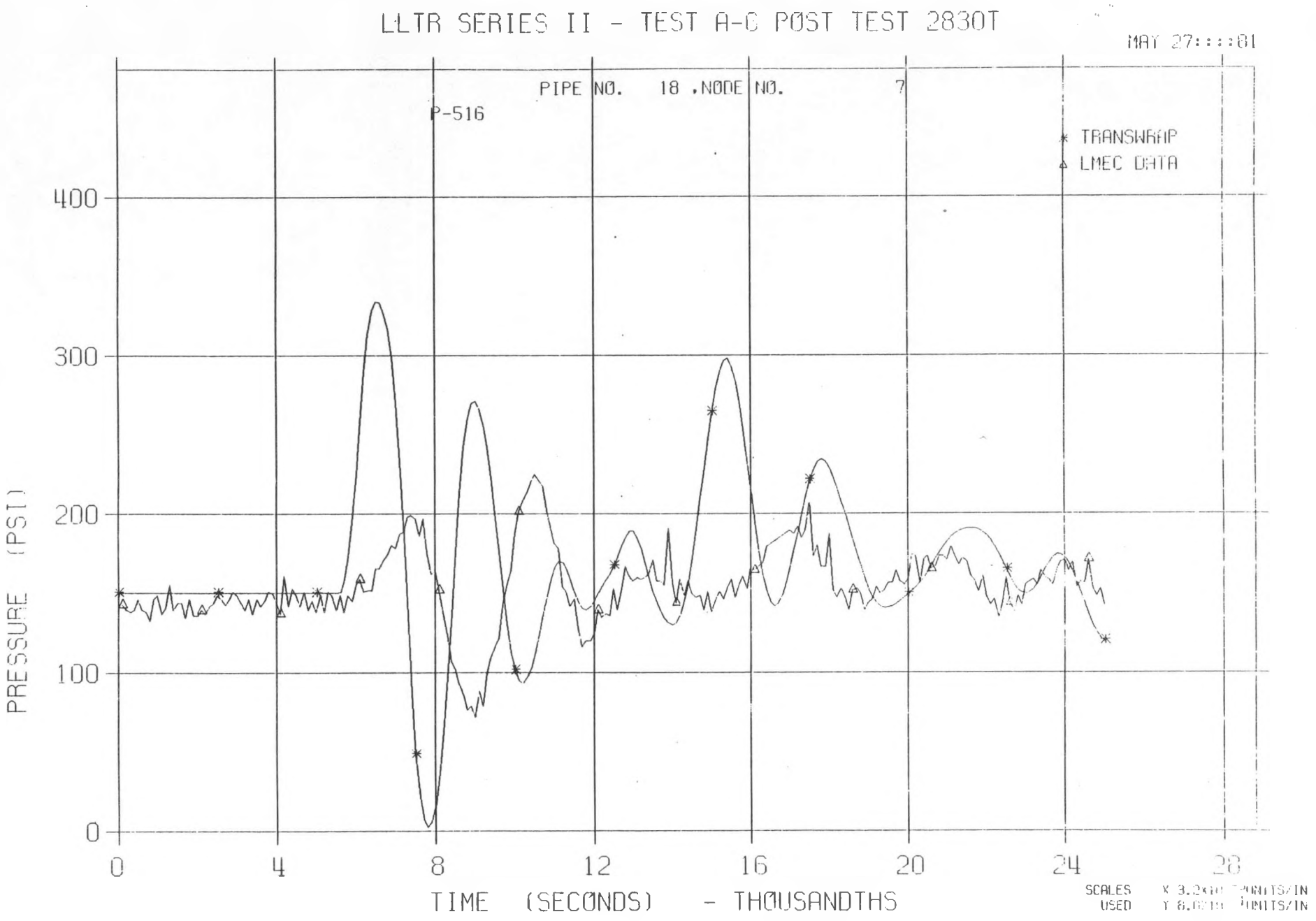
LLTR SERIES II - TEST A-C POST TEST 2830T
MAY 27::::81
PIPE NO. 18 .NODE NO. 7
P-516
TRANSWRAP
LMEC DATA
400
300
200
100
0
PRESSURE (PSI)
0
4
8
12
16
20
24
28
TIME (SECONDS) - THOUSANDTHS
SCALES USED

D-13

PL 13

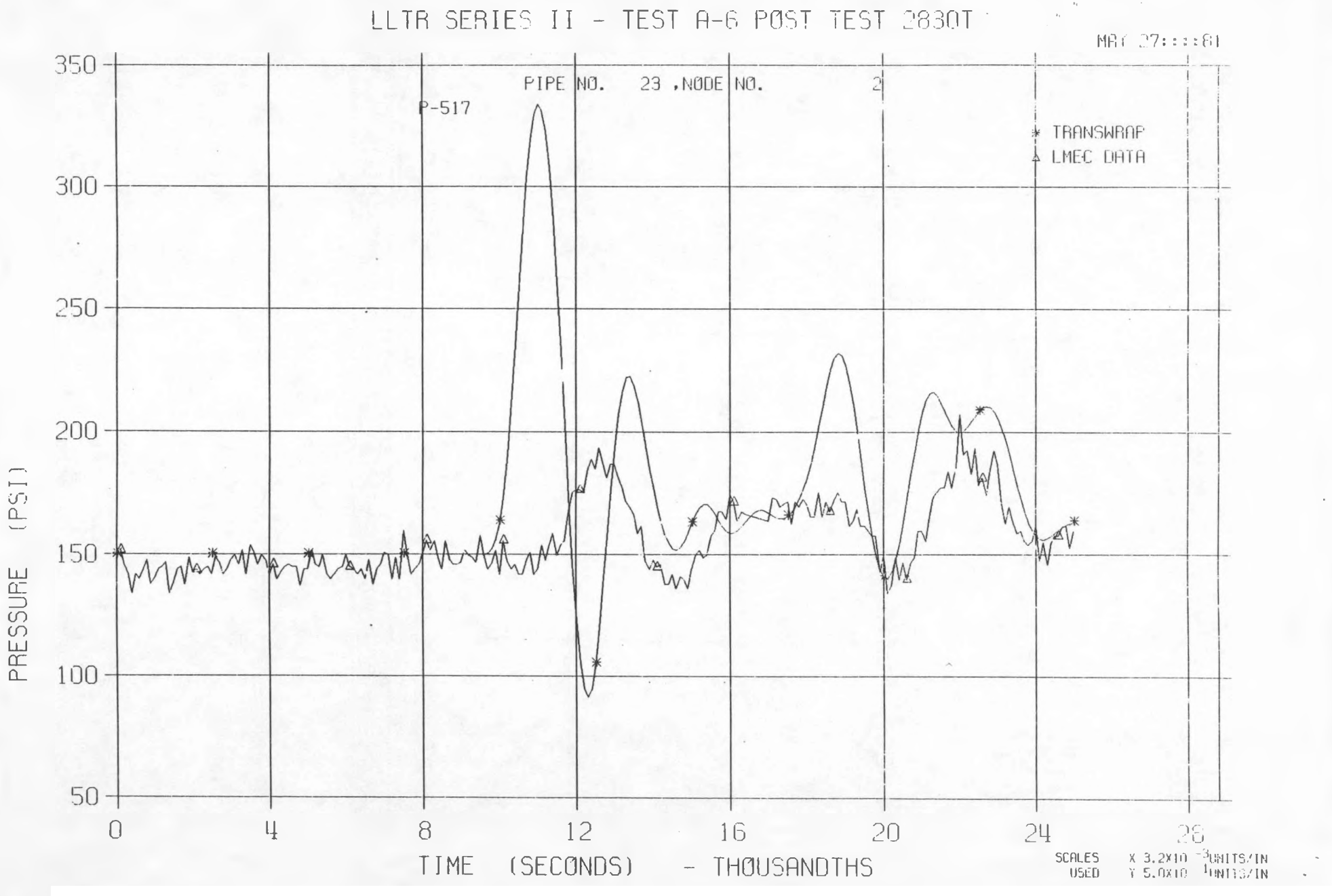
LLTR SERIES II - TEST A-6 POST TEST 2830T
MAY 27::::81
PIPE NO. 23 ,NODE NO. 2
P-517
* TRANSWRAP
Δ LMEC DATA
350
300
250
200
150
100
50
PRESSURE (PSI)
0
4
8
12
16
20
24
28
TIME (SECONDS) - THOUSANDTHS
SCALES USED
X 3.2X10 -3 UNITS/IN
Y 5.0X10 1 UNITS/IN

h1-a

PL 14

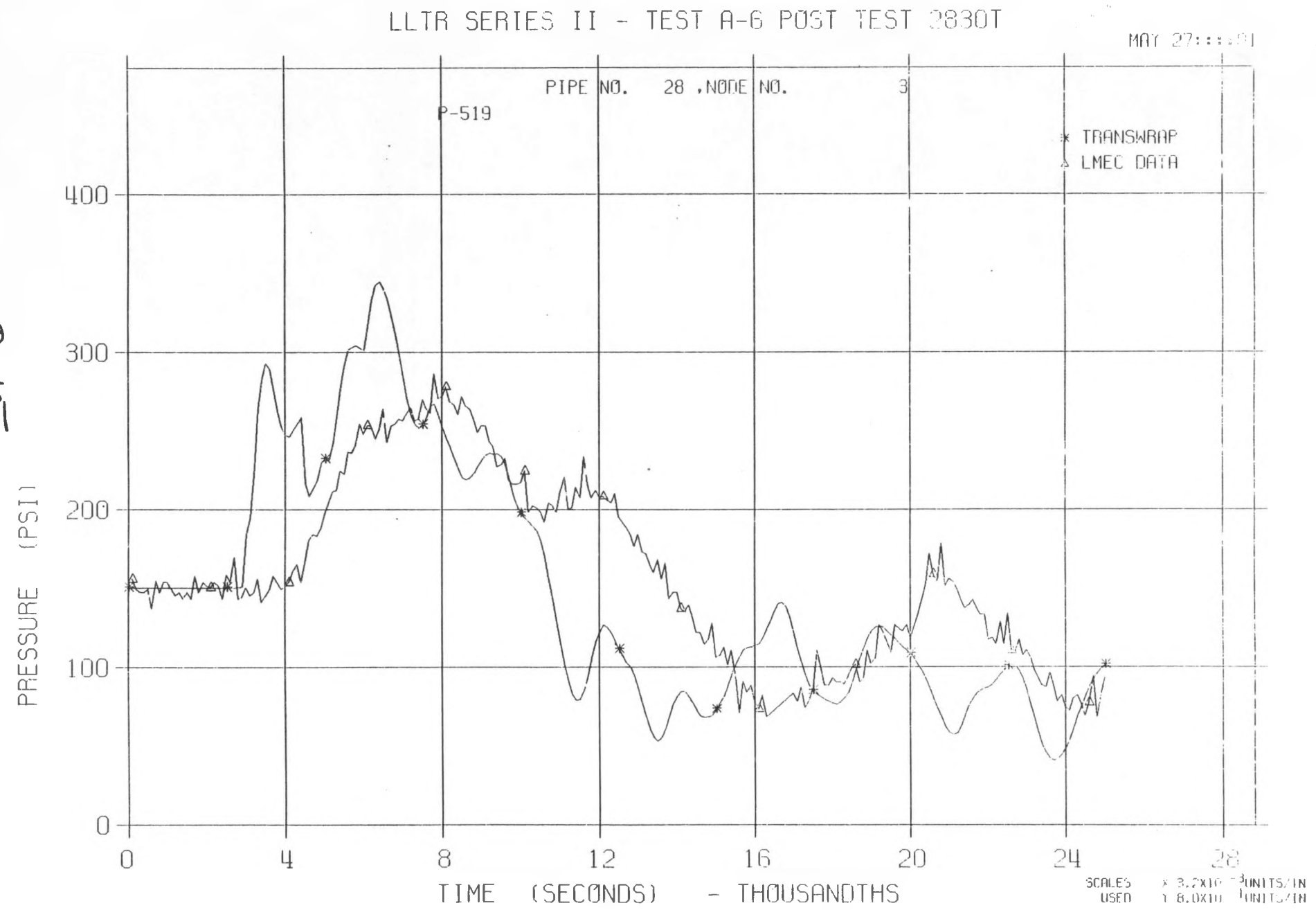
LLTR SERIES II - TEST A-6 POST TEST 2830T
MAY 27::::91
PIPE NO. 28 ,NODE NO. 3
P-519
TRANSWRAP
LMEC DATA
400
300
200
100
0
PRESSURE (PSI)
0
4
8
12
16
20
24
28
TIME (SECONDS) - THOUSANDTHS
SCALES USED

D-15

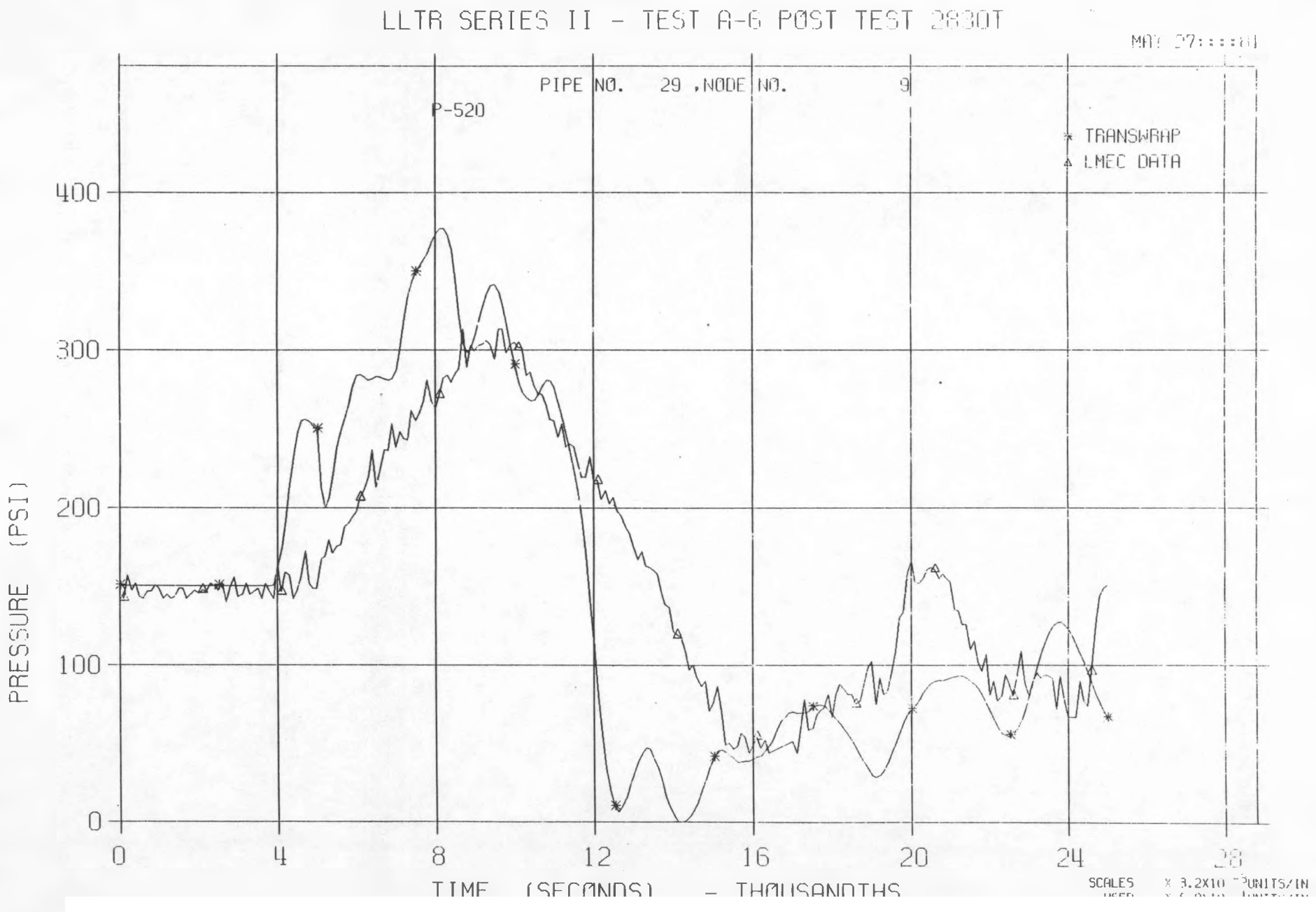
LLTR SERIES II - TEST A-6 POST TEST 2830T
PIPE NO. 29 ,NODE NO. 9
P-520
TRANSWRAP
LMEC DATA
PRESSURE (PSI)
0
100
200
300
400
0
4
8
12
16
20
24
TIME (SECONDS) - THOUSANDTHS
SCALES

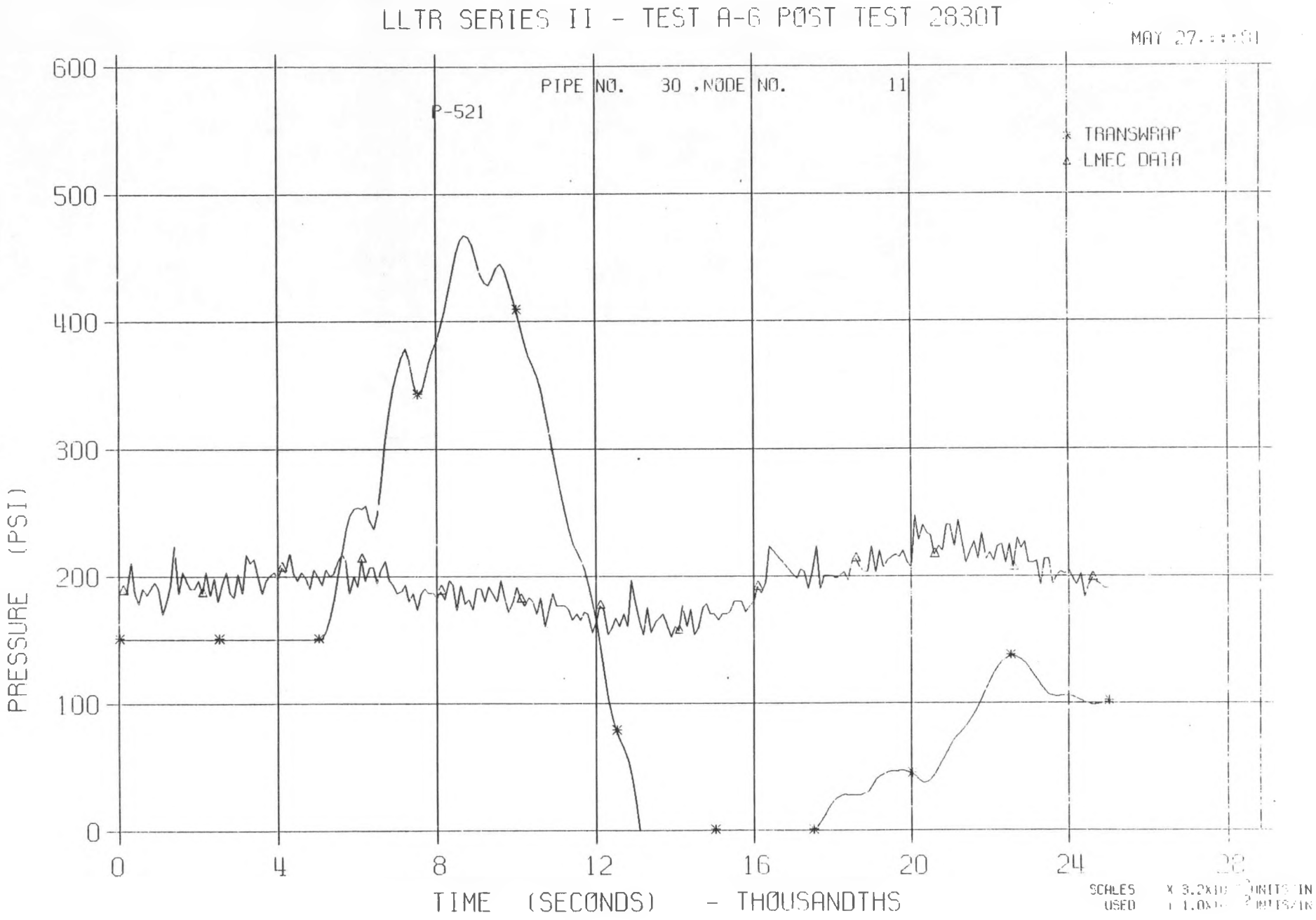
LLTR SERIES II - TEST A-6 POST TEST 2830T
MAY 27.
PIPE NO. 30 , NODE NO. 11
P-521
TRANSWRAP
LMEC DATA
600
500
400
300
200
100
0
PRESSURE (PSI)
0
4
8
12
16
20
24
TIME (SECONDS) - THOUSANDTHS
SCALES USED
UNITS IN

D-17

PL 17

D-18

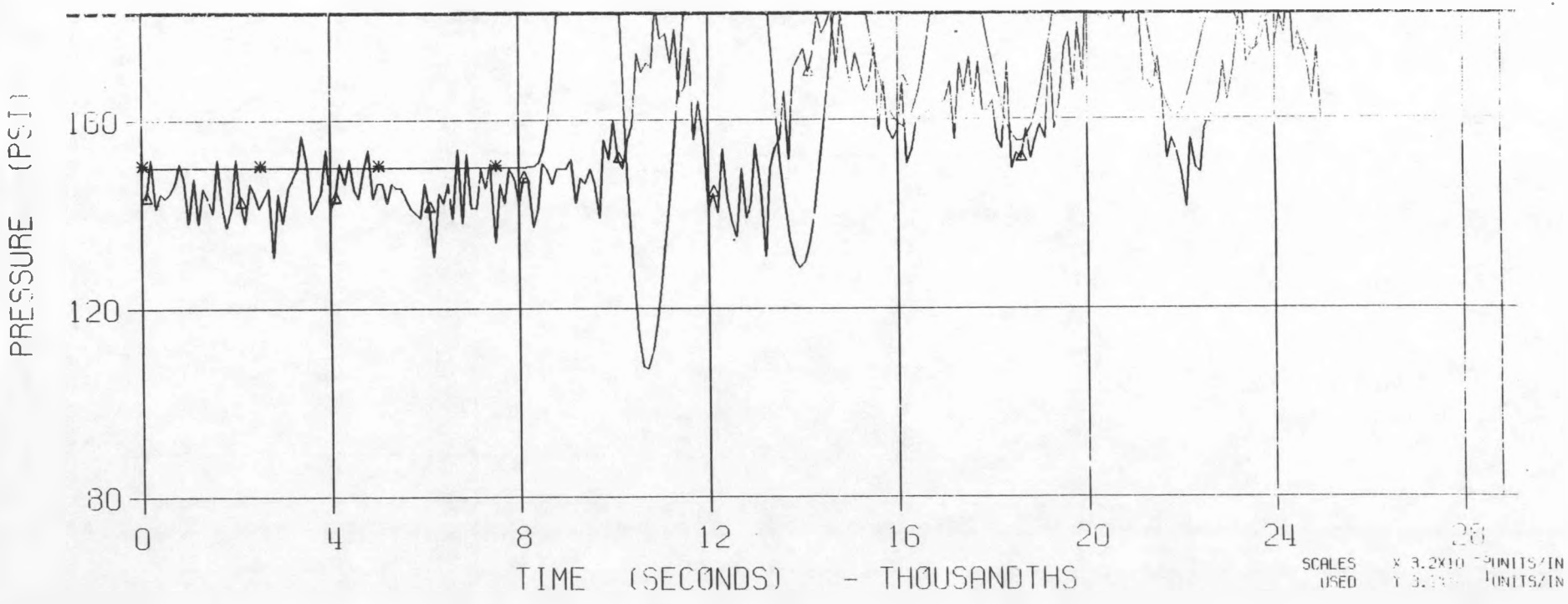
PRESSURE (PSI)
160
120
80
0
4
8
12
16
20
24
28
TIME (SECONDS) - THOUSANDTHS
SCALES USED

PL 13

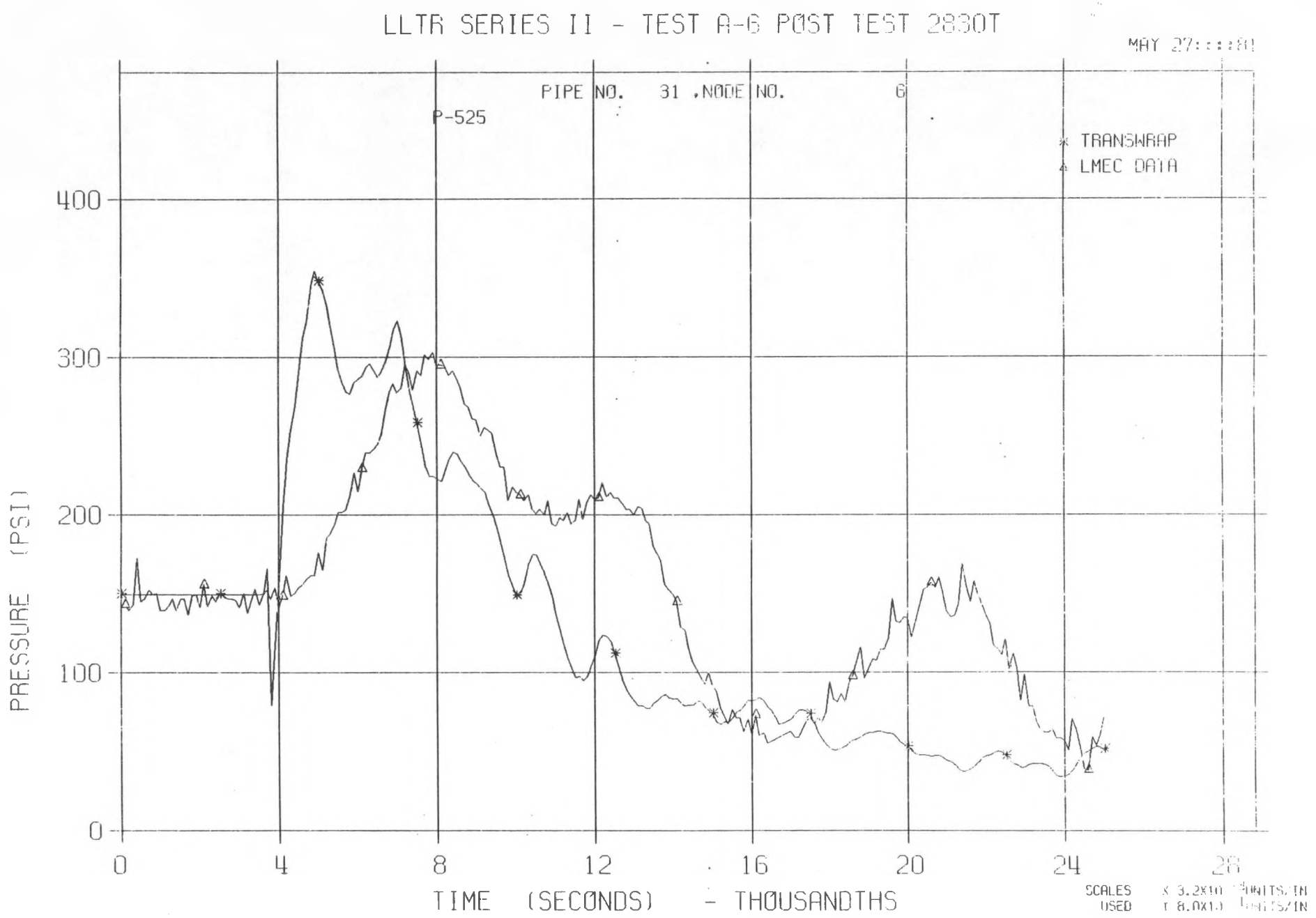
LLTR SERIES II - TEST A-6 POST TEST 2830T
MAY 27::::81
PIPE NO. 31 ,NODE NO. 6
P-525
* TRANSWRAP
Δ LMEC DATA
400
300
200
100
0
PRESSURE (PSI)
0
4
8
12
16
20
24
28
TIME (SECONDS) - THOUSANDTHS
SCALES USED
X 3.2X10 UNITS/IN
Y 8.0X10 UNITS/IN

D-19

PL 19

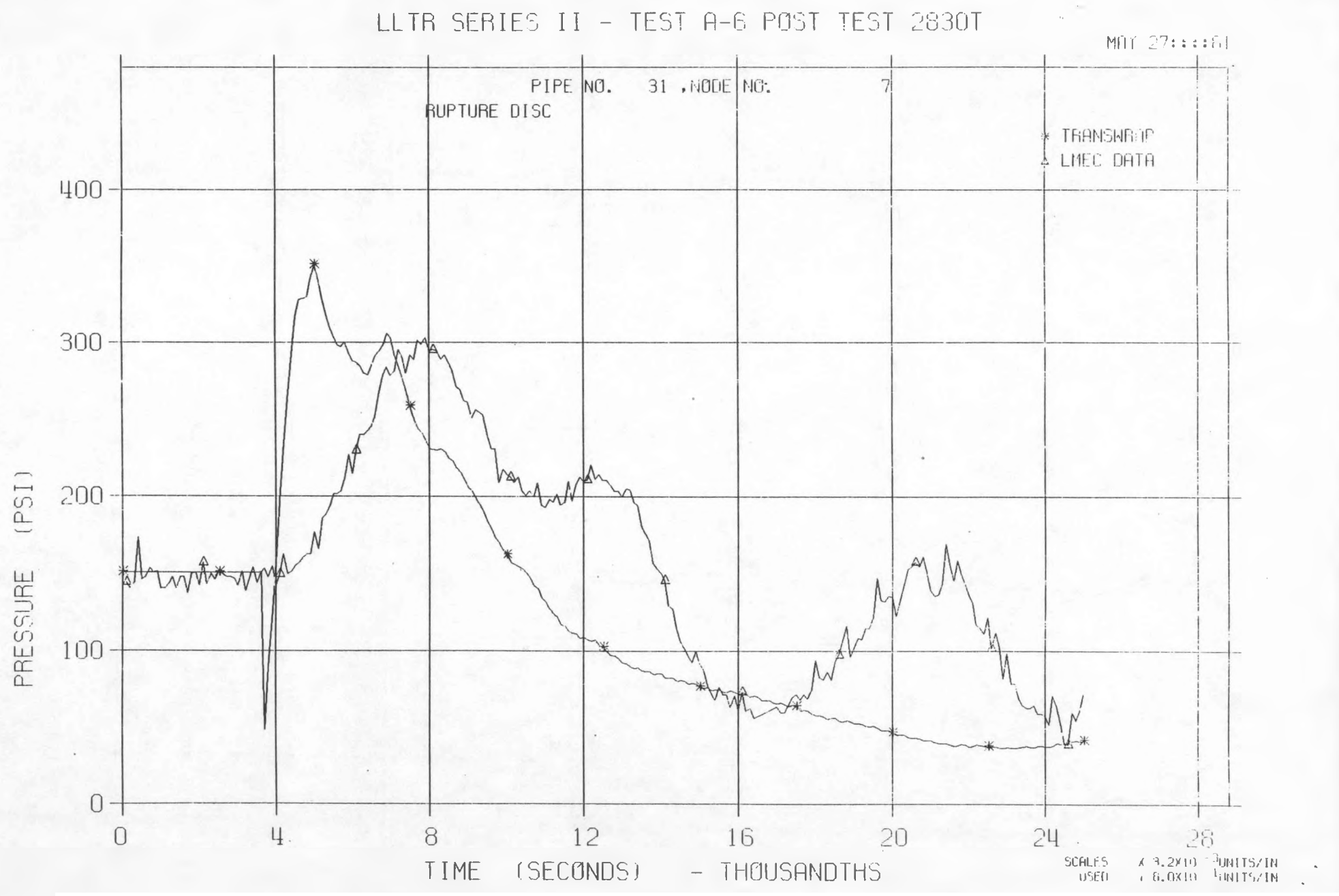
LLTR SERIES II - TEST A-6 POST TEST 2830T
MAY 27::::81
PIPE NO. 31 ,NODE NO: 7
RUPTURE DISC
TRANSWRAP
LMEC DATA
400
300
200
100
0
PRESSURE (PSI)
0
4
8
12
16
20
24
28
TIME (SECONDS) - THOUSANDTHS
SCALES USED
X 3.2X10 -3 UNITS/IN
Y 6.0X10 1 UNITS/IN

PL 20

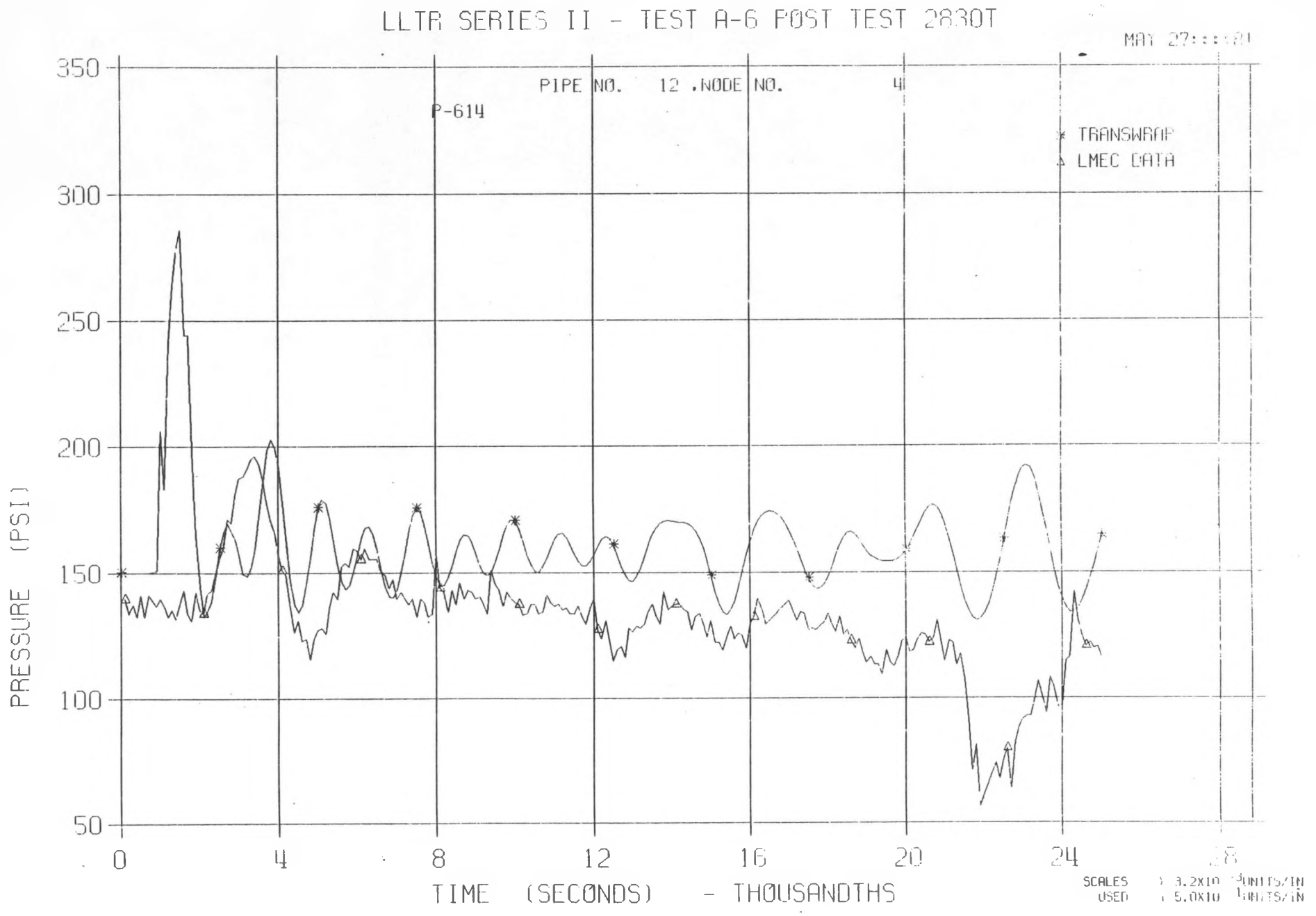
LLTR SERIES II - TEST A-6 POST TEST 2830T
MAY 27:::21
PIPE NO. 12 ,NODE NO. 4
P-614
* TRANSWRAP
Δ LMEC DATA
350
300
250
200
150
100
50
PRESSURE (PSI)
0
4
8
12
16
20
24
28
TIME (SECONDS) - THOUSANDTHS
SCALES USED
3.2X10 -3 UNITS/IN
5.0X10 1 UNITS/IN

D-21

PL 21

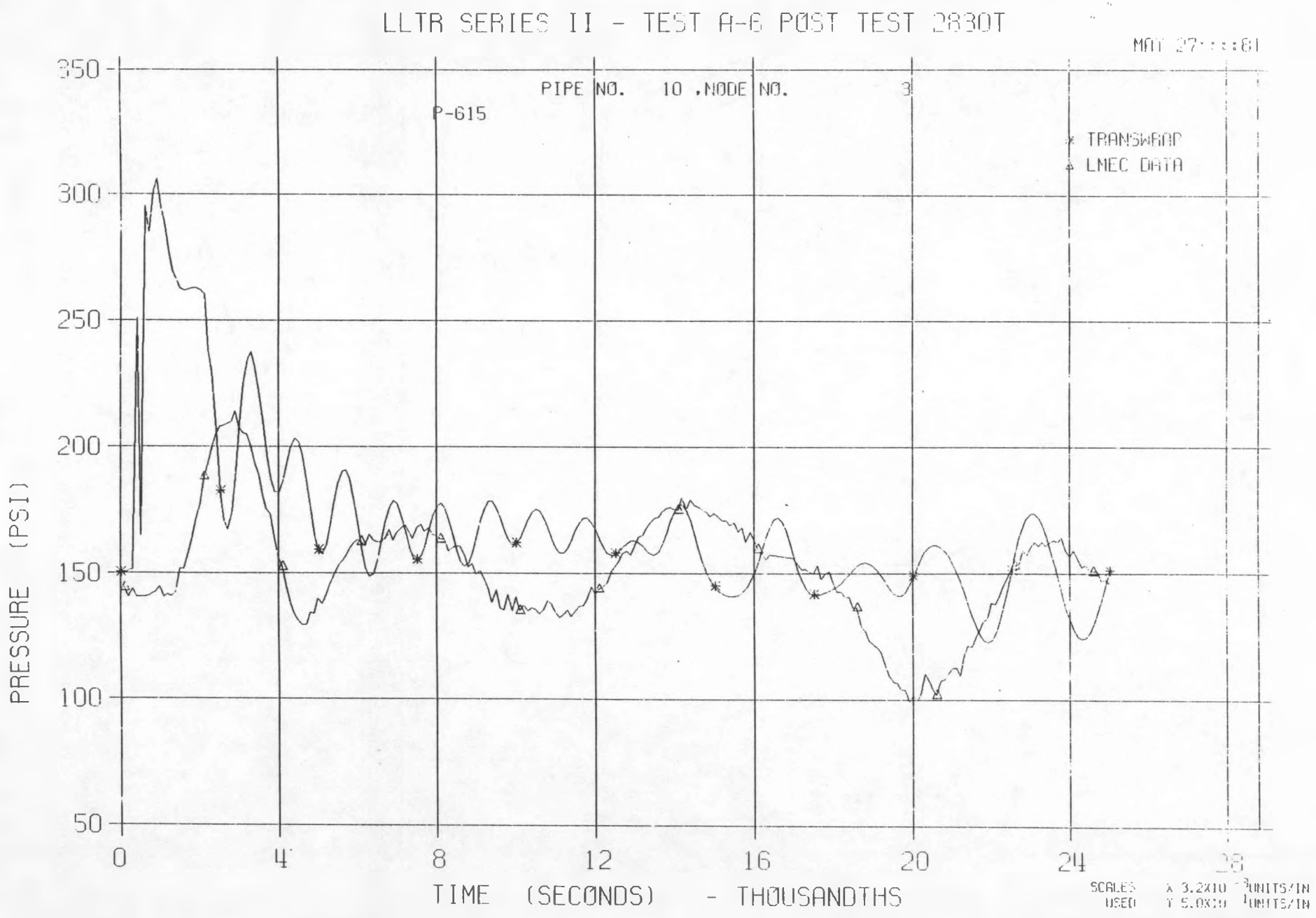
LLTR SERIES II - TEST A-6 POST TEST 2830T
MAY 27 : : : 81
PIPE NO. 10 , NODE NO. 3
P-615
TRANSWRAP
LNEC DATA
350
300
250
200
150
100
50
PRESSURE (PSI)
0
4
8
12
16
20
24
28
TIME (SECONDS) - THOUSANDTHS
SCALES USED
X 3.2X10 -3 UNITS/IN
Y 5.0X10 1 UNITS/IN

D-22

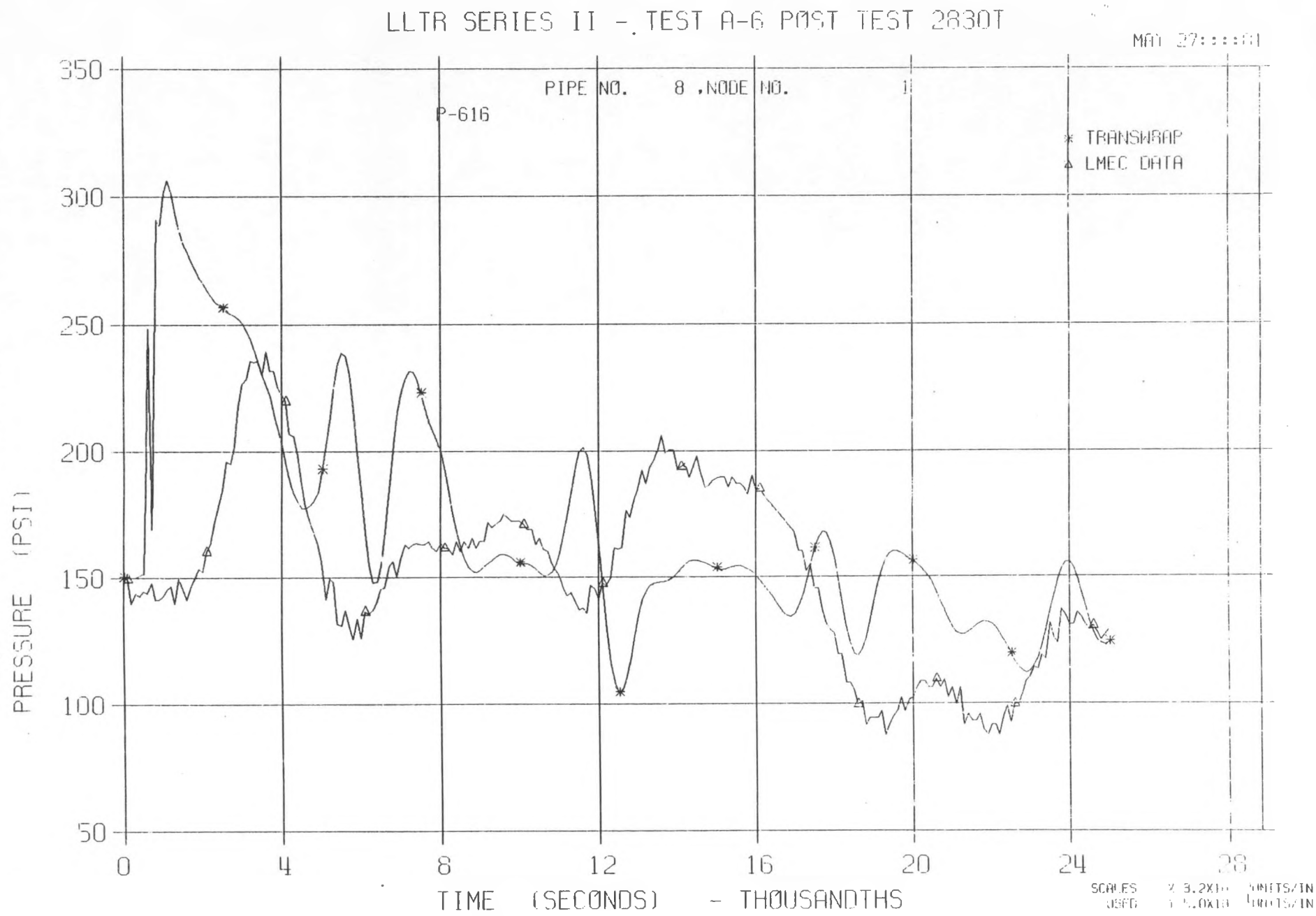
LLTR SERIES II - TEST A-6 POST TEST 2830T
MAY 27:::::81
PIPE NO. 8 ,NODE NO. 1
P-616
* TRANSWRAP
Δ LMEC DATA
PRESSURE (PSI)
350
300
250
200
150
100
50
0
4
8
12
16
20
24
28
TIME (SECONDS) - THOUSANDTHS

D-23

PL 23

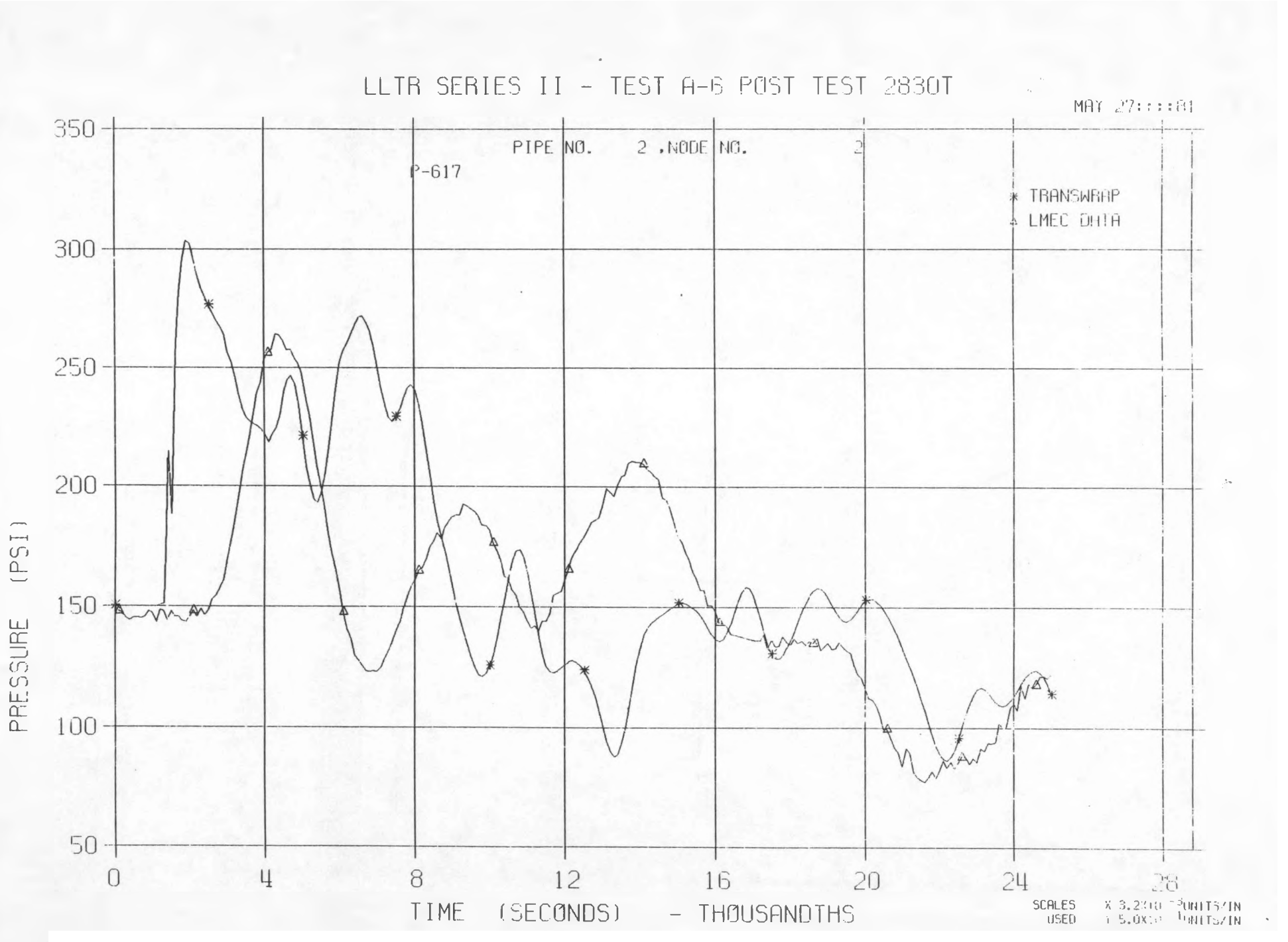
LLTR SERIES II - TEST A-6 POST TEST 2830T
MAY 27
PIPE NO. 2 ,NODE NO. 2
P-617
TRANSWRAP
LMEC DATA
350
300
250
200
150
100
50
PRESSURE (PSI)
0
4
8
12
16
20
24
28
TIME (SECONDS) - THOUSANDTHS
SCALES USED

D-24

PL 24

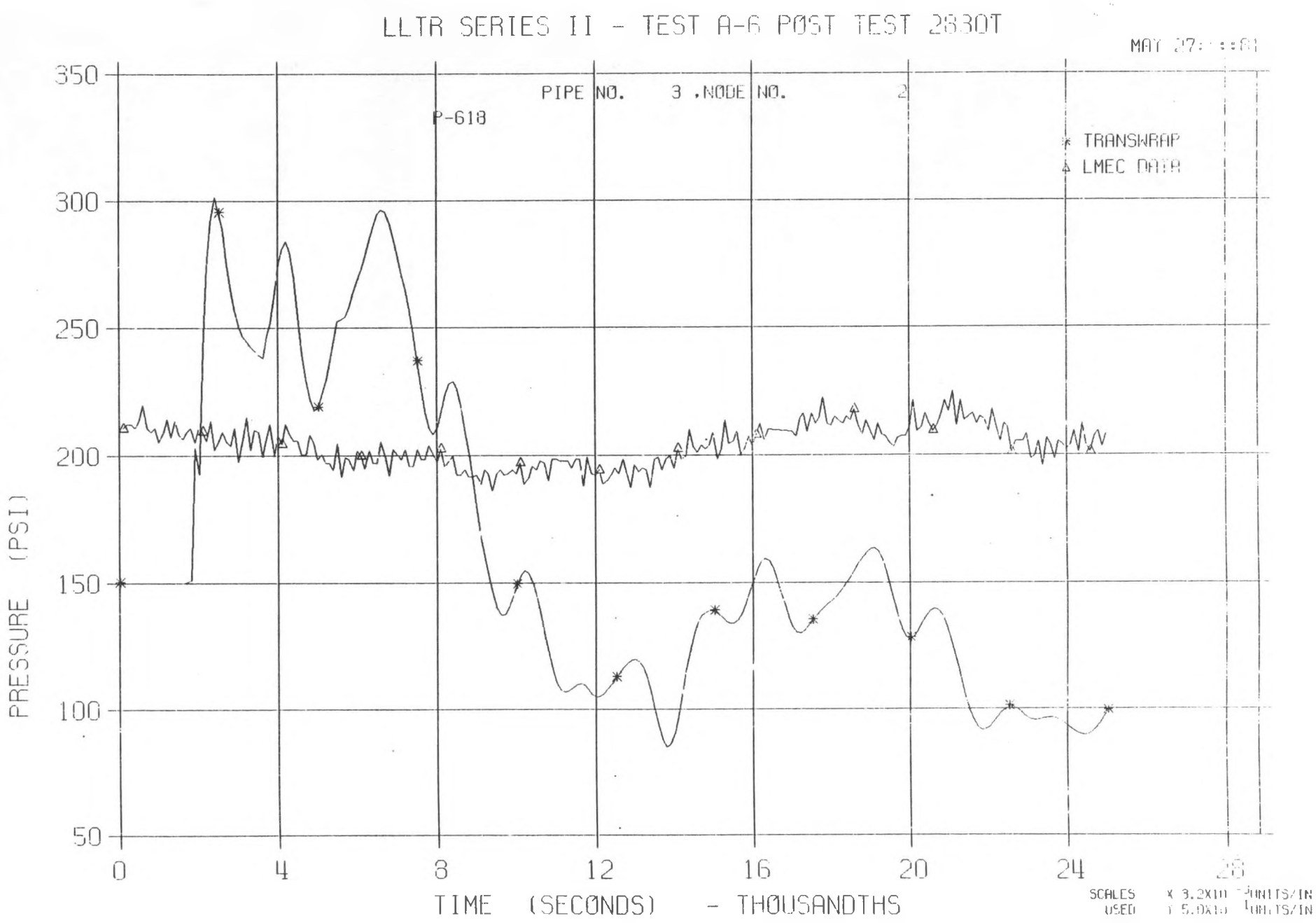
LLTR SERIES II - TEST A-6 POST TEST 2830T
MAY 27
PIPE NO. 3 .NODE NO. 2
P-618
TRANSWRAP
LMEC DATA
350
300
250
200
150
100
50
PRESSURE (PSI)
0
4
8
12
16
20
24
28
TIME (SECONDS) - THOUSANDTHS
SCALES USED

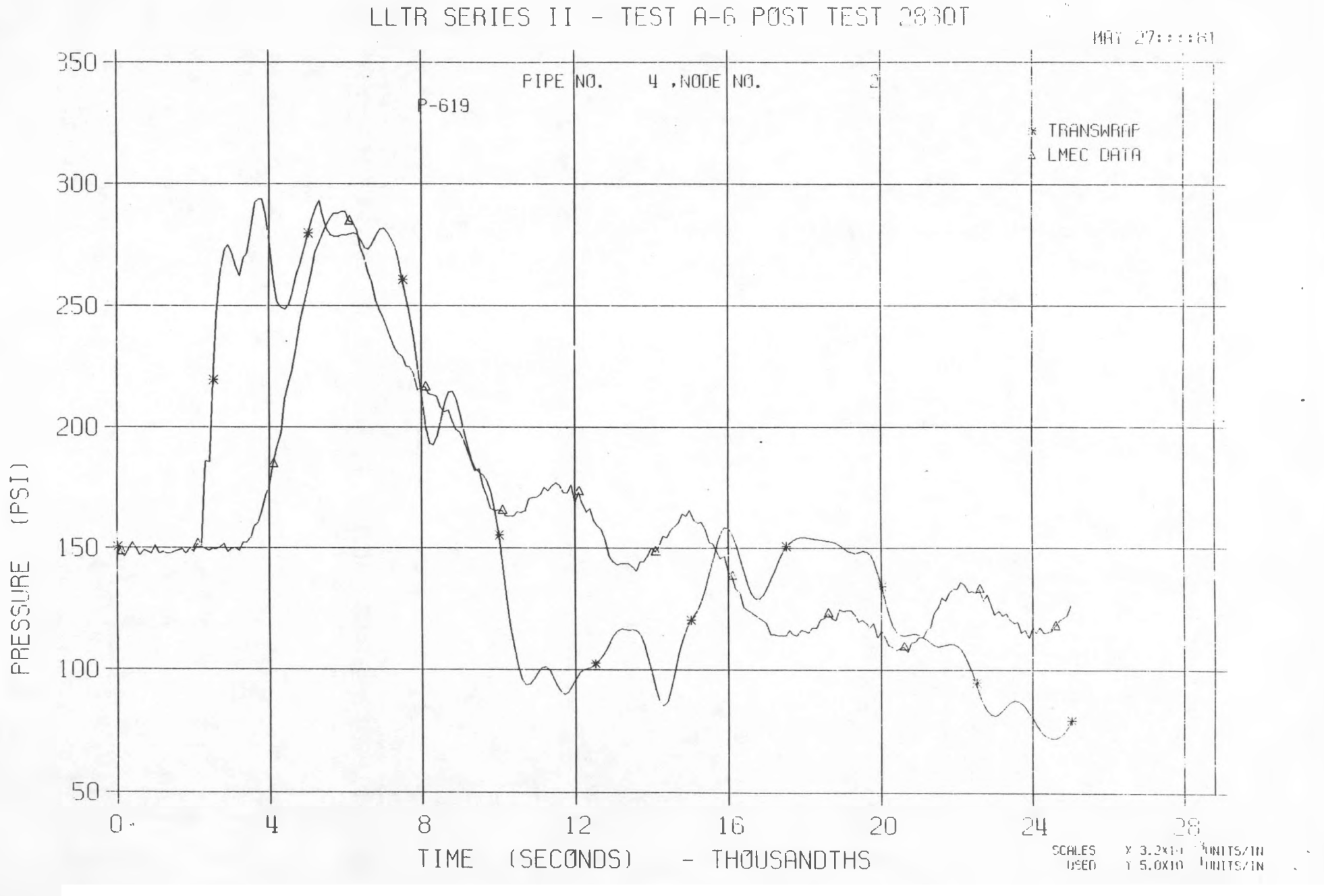
LLTR SERIES II - TEST A-6 POST TEST 2830T
MAY 27::::81
PIPE NO. 4 ,NODE NO. 2
P-619
* TRANSWRAP
Δ LMEC DATA
350
300
250
200
150
100
50
PRESSURE (PSI)
0
4
8
12
16
20
24
28
TIME (SECONDS) - THOUSANDTHS
SCALES USED
X 3.2X10 UNITS/IN
Y 5.0X10 UNITS/IN

D-26

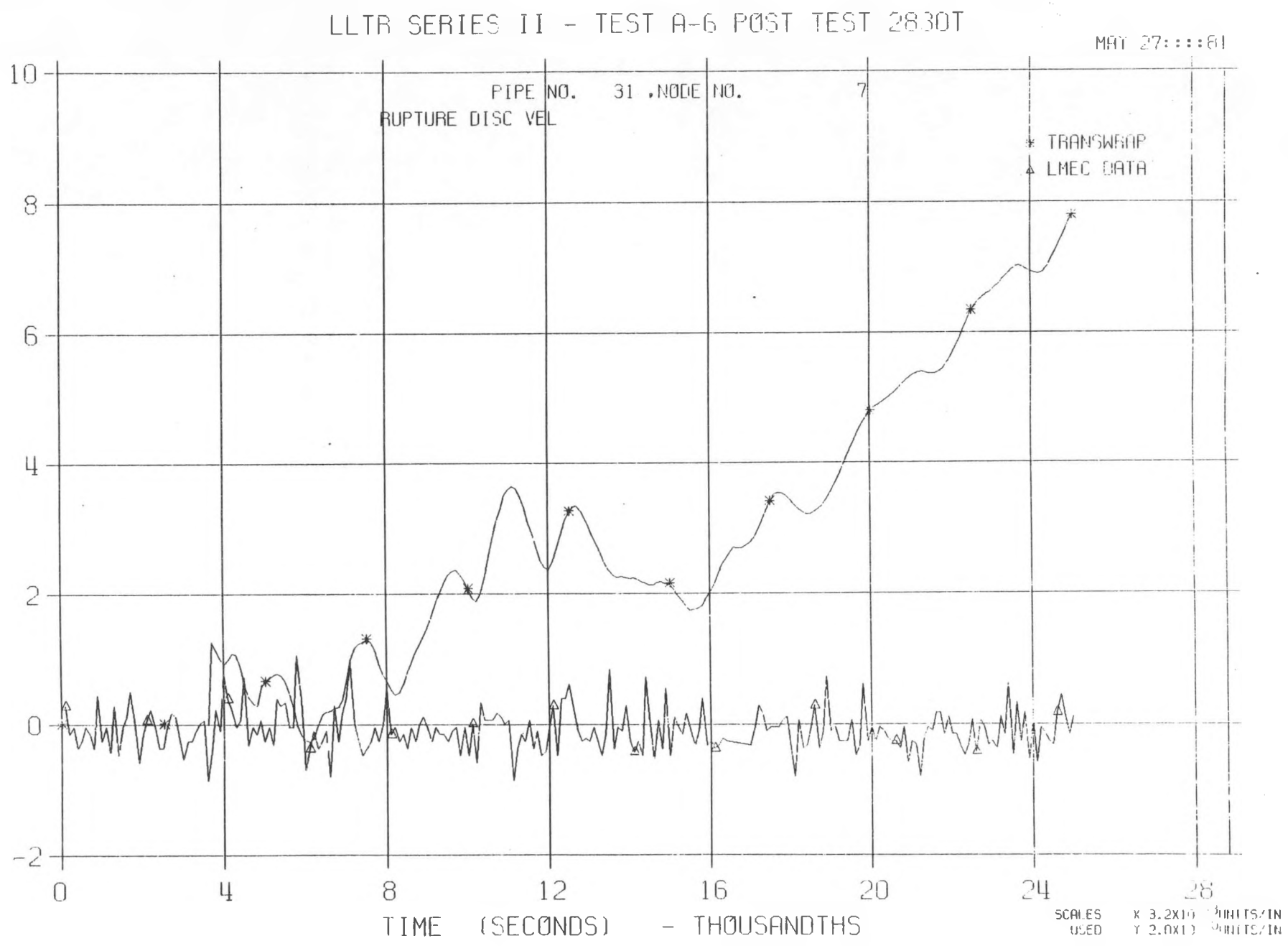
LLTR SERIES II - TEST A-6 POST TEST 2830T
MAY 27::::81
PIPE NO. 31 ,NODE NO. 7
RUPTURE DISC VEL
* TRANSWRAP
Δ LMEC DATA
VELOCITY (FT/SEC)
10
8
6
4
2
0
-2
0
4
8
12
16
20
24
28
TIME (SECONDS) - THOUSANDTHS
SCALES USED
X 3.2X10 UNITS/IN
Y 2.0X10 UNITS/IN

PL 28

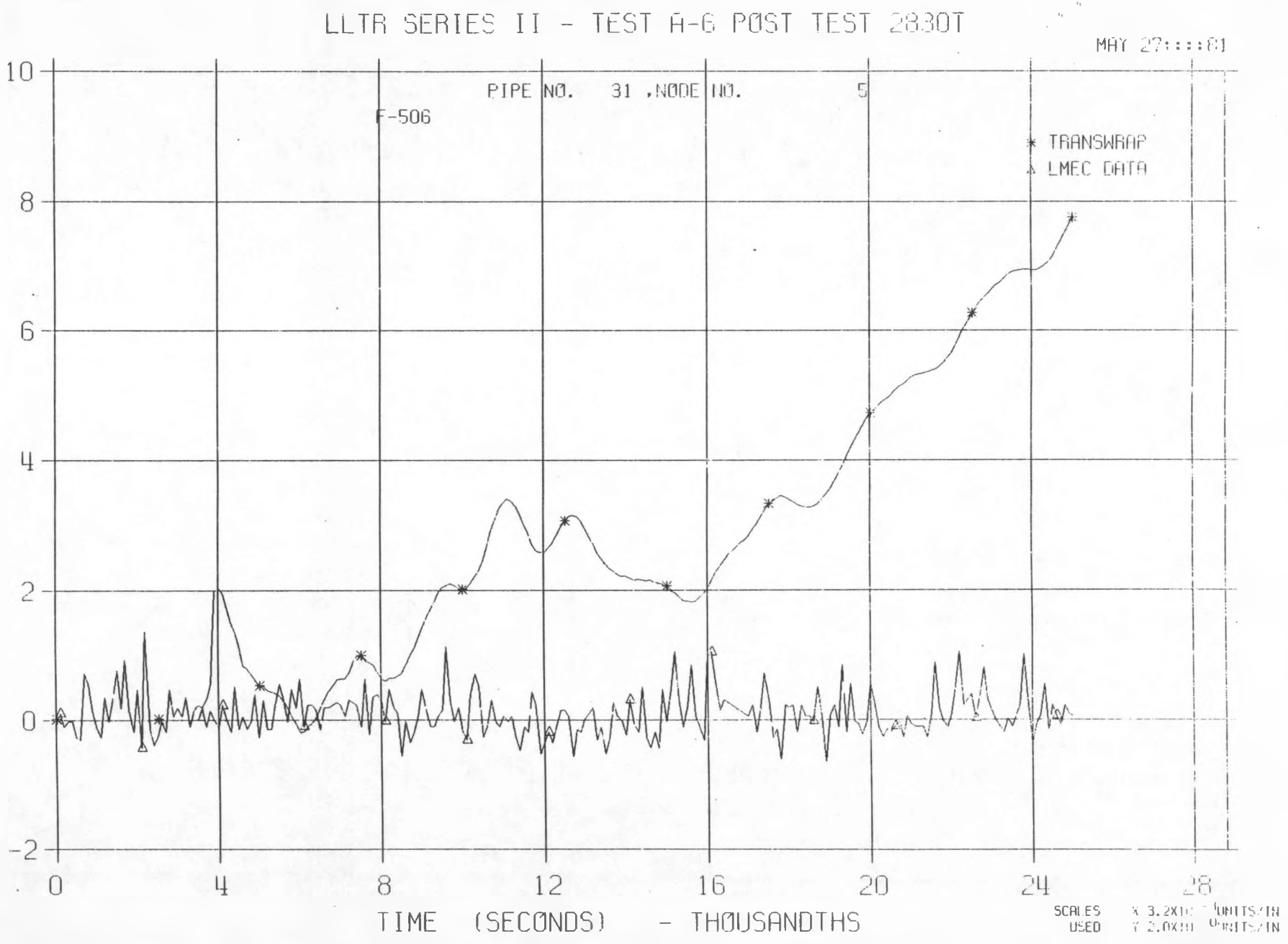
LLTR SERIES II - TEST A-6 POST TEST 28.30T
MAY 27::::81
PIPE NO. 31 ,NODE NO. 5
F-506
TRANSWRAP
LMEC DATA
10
8
6
4
2
0
-2
0
4
8
12
16
20
24
28
VELOCITY (FT/SEC)
TIME (SECONDS) - THOUSANDTHS
SCALES USED

D-28

PL 29

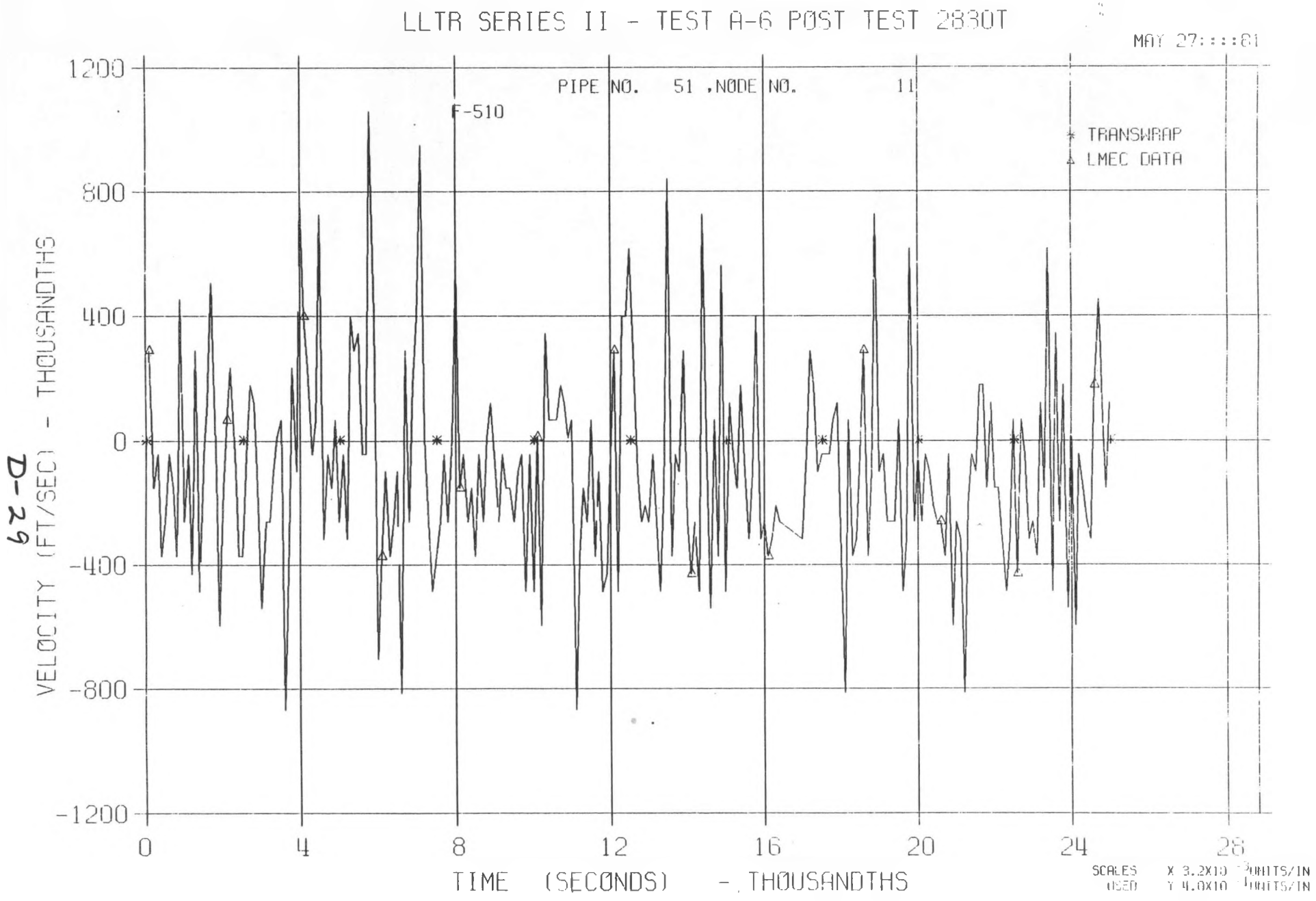
LLTR SERIES II - TEST A-6 POST TEST 2830T
MAY 27::::81
PIPE NO. 51 ,NODE NO. 11
F-510
* TRANSWRAP
Δ LMEC DATA
1200
800
400
0
-400
-800
-1200
VELOCITY (FT/SEC) - THOUSANDTHS
0
4
8
12
16
20
24
28
TIME (SECONDS) - THOUSANDTHS
SCALES USED
X 3.2X10 UNITS/IN
Y 4.0X10 UNITS/IN

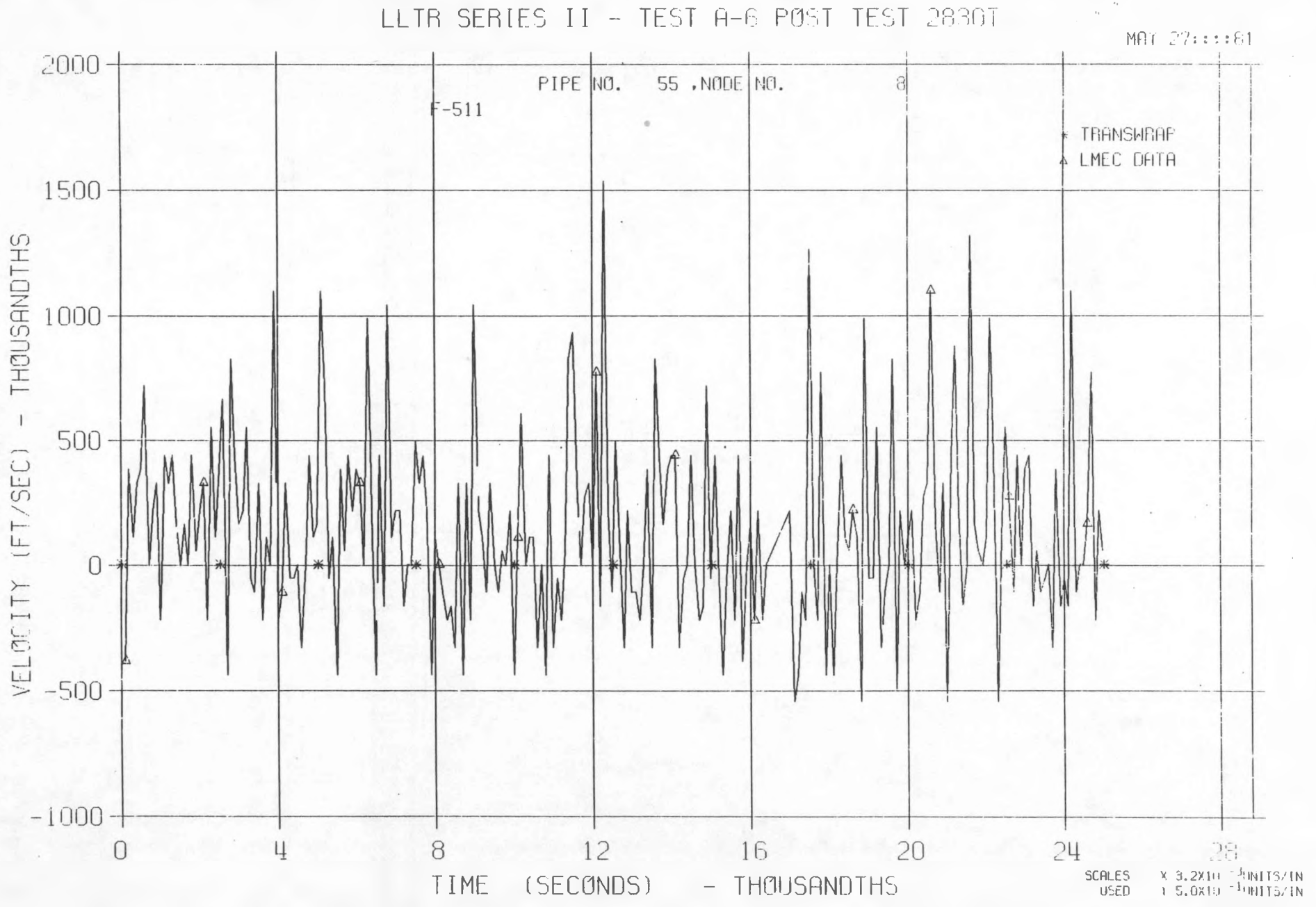
LLTR SERIES II - TEST A-6 POST TEST 2830T
MAY 27::::81
PIPE NO. 55 ,NODE NO. 8
F-511
* TRANSWRAP
Δ LMEC DATA
VELOCITY (FT/SEC) - THOUSANDTHS
2000
1500
1000
500
0
-500
-1000
0
4
8
12
16
20
24
28
TIME (SECONDS) - THOUSANDTHS
SCALES USED
X 3.2X10 -4 UNITS/IN
Y 5.0X10 -4 UNITS/IN

PL 31

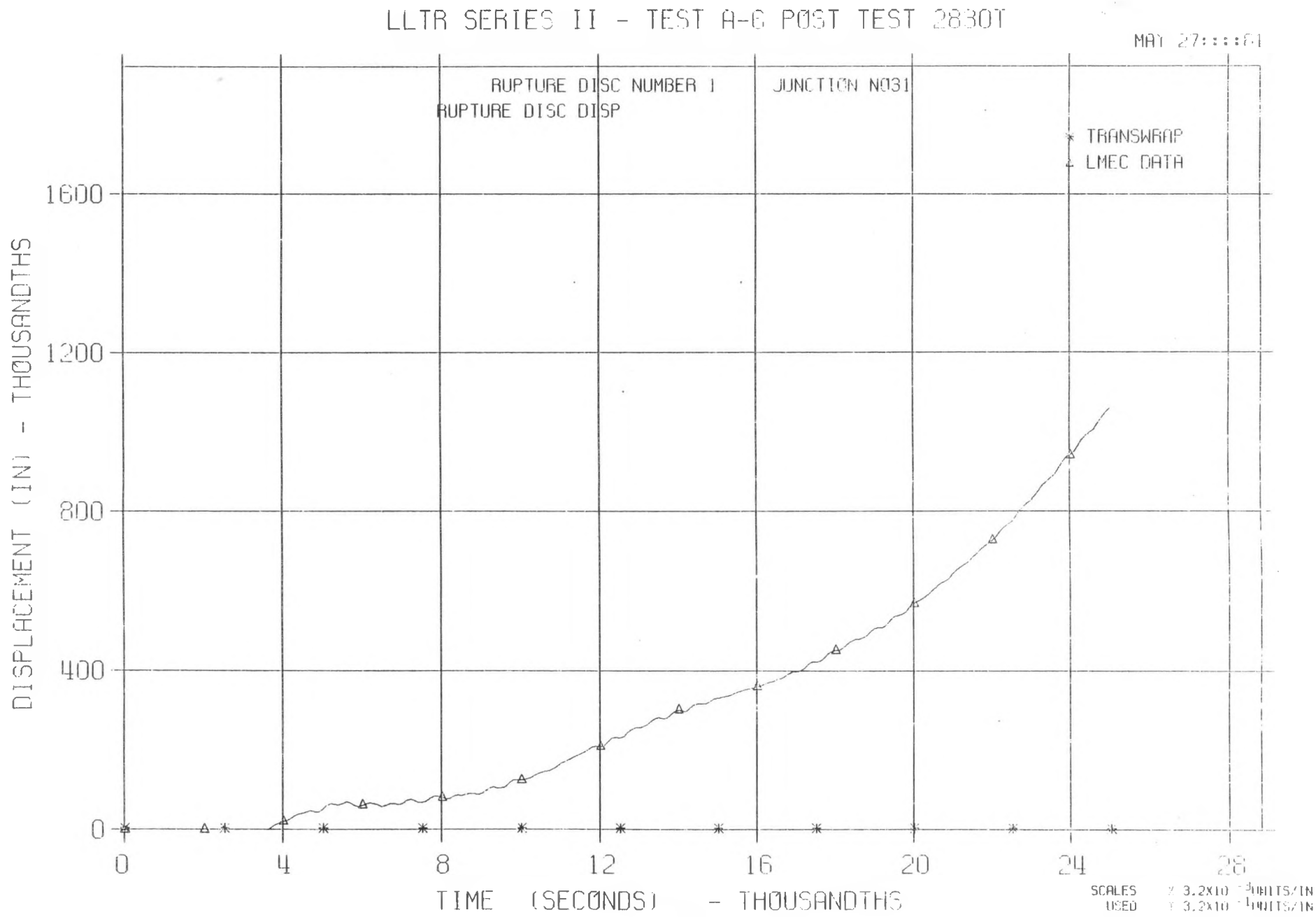
LLTR SERIES II - TEST A-6 POST TEST 2830T
MAY 27::::81
RUPTURE DISC NUMBER 1
RUPTURE DISC DISP
JUNCTION N031
TRANSWRAP
LMEC DATA
DISPLACEMENT (IN) - THOUSANDTHS
1600
1200
800
400
0
0
4
8
12
16
20
24
28
TIME (SECONDS) - THOUSANDTHS
SCALES USED
X 3.2X10 -3 UNITS/IN
Y 3.2X10 -4 UNITS/IN

D-31

PL 32

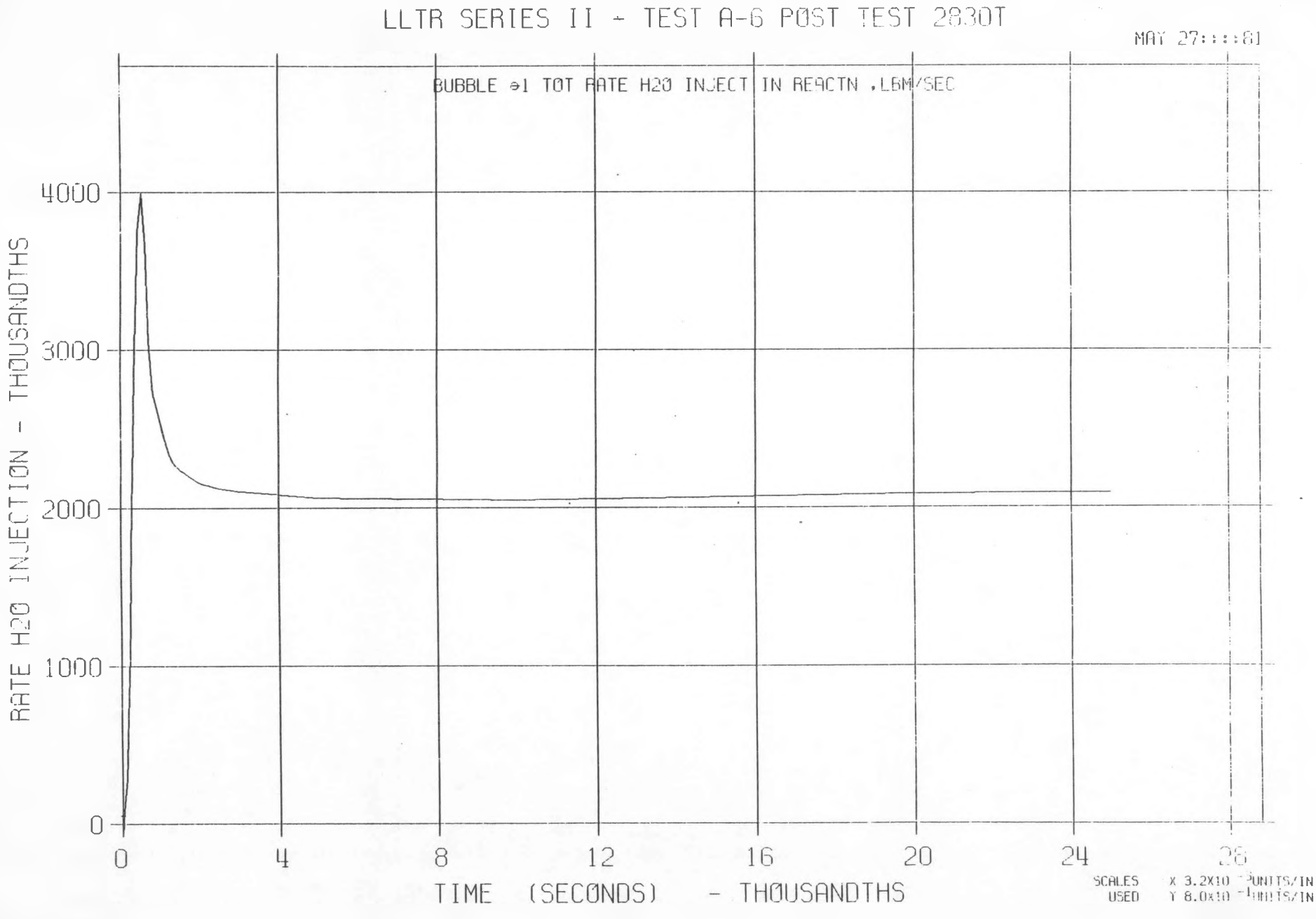
LLTR SERIES II - TEST A-6 POST TEST 2830T
MAY 27::::81
BUBBLE ⊖1 TOT RATE H20 INJECT IN REACTN ,LBM/SEC
4000
3000
2000
1000
0
RATE H20 INJECTION - THOUSANDTHS
0
4
8
12
16
20
24
28
TIME (SECONDS) - THOUSANDTHS
SCALES USED
X 3.2X10 -3 UNITS/IN
Y 8.0x10 -1 UNITS/IN

D-32

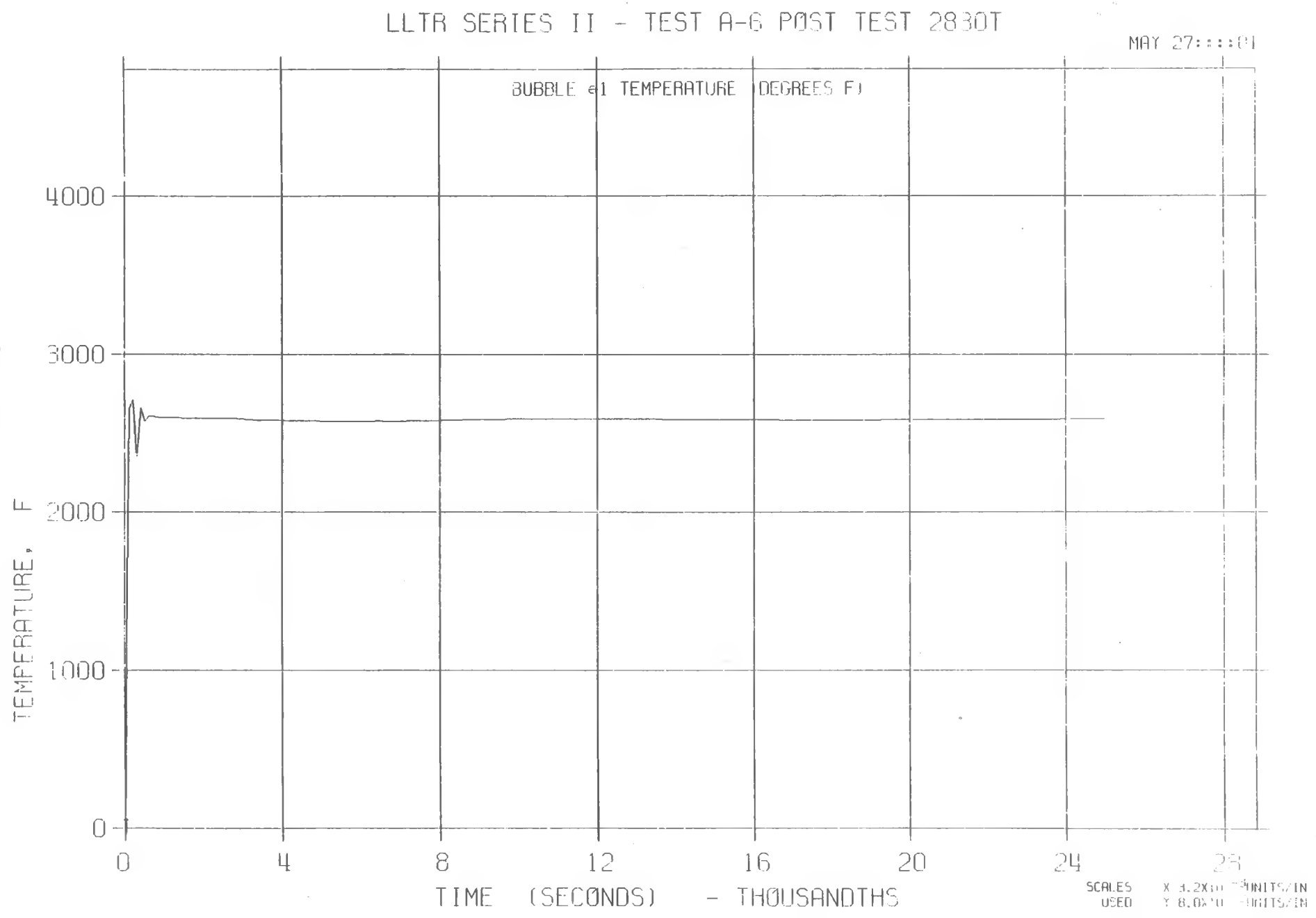
LLTR SERIES II - TEST A-6 POST TEST 2830T
MAY 27::::81
BUBBLE #1 TEMPERATURE (DEGREES F)
4000
3000
2000
1000
0
TEMPERATURE, F
0
4
8
12
16
20
24
28
TIME (SECONDS) - THOUSANDTHS
SCALES USED

PL 38

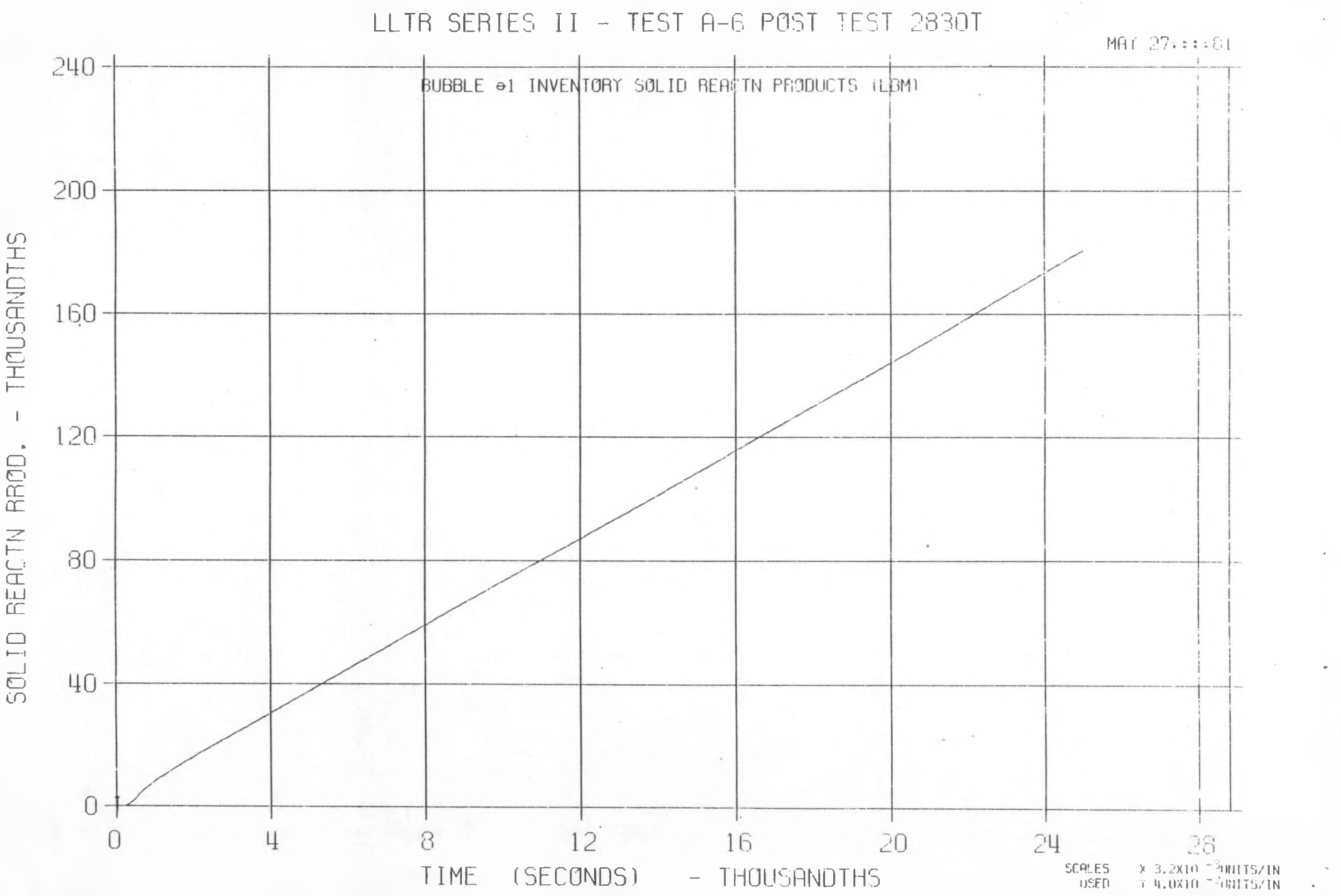
LLTR SERIES II - TEST A-6 POST TEST 2830T
MAY 27:::81
BUBBLE #1 INVENTORY SOLID REACTN PRODUCTS (LBM)
SOLID REACTN PROD. - THOUSANDTHS
240
200
160
120
80
40
0
0
4
8
12
16
20
24
28
TIME (SECONDS) - THOUSANDTHS
SCALES USED
X 3.2X10 UNITS/IN
Y 4.0X10 UNITS/IN

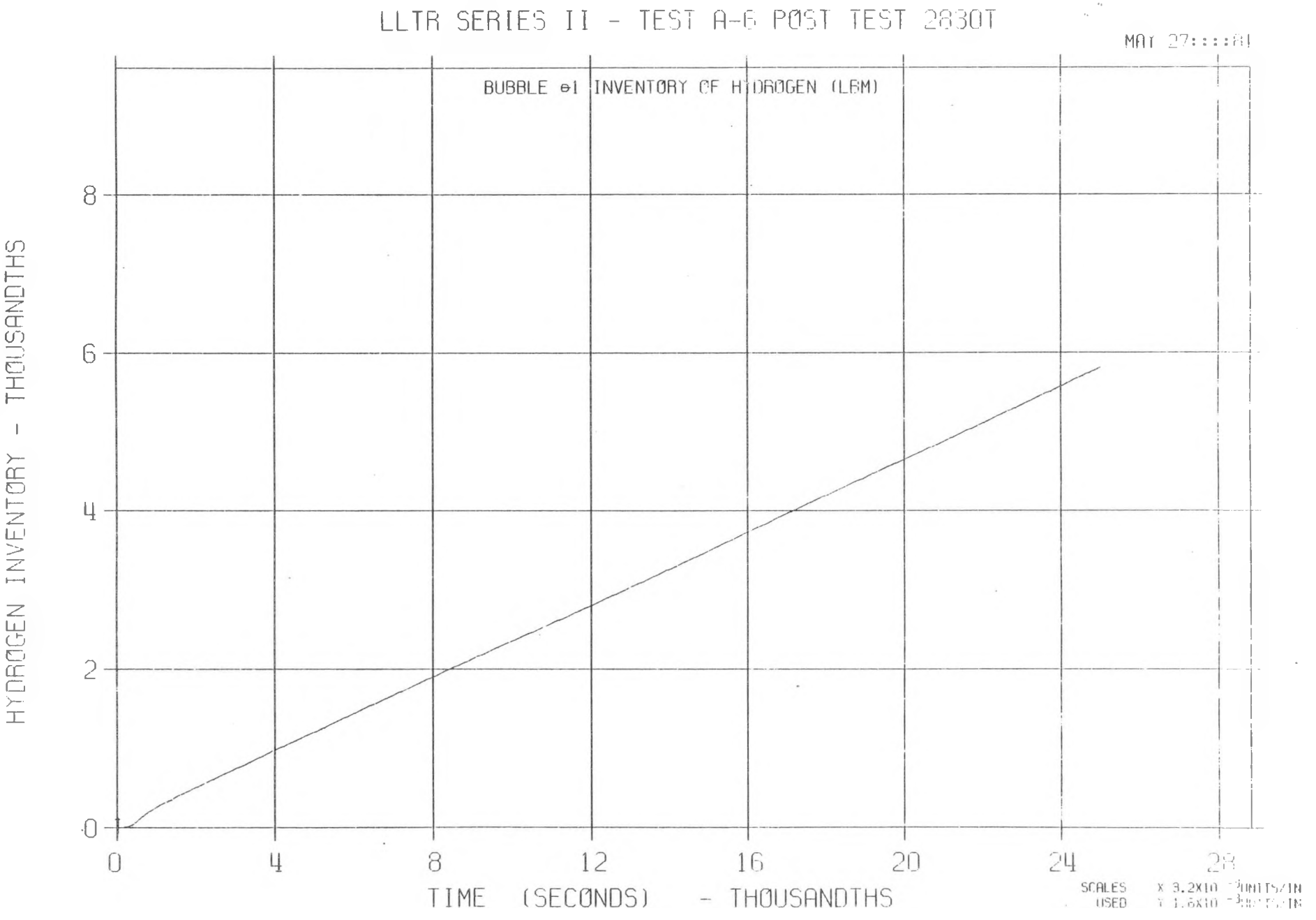
LLTR SERIES II - TEST A-6 POST TEST 2830T
MAY 27::::81
BUBBLE el INVENTORY OF HYDROGEN (LBM)
HYDROGEN INVENTORY - THOUSANDTHS
0
2
4
6
8
0
4
8
12
16
20
24
28
TIME (SECONDS) - THOUSANDTHS
SCALES USED

PL 40

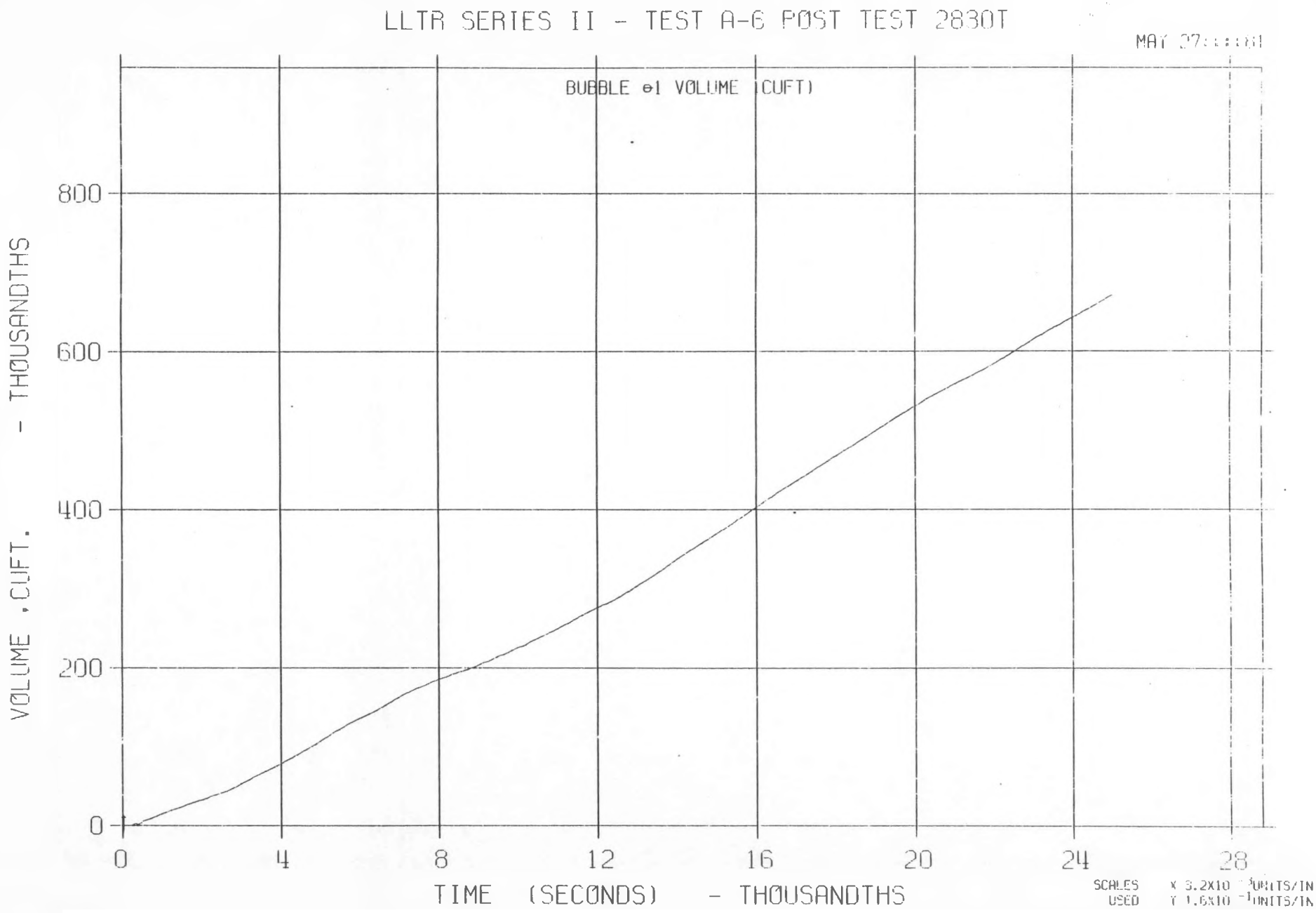
LLTR SERIES II - TEST A-6 POST TEST 2830T
MAY 27
BUBBLE #1 VOLUME (CUFT)
VOLUME ,CUFT. - THOUSANDTHS
800
600
400
200
0
0
4
8
12
16
20
24
28
TIME (SECONDS) - THOUSANDTHS
SCALES USED
X 5.2X10 -3 UNITS/IN
Y 1.6X10 -1 UNITS/IN

D-36

PL 41

APPENDIX E

TRANSWRAP MODEL E

A-6 TEST

IX SWR

GAS VOID AT TOP OF LLTV

LARGE SODIUM CORE

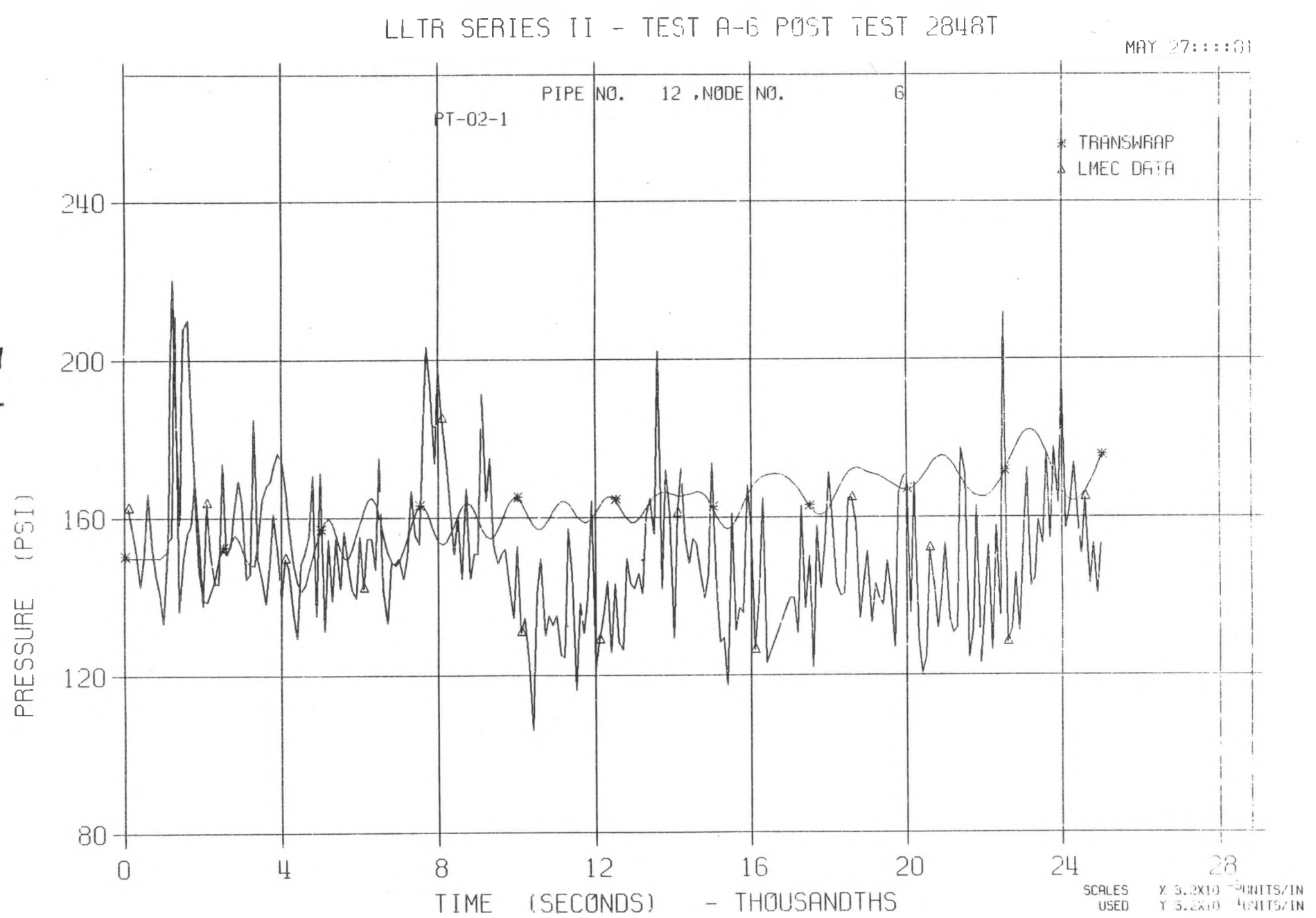
LLTR SERIES II - TEST A-6 POST TEST 2848T
MAY 27::::01
PIPE NO. 12 ,NODE NO. 6
PT-02-1
* TRANSWRAP
Δ LMEC DATA
240
200
160
120
80
PRESSURE (PSI)
0
4
8
12
16
20
24
28
TIME (SECONDS) - THOUSANDTHS
SCALES USED
X 3.2X10 -3 UNITS/IN
Y 3.2X10 1 UNITS/IN

E-1

PL 1

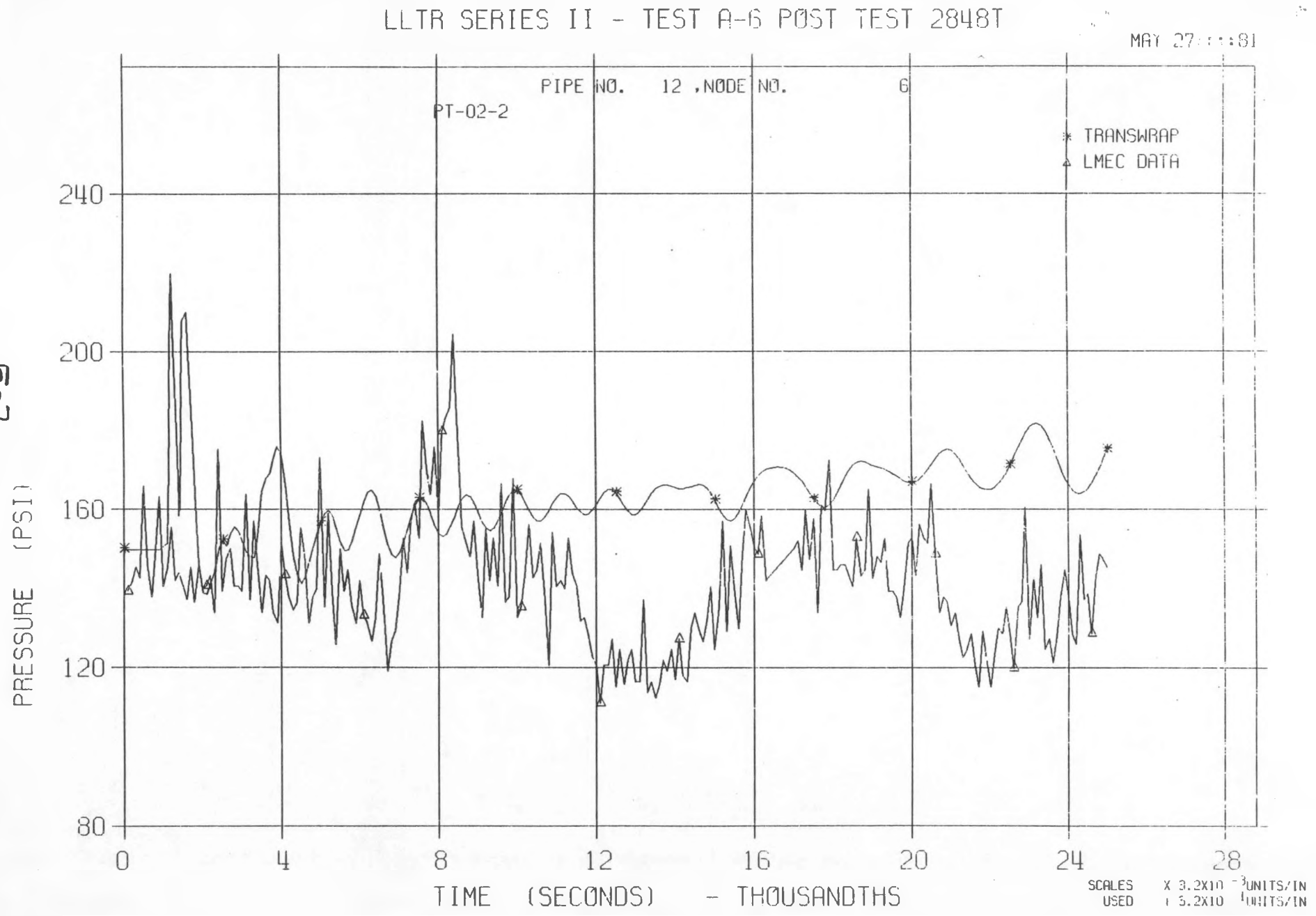
LLTR SERIES II - TEST A-6 POST TEST 2848T
MAY 27
PIPE NO. 12 ,NODE NO. 6
PT-02-2
TRANSWRAP
LMEC DATA
240
200
160
120
80
PRESSURE (PSI)
0
4
8
12
16
20
24
28
TIME (SECONDS) - THOUSANDTHS
SCALES USED
X 3.2X10 -3 UNITS/IN
Y 5.2X10 1 UNITS/IN

E-2

PL 2

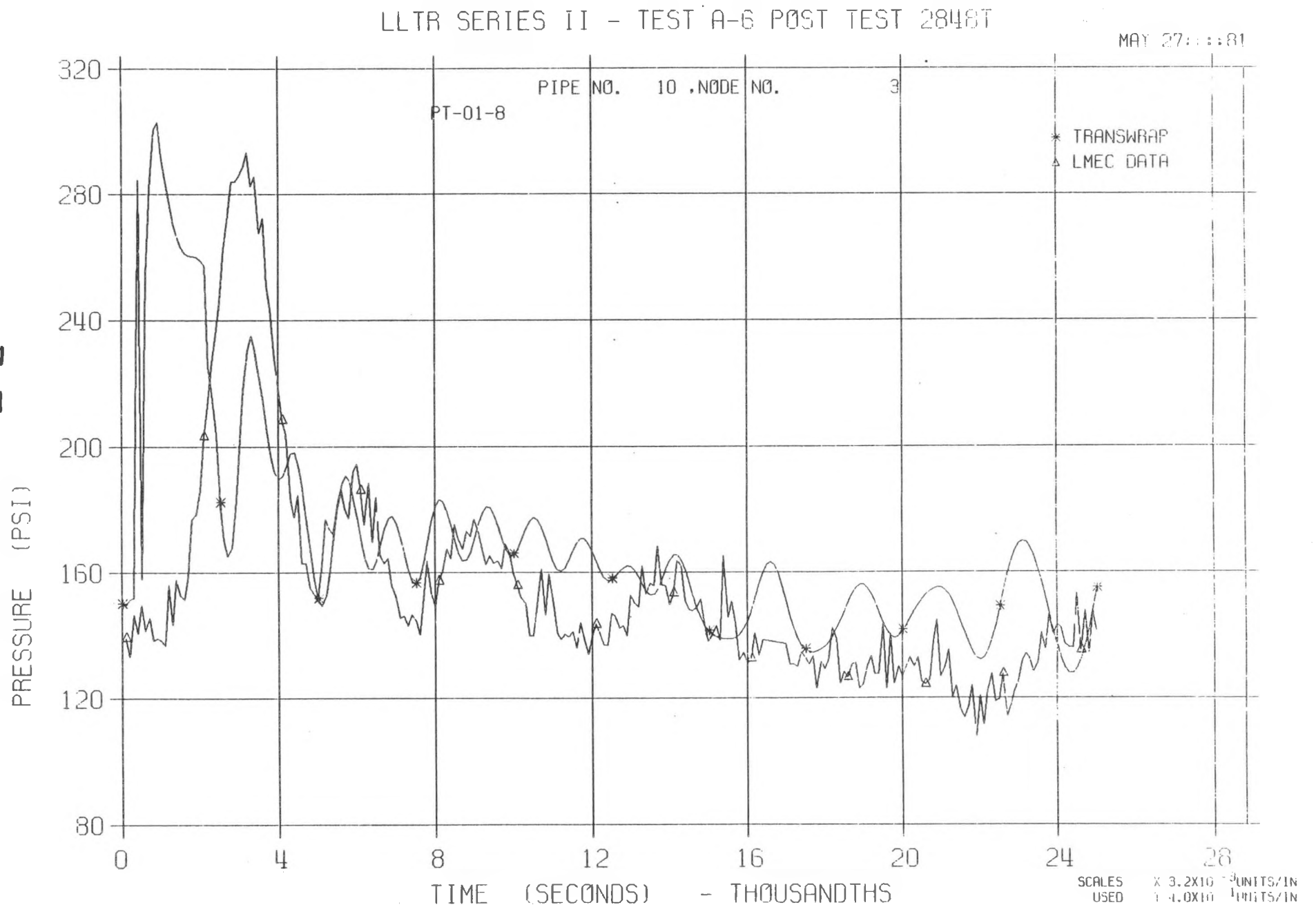
LLTR SERIES II - TEST A-6 POST TEST 2848T
MAY 27
PIPE NO. 10 ,NODE NO. 3
PT-01-8
TRANSWRAP
LMEC DATA
320
280
240
200
160
120
80
PRESSURE (PSI)
0
4
8
12
16
20
24
28
TIME (SECONDS) - THOUSANDTHS
SCALES USED
UNITS/IN
UNITS/IN

E-3

PL 3

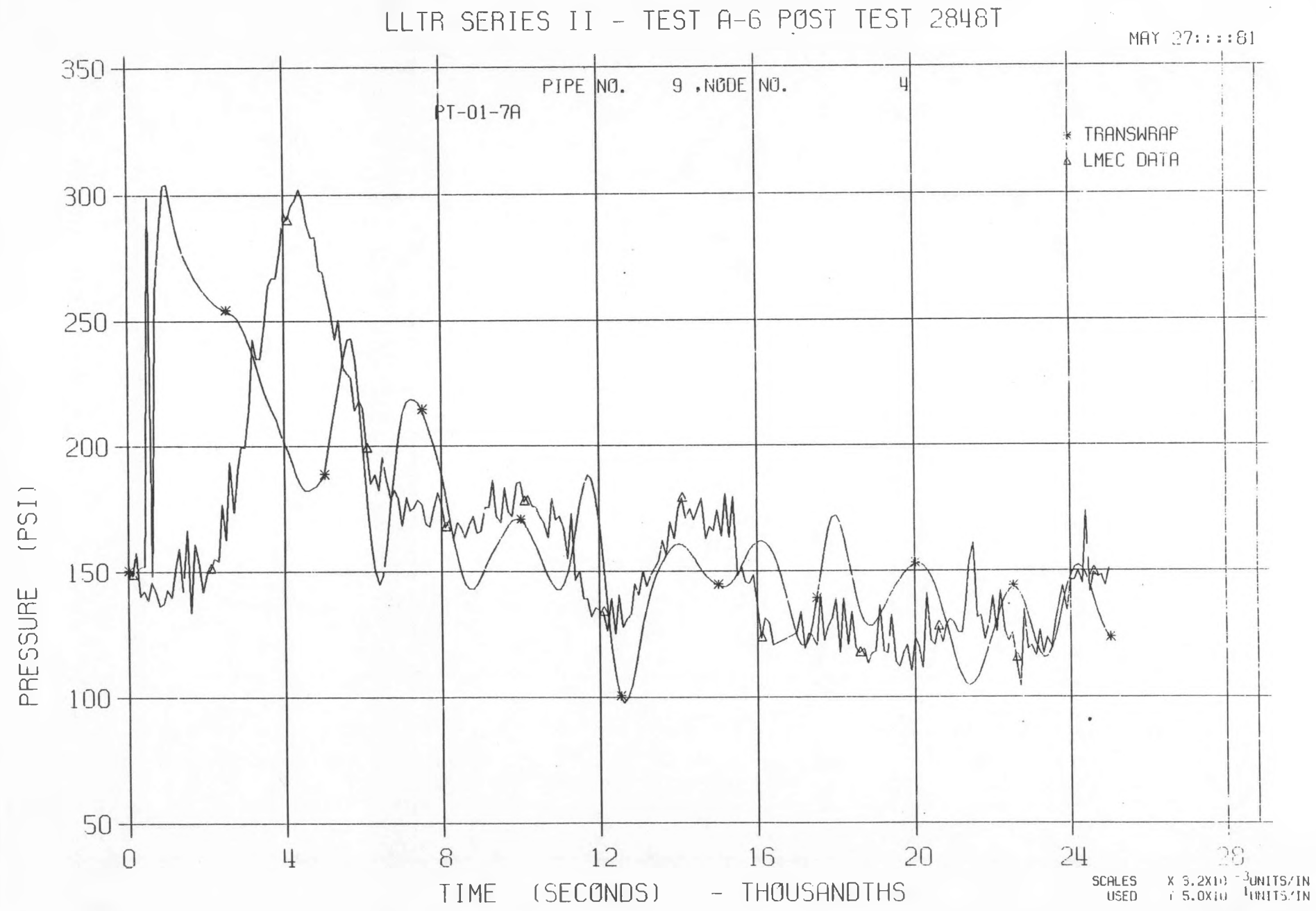
LLTR SERIES II - TEST A-6 POST TEST 2848T
MAY 27::::81
PIPE NO. 9 ,NODE NO. 4
PT-01-7A
TRANSWRAP
LMEC DATA
PRESSURE (PSI)
350
300
250
200
150
100
50
0
4
8
12
16
20
24
28
TIME (SECONDS) - THOUSANDTHS
SCALES USED
X 5.2X10 -3 UNITS/IN
Y 5.0X10 1 UNITS/IN

E-4

PL 4

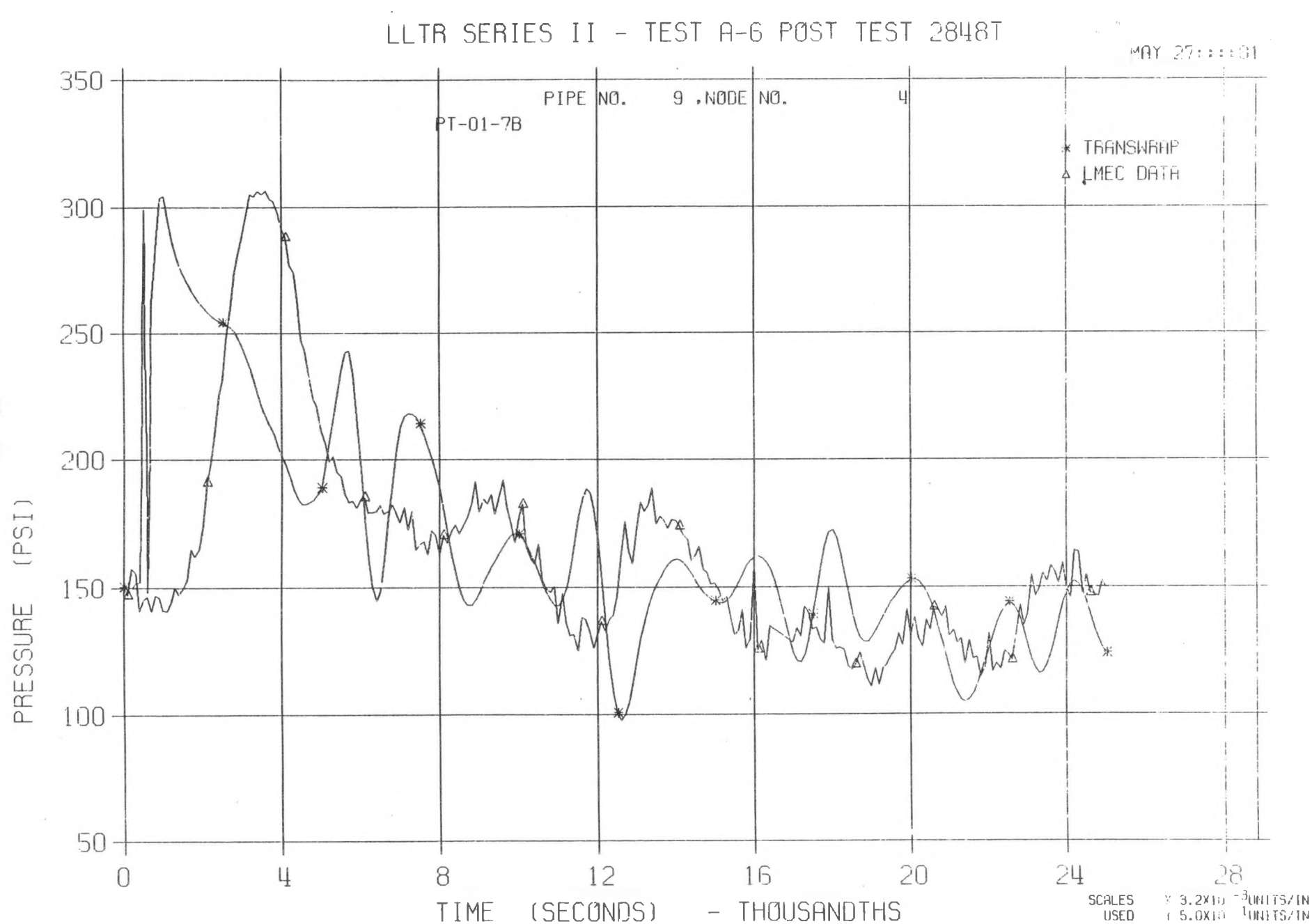
LLTR SERIES II - TEST A-6 POST TEST 2848T
MAY 27
PIPE NO. 9 ,NODE NO. 4
PT-01-7B
* TRANSWRAP
Δ LMEC DATA
350
300
250
200
150
100
50
PRESSURE (PSI)
0
4
8
12
16
20
24
28
TIME (SECONDS) - THOUSANDTHS
SCALES USED
UNITS/IN
UNITS/IN

PL 5

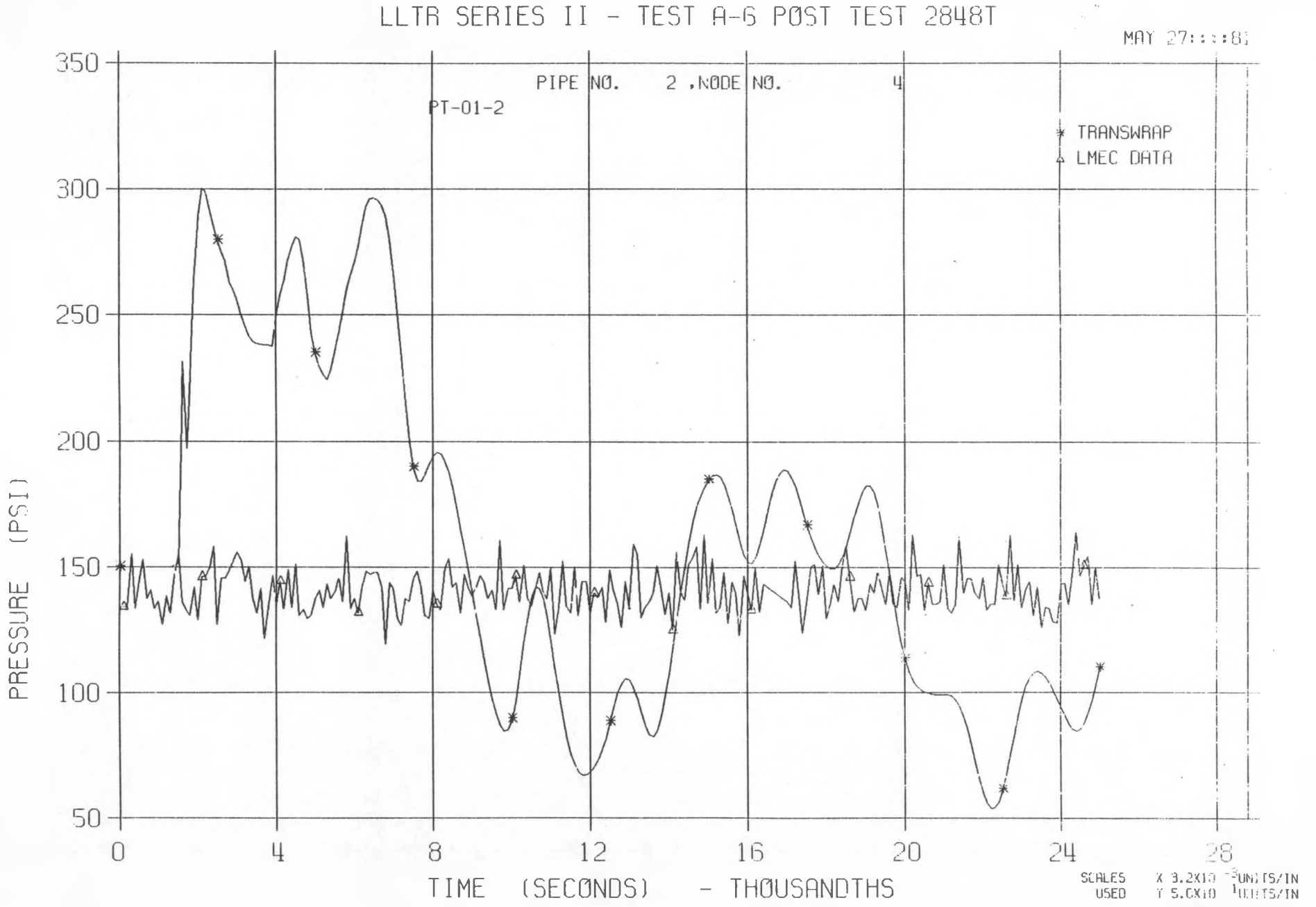
LLTR SERIES II - TEST A-6 POST TEST 2848T
MAY 27::::81
PIPE NO. 2 ,NODE NO. 4
PT-01-2
TRANSWRAP
LMEC DATA
350
300
250
200
150
100
50
PRESSURE (PSI)
0
4
8
12
16
20
24
28
TIME (SECONDS) - THOUSANDTHS
SCALES USED
X 3.2X10 -3 UNITS/IN
Y 5.0X10 1 UNITS/IN

PL 6

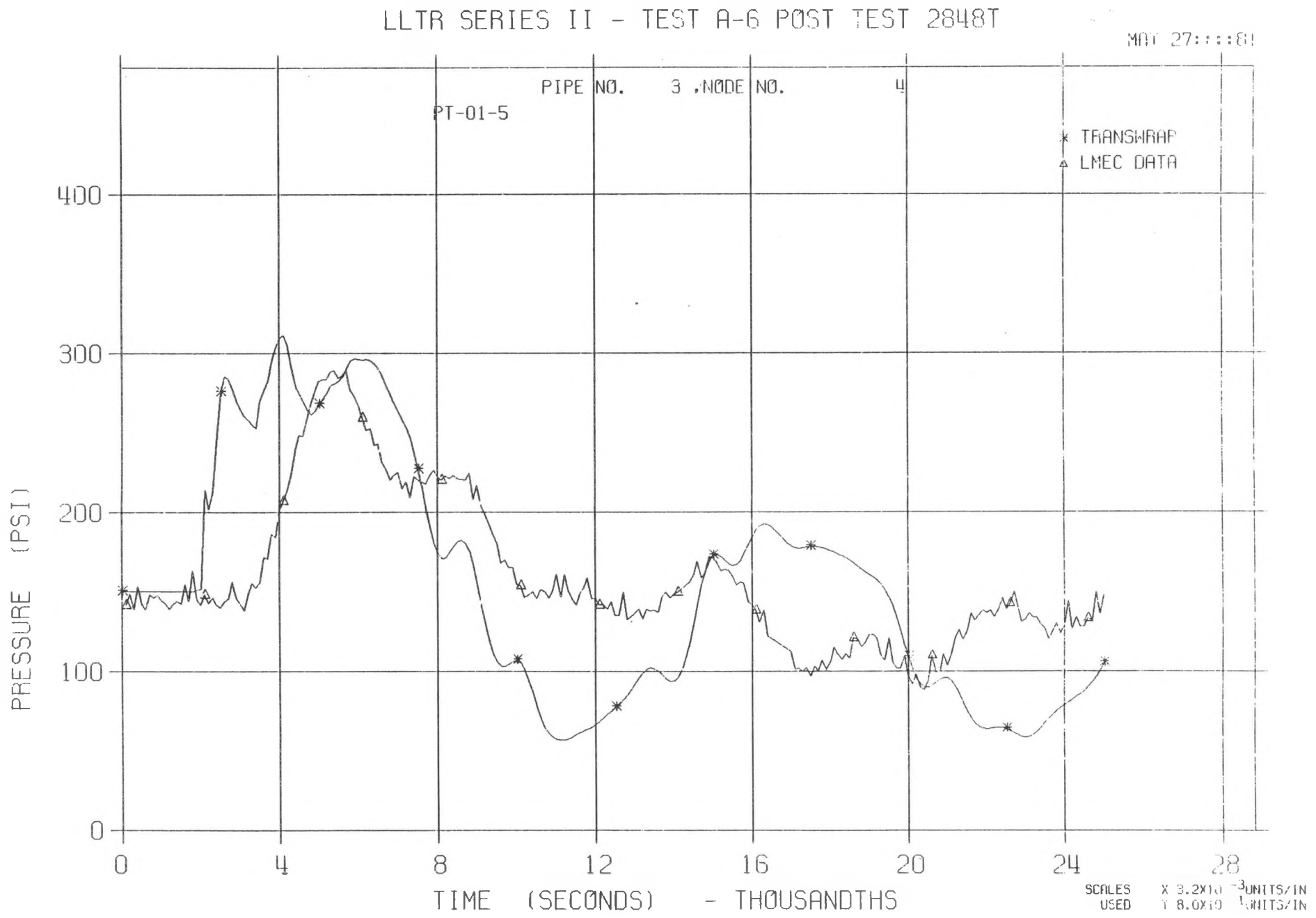
LLTR SERIES II - TEST A-6 POST TEST 2848T
MAY 27::::81
PIPE NO. 3 ,NODE NO. 4
PT-01-5
* TRANSWRAP
Δ LMEC DATA
400
300
200
100
0
PRESSURE (PSI)
0
4
8
12
16
20
24
28
TIME (SECONDS) - THOUSANDTHS
SCALES USED
X 3.2X10 -3 UNITS/IN
Y 8.0X10 1 UNITS/IN

E-7

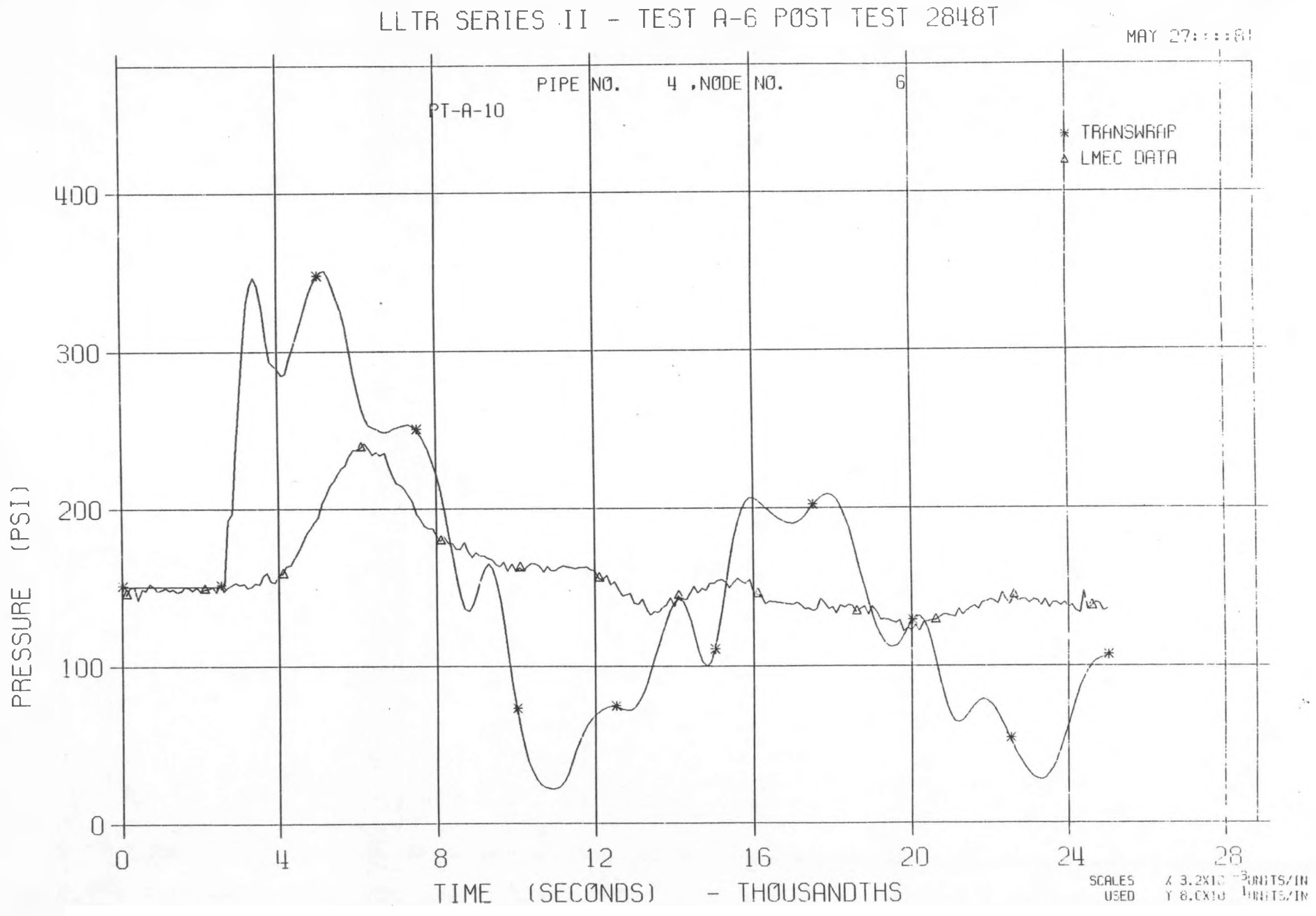
LLTR SERIES II - TEST A-6 POST TEST 2848T
MAY 27::::81
PIPE NO. 4 ,NODE NO. 6
PT-A-10
* TRANSWRAP
Δ LMEC DATA
400
300
200
100
0
PRESSURE (PSI)
0
4
8
12
16
20
24
28
TIME (SECONDS) - THOUSANDTHS
SCALES USED

E-66

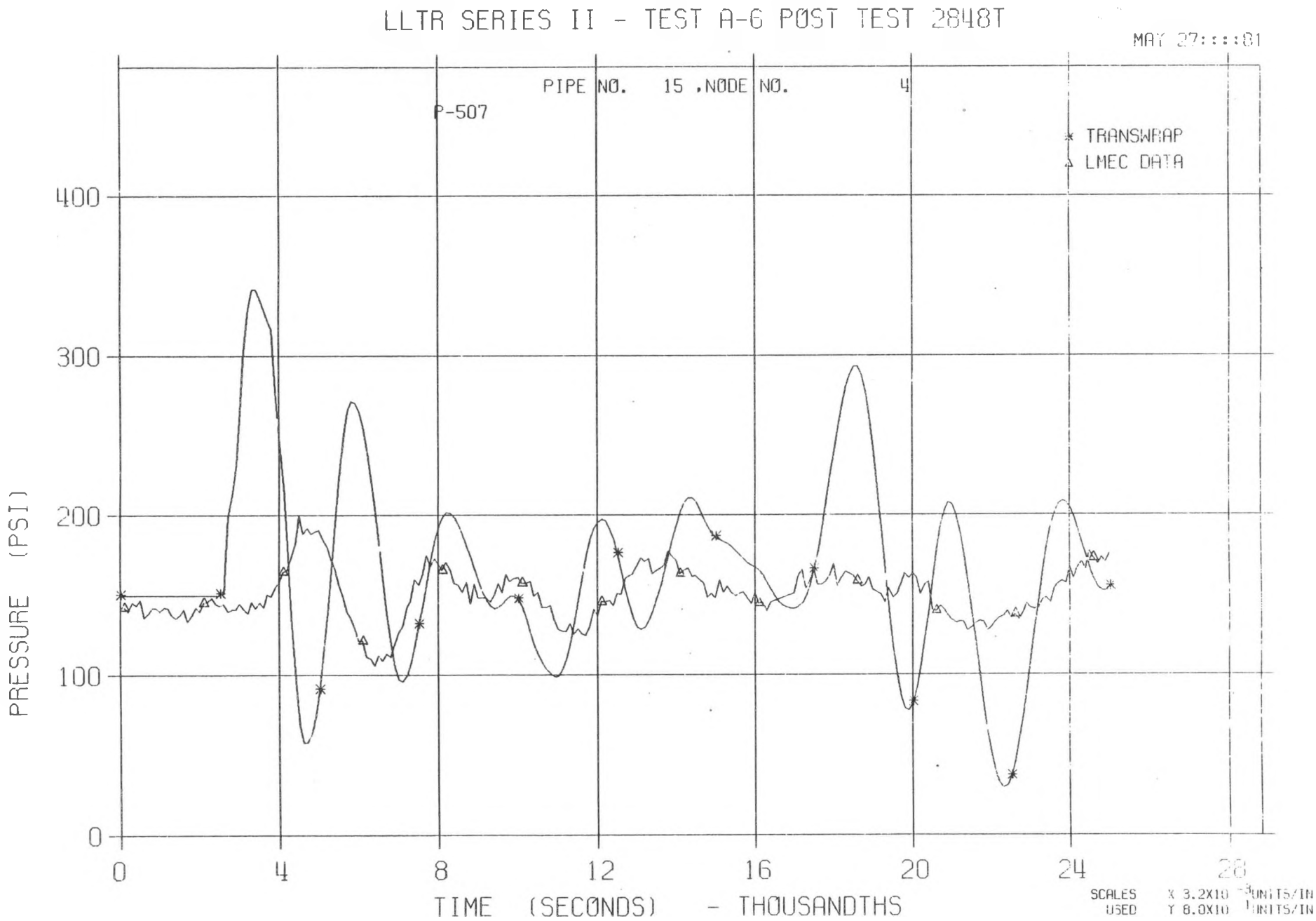
LLTR SERIES II - TEST A-6 POST TEST 2848T
MAY 27::::81
PIPE NO. 15 ,NODE NO. 4
P-507
TRANSWRAP
LMEC DATA
400
300
200
100
0
PRESSURE (PSI)
0
4
8
12
16
20
24
28
TIME (SECONDS) - THOUSANDTHS
SCALES USED
X 3.2X10 -3 UNITS/IN
Y 8.0X10 1 UNITS/IN

E-9

PL 9

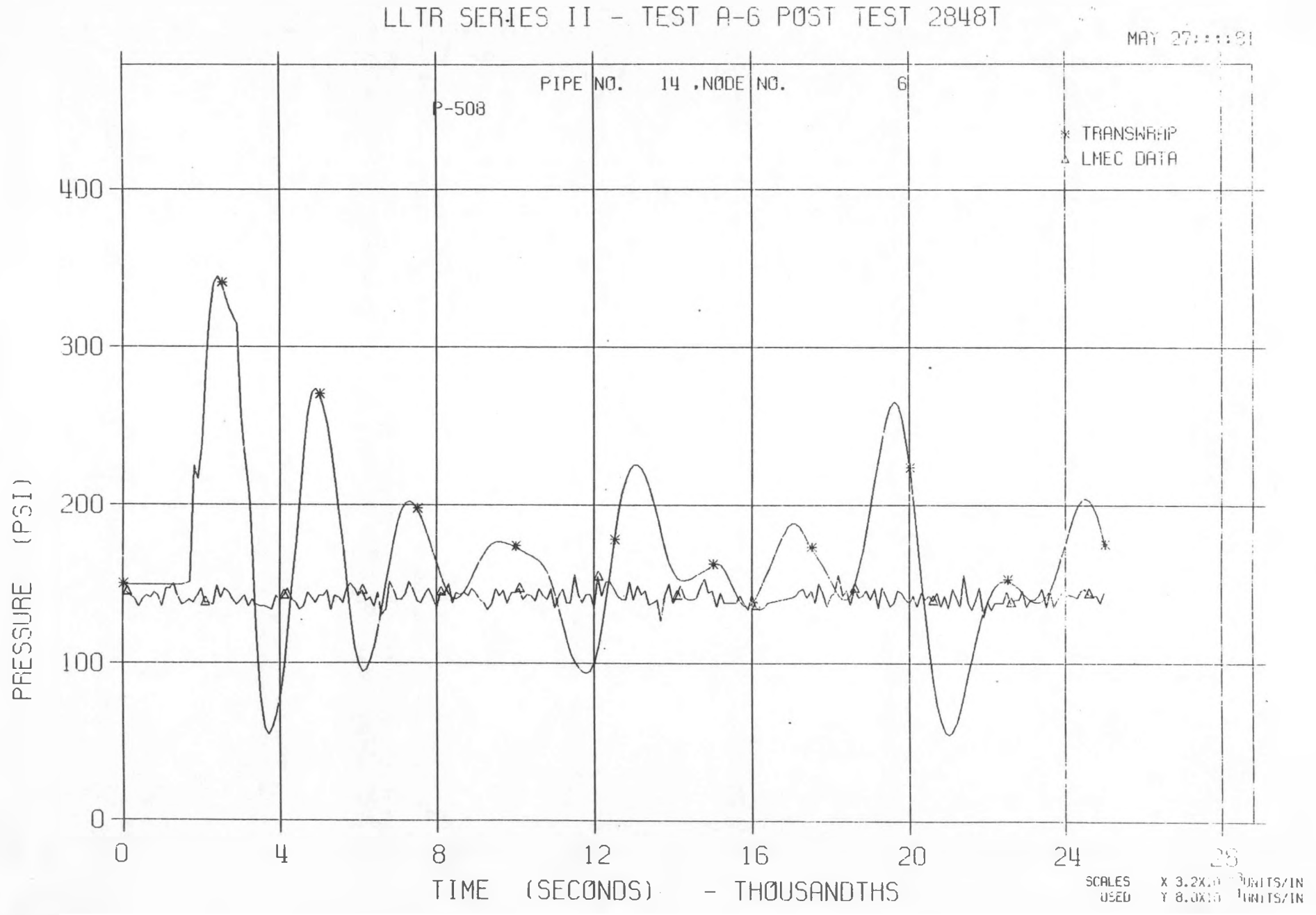
LLTR SERIES II - TEST A-6 POST TEST 2848T
MAY 27
PIPE NO. 14 ,NODE NO. 6
P-508
TRANSWRAP
LMEC DATA
400
300
200
100
0
PRESSURE (PSI)
0
4
8
12
16
20
24
TIME (SECONDS) - THOUSANDTHS
SCALES USED
X 3.2X
Y 8.0X

E-10

PL 10

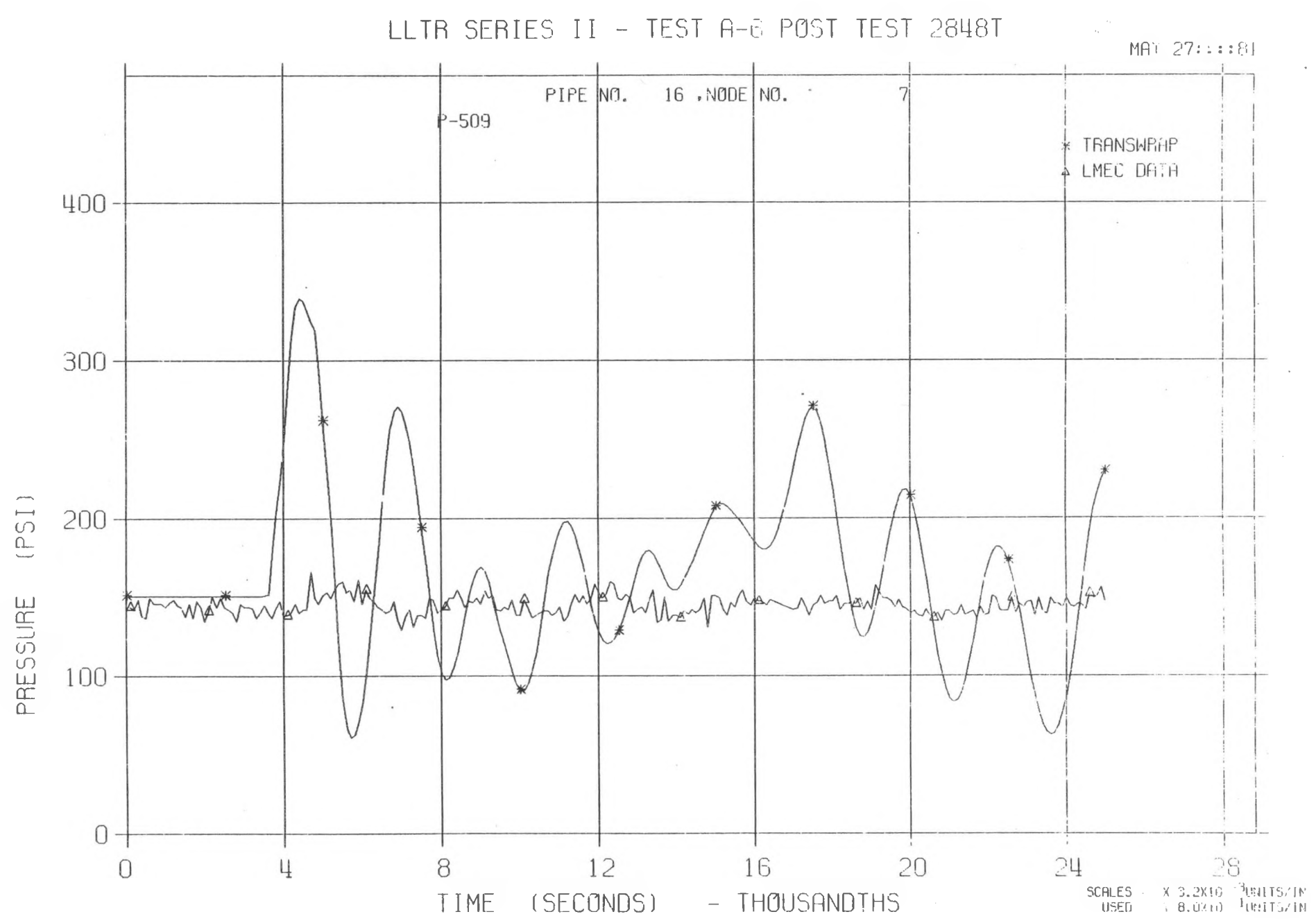
LLTR SERIES II - TEST A-8 POST TEST 2848T
MAY 27::::81
PIPE NO. 16 ,NODE NO. 7
P-509
TRANSWRAP
LMEC DATA
400
300
200
100
0
PRESSURE (PSI)
0
4
8
12
16
20
24
28
TIME (SECONDS) - THOUSANDTHS
SCALES USED
X 3.2X10 UNITS/IN
Y 8.0X10 UNITS/IN

E-11

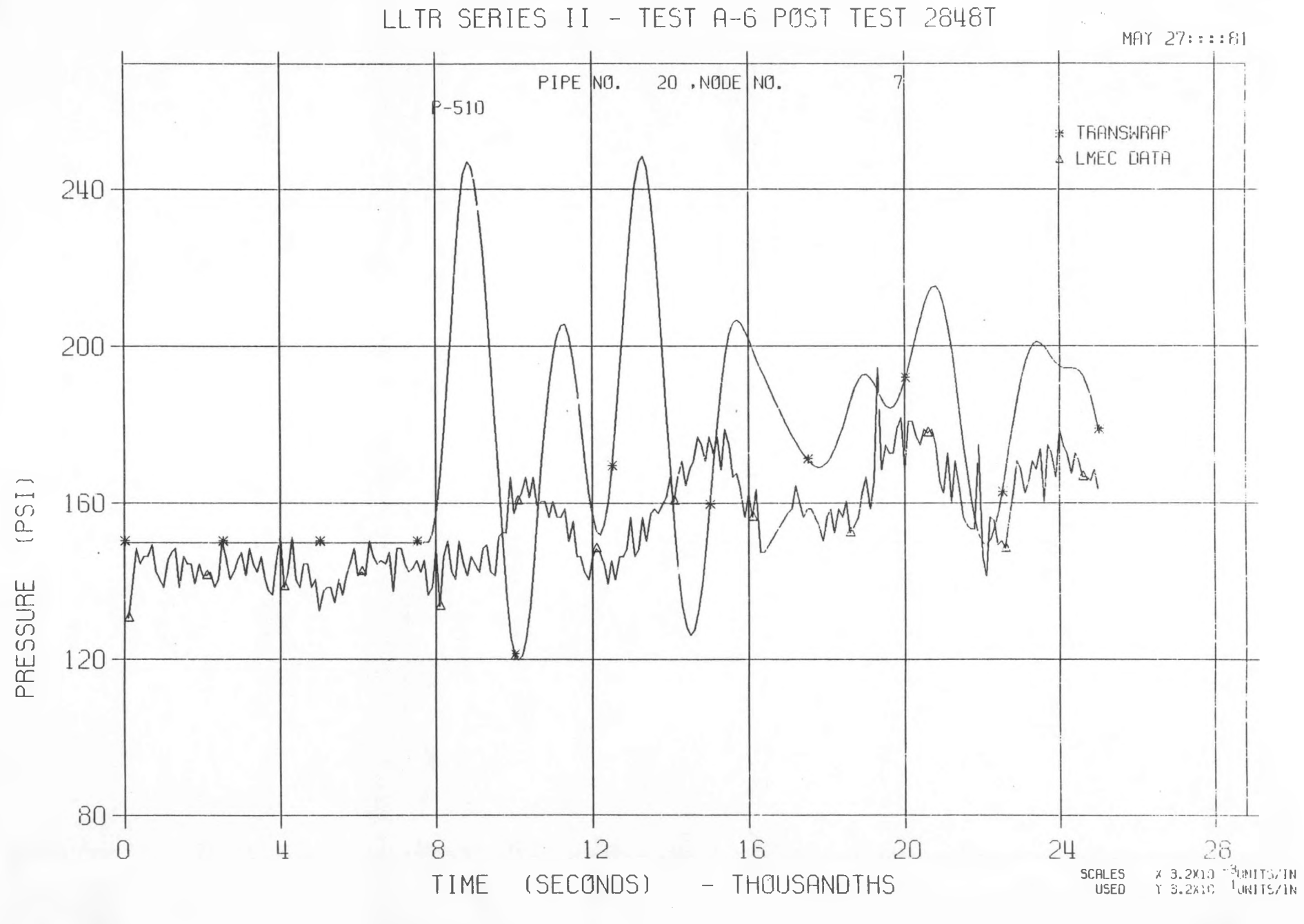
LLTR SERIES II - TEST A-6 POST TEST 2848T
MAY 27::::81
PIPE NO. 20 ,NODE NO. 7
P-510
* TRANSWRAP
Δ LMEC DATA
240
200
160
120
80
PRESSURE (PSI)
0
4
8
12
16
20
24
28
TIME (SECONDS) - THOUSANDTHS
SCALES USED
X 3.2X10 -3 UNITS/IN
Y 5.2X10 1 UNITS/IN

PL 12

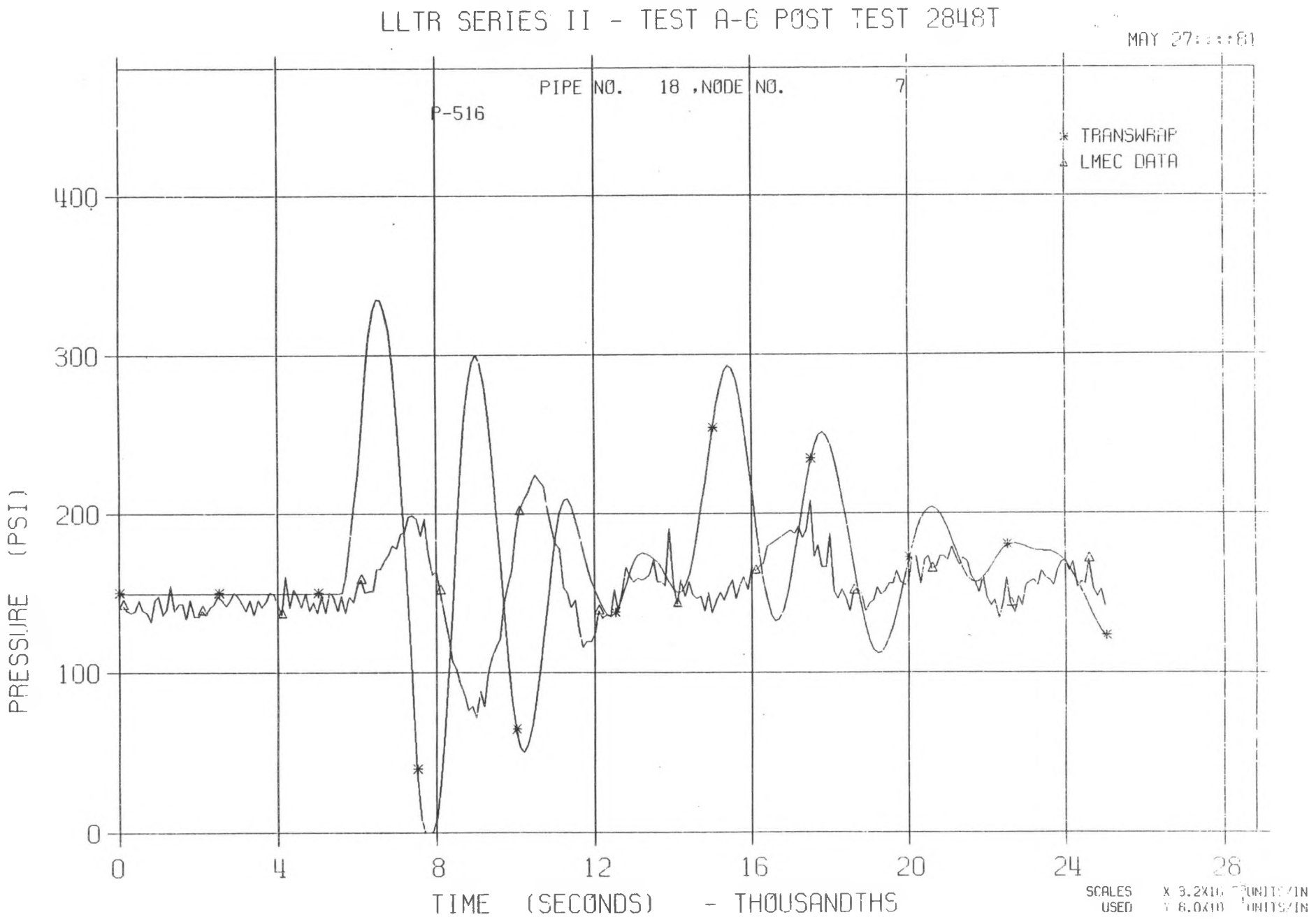
LLTR SERIES II - TEST A-6 POST TEST 2848T
MAY 27
PIPE NO. 18 ,NODE NO. 7
P-516
TRANSWRAP
LMEC DATA
400
300
200
100
0
PRESSURE (PSI)
0
4
8
12
16
20
24
28
TIME (SECONDS) - THOUSANDTHS
SCALES USED

PL 13

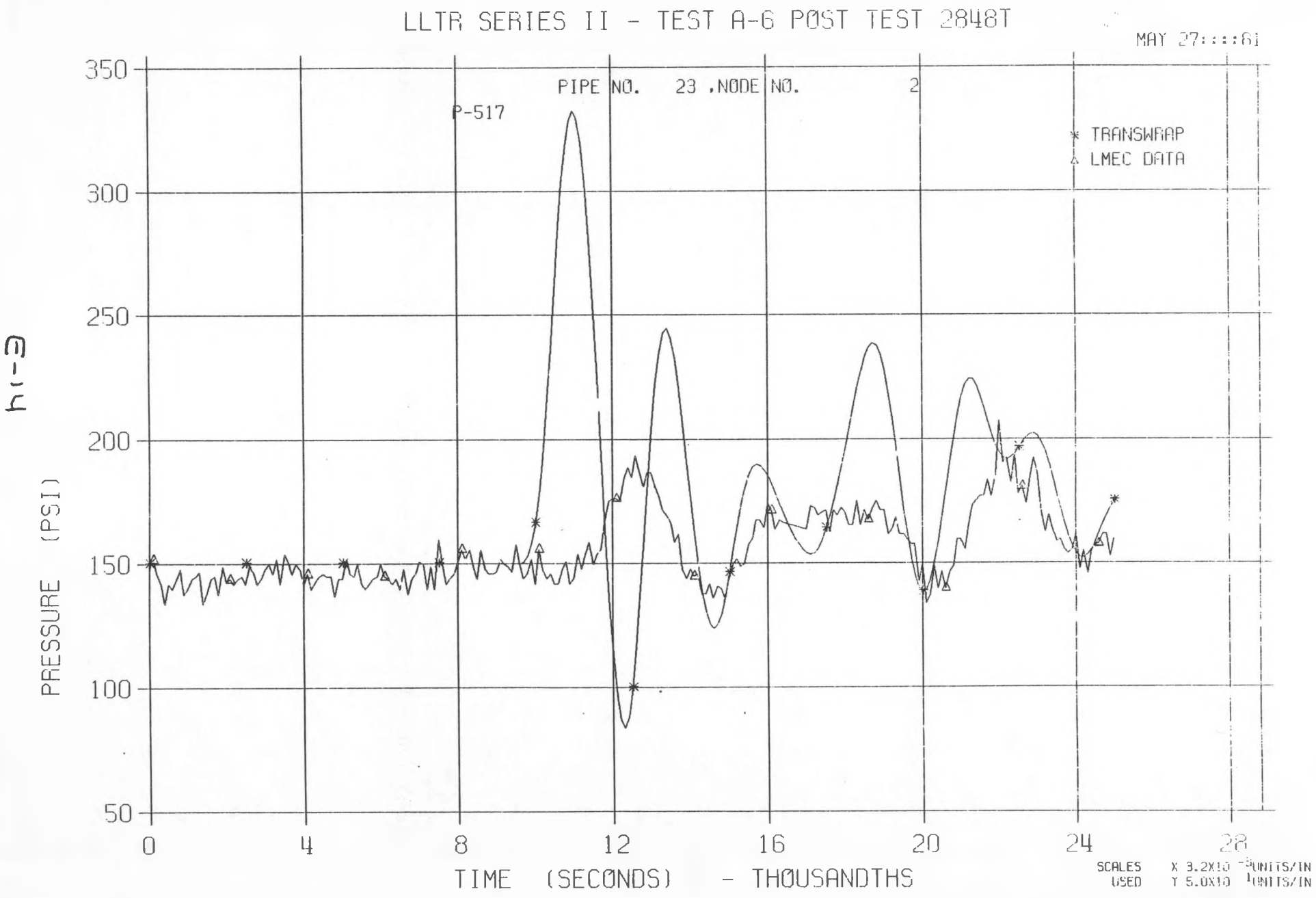
LLTR SERIES II - TEST A-6 POST TEST 2848T
MAY 27::::61
PIPE NO. 23 ,NODE NO. 2
P-517
* TRANSWRAP
Δ LMEC DATA
PRESSURE (PSI)
350
300
250
200
150
100
50
0
4
8
12
16
20
24
28
TIME (SECONDS) - THOUSANDTHS
SCALES USED
X 3.2X10 -3 UNITS/IN
Y 5.0X10 1 UNITS/IN

H-3

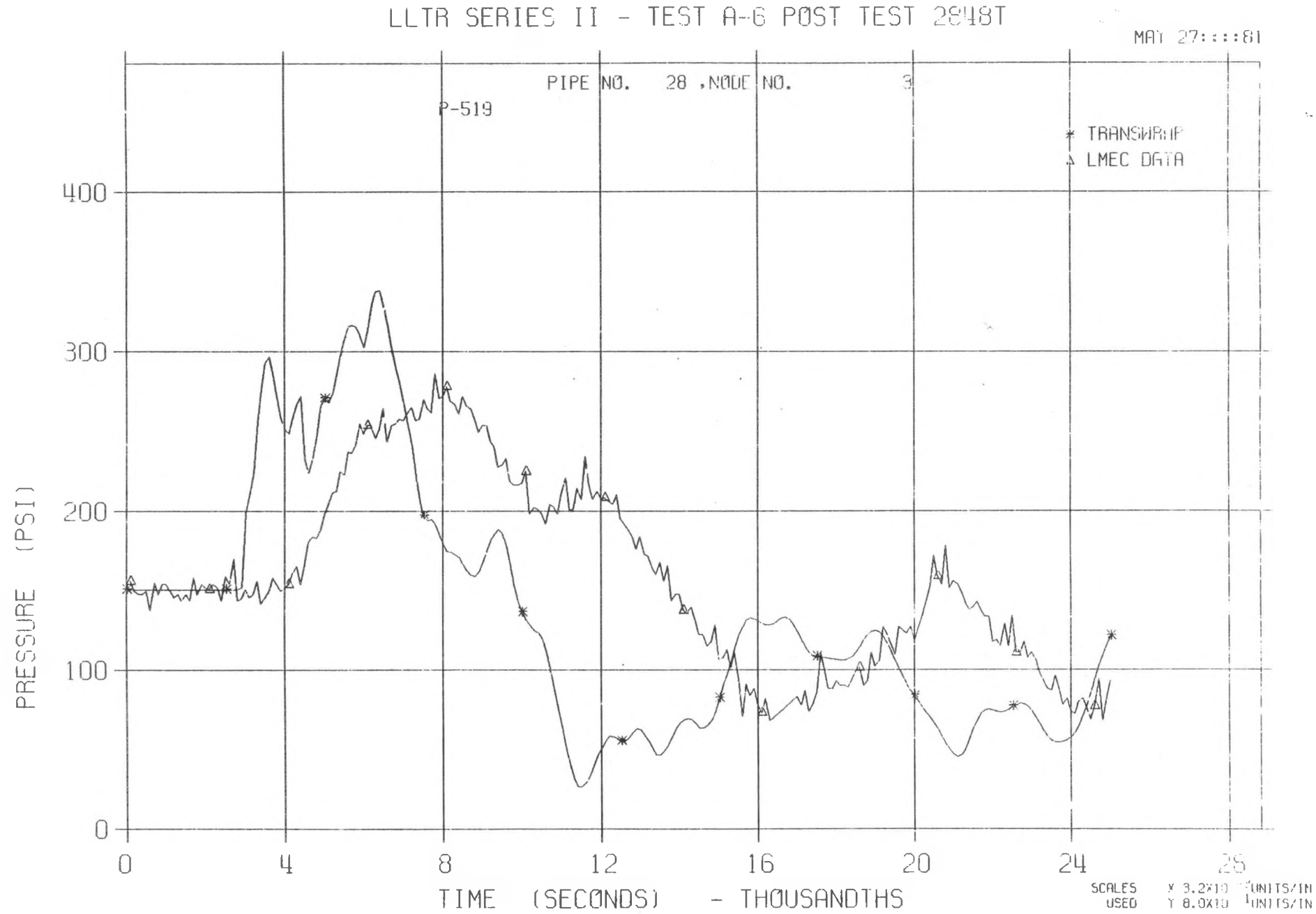
LLTR SERIES II - TEST A-6 POST TEST 2848T
MAY 27::::81
PIPE NO. 28 ,NODE NO. 3
P-519
TRANSWRAP
LMEC DATA
400
300
200
100
0
PRESSURE (PSI)
0
4
8
12
16
20
24
28
TIME (SECONDS) - THOUSANDTHS
SCALES USED
X 3.2X10 UNITS/IN
Y 8.0X10 UNITS/IN

E-15

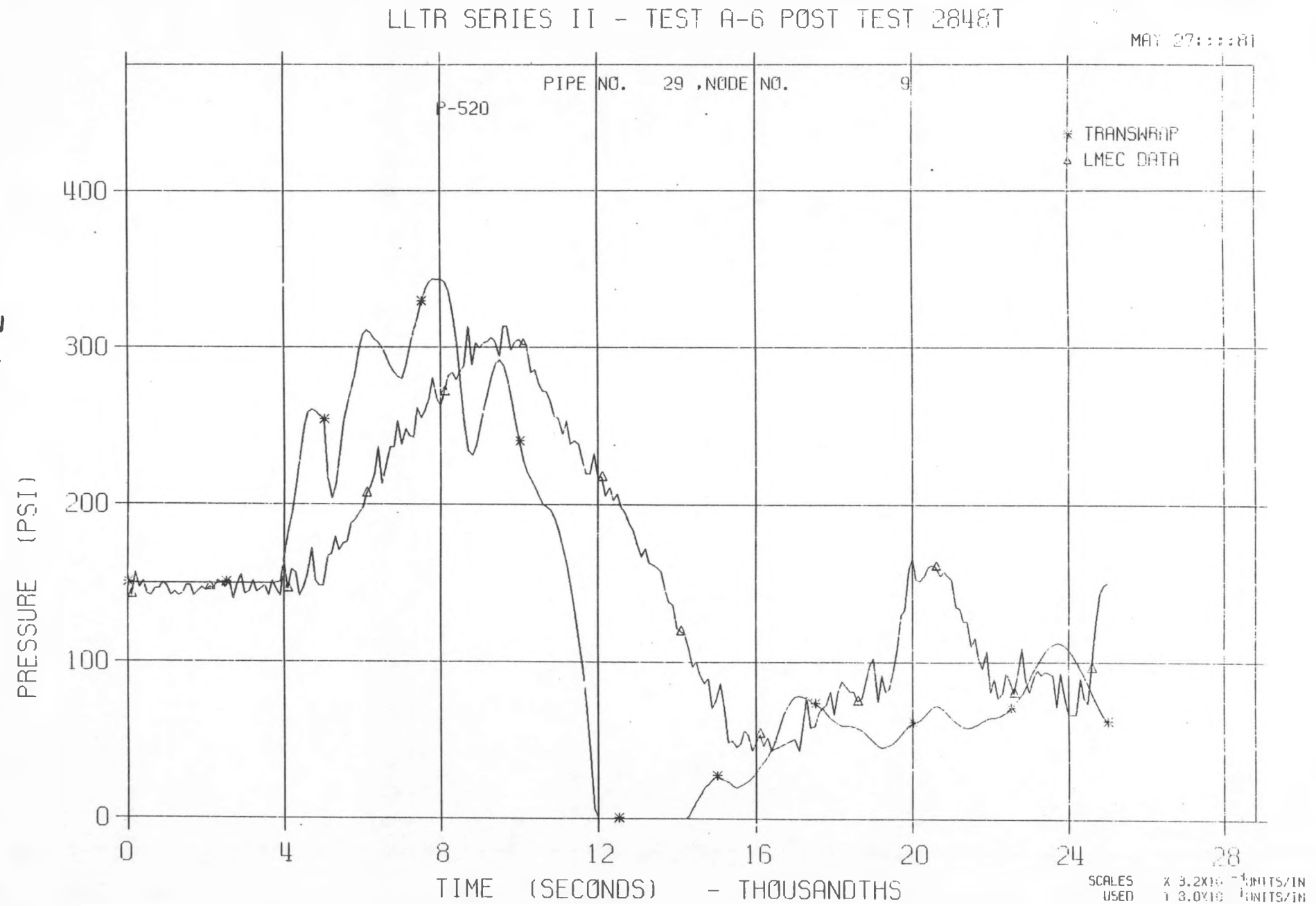
LLTR SERIES II - TEST A-6 POST TEST 2848T
MAY 27:::81
PIPE NO. 29 ,NODE NO. 9
P-520
TRANSWRAP
LMEC DATA
400
300
200
100
0
PRESSURE (PSI)
0
4
8
12
16
20
24
28
TIME (SECONDS) - THOUSANDTHS
SCALES USED
X 3.2X10 UNITS/IN
Y 3.0X10 UNITS/IN

F-16

PL 16

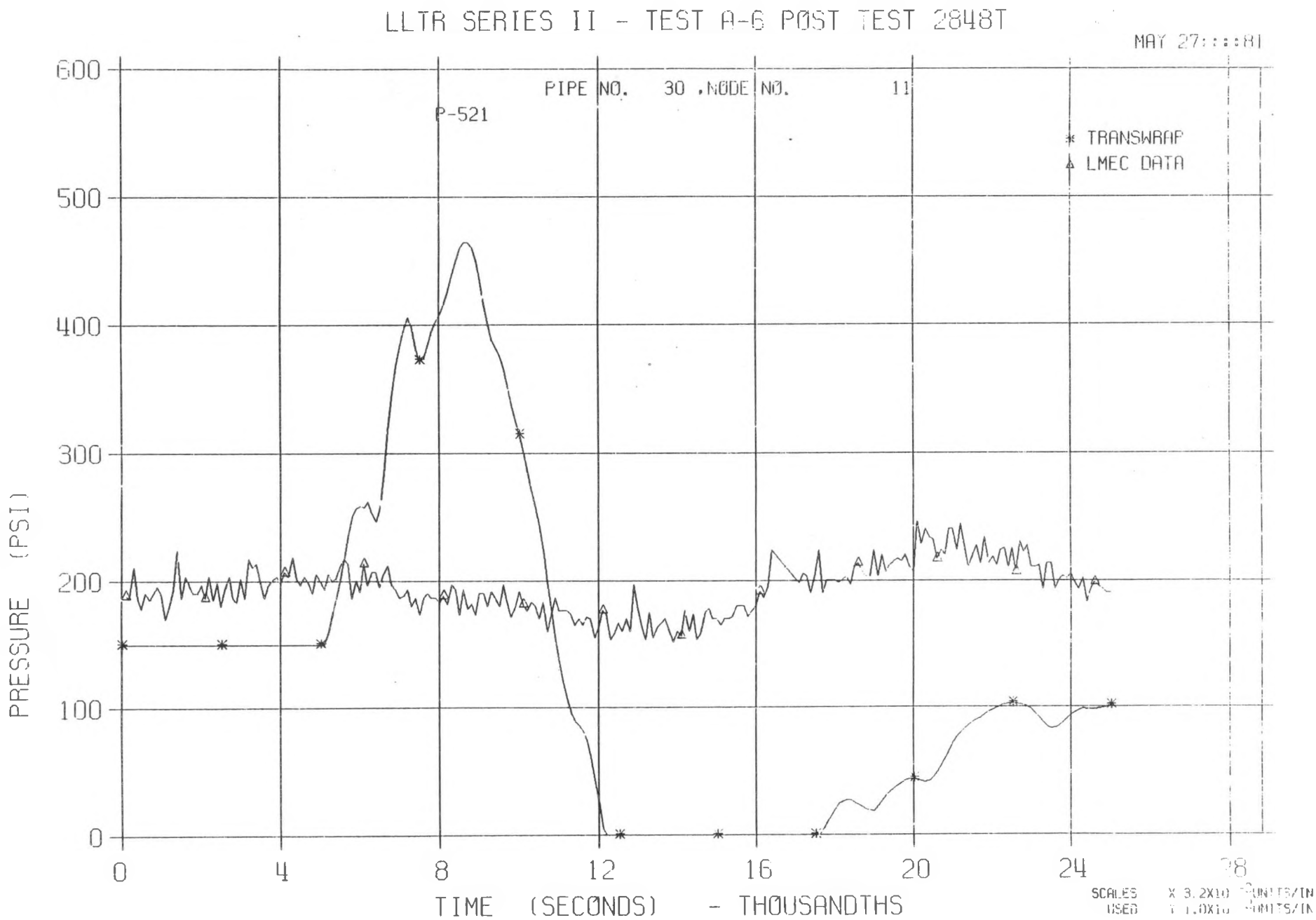
LLTR SERIES II - TEST A-6 POST TEST 2848T
MAY 27::::81
PIPE NO. 30 ,NODE NO. 11
P-521
* TRANSWRAP
Δ LMEC DATA
600
500
400
300
200
100
0
PRESSURE (PSI)
0
4
8
12
16
20
24
28
TIME (SECONDS) - THOUSANDTHS
SCALES USED
X 3.2X10
Y 1.0X10

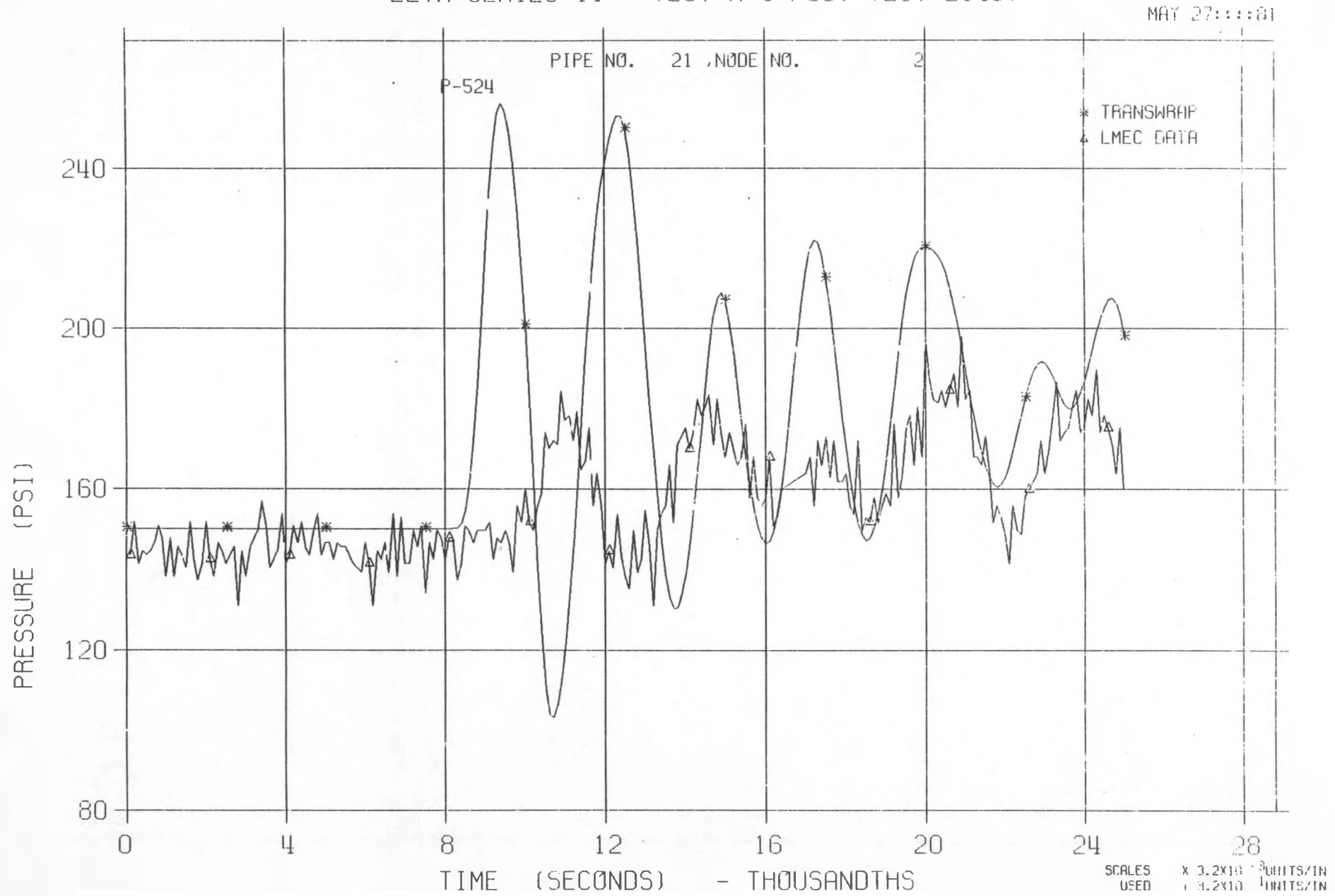
LLTR SERIES II - TEST A-6 POST TEST 2848T
MAY 27::::81
PIPE NO. 21 ,NODE NO. 2
P-524
* TRANSWRAP
Δ LMEC DATA
240
200
160
120
80
PRESSURE (PSI)
0
4
8
12
16
20
24
28
TIME (SECONDS) - THOUSANDTHS
SCALES USED
X 3.2X10 UNITS/IN
Y 3.2X10 UNITS/IN

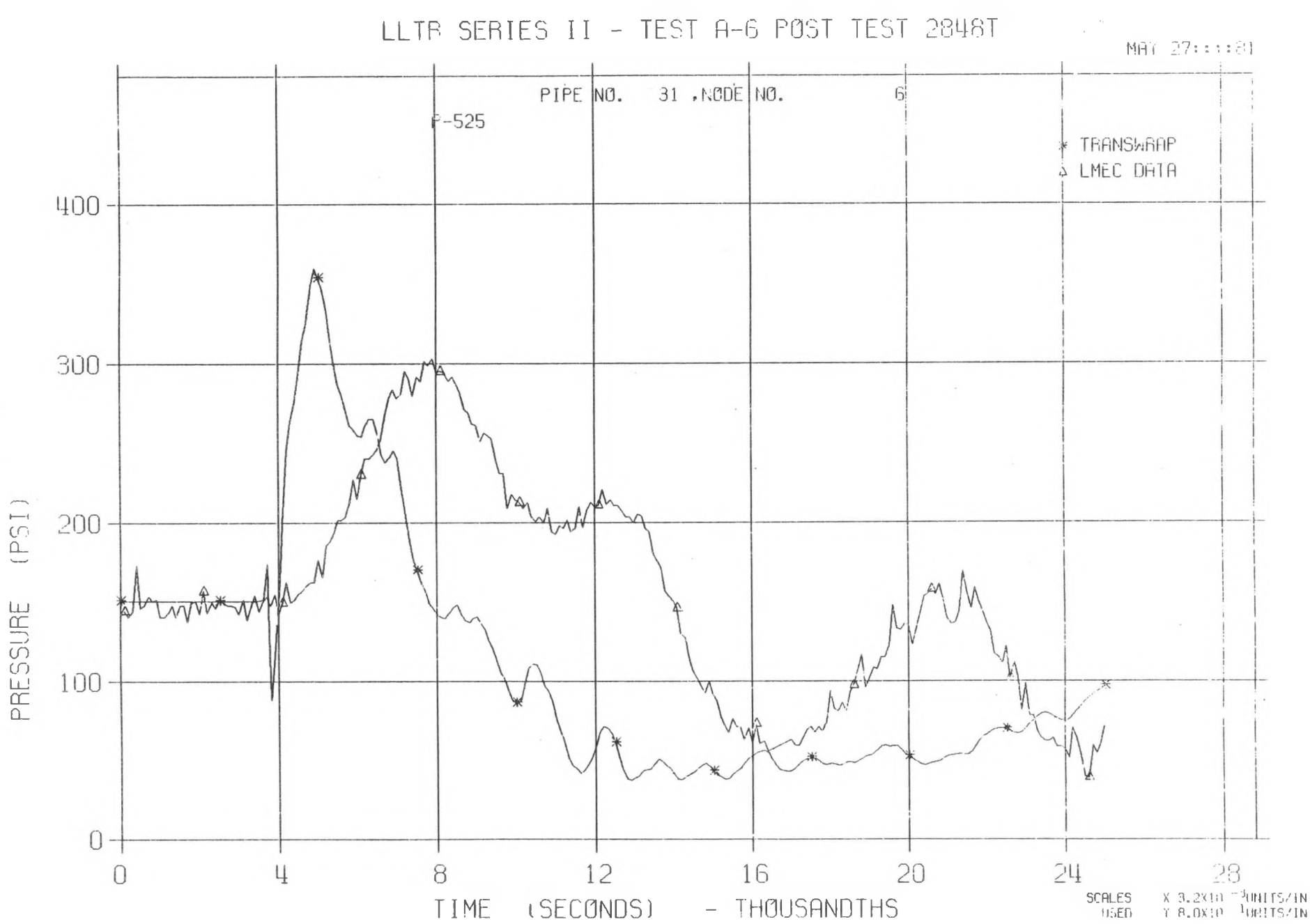
LLTR SERIES II - TEST A-6 POST TEST 2848T
MAY 27::::81
PIPE NO. 31 ,NODE NO. 6
P-525
* TRANSWRAP
Δ LMEC DATA
400
300
200
100
0
PRESSURE (PSI)
0
4
8
12
16
20
24
28
TIME (SECONDS) - THOUSANDTHS
SCALES USED
X 3.2X10 -3 UNITS/IN
Y 8.0X10 1 UNITS/IN

PL 19

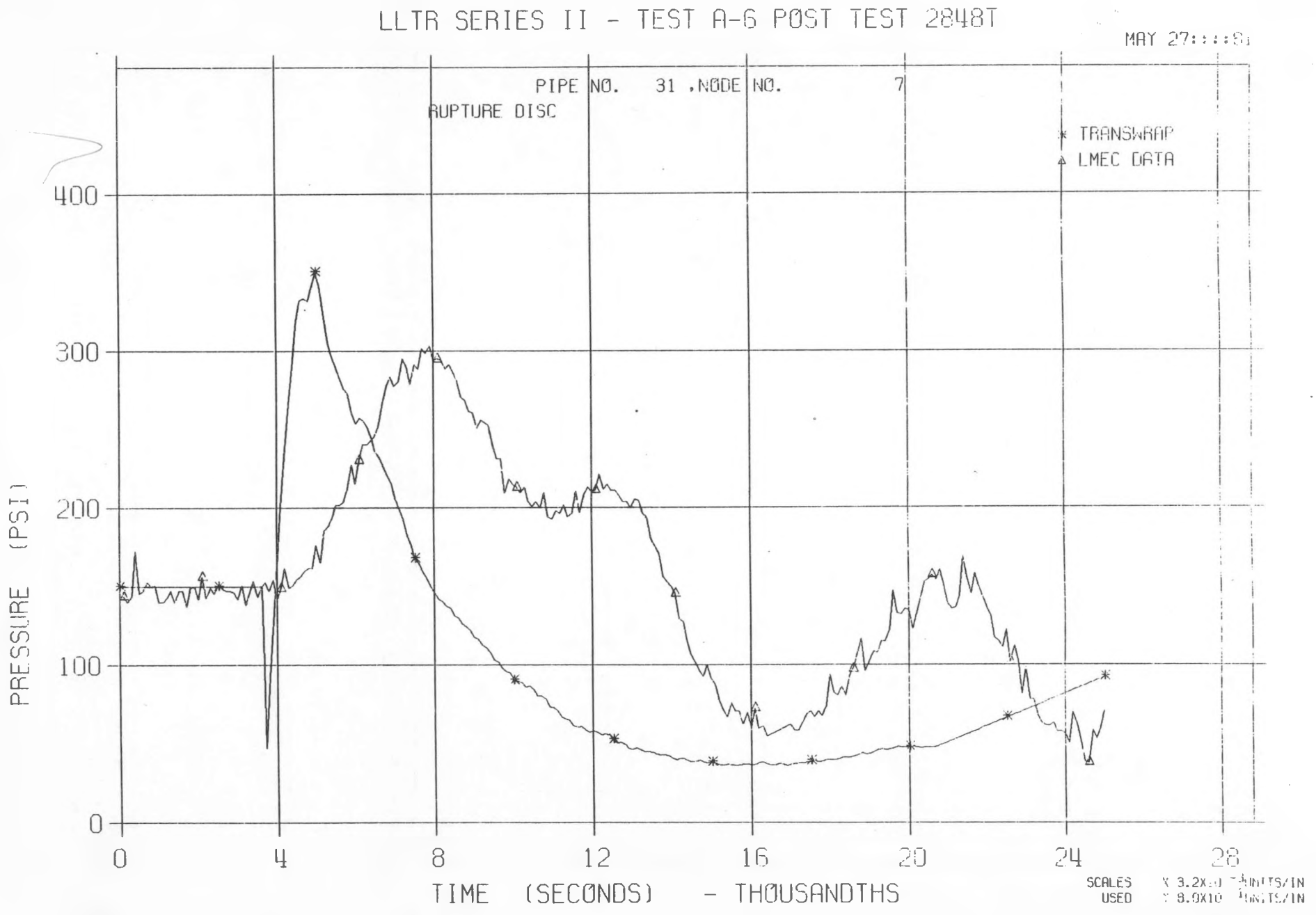
LLTR SERIES II - TEST A-6 POST TEST 2848T
MAY 27
PIPE NO. 31 ,NODE NO. 7
RUPTURE DISC
TRANSWRAP
LMEC DATA
400
300
200
100
0
PRESSURE (PSI)
0
4
8
12
16
20
24
28
TIME (SECONDS) - THOUSANDTHS
SCALES USED

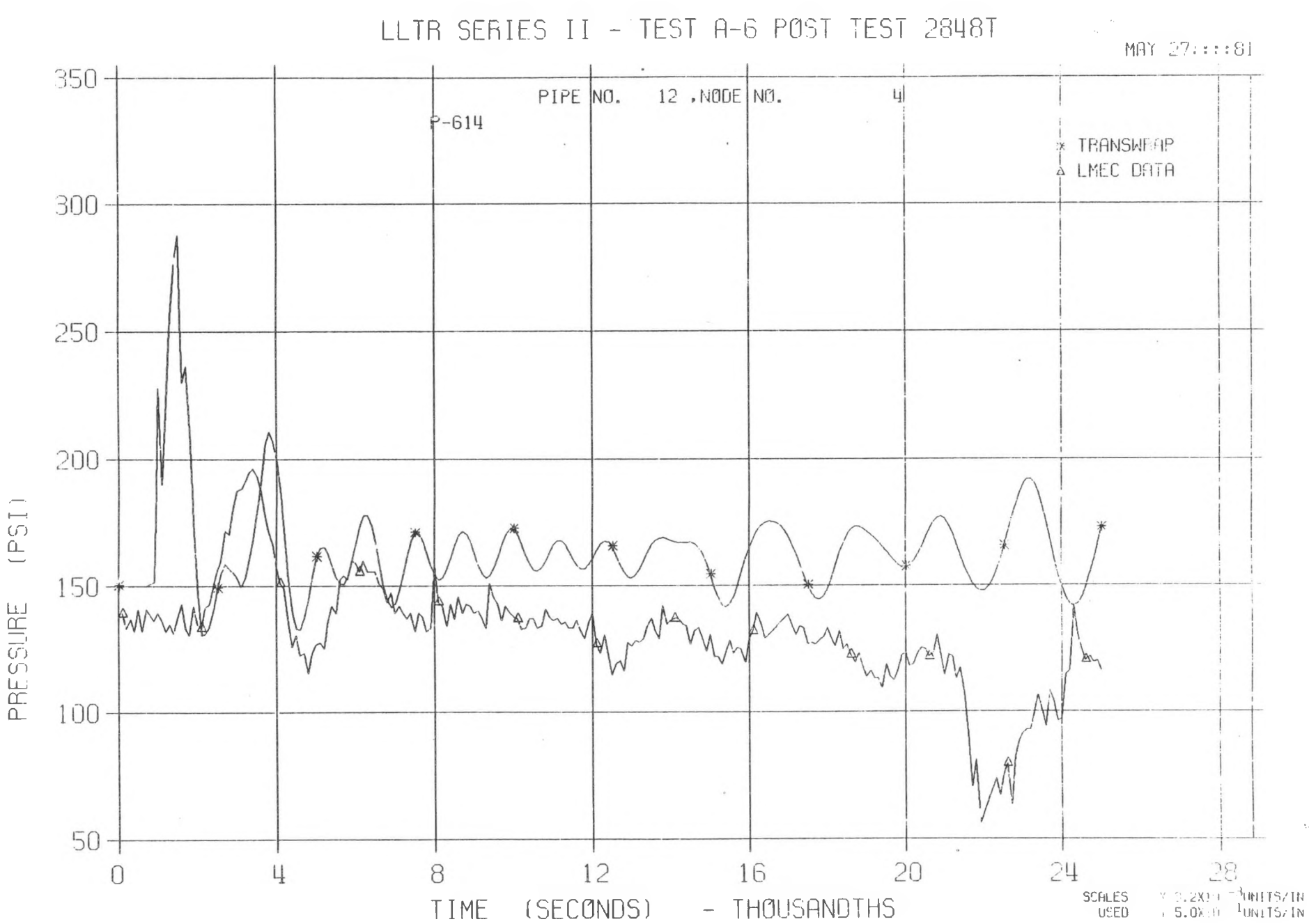
LLTR SERIES II - TEST A-6 POST TEST 2848T
MAY 27::::81
PIPE NO. 12 ,NODE NO. 4
P-614
* TRANSWRAP
Δ LMEC DATA
PRESSURE (PSI)
350
300
250
200
150
100
50
0
4
8
12
16
20
24
28
TIME (SECONDS) - THOUSANDTHS
SCALES USED
UNITS/IN
UNITS/IN

E-21

PL 21

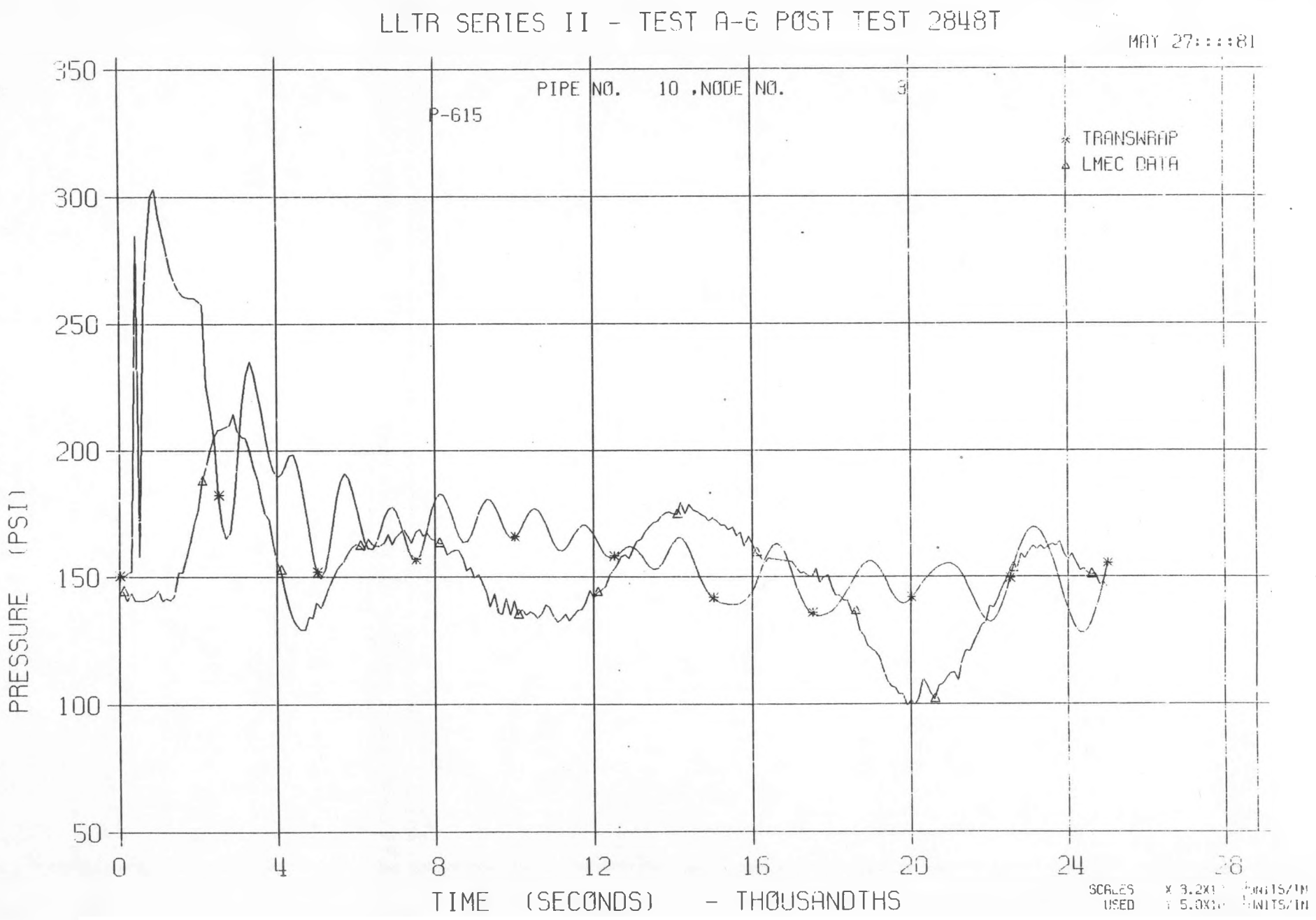
LLTR SERIES II - TEST A-6 POST TEST 2848T
MAY 27::::81
PIPE NO. 10 .NODE NO. 3
P-615
* TRANSWRAP
Δ LMEC DATA
PRESSURE (PSI)
350
300
250
200
150
100
50
0
4
8
12
16
20
24
28
TIME (SECONDS) - THOUSANDTHS
SCALES USED
X 3.2X1 UNITS/IN
Y 5.0X1 UNITS/IN

E-22

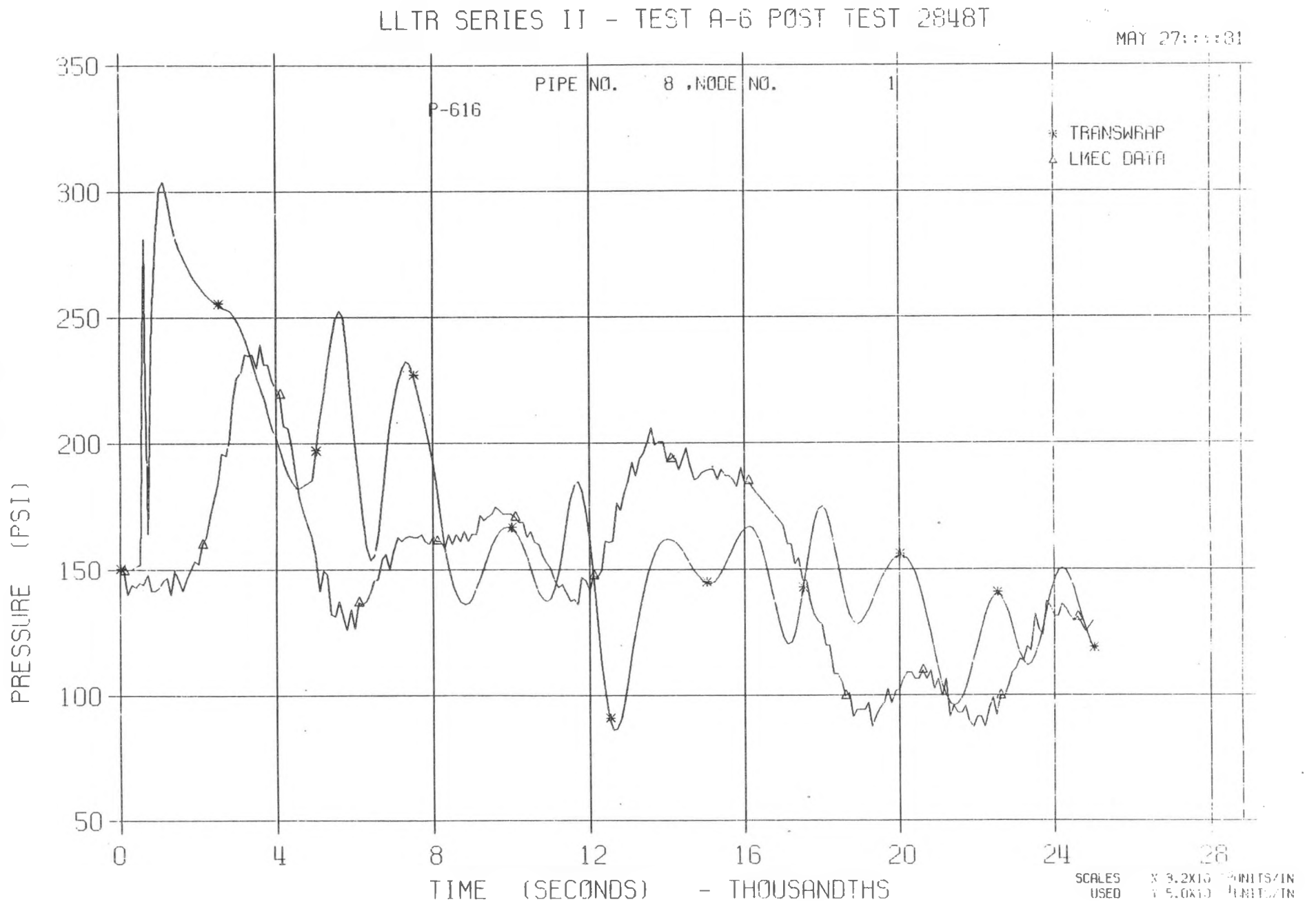
LLTR SERIES II - TEST A-6 POST TEST 2848T
MAY 27
PIPE NO. 8 ,NODE NO. 1
P-616
TRANSWRAP
LMEC DATA
350
300
250
200
150
100
50
PRESSURE (PSI)
0
4
8
12
16
20
24
28
TIME (SECONDS) - THOUSANDTHS
SCALES USED

E-23

PL 23

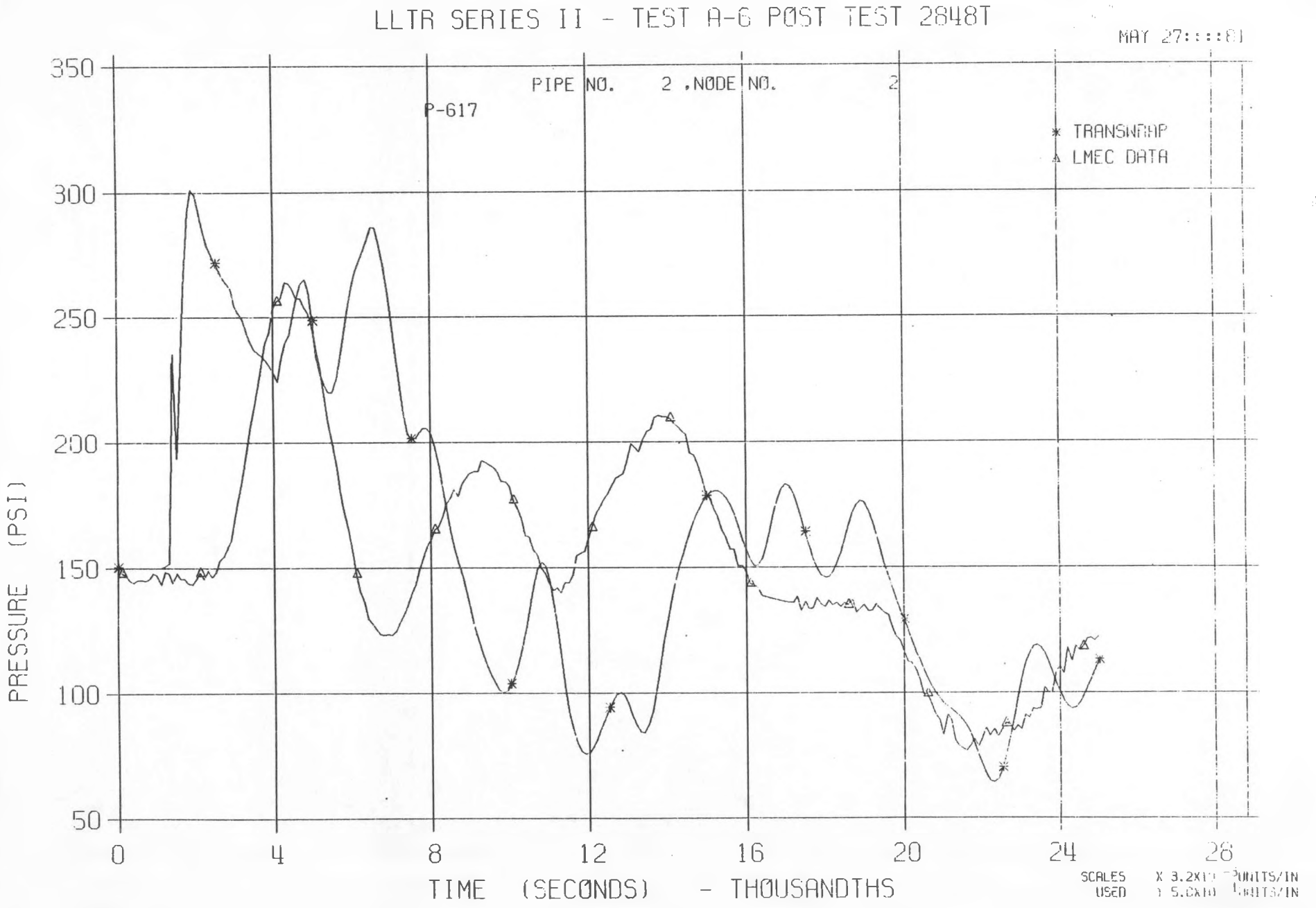
LLTR SERIES II - TEST A-6 POST TEST 2848T
MAY 27::::81
PIPE NO. 2 ,NODE NO. 2
P-617
* TRANSWRAP
Δ LMEC DATA
350
300
250
200
150
100
50
PRESSURE (PSI)
0
4
8
12
16
20
24
28
TIME (SECONDS) - THOUSANDTHS
SCALES USED
X 3.2X10 -2 UNITS/IN
Y 5.0X10 1 UNITS/IN

E-24

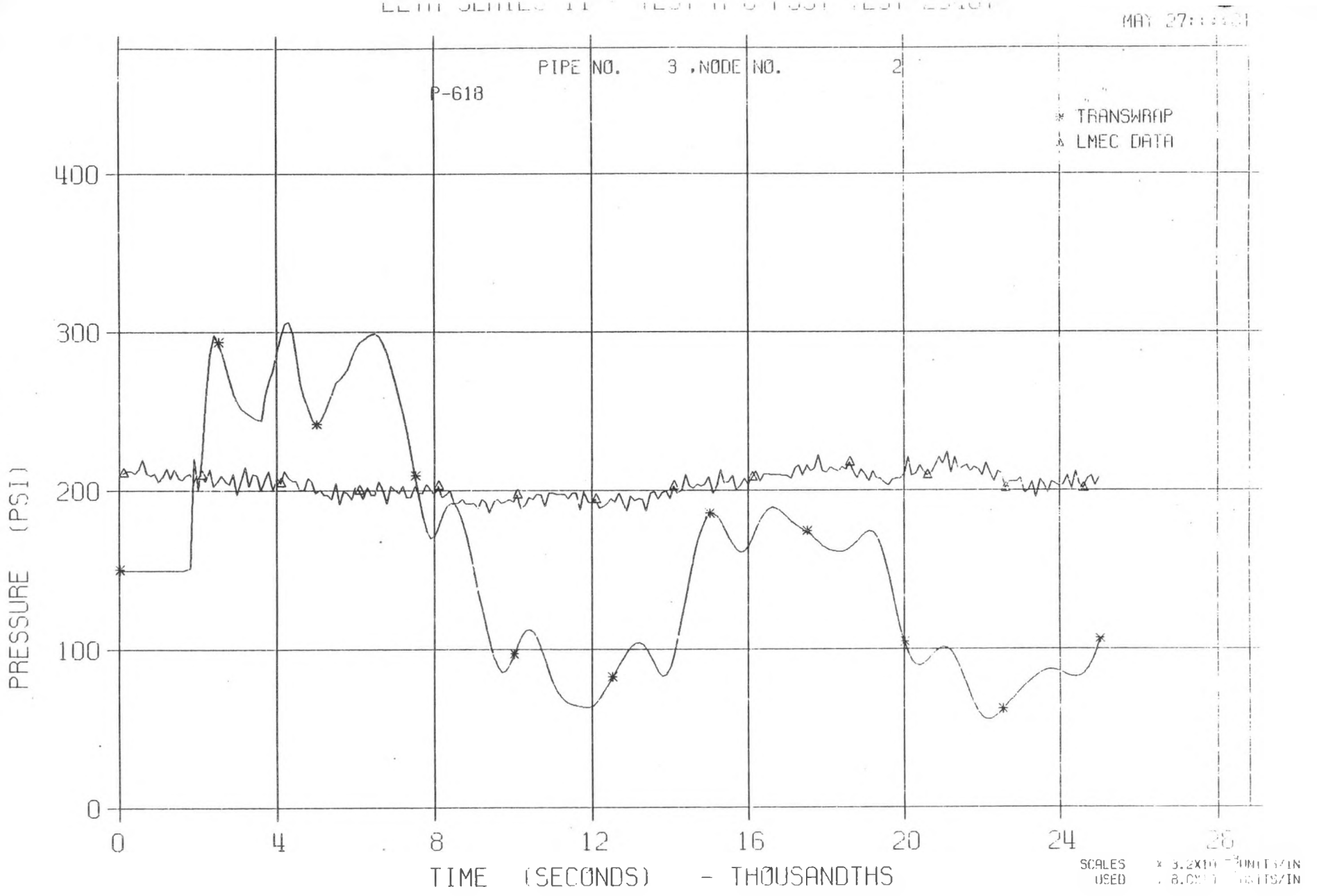

PL 25

TIME (SECONDS) - THOUSANDTHS

PL 25

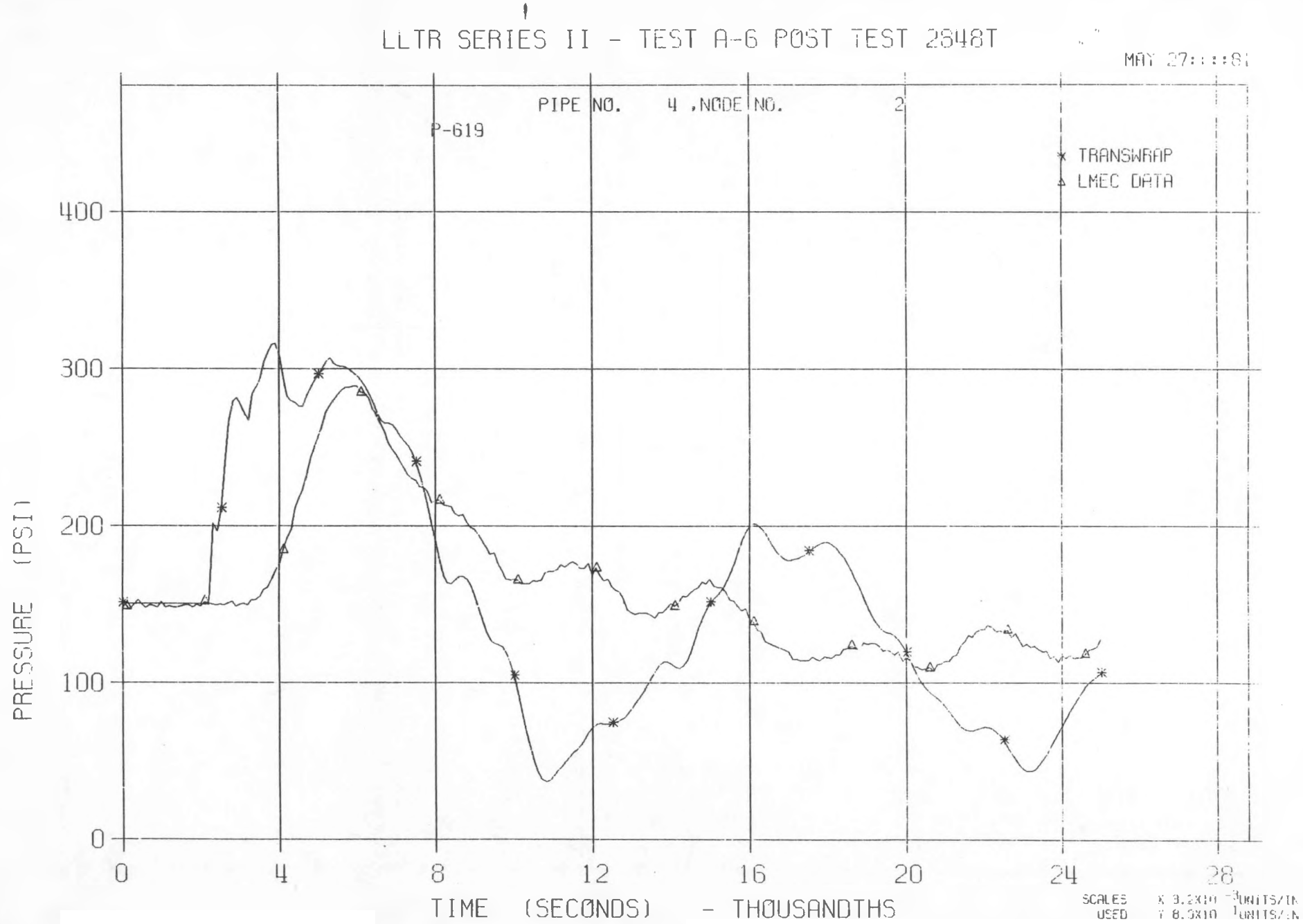
LLTR SERIES II - TEST A-6 POST TEST 2648T
MAY 27
PIPE NO. 4 ,NODE NO. 2
P-619
TRANSWRAP
LMEC DATA
400
300
200
100
0
PRESSURE (PSI)
0
4
8
12
16
20
24
28
TIME (SECONDS) - THOUSANDTHS
SCALES USED

E-26

PL 25

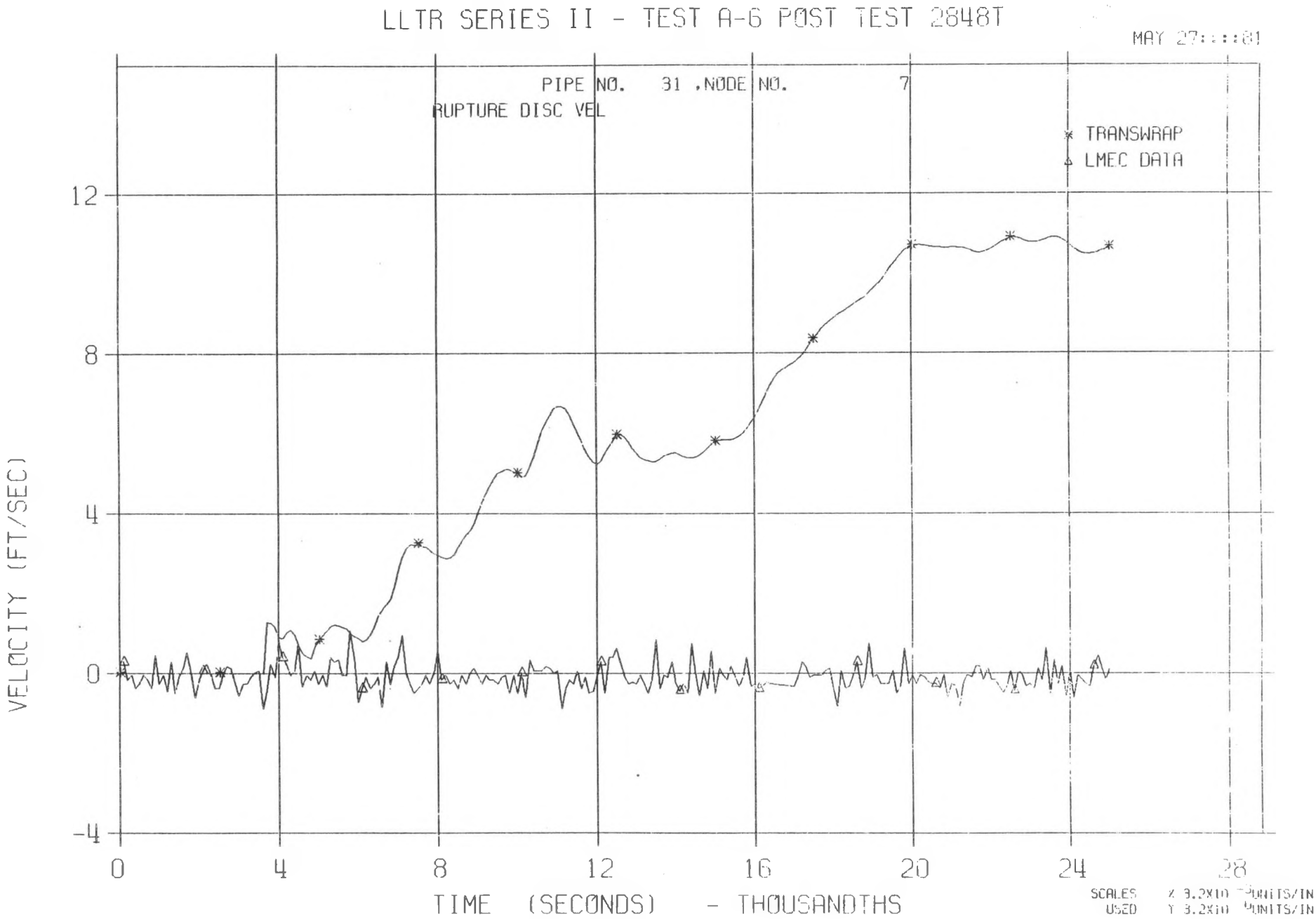
LLTR SERIES II - TEST A-6 POST TEST 2848T
MAY 27::::81
PIPE NO. 31 ,NODE NO. 7
RUPTURE DISC VEL
TRANSWRAP
LMEC DATA
12
8
4
0
-4
VELOCITY (FT/SEC)
0
4
8
12
16
20
24
28
TIME (SECONDS) - THOUSANDTHS
SCALES USED
X 3.2X10 -3UNITS/IN
Y 3.2X10 0UNITS/IN

E-27

PL 28

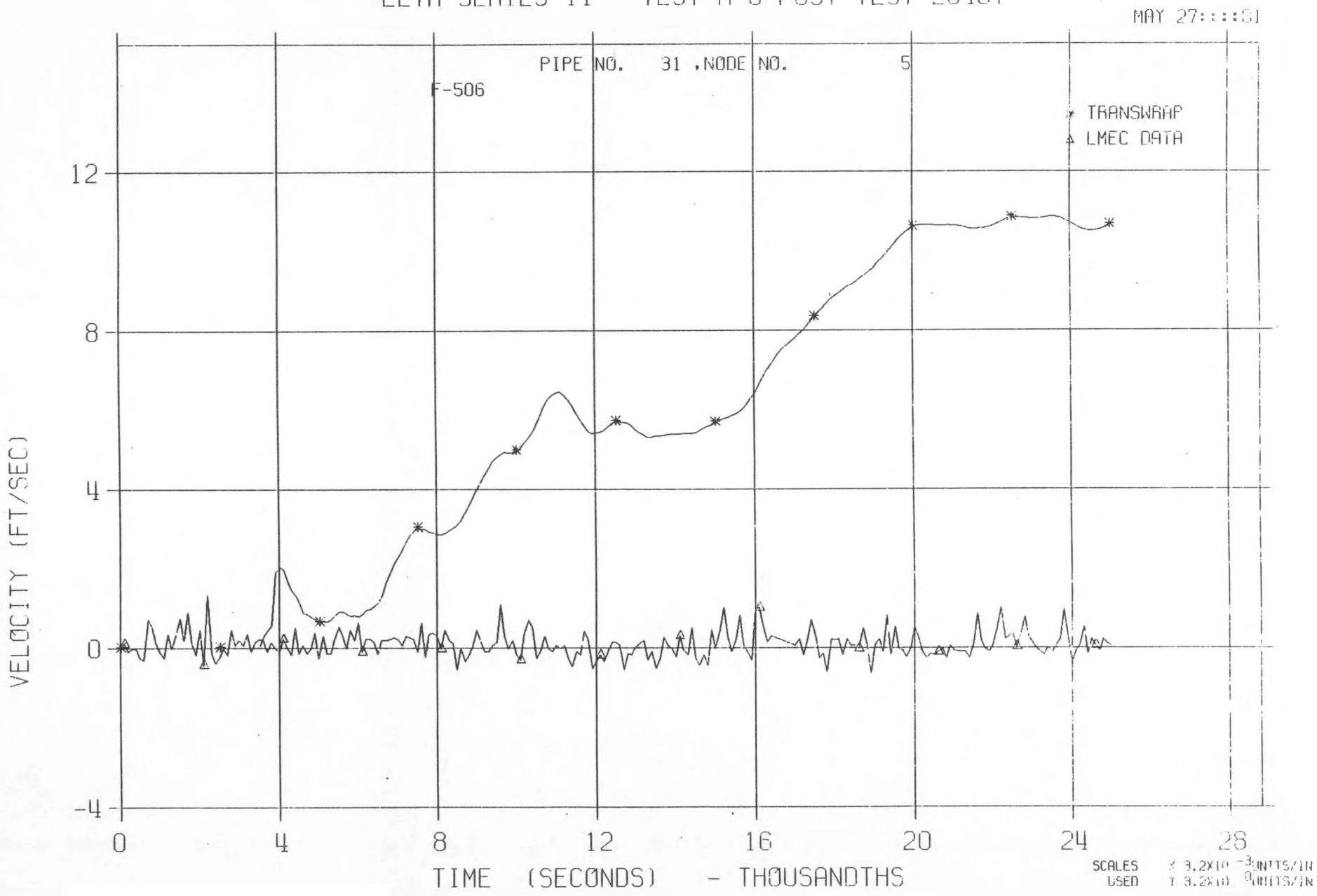
LLTR SERIES II - TEST A-6 POST TEST 2848T
MAY 27::::81
PIPE NO. 31 ,NODE NO. 5
F-506
TRANSWRAP
LMEC DATA
12
8
4
0
-4
VELOCITY (FT/SEC)
0
4
8
12
16
20
24
28
TIME (SECONDS) - THOUSANDTHS
SCALES USED

E-28

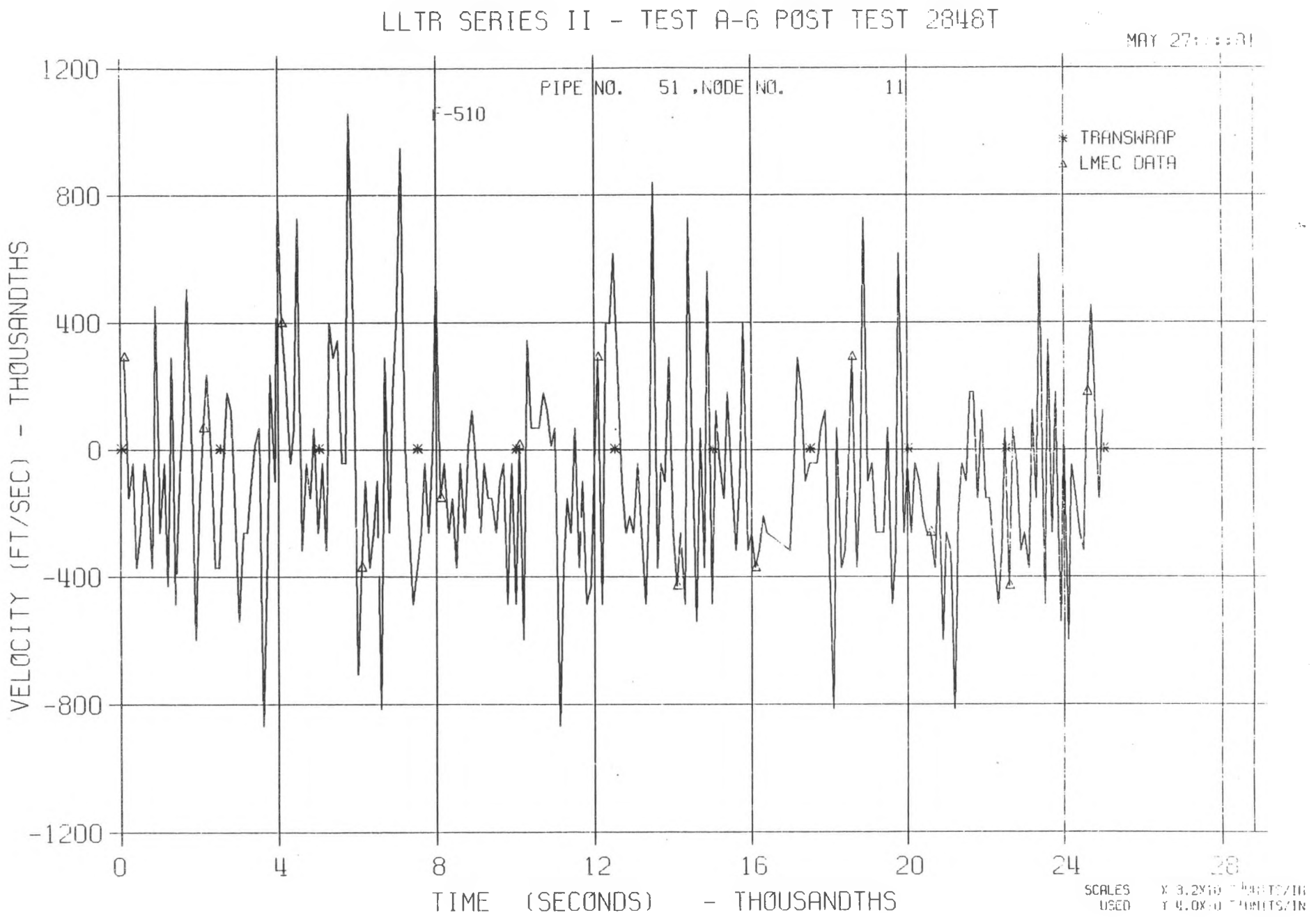
LLTR SERIES II - TEST A-6 POST TEST 2848T
MAY 27
PIPE NO. 51 ,NODE NO. 11
F-510
* TRANSWRAP
Δ LMEC DATA
1200
800
400
0
-400
-800
-1200
VELOCITY (FT/SEC) - THOUSANDTHS
0
4
8
12
16
20
24
28
TIME (SECONDS) - THOUSANDTHS
SCALES USED

PL 30

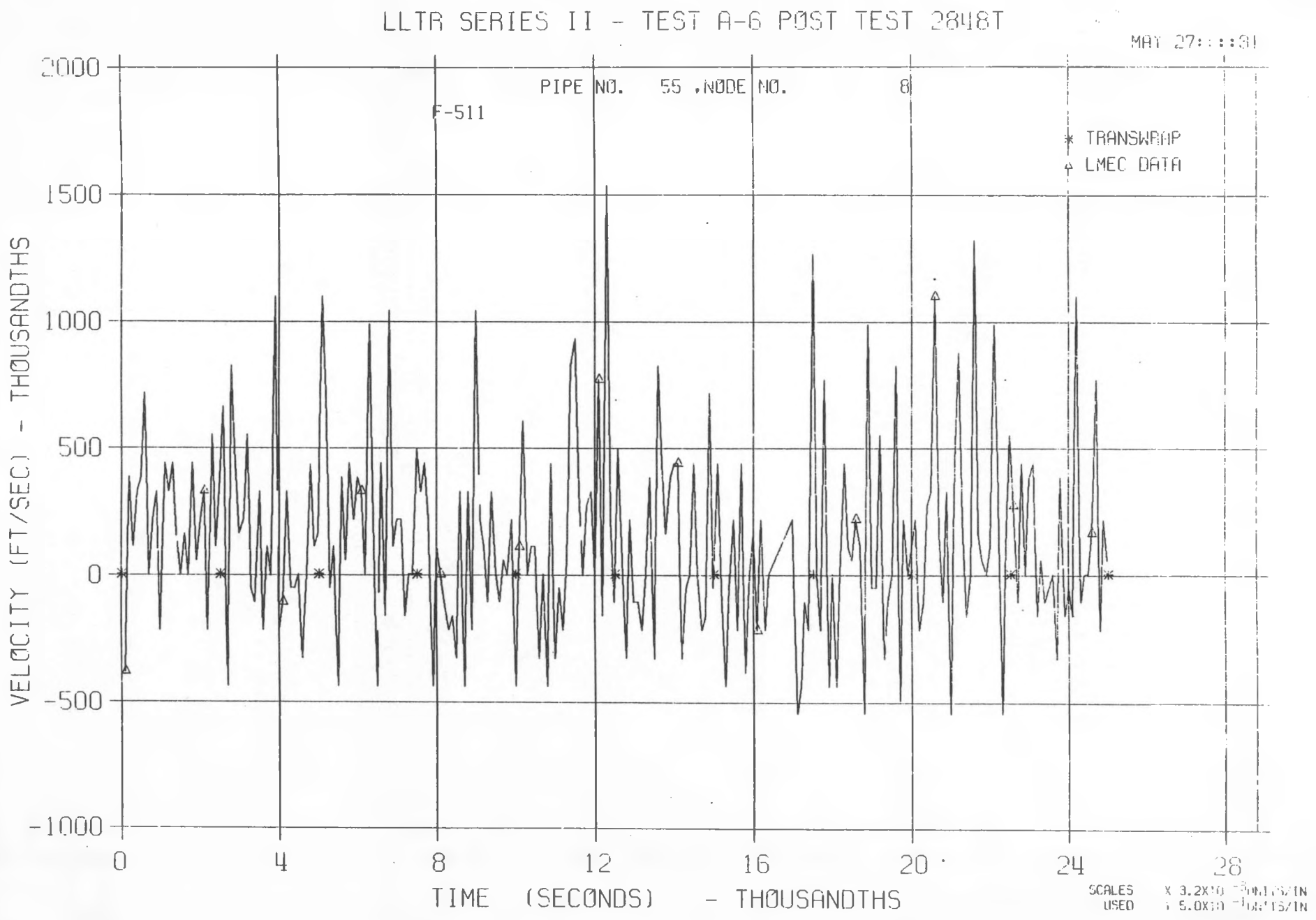
LLTR SERIES II - TEST A-6 POST TEST 2848T
MAY 27::::31
PIPE NO. 55 ,NODE NO. 8
F-511
* TRANSWRAP
Δ LMEC DATA
VELOCITY (FT/SEC) - THOUSANDTHS
2000
1500
1000
500
0
-500
-1000
0
4
8
12
16
20
24
28
TIME (SECONDS) - THOUSANDTHS
SCALES USED

PL 31

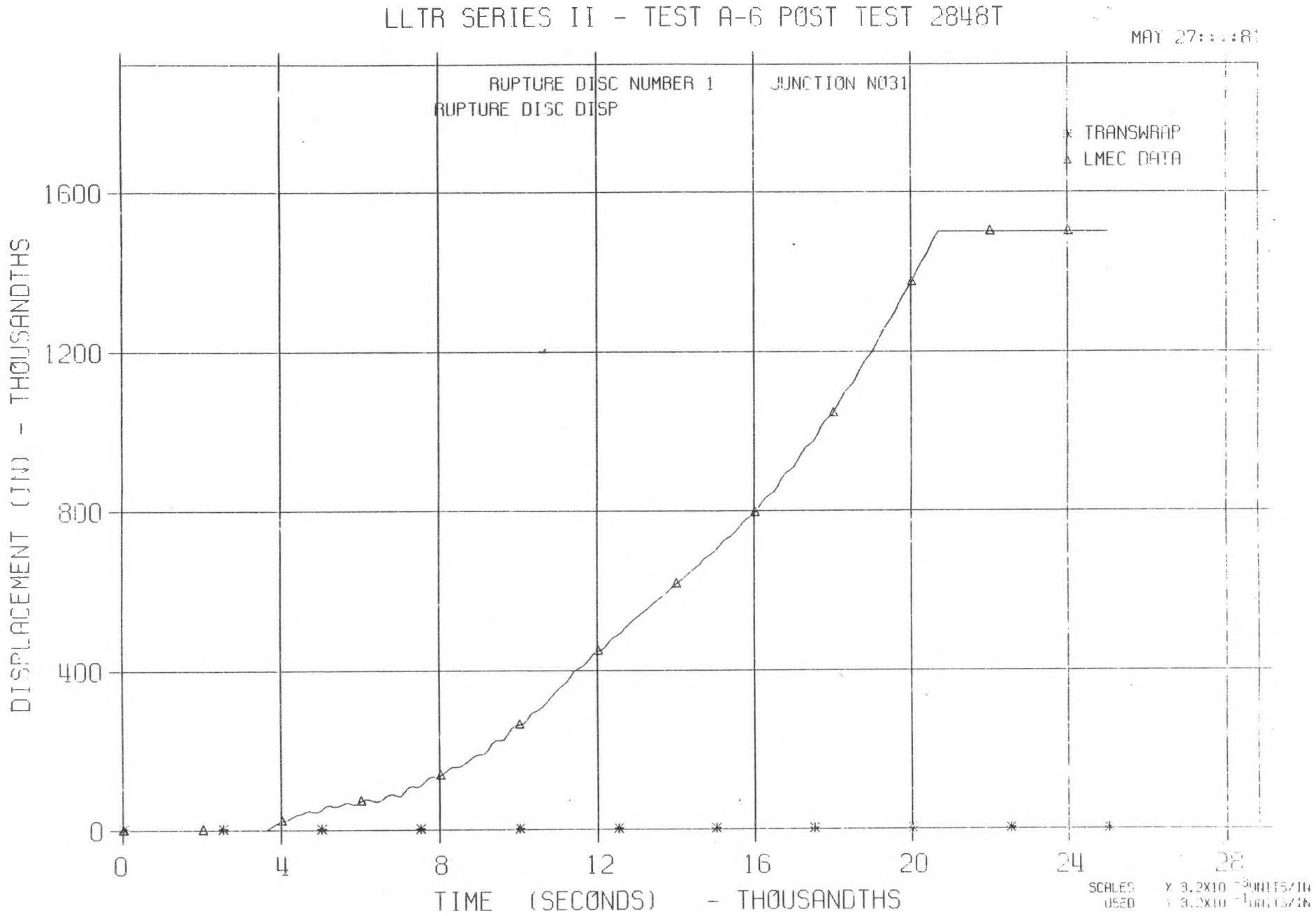
LLTR SERIES II - TEST A-6 POST TEST 2848T
MAY 27:::81
RUPTURE DISC NUMBER 1
RUPTURE DISC DISP
JUNCTION N031
TRANSWRAP
LMEC DATA
DISPLACEMENT (IN) - THOUSANDTHS
1600
1200
800
400
0
0
4
8
12
16
20
24
28
TIME (SECONDS) - THOUSANDTHS
SCALES USED

E-31

PL 32

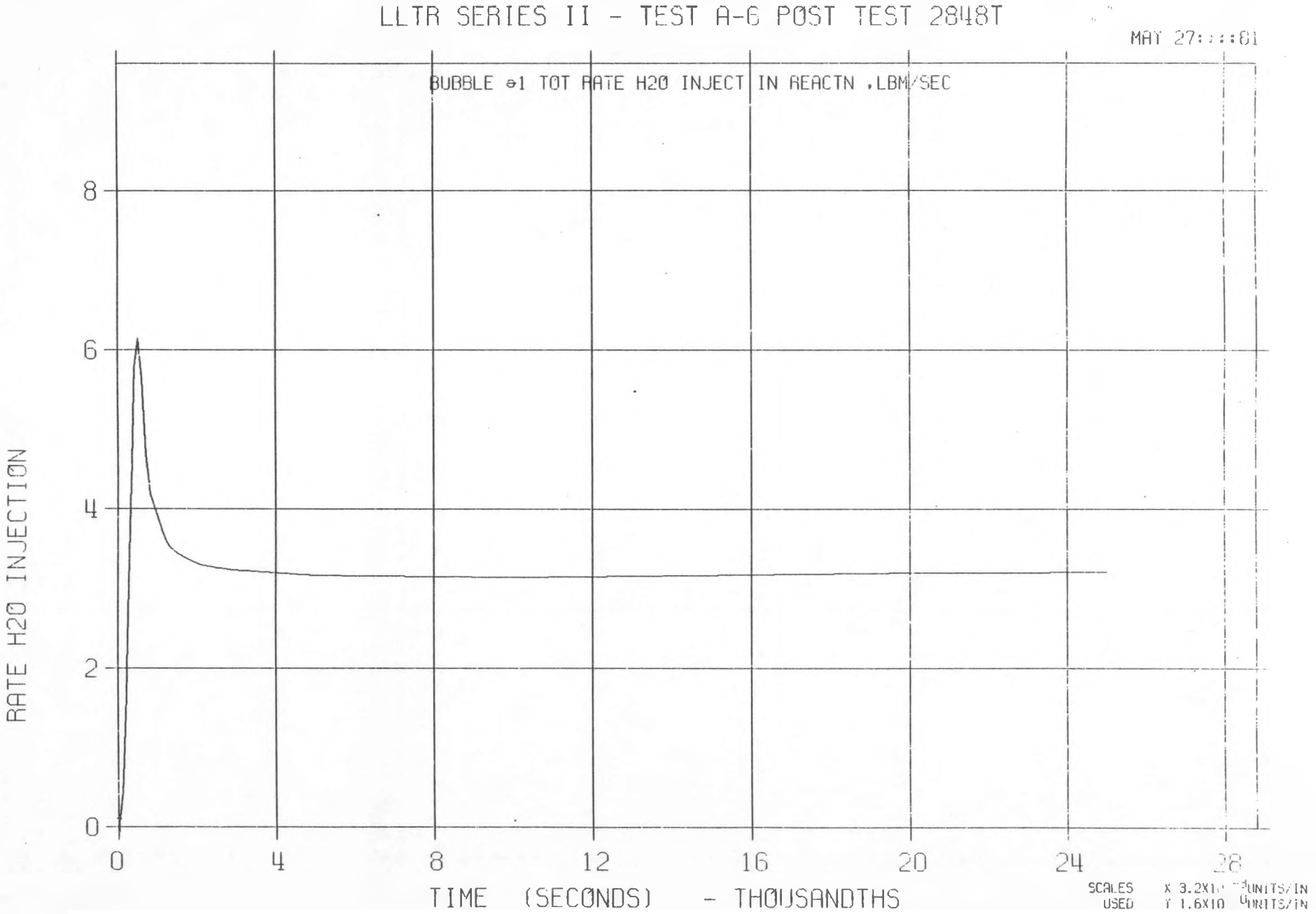
LLTR SERIES II - TEST A-6 POST TEST 2848T
MAY 27::::81
BUBBLE 61 TOT RATE H20 INJECT IN REACTN ,LBM/SEC
8
6
4
2
0
RATE H20 INJECTION
0
4
8
12
16
20
24
28
TIME (SECONDS) - THOUSANDTHS
SCALES USED
X 3.2X10 -3 UNITS/IN
Y 1.6X10 4 UNITS/IN

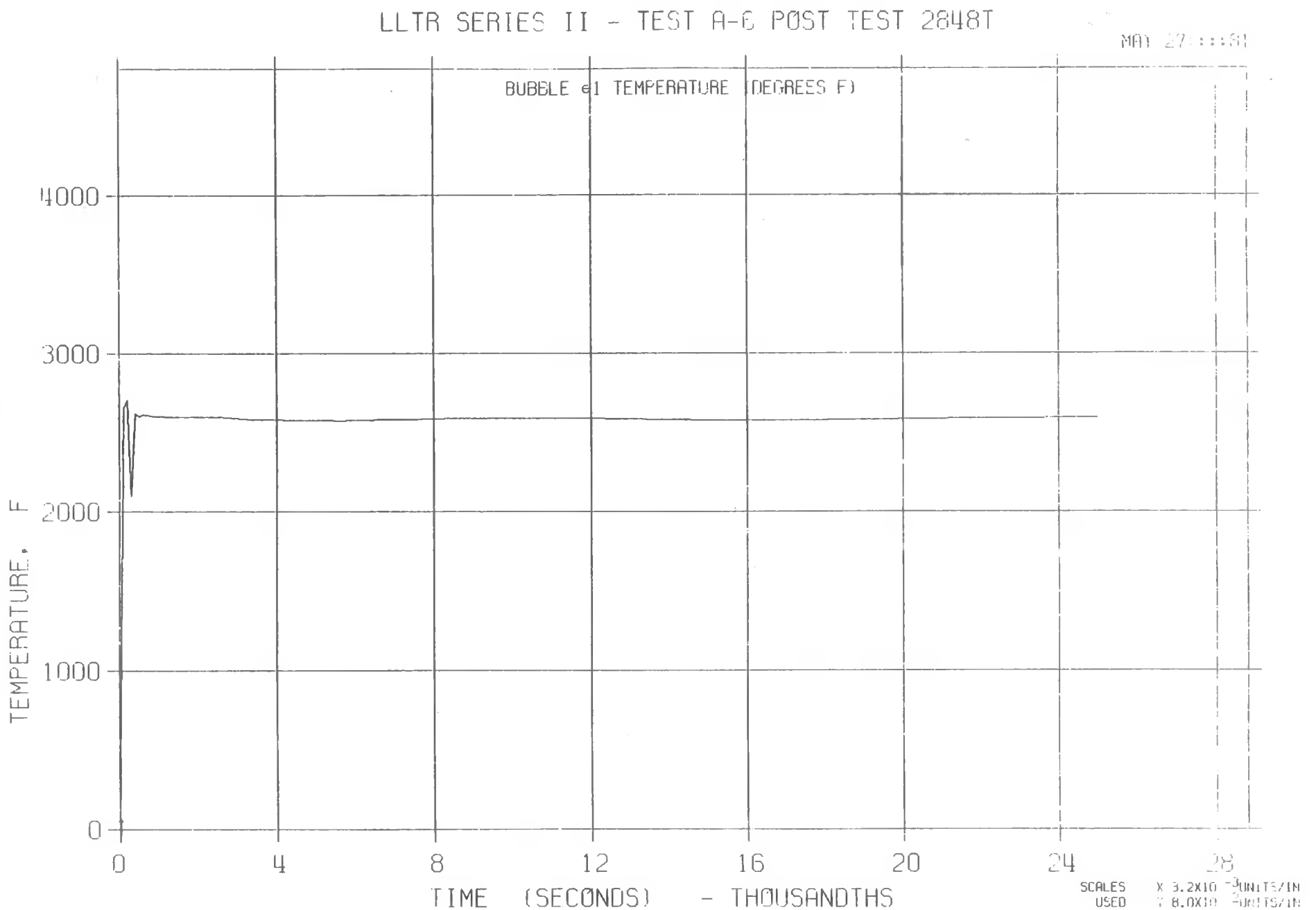
LLTR SERIES II - TEST A-6 POST TEST 2848T
BUBBLE e1 TEMPERATURE (DEGREES F)
4000
3000
2000
1000
0
TEMPERATURE, F
0
4
8
12
16
20
24
28
TIME (SECONDS) - THOUSANDTHS
SCALES USED

PL 38

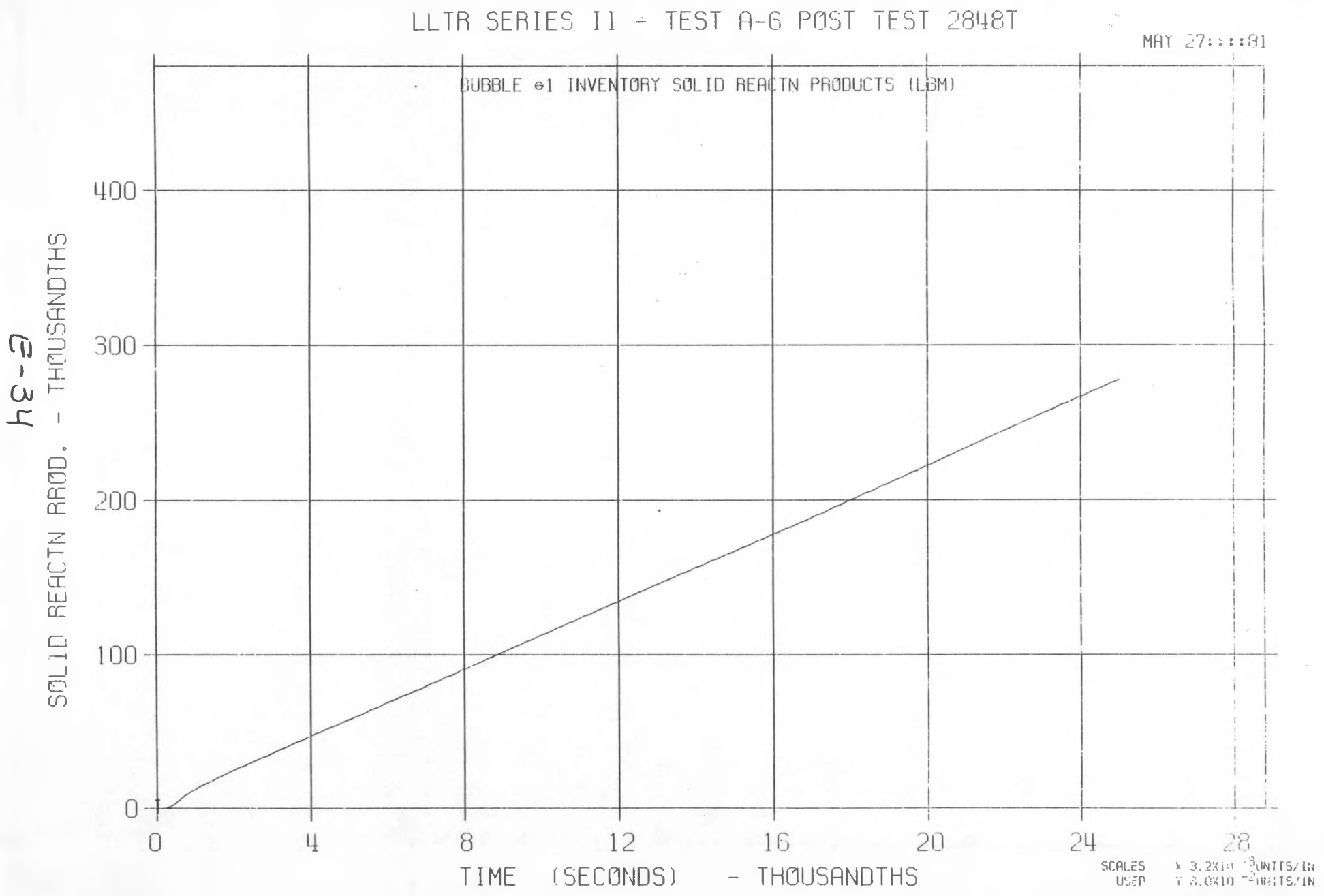
LLTR SERIES II - TEST A-6 POST TEST 2848T
MAY 27::::81
BUBBLE #1 INVENTORY SOLID REACTN PRODUCTS (LBM)
SOLID REACTN RROD. - THOUSANDTHS
400
300
200
100
0
0
4
8
12
16
20
24
28
TIME (SECONDS) - THOUSANDTHS
SCALES USED

E-34

PL 39

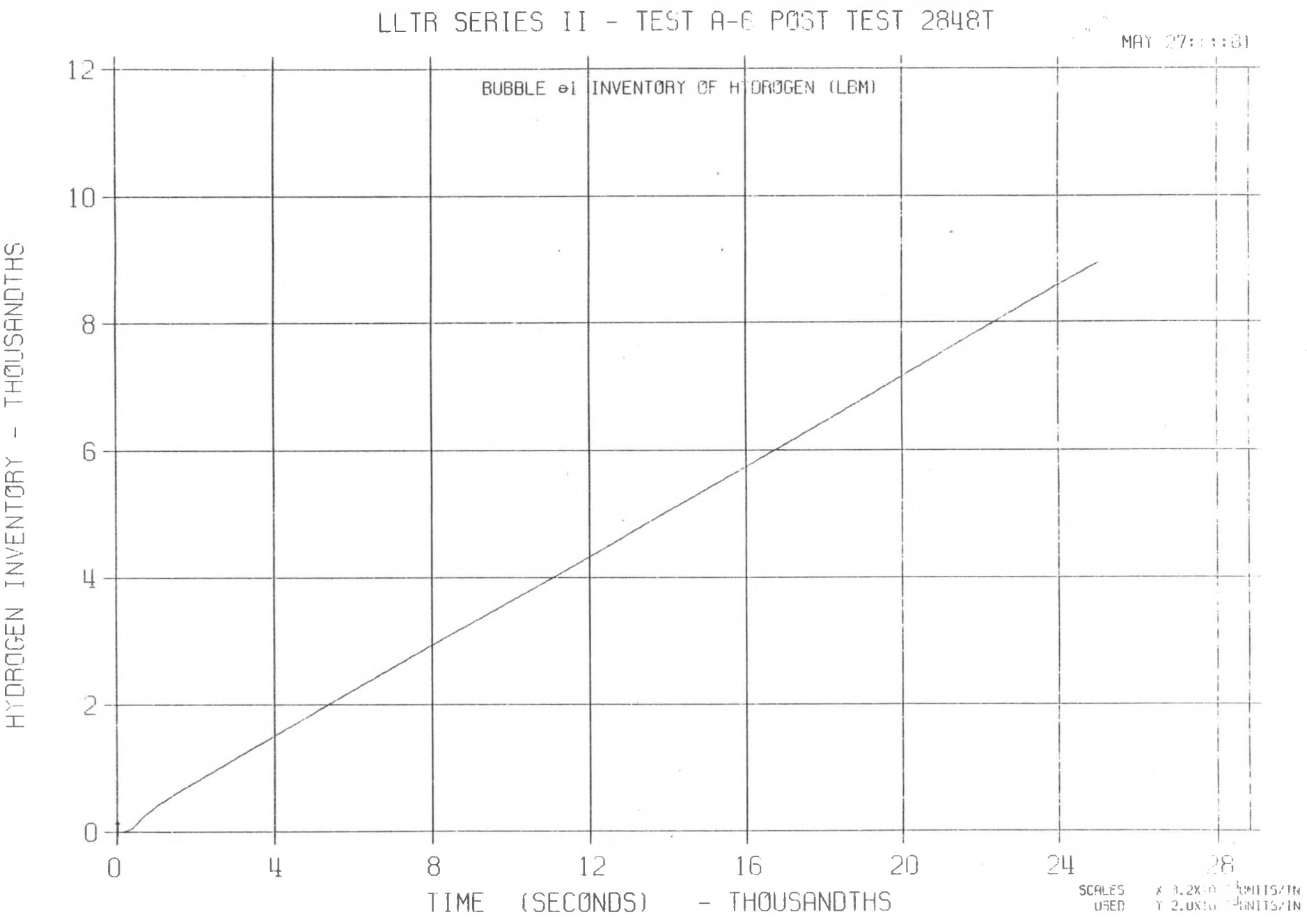
LLTR SERIES II - TEST A-6 POST TEST 2848T
MAY 27:::81
BUBBLE ei INVENTORY OF HYDROGEN (LBM)
HYDROGEN INVENTORY - THOUSANDTHS
12
10
8
6
4
2
0
0
4
8
12
16
20
24
28
TIME (SECONDS) - THOUSANDTHS
SCALES USED
X 1.2X10 UNITS/IN
Y 2.0X10 UNITS/IN

PL 40

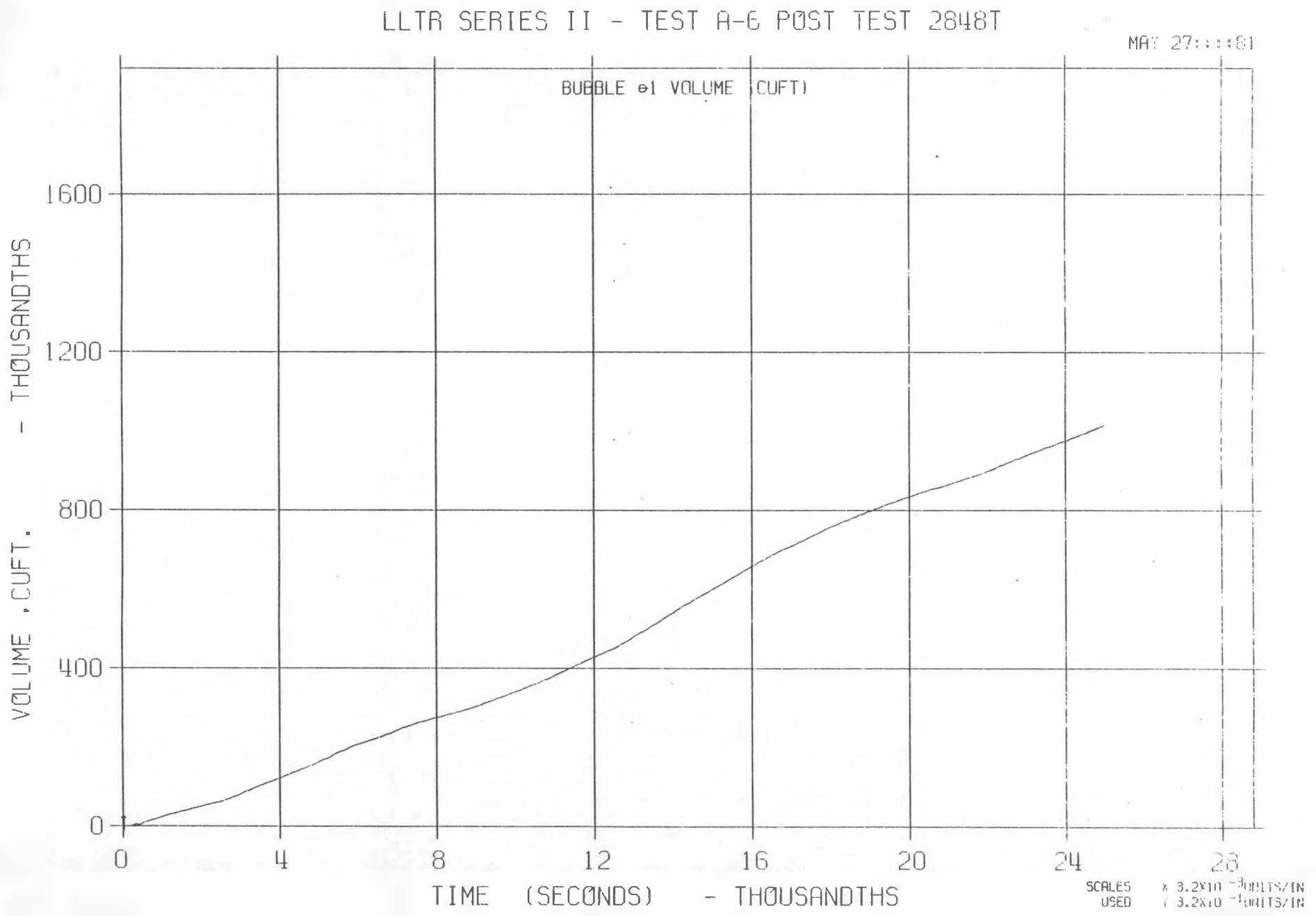
LLTR SERIES II - TEST A-6 POST TEST 2848T
MAY 27::::81
BUBBLE #1 VOLUME (CUFT)
VOLUME , CUFT. - THOUSANDTHS
1600
1200
800
400
0
0
4
8
12
16
20
24
28
TIME (SECONDS) - THOUSANDTHS
SCALES USED
X 3.2X10 -3 UNITS/IN
Y 3.2X10 -4 UNITS/IN

PL 41

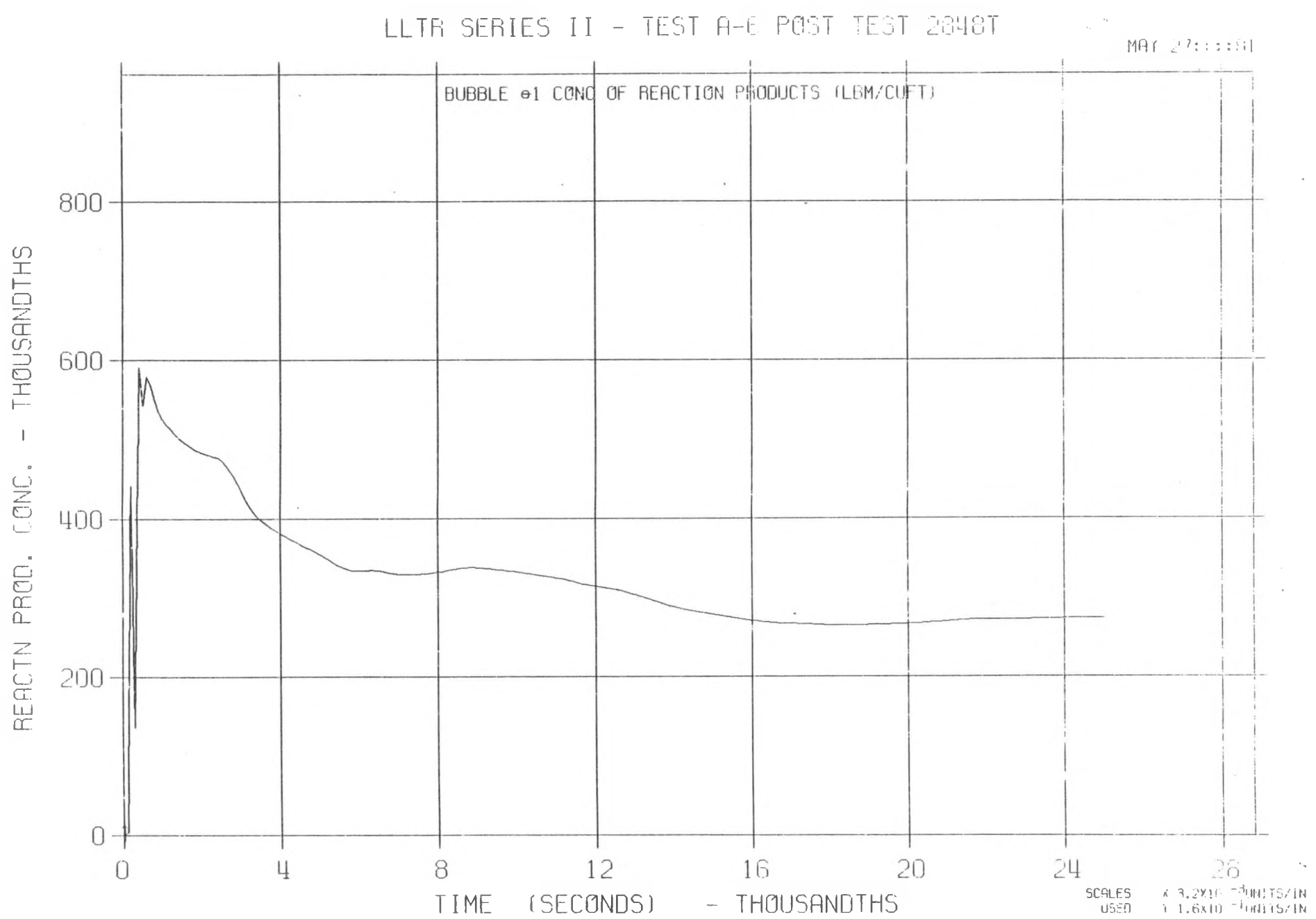
LLTR SERIES II - TEST A-6 POST TEST 2848T
BUBBLE @1 CONC OF REACTION PRODUCTS (LBM/CUFT)
REACTN PROD. CONC. - THOUSANDTHS
800
600
400
200
0
0
4
8
12
16
20
24
28
TIME (SECONDS) - THOUSANDTHS
SCALES
USED

PL 42